Programme and abstract booklet

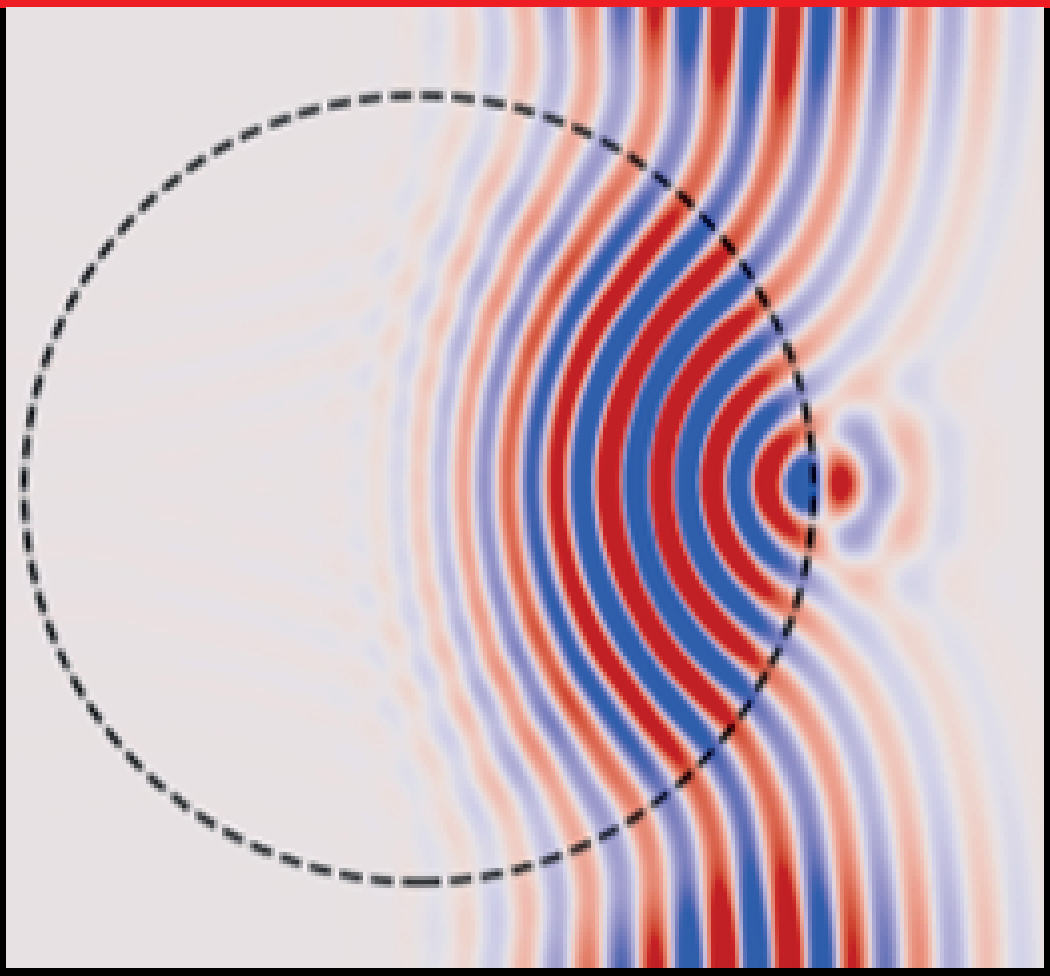

Image credit Natalie Whitehead and Volodymyr Kruglyak

Magnetism 2022

28-29 March 2022
University of York
York
UK

magnetism2022.iopconfs.org

IOP Institute of Physics

ProteusQ

Qnami

the quantum wave

Qnami ProteusQ™

Capture surface magnetic fields at the atomic scale

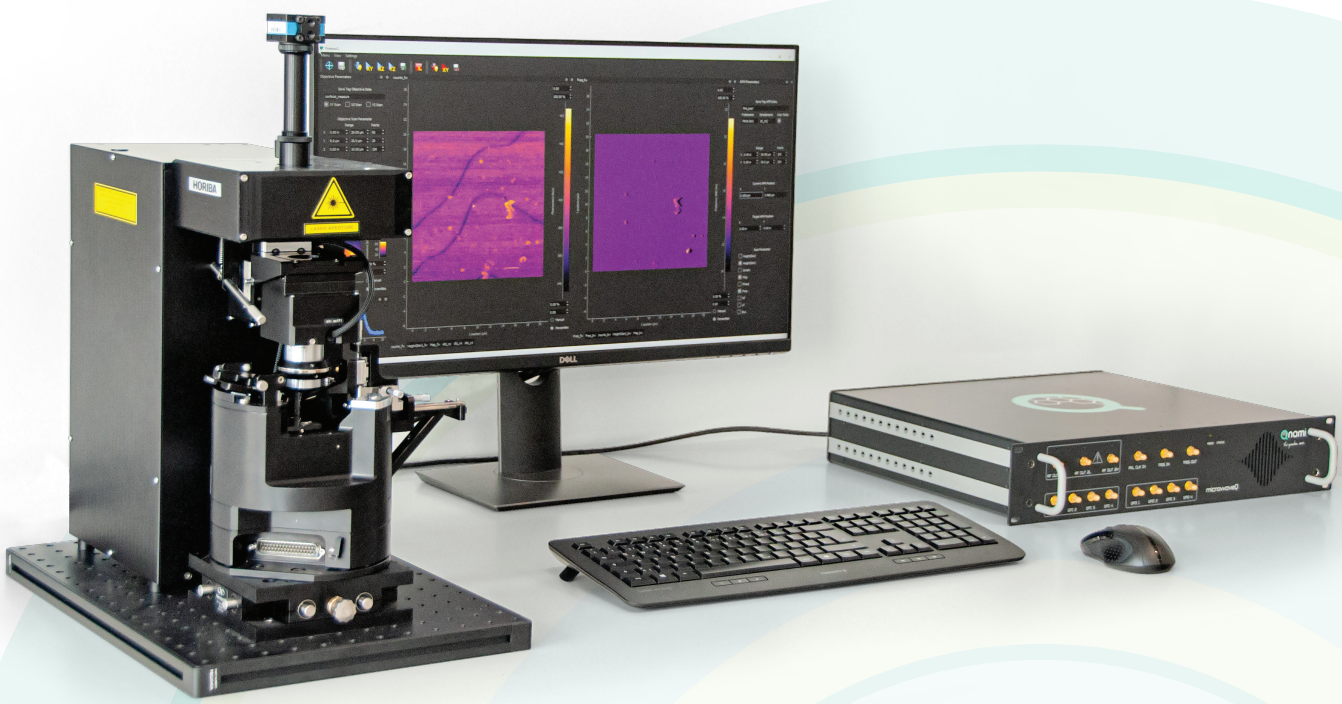

The first Scanning NV Magnetometer

To unlock your research potential

Qnami AG Hofackerstr. 40B • CH-4132 Muttenz • Switzerland
+41 (0) 61 511 89 60 • contact@qnami.ch • www.qnami.ch

attocube
WITTENSTEIN Group

Your partner for magnetic imaging

cutting-edge cryogenic measurement instrumentation

attoAFM

cryogenic atomic force microscope

mK .. 300 K

temperature rang compabilty

0 .. 12 T

available magnetic field range

1 nm

lateral closed loop scan resolution

sub -pm

vertical PFM resolution incl. amplitude calibration

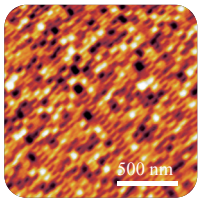

Magnetic Force Microscopy (MFM)

- Superconductors (high-T_c, pnictides, vortex imaging,...)
- Skyrmions & helimagnet phases
- Artificial spin ice
- Next generation storage media (bit patterned media,...)

Cryogenic Nanopositioners

- Non-magnetic low temperature nanopositioners
- Precise positioning of probe tips and specimens
- Exact and repeatable positioning
- Synonymous with attocube over the last 20 years

OXFORD INSTRUMENTS

Ultra Low Temperature Cryostats with Both Solenoid and Vector Magnets Available as Standard

#OxInstisListening

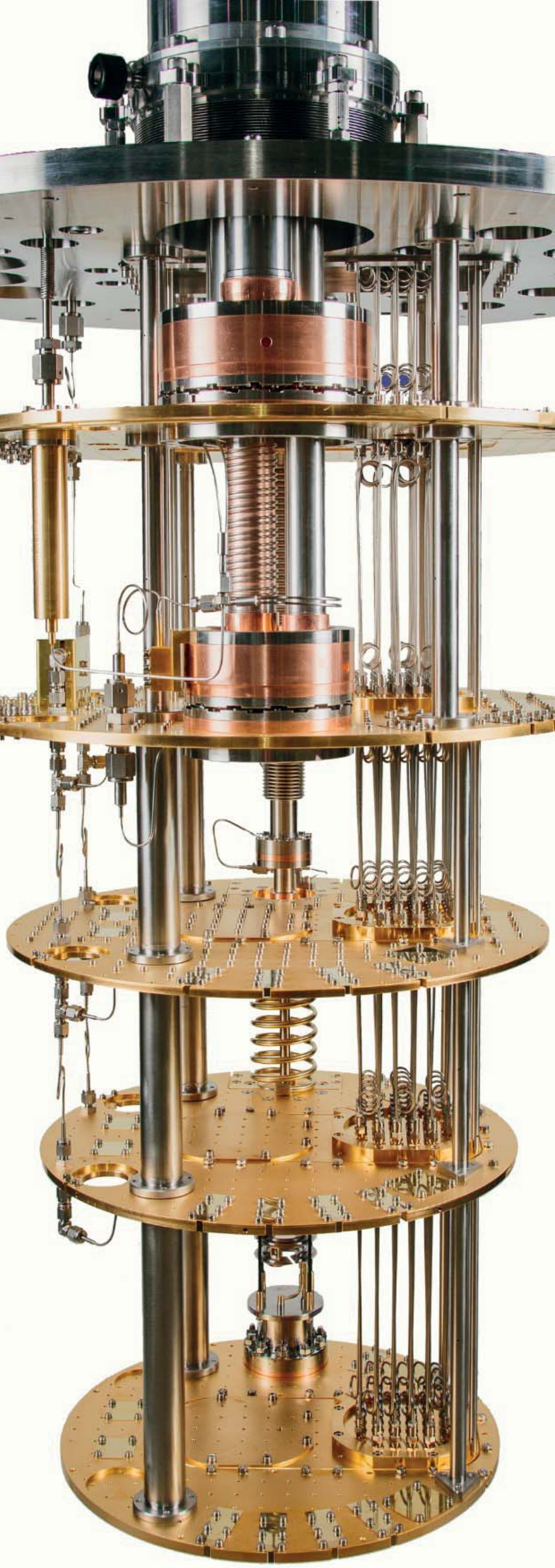

nanoscience.oxinst.com

Monday 28 March 2022

09:00 **Coffee and registration**
Exhibition Centre

Thin films & Dynamics

Parallel Session 1
P/L002
Chair: Tom Hayward

10:00 **Ultrafast magnetisation dynamics in CrI3,** Mara Strungaru, University of Edinburgh, UK

10:15 **Sub-ps Investigation of FeRh Structural Dynamics,** Michael Grimes, University of Manchester, UK

10:30 **Enhanced magnon transport through an amorphous magnetic insulator,** Daniel Cheshire, University of York, UK

10:45 **Local anisotropy control of Pt/Co/Ir thin films with perpendicular magnetic anisotropy by surface acoustic waves,** Jintao Shuai, University of Leeds, UK

11:00 **Low power continuous-wave all-optical magnetic switching in ferromagnetic nanoarrays,** Kilian Stenning, Imperial College

Correlated Electron Systems

Parallel session 2
P/L001
Chair: Helen Walker

10:00 **(Invited) Magnetic monopole density and antiferromagnetic domain control in spin-ice iridates,** Paul Goddard, University of Warwick, UK

10:30 **Evidence for emergent magnetic phase in LaFe11.8Si1.2?,** Kelly Morrison, Loughborough University, UK

10:45 **Magnetism on the stretched diamond lattice in lanthanide orthotantalates,** Nicola Kelly, University of Cambridge, UK

11:00 **Evidence of Covalent Mixing in the van der Waals Ferromagnet CrSiTe3 by Magnetic X-Ray Circular Dichroism,** Barat Achinuq, University of Oxford, UK

11:15 **Break**
Exhibition Centre

Thin films & Dynamics 2

Parallel Session 3
P/L002
Chair: Sam Ladak

11:45 **Scanning NV Magnetometry for Magnetic Memory Devices,** Peter Rickhaus, Qnami AG, Switzerland

12:00 **Polarised neutron reflectometry characterisation of interfacial magnetism in an FePt/FeRh exchange spring,** Will Griggs, The University of Manchester, UK

12:15 **Imprinting magnetic micropatterns through geometrical transformation,** Volker Neu, Leibniz IFW Dresden, Germany

12:30 **Microstate control via direct writing of vortices in an Artificial Spin-Vortex Ice,** Holly Holder, Imperial College London, UK

12:45 **Structural, chemical, and magnetic investigation of a graphene/cobalt/platinum multilayer system on silicon carbide**, Philipp Weinert, TU Dortmund University, Germany

Spintronics 1

Parallel Session 4
P/L001
Chair: Christy Kinane

11:45 **(Invited) Ferromagnetic Josephson junctions for cryogenic memory,** Nathan Satchell, University of Leeds, UK

12:15 **Spintronic terahertz emitters exploiting uniaxial magnetic anisotropy for field-free emission and polarisation control,** Charlotte Bull, University of Manchester, UK

12:30 **Voltage-Controlled Skyrmionic Interconnect with Multiple Magnetic Quasiparticles**, Will Griggs, The University of Manchester, UK

12:45 **The role of proximity induced magnetism on spin transport in multilayered systems**, Charles Swindells, University of Sheffield, UK

13:00 **Lunch break**
Exhibition Centre

14:00 **IEEE UK and Ireland Magnetic Chapter AGM**
P/L001

14:30 **Plenary Lecture**
Main plenary room - P/X001
Chair: Tom Moore
(Plenary talk) Fully-nano spintronic neural networks with radio-frequency connections
Julie Grollier, CNRS/Thales, France

High Frequency Spin Dynamics
Parallel Session 5
P/L002
Chair: Paul Keatley

15:30 **(Invited) Spin transport in a conventional superconductor,** Chiara Ciccarelli, University of Cambridge, UK

16:00 **Control of spin wave propagation in YIG by overlaying chiral magnonic resonators,** Yat-Yin Au, University of Exeter, UK

16:15 **Timescales and contribution of heating and helicity effect in helicity-dependent all-optical switching**, Jing Wu, University of York, UK

16:30 **Reservoir Computing via Spin-Wave Fingerprinting in an Artificial Spin-Vortex Ice**, Jack C. Gartside, Imperial College London, UK

16:45 **Optical generation and detection of coherent propagating magnons in an antiferromagnet**, Rostislav Mikhaylovskiy, Lancaster University, UK

Computation and Theory
Parallel Session 6
P/L001
Chair: TBC

15:30 **(Invited) Revealing the ultrafast domain wall motion in Manganese Gold through Permalloy capping**, Sarah Jenkins, University of York, UK

16:00 **Decreasing the magnetic anisotropy of Fe3O4 by Co-doping?,** David Serantes, Universidade de Santiago de Compostela, Spain

16:15 **Quantifying temperature-induced magnetic disorder effects in the anisotropy of MnBi**, Christopher Patrick, University of Oxford, UK

16:30 **Spin transport in easy-axis and easy-plane antiferromagnetic insulator thin films**, Verena Brehm, QuSpin, NTNU Trondheim, Norway

16:45 **The thermodynamic properties of exchange stiffness**, Sean Stansill, University of Leeds, UK

17:00 **Poster and exhibition session**
Exhibition Centre

19:00 **Conference Dinner**
The Principal Hotel York

Tuesday 29 March 2022

08:30 **Coffee and registration**
Exhibition Centre

09:00 **(Wohlfarth Lecture) Controlling and utilising antiferromagnetic order**
Peter Wadley, University of Nottingham, UK
Chair: Nicola Morley

10:00 **Break**
Exhibition Centre

10:30 Spintronics 2
Parallel Session - P/L002
Chair: Ivan Vera-Marun

10:30 **(Invited) Memristor controlled mutual synchronization of spin Hall nano-oscillator arrays for neuromorphic computing and spintronic Ising Machines**, Johan Åkerman, University of Gothenburg, Sweden

11:00 **All-optical switching in Ni3Pt/Ir/Co synthetic ferrimagnets driven by spin current**, Maciej Dabrowski, University of Exeter, UK

11:15 **Oblique spin injection and gate-controlled spin polarity in 1D-contact architectures**, Jesús Carlos Toscano Figueroa, University of Manchester, UK

11:30 **Computation with Magnetic Domain Walls and Oscillators**, Ales Hrabec, ETH Zurich, Switzerland

11:45 **Dipolar and quadrupolar spontaneous magnetic ordering in an atomic spin system mediated by ligh**, Thorsten Ackemann, University of Strathclyde, UK

10:30 General 1
Parallel Session - P/L001
Chair: Tom Ostler

10:30 **(Invited - IEEE) Exploring the Potentials of Spin-Orbitronics**, Aurélien Manchon, Aix-Marseille University, France

11:15 **Energy based model for Twin boundary prediction in the Sm-Fe-Co 1:12 phase**, Gino Hrkac, University of Exeter, UK

11:30 **Atomic Level Analysis of the Oxidation Pathways in Magnetic Fe/Fe Oxide Particles**, Toby Bird, University of York, UK

11:45 **Optimising Laser Additive Manufacturing Process for Amorphous Magnetic Materials**, Merve Ozden, University of Sheffield/Material Science and Engineering, UK

12:00 **Structural Explanation for Titanium Stability Range in RFe12-xTix**, Connor Skelland, University of Exeter, UK

12:15 **Lunch Break**
Exhibition Centre

13:30 EPSRC, MagSoc, AGM
Main plenary room - P/X001
Chair: Tim Mercer

14:00 Poster prizes and AGM
Main plenary room - P/X001

Invited: IEEE presentation

Parallel Session - P/L002

Chair: Christoforos Moutafis

14:30 **(Invited) Coherent Magnonics for Quantum Infor**
Michael Flatté, The University of Iowa, USA

15:15 **Break**
Exhibition Centre

Thin Films 3

Parallel Session - P/L002

Chair: Liam O'Brien

15:45 **Current induced crystallisation in Heusler alloy films for memory potentiation in neuromorphic computation**, William Frost, University of York, UK

16:00 **Experimental Demonstration of Reservoir Computation using Emergent Domain Wall Dynamics in a Patterned Magnetic Substrate**, Ian Vidamour, University of Sheffield, UK

16:15 **Obtaining additional behaviour from magnetic ring arrays for reservoir computing**, Guru Venkat, University of Sheffield, UK

16:30 **Thermal and edge roughness effects on domain wall based reservoir computing**, Matthew Ellis, University of Sheffield, UK

16:45 **Voltage Controlled Superparamagnetic Ensembles for Low Power Reservoir Computing**, Alexander Welbourne, University of Sheffield, UK

17:00 **Conference close**

Invited: IEEE presentation

Parallel Session - P/L001

Chair: Gonzalo Vallejo Fernandez

14:30 **(Invited) Symmetry Breaking by Materials Engineering for Spin-Orbit-Torque Technology**
Jingsheng Chen, National University of Singapore, Singapore

General 2

Parallel Session - P/L001

Chair: Matthew Swallow

15:45 **(Invited) Magnetic Nanoparticles as a Theranostic Platform for Cardiovascular Diseases**, David Cabrera, Keele University, UK

16:15 **Elasto-Magnetic Pumps for Point-of-Care Diagnostics**, Jacob Binsley, University of Exeter, UK

16:30 **SAR determination from temperature measurement using repeated heating-cooling cycles**, Sergiu Ruta, Sheffield Hallam University, UK

16:45 **Thinking Magneto-ionics: Neuromorphic Functionalities in Magnetic Nitride Films**, Julius de Rojas, Durham University, UK

Poster programme

Topic: Bulk Magnetic Materials

P1* **Band magnetism in doped GdTSi compounds**
Sergey Platonov, M.N. Mikheev Institute of Metal Physics of Ural Branch of Russian Academy of Sciences, Russia

P2 **Tailoring the structural and magnetic properties of CoFeNi0.5AlCrx**
Nicola Morley, University of Sheffield, United Kingdom

P3 **Unravelling magnetoelectriceffects in doped M-type hexaferrites**
Ohoud Alsaqer, University of York, UK

P4 **Magnetic Structure and Highly Unusual In-field Behaviour of D-type Erbium Disilicate**
Manisha Islam, University of Warwick, UK

Topic: Carbon-based Materials and Molecular Magnetism

P5 **The Impact of Finite Phonon Lifetimes on the Spin Dynamics in Single-Molecule Magnets**
Rizwan Nabi, The University of Manchester, UK

P6 **Characterisation of magnetic relaxation on extremely long timescales**
William Blackmore, The University of Manchester, UK

P7* **Intrinsic Magnetism of Spider Dragline Silks**
Varun Ranade, Indian Institute of Science Education and Research Mohali, India

P8 **Magnetic and Structural Effects of Boron Migration in C60/CoB/C60 Structures**
Daniel Roe, University of Leeds, UK

Topic: Computational and Theoretical Magnetism

P9 **Longitudinal spin fluctuations in atomistic spin models**
David Papp, University of York, UK

P10 **Atomistic simulations on the effect of grain size in HAMR**
David Papp, University of York, UK

P11 **Collective Skyrmion Motion Under the Influence of an Additional Interfacial Spin-Transfer Torque**
Callum MacKinnon, University of Central Lancashire, UK

P12 **3D FDTD-LLG modelling of electromagnetic shock waves**
Feodor Ogrin, University of Exeter, UK

P13 **Current-induced resonance in long conductive ferromagnetic nano-wires**
Mohammad Alneari, University of Exeter, UK

P14 **Free-Energy Landscapes of Nanomagnetic Skyrmion Host Systems**
Ioannis Charalampidis, University of Leeds, UK

P15 **A route towards stable homochiral topological textures in A-type antiferromagnets.**
Jack Harrison, University of Oxford, UK

P16 **Multiscale Modelling of the Antiferromagnet Mn2Au**
Joel Hirst, Sheffield Hallam University, UK

P17 **Effect of geometry on magnetism of Hund's metals: A case study with BaRuO3**
Hrishit Banerjee, University of Cambridge, UK

P18 **The effect of transmitted Spin Wave to Transient retrograde motion of skyrmions in multilayer wave guides**
Lin Huang, University of Leeds, UK

P19 **The Micromagnetic Effect of Magnetoelasticity on Antiferromagnets**
Robert Mackay, University of Leeds, UK

P20 **Coherent spin states path integral spin dynamics**
Thomas Nussle, University of Leeds, UK

P21 **Breaking through the Mermin-Wagner limit in 2D van der Waals magnets**
Sarah Jenkins, University of York, UK

P22 **Ab-inito and atomistic spin dynamics characterisation of antiferromagnetic materials Mn2Au and CuMnAs**
Sergiu Ruta, Sheffield Hallam University, UK

P23 **Investigating the exchange through the amorphous inter-granular phase in NdFeB permanent magnets**
Jack Collings, University of York, UK

P24 **Higher-order Magnetic Anisotropy in Soft-hard Nanocomposite Materials**
THANH BINH Nguyen, The University of York, UK

P25 **Switching Efficiency in Coreshell L10/A1-FePt Grain**
THANH BINH Nguyen, The University of York, UK

P26 **Electronic Heat Bath Simulations for Ultra-fast Spin Dynamics**
Jackson Ross, The University of York, UK

P27* **An ab initio study of anomalous magneto-volumetric behavior of ferrimagnetic Ni31Mn25Sn8 alloy**
Martin Friák, Institute of Physics of Materials, v.v.i., Czech Academy of Sciences, Czech Republic

Topic: Correlated Electron Systems

P28 **Site-specific Kondo and Spin-flip spectral signatures in chains of magnetic molecules on Au(111) surface**
Yingzheng Gao, École Superieure De Physique Et De Chimie Industrielles De La Ville De Paris, France

Topic: High Frequency Spin Dynamics

P29 **Reconfigurable stripe array metamaterial for control of surface acoustic wave propagation**
Yat-Yin Au, University of Exeter, UK

P30 **Exchange constant determination using multiple-mode FMR perpendicular standing spin waves**
Harry Waring, University of Manchester, UK

P31 **Enhancing the zero field resonances in synthetic antiferromagnets**
Harry Waring, University of Manchester, UK

P32 **Theory of THz-Driven Rare-Earth Dynamics in RFeO3**
Mykola Vovk, Lancaster University, UK

P33 **Tuneable NiFe Multilayers for High Frequency Applications**
Jade Scott, Queen's University Belfast, UK

P34 **Magnetisation dynamics in thin ferromagnetic films with Hybrid Anisotropy**
Jaime Leon, University of Manchester, UK

P35 **The THz-driven nonlinear spin wave propagation in an antiferromagnet**
Yuichi Saito, Lancaster University, UK

Topic: Nanoparticles

P36* **Signature of coexistent Ferromagnetism and Superconductivity in Bi coated Ni nanoparticles**
Laxmipriya Nanda, NISER institute, India

P37 **High-Moment Films Produced by Depositing Gas-Phase Nanoparticles**
Raul Lopez-Martin, Universidad de Castilla-La Mancha, Spain

P38 **Magnetic nanoparticles for spin Seebeck based thermoelectrics**
Mohamed Awad, Loughborough University, UK

P39 **Synthesis, characterisation and biofunctionlisation of BaTiO3 – CoFe2O4 magnetoelectric nanoparticles for biomedical applications**
Samyog Adhikari, University College London, UK

P40 **Magnetic anisotropy in relation to nanoparticle agglomeration and hyperthermia**
David Serantes, Universidade de Santiago de Compostela, Spain

Topic: Spintronics

P41 **Growing and characterising magnetic tunnel junction structures**
Meg Smith, University of Manchester, UK

P42 **Spintronic terahertz emitters exploiting uniaxial magnetic anisotropy for field-free emission and polarisation control**
Charlotte Bull, University of Manchester, UK

P43* **A 3D magnetic field sensor based on one single spin–orbit torque device**
Ruofan Li, Huazhong University of Science and Technology, China

P44 **Extrinsic contributions to spin Hall angle in Cu induced by impurities**
Jordan Harknett, Loughborough University, UK

P45 **Atomistic simulations of spin-orbit torque switching of Pt/MnPt bilayers**
Carenza Cronshaw, University of York, UK

P46 **Investigating ballistic transport in 1D graphene/FM spin injectors**
Daniel Burrow, University of Manchester, UK

P47 **Magneto-Optic Imaging of Coupled Domains in BaTiO3(111)/CoFeB Heterostructures**
Robbie Hunt, University of Leeds, UK

P48 **Combined spin transfer torque and spin orbit torque for low power magnetisation dynamics in magnetic tunnel junctions**
Andrea Meo, University of York, UK

P49 **Thermodynamic properties and switching dynamics of perpendicular shape anisotropy MRAM**
Wayne Lack, University of York, UK

P50 **Ultrafast magnetization dynamics in Ni80Fe20/Neodymium bilayer films**
Lulu Cao, Southeast University, China

P51 **Spin Torque Nano Oscillators as MIMO sources for 5G telecommunications**
Richard Evans, University of York, UK

Topic: Thin Films/General Submission

P52 **Development of a variable frequency, low current, low volume hysteresis loop tracer**
Gonzalo Vallejo Fernandez, University of York, UK

P53 **ISIS Neutron and Muon Source: The one-stop Magnetism Characterisation Shop**
Christy Kinane, ISIS, STFC, UK

Topic: Thin Films and nanostructures

P54 **Magnetoelectric Coupling in Inorganic/Organic Hybrid Composite Thin Films**
Muireann de h-Óra, University of Cambridge, UK

P55 **Controlling Piezoelectric Love Waves in Magnetoacoustic Devices**
Oliver Latcham, Exeter University, UK

P56 **Vortex dynamics in microscopic magnetic thin film spherical shells**
Katie Lewis, University of Exeter, UK

P57 **Spin pumping between two identical CoFe layers separated by an Ag layer**
Kalel Alsaeed, Durham University, UK

P58 **Paradigm of Magnetic Domain Wall-Based In-Memory Computing**
Wenjia Li, University of York, UK

P59 **A Study of the Dispersive Nature of the Voigt Effect in Thin Magnetic Films**
Neil Collings, Retired from University of Cambridge, UK

P60 **Exploring magnetic responses In interconnected magnetic nanoring arrays**
Charles Swindells, University of Sheffield, UK

P61 **Structural and magnetic properties of MBE grown Co2FeSi/Si(111) films**
Stuart Cavill, University of York, UK

P62 **Optimisation of CoFe/IrMn bilayers For Tunnel Anisotropic Magnetoresistance (TAMR) Applications**
Jade Scott, Queen's University Belfast, UK

P63 **Phase Coexistence and Transitions between Anti- and Ferromagnetic States in a Synthetic Antiferromagnet**
Christopher Barker, University of Leeds, UK

P64 **Structural and Magnetic Properties of CoIrMnAl Heusler Alloy Epitaxial Films Fabricated with Magnetron Sputtering for Spintronics Applications**
David Lloyd, University of York, UK

P65 **All optical switching in transition metal synthetic ferrimagnetic multilayer systems with enhanced interlayer exchange coupling**
Connor Sait, University of Exeter, UK

P66* **Skyrmions, stripe domains and AFM-FM phase coexistence observed in a synthetic antiferromagnetic system using Lorentz transmission electron microscopy**
Kayla Fallon, University of Glasgow, UK

P67 **Scanning Probe Microscopy Studies of Ion-Patterned FeRh**
Adrian Peasey, University of Manchester, UK

P68 **Spintronic Computing @ Sheffield**
Tom Hayward, Department of Materials Science and Engineering, UK

P69 **Stochastic Computing and Machine Learning with Magnetic Domain Wall Devices**
Alexander Welbourne, University of Sheffield, UK

P70 **Engineering exchange bias at the NiO/Fe3O4 interface by the varying surface termination of MgO**
Barat Achinuq, University of Oxford, UK

P71 **Pinning sites and defect phenomena on 2D magnetic materials**
Leopoldine Parczanny, University of Edinburgh, UK

P72 **Two-dimensional magnetic order in Cr-based chalcogenides**
Jan Phillips, Universidade de Santiago de Compostela, Spain

P73 **POLREF: Time of flight Polarised Reflectometer for Magnetism in Thin Films**
Christy Kinane, ISIS, STFC, UK

P74 **Refl1d: Advanced Neutron and X-ray reflectivity modelling with Bayesian Uncertainty analysis**
Christy Kinane, ISIS, STFC, UK

P75 **Fine-tuning of the compensation point in ferrimagnetic TbFe alloys by He+ irradiation and surface to bulk ratio**
Paweł Sobieszczyk, University of York, UK

Topic: Topological Materials for Spintronics

P76 **Antiferromagnetic Materials Optimisation for Next Generation Low Power Electronic Devices Using First-Principles Simulation**
Ieuan Wilkes, University of York Physics Department, UK

P77 **Measurement of the Skyrmion Pseudo-Liquid Phase using Resonant Elastic X-ray Scattering**
Jack Bollard, University of Oxford, UK

***Posters available but presenters not on site**

Monday 28 March 2022

Thin films & Dynamics

Ultrafast magnetisation dynamics in CrI_3

Mara Strungaru, and Elton J G Santos

The University of Edinburgh, UK

This discovery of intrinsic magnetism at the two-dimensional level has opened up the possibility of creating devices that exploit the magnetic order in 2D. The laser-induced manipulation of spins promises to revolutionise the magnetic storage technologies by using ultrafast processes with low dissipation. With the discovery of 2D materials having high Curie temperatures such as Fe_3GeTe_2, the applications based on ultrafast excitation in 2D materials are becoming feasible.

In this work we explore the typical example of a 2D magnetic material, CrI_3 under the effect of an ultrafast laser pulse. CrI_3 is an interesting example of 2D material, that holds a ferromagnetic order at the monolayer limit, however, for even numbers of atomic layers, an antiferromagnetic order is stabilised [1]. Starting from experimental measurements [2], we reproduce the ultrafast magnetisation dynamics in bulk CrI_3 (Fig. 1) and extend our study to monolayer CrI_3. By using atomistic simulation methods [3], which include complex spin interactions (e.g. biquadratic [4], Dzyaloshinskii-Moriya interactions (DMI), dipolar interactions), we were able to create dynamically topologically protected spin structures (e.g. skyrmions) in CrI_3 layers at different temperatures and energy fluencies. Our findings indicate that ultrafast laser pulses can be used to manipulate spin textures efficiently at atomically thin van der Waals layers, similarly to other conventional ferromagnets [5].

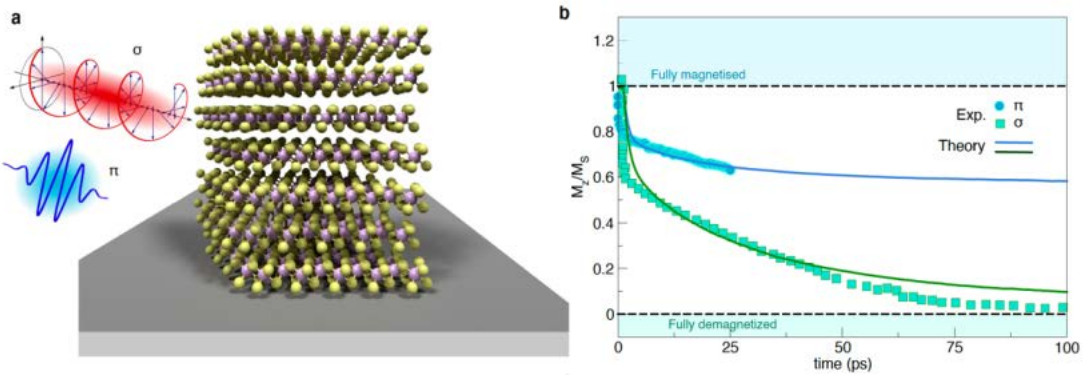

Fig. 1: Magnetisation dynamics in bulk CrI3 under laser pulse excitation. Panel a) - schematics of bulk CrI3 excited via a circular or linear polarised laser pulse. Panel b) Comparison between atomistic spin dynamics simulations and experimental results [2].

[1] Huang, B. et al. Nature 2017, 546, 270–273
[2] Padmanabhan, P. et al. arXiv preprint arXiv:2010.04915 (2020).
[3] https://vampire.york.ac.uk
[4] Wahab, D. A. et al. Advanced Materials 2021, 33, 2004138.
[5] Olleros-Rodriguez, P. arXiv preprint arXiv:2011.06093 2020

Sub-ps Investigation of FeRh Structural Dynamics

Michael Grimes[1,2,3], Hiroki Ueda[2], Dmitry Ozerov[2] , Federico Pressacco[4,5], Sergii Parchenko[2,3] , Andreas Asperos[2,3], Markus Scholz[4] , Yuya Kubota[6] , Tadashi Togashi[6] , Yoshikazu Tanaka[6] , Thomas Thomson[1] , and Valerio Scagnoli[2,3]

[1]The University of Manchester, UK, [2]Paul Scherrer Institut, Switzerland, [3]ETH Zurich, Switzerland, [4]DESY, Germany, [5]Universität Hamburg, Germany, [6]RIKEN SPring-8, Japan

FeRh is an archetypal system for the investigation of ultrafast behaviour in coupled transitions due to its meta-magnetic phase transition occurring around 380 K [1]. In this coupled phase transition, the electronic structure transforms lowering the resistivity by ≈ 33%, the lattice expands isotropically with a volumetric expansion of ≈ 1%, and the magnetic order changes from a G-type antiferromagnet (AF) to a ferromagnet (FM) [1], [2]. Previous x-ray diffraction (XRD) studies have indicated that the lattice expands with first order dynamics within 10-30 ps [3], with long-range AF order throughout the transition [4]. The sub-ps capabilities of the SACLA free-electron laser allowed for investigation of the ultrafast behaviour of the FeRh lattice upon laser excitation. This shows new dynamics at high fluences which were compared to the static behaviour of the Bragg peaks as measured using heated XRD. We describe the lattice temperature and expansion as a function of pump-probe delay. We have observed a perturbation to the expected dynamics above fluences of 5 mJ cm-2 where the lattice initially contracts before finally expanding as predicted. We demonstrate that a model using an excited lattice state [5] can explain the observed behaviour. Our model suggests the system relaxes through a subset of the phonon bands which are preferentially coupled to the electronic system.

[1] J. S. Kouvel and C. C. Hartelius, J. Appl. Phys., 33, no. 3, 1343, (1962).
[2] J. S. Kouvel, J. Appl. Phys., 37, no. 3, 1257–1258, (1966).
[3] S. O. Mariager, F. Pressacco, G. Ingold, et al., Phys. Rev. Lett., 108, no. 8, 087201, (2012).
[4] M. Grimes, N. Gurung, H. Ueda, et al., AIP Adv., [In Press], (2022).
[5] B. Mansart, M. J. G. Cottet, G. F. Mancini, et al., Phys. Rev. B - Condens. Matter Mater. Phys., 88, no. 5, 054507, (2013).

Enhanced magnon transport through an amorphous magnetic insulator

D M Cheshire and S A Cavill

Department of Physics, University of York, UK

Magnonics research is focused on the transport of spin information via spin-wave, or magnon, excitations in magnetic materials. Due to its exceptionally low damping, even in thin films, the magnetic insulator Yttrium Iron Garnet (YIG) is considered the most prominent material in this field being widely used in spin transport experiments. New research has been stimulated by a report of the observation of exceptionally long μm magnon diffusion lengths in amorphous YIG (a-YIG) where there is no significant long range structural or ferrimagnetic order (M ≈ 0) [1]. Spin transport through disordered magnetic insulators is suggested to be mediated by short range spin correlations and is highly dependent on the relative size of the correlation length to grain size [2].

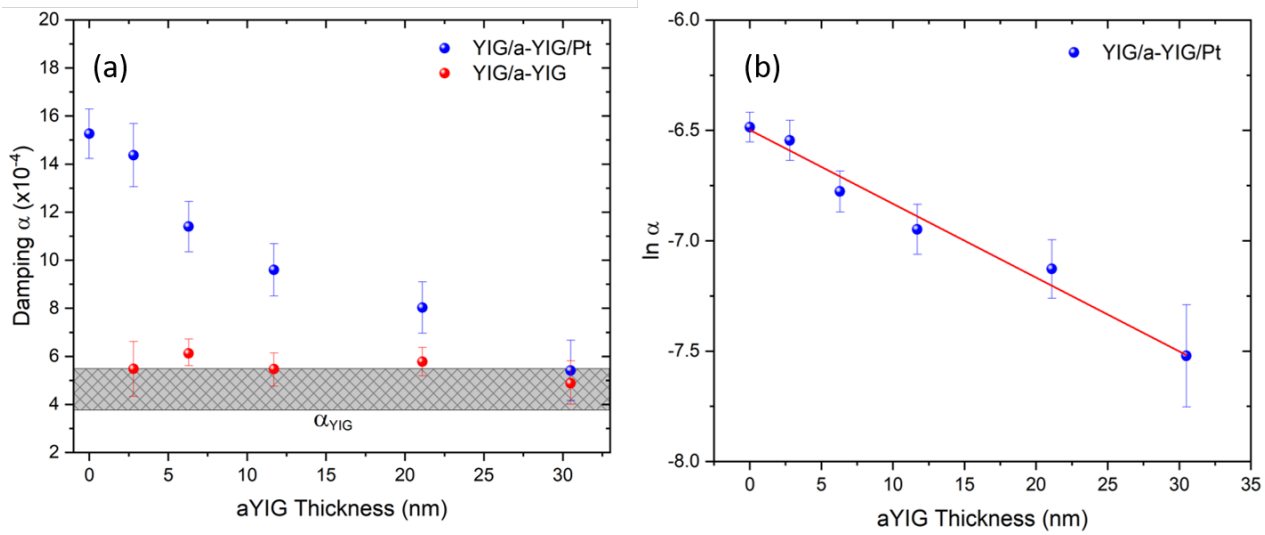

Fig. 1: (a) Gilbert damping, α, for YIG(45nm)/a-YIG(t nm)/Pt(5nm) trilayers as a function of a-YIG thickness and (b) ln(α) vs t

Similar non local experiments have failed to observe long range spin transport through a-YIG [3] and FMR spin-pumping in Permalloy/a-YIG/Pt trilayers provides a much lower (3.6nm) magnon diffusion length for a-YIG [4]. We hypothesise that samples of a-YIG may, in fact, have differing levels of 'amorphousness' and Fe cation distributions, which are highly dependent on growth conditions, leading to differences in the reported behaviour.

In this study we report on the magnon diffusion length in YIG (45nm)/a-YIG/Pt (5nm) trilayer structures fabricated on Gadolinium Gallium Garnet (GGG) substrates by pulsed laser deposition (PLD). In-plane VNA-FMR spectroscopy was performed to obtain the damping of the YIG in the trilayer, as a function of a-YIG thickness, and extract the magnon diffusion length. The experimental data (Figure 1a) shows a large change in damping with the addition of either Pt, or a-YIG plus Pt; indicating spin-pumping thought the a-YIG spacer into the Pt. Unlike Wang *et al*/[4] we do not observe significant additional damping when a-YIG is grown on YIG for thicknesses between 0 and 30nm without the Pt layer. As the thickness of the a-YIG layer is increased the additional damping due to spin pumping into the Pt is reduced. The relationship between damping and a-YIG thickness is described by diffusive magnon transport (Fig.1b). However, a significantly longer magnon diffusion length of 28nm for a-YIG is observed; approximately an order of magnitude larger than that observed in previous spin-pumping studies [4-5].

[1] D. Wesenberg *et al*. NPhys **13**, 987 (2017).
[2] H. Ochoa *et al*. Phys. Rev. B **98**, 054424 (2018).
[3] J. Gomez-Perez *et al*. Appl. Phys. Lett.**116**, 032401 (2020).
[4] H. Wang *et al*. Phys. Rev. B. **91**, 220410 (2015).
[5] L. Yang *et al*. Phys. Rev. B. **104**, 144415 (2021).

Local anisotropy control of Pt/Co/Ir thin films with perpendicular magnetic anisotropy by surface acoustic waves

Jintao Shuai[1], Mannan Ali[1], Li Chen[2] , John E Cunningham[2], and Thomas A Moore[1]

[1]School of Physics and Astronomy, University of Leeds, UK, [2]School of Electronic and Electrical Engineering, University of Leeds, UK

Encoding information in thin films with perpendicular magnetic anisotropy (PMA) holds promise for the next generation of data storage and logic operation applications [1]. Thin films with a large anisotropy provide high stability of the encoded information but cause a high energy cost of writing data [2]. Controlling anisotropy on demand is a practical method to decrease the energy cost. Here, we experimentally demonstrated the control of local anisotropy in a PMA thin film using standing surface acoustic waves (SAWs), which can introduce oscillating strain waves in the thin films over millimetric distances. Two interdigitated transducers (IDTs), whose centre frequency is 93.35 MHz, were patterned on opposite ends of a 2-mm-wide stripe of Ta(50)/Pt(25)/Co(11)/Ir(15)/Ta (50) thin film (thickness in Å). The film was prepared by dc magnetron sputtering onto a lithium niobate substrate, which can support the propagation of SAWs. A wide-field Kerr microscope was used to measure the hysteresis loops of the thin film and image the domain patterns with SAW both on and off at room temperature. Micromagnetic simulations were performed by Mumax to reveal the effect of the nodes and anti-nodes of the standing SAW on magnetisation reversal. Results showed that the standing SAW significantly reduce the coercivity of the thin films from 4.95 ± 0.03 mT to 3.90 ± 0.03 mT (~21% reduction). With the presence of the standing SAW, domain nucleated at certain locations of the thin film, forming lined-up domain patterns with the spacing of half-wavelength (40 μm). Whereas domains nucleated and propagated randomly without SAW. The domain patterns and simulation results suggested that the anti-nodes of the standing SAW locally reduce the anisotropy of the thin film due to magneto-elastic coupling, favouring magnetisation reversal [3]. This study indicates the possibility of remote and energy-efficient control of magnetization switching.

Keywords: magnetization switching, magneto-elastic coupling, anisotropy control, surface acoustic waves, PMA

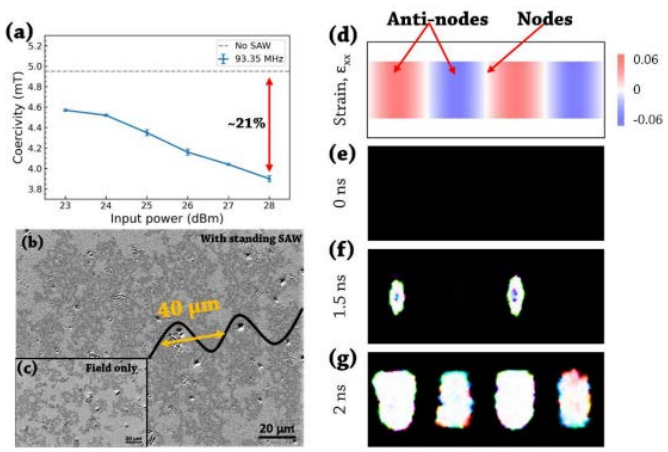

Fig.1 (a) Coercivity of the Ta(50)/Pt(25)/Co(11)/Ir(15)/Ta (50) thin film (thickness in Å) against input SAW power. Up to 21% coercivity reduction can be observed at input SAW power of 28 dBm. (b) Domain patterns with the presence of standing SAW. Domains nucleated and lined up at the anti-nodes of the standing SAW with the spacing of half SAW wavelength of 40 μm. (c) Domain patterns without SAW presence. Domains nucleated and propagated randomly. (d) Strain distribution in the simulation. The amplitude (strain) of the SAW is 0.06. (e)-(f) Magnetisation at 0, 1.5, and 2 ns. The magnetisation reversal occurred at the anti-nodes of the standing SAW first and then propagated towards the nodes.

[1] B. Tudu et al., Vacuum, 14, 329, (2017)
[2] W. Li et al., J. Appl. Phys, 115, 17E307 (2014)
[3] P.M. Shepley et al., Sci. Rep. 5, 7921 (2015)

Low power continuous-wave all-optical magnetic switching in ferromagnetic nanoarrays

Kilian D Stenning[1,3], Xiaofei Xiao[1,3], Holly H Holder[1], Jack C Gartside[1], Alex Vanstone[1,2], Oscar W Kennedy[1,2], Rupert F Oulton[1], and Will R Branford[1]

[1]Blackett Laboratory, Imperial College London, UK [2]London Centre for Nanotechnology, University College London, UK

All-optical magnetic switching[1–3] represents a next-generation class of local magnetisation control, with wide-ranging technological implications. 75% of all data is stored magnetically and the predominant recording technology uses power-consuming magnetic fields with plasmonic focusing of laser heating for Heat Assisted Magnetic Recording (HAMR)[4,5].

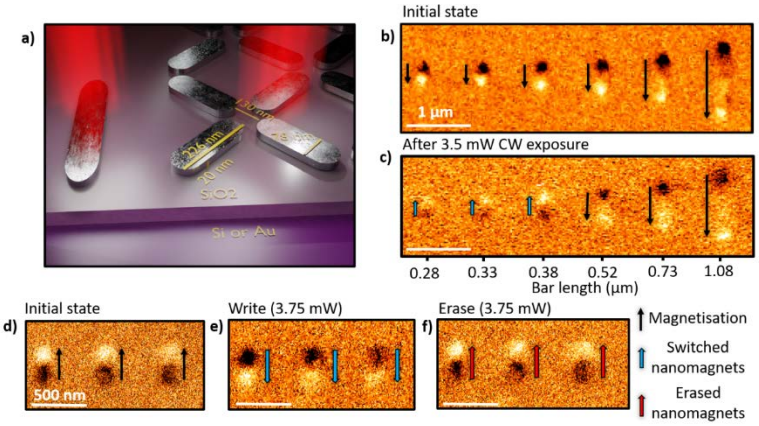

Fig. 2: a) Schematic of linearly-polarised CW laser exposure of isolated nanomagnets (left) and densely-packed Py nanomagnets in a square. MFM images of isolated nanomagnets b) in the saturated state and c) after linearly-polarised CW laser exposure with 3.5 mW power. Bars with length (L) ≤ 380 nm switch. MFM images of d) three nanomagnets with L = 280 nm in an initial saturated state. e) Subsequent switching after linearly-polarised CW exposure with 3.75 mW. f) Switching after a second 3.75 mW exposure demonstrating the ability to rewrite / erase previously written states

Existing (field-free) all-optical switching schemes are unsuitable for device integration, typically requiring power-hungry femtosecond-pulsed lasers and complex magnetic materials, rendering them unsuitable for device integration and up-scaling for application. Additionally, the majority of studies concern continuous thin films or well-spaced single nanostructures, restricting write-density.

In this talk, we demonstrate deterministic, all-optical magnetic switching using a low-power, linearly-polarised continuous-wave laser in nanostructures with sub-diffraction limit dimensions composed of simple earth abundant ferromagnetic alloys ($Ni_{81}Fe_{19}$, $Ni_{50}Fe_{50}$) and dielectrics (Fig. 1a). An interference effect dramatically enhances absorption in the nanomagnets, enabling high fidelity writing at powers as low as 2.74 mW. Isolated (Fig. 1b-f) and densely-packed nanomagnets are switched across a range of dimensions, laser wavelengths and powers. All artificial spin ice[6] vertex configurations are written with high fidelity, including energetically and entropically unfavourable 'monopole-like' states inaccessible by thermalisation methods. No switching is observed in equivalent structures with pure Co magnets, suggesting multi-species interactions within the nanomagnet play a role. The results presented here usher in low-cost, low-power optically-controlled devices with impact across data storage, neuromorphic computation and reconfigurable magnonics.

[1] Stanciu, Claudiu D., et al. *Physical review letters* 99.4 (2007): 047601.
[2] Kirilyuk, A., Kimel, A. V. & Rasing, T. Phys. 82, 2731 (2010).
[3] Kimel, A. V. & Li, M. Nat. Rev. Mater. 4, 189–200 (2019).

[4] Pancaldi, M., Leo, N. & Vavassori, P. Nanoscale 11, 253 7656–7666 (2019).
[5] Kryder, M. H. et al. Proc. IEEE 96, 1810–1835 (2008).
[6] Wang, R. et al. Nature 439, 256 303–306 (2006).

Correlated Electron Systems

(Invited) Magnetic monopole density and antiferromagnetic domain control in spin-ice iridates

Paul Goddard

University of Warwick, UK

Magnetically frustrated systems provide fertile ground for complex behaviour, including unconventional ground states with emergent symmetries, topological properties, and exotic excitations. A canonical example is the emergence of magnetic-charge-carrying quasiparticles in spin-ice compounds. Despite extensive work, a reliable experimental indicator of the density of these magnetic monopoles is yet to be found. Using measurements on single crystals of Ho2Ir2O7 combined with dipolar Monte Carlo simulations, we show that the isothermal magnetoresistance is highly sensitive to the monopole density. Moreover, we uncover an unexpected and strong coupling between the monopoles on the holmium sublattice and the antiferromagnetically ordered iridium ions. These results pave the way towards a quantitative experimental measure of monopole density and demonstrate the ability to control antiferromagnetic domain walls using a uniform external magnetic field, a key goal in the design of next-generation spintronic devices.

Evidence for emergent magnetic phase in $LaFe_{11.8}Si_{1.2}$?

K Morrison[1], J Betouras[1], G Venkat[2], R A Ewings[3], A Caruana[3], K Skokov[4], O Gutfleisch[4] & L F Cohen[5]

[1]Physics Department, Loughborough University, UK, [2]Department of Materials Science and Engineering, University of Sheffield, UK [3]ISIS Pulsed Neutron and Muon Source, STFC Rutherford Appleton Laboratory, UK, [4]Technical University Darmstadt, Material Science, Functional Materials, Germany, [5]The Blackett Laboratory, Imperial College London, UK

The $LaFe_{13-x}Si_x$ system ($x<1.6$) has a first order ferromagnetic, FM, to paramagnetic, PM, transition that is tunable in magnetic field and ends at a (tri)critical point (H_{crit}, T_{crit}) beyond which it is second order. In this large family of materials T_c can be easily tailored by changing the Fe content or by hydrogenation, and $La(Fe,Si)_{13}$ has attracted huge interest due to its potential for room temperature magnetic cooling [1] or harvesting of waste heat [2]. One of the fundamental reasons for this is that despite the magnetic transition being strongly first order, there is almost no magnetic or thermal hysteresis (an advantage for cooling applications).

We used a novel microcalorimetry method [3] to isolate the contributions to heat capacity and latent heat as a function of magnetic field and temperature, which can be used to distinguish between first and second order phase transitions. The results have previously been compared for a series of intermetallics such as $Gd_5Ge_2Si_2$, $DyCo_2$, $LaCaMnO_3$ and $LaFe_{13-x}Si_x$ with respect to the hysteresis at the phase transition [4]. For the $LaFe_{13-x}Si_x$ system, with $x=1.2$ we observed that a giant increase in the heat capacity evolved as the system approaches the tricritical point[5] and argued that this enhancement of the heat capacity is due to anomalously large spin fluctuations that are enabled by a multiple minima energy landscape.[6]

Inelastic neutron scattering of $LaFe_{11.8}Si_{1.2}$ was carried out on the LET beamline at ISIS in order to test this theory, where we found evidence of broad, quasielastic paramagnetic fluctuations for $Q<0.7$ Å^{-1} supporting the presence of large spin fluctuations. In addition, we observed emergence of a finite-Q quasielastic feature

at Q=0.52 Å^{-1}, which is close to the (100) Bragg reflection (but not expected for this structure). We will show the results of these measurements as a function of magnetic field and temperature, including the development of this finite-Q feature, as we approach T_{crit} and discuss its potential origin.

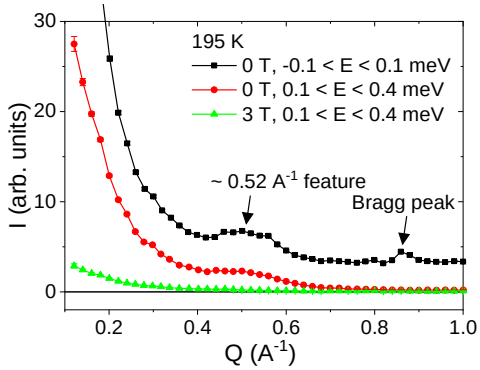

Fig. 1 – Example line-scan of inelastic neutron scattering data as a function of the momentum transfer, Q. Black squares show data integrated about the elastic line (±0.1 meV), red circles and green triangles show data integrated in the quasielastic regime (0.1-0.4 meV) when sample was in the paramagnetic and ferromagnetic state, respectively. The finite-Q feature at 0.5 Å^{-1} is observed in the quasielastic regime only when the sample is in the paramagnetic state and close to T_c.

[1] B.G. Shen *et al.*, *Adv. Mat.*, 21, 4545-4564 (2009).
[2] A. Waske *et al.*, *Nature Energy* **4**, 68–74 (2019).
[3] K. Morrison *et al.*, *Phil. Mag.*, **92**, 292-303 (2012); Y. Miyoshi *et al.*, *Rev. Sci. Instrum.*, **79**, 074901 (2008).
[4] K. Morrison & L. F. Cohen, *Metallurgical and Materials Transactions E* **1**, 153-159 (2014).
[5] K. Morrison *et al.*, *J. Phys. D*, **43**, 132001 (2010).
[6] M.D. Kuz'min *et al.*, *Phys. Rev. B*, **76**, 092401 (2007).

Magnetism on the stretched diamond lattice in lanthanide orthotantalates

Nicola D Kelly[1], Lei Yuan[1], Rosalyn L Pearson[1] , Emmanuelle Suard[2] , Inés Puente Orench[2,3] and Siân E Dutton[1]

[1]Cavendish Laboratory, University of Cambridge, UK, 2Institut Laue-Langevin, France, [3]Instituto de Nanociencia y Materiales de Aragón (INMA), CSIC-Universidad de Zaragoza, Spain

In this contribution I will discuss the structural and magnetic properties of lanthanide tantalates, $LnTaO_4$ (Ln = Nd, Sm, Eu, Gd, Tb, Dy, Ho, Er). Bulk magnetometry and heat capacity measurements indicate the absence of long-range ordering above 2 K in all samples except $TbTaO_4$. Powder neutron diffraction [1] on $TbTaO_4$ above and below its Néel temperature of 2.25 K reveals A-type antiferromagnetic ordering with collinear Tb^{3+} spins, Fig. 1.

The arrangement of magnetic ions in $LnTaO_4$ is discussed with reference to the so-called "harmonic honeycomb" series of geometrically frustrated magnets [2], and the results are compared to other materials with the same "stretched" or elongated diamond-like network. The stretched diamond lattice is expected to produce unusual magnetic ground states in the presence of competing nearest- and next-nearest-neighbour exchange interactions.

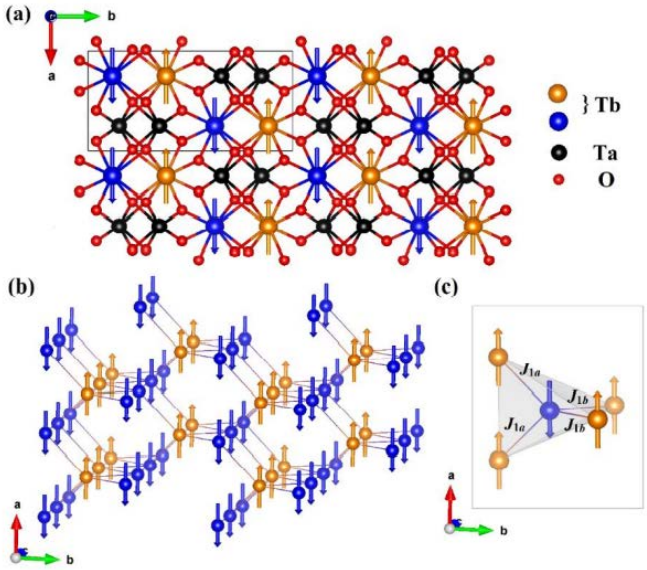

Fig. 1: Magnetic structure of TbTaO4 obtained by powder neutron diffraction: (a) all atoms, (b) Tb spins only, (c) illustration of nearest-neighbour magnetic interactions J_{1a} and J_{1b}.

[1] N. D. Kelly et al., Nuclear and magnetic diffraction study of monoclinic TbTaO4, https://doi.org/10.5291/ILL-DATA.5-31-2854

[2] K. A. Modic et al., Realization of a three-dimensional spin-anisotropic harmonic honeycomb iridate, Nat. Commun. 5:4203 (2014)

Evidence of Covalent Mixing in the van der Waals Ferromagnet $CrSiTe_3$ by Magnetic X-Ray Circular Dichroism

Barat Achinuq[1], Ryuji Fujita[1], Wei Xia[2], Yanfeng Guo[2], Peter Bencok[3], Gerrit van der Laan[3], and Thorsten Hesjedal[1]

[1]University of Oxford, UK, [2] School of Physical Science and Technology, ShanghaiTech University, China, [3]Diamond Light Source Ltd, Harwell Science and Innovation Campus, UK

$CrSiTe_3$ is a van der Waals type ferromagnetic semiconductor with a magnetic bulk transition temperature of 33 K, which can reach up to 80 K in single- and few-layer flakes. X-ray absorption spectroscopy (XAS) and X-ray magnetic circular dichroism (XMCD) on in vacuo-cleaved $CrSiTe_3$ crystals measured at ~10 K, indicate a hybridization-mediated superexchange between the Cr atoms. The observed chemical shift in the XAS and the XMCD of Cr $L_{2,3}$ multiple spectra confirm a strong covalent bond between the Cr 3*d(eg)* and Te 5*p* states. Furthermore, application of the XMCD sum rules gives a nonvanishing orbital moment, suggesting a partial occupation of the e_g states, apart from t_{2g}. We also show that the presence of a nonzero XMCD signal at the Te M_5 edge, which confirms a Te 5*p* spin polarization due to mixing with the Cr e_g bonding states. The results indicate that superexchange, instead of the previously suggested single-ion anisotropy, is responsible for the low-temperature ferromagnetic ordering of van deer Waals materials such as $CrSiTe_3$ and $CrGeTe_3$. This sheds light on the mechanism of ferromagnetism in 2D materials.

Thin films & Dynamics 2

Scanning NV Magnetometry for Magnetic Memory Devices

Peter Rickhaus[2], Umberto Celano[1], Hai Zhong[2], Florin Ciubotaru[1] , Laurentiu Stoleriu[3] , Alexander Stark[2], Felipe Favaro de Oliveira[2], Matthieu Munsch[2], Paola Favia[1], Maxim Korytov[1], Patricia Van Marcke[1], Patrick Maletinsky[2], Christoph Adelmann[1], and Paul van der Heide[1]

[1]IMEC, Leuven, Belgium, [2]Qnami AG, Muttenz, Switzerland, [3]Alexandru Ioan Cuza University, Iasi, Romania

Scanning NV magnetometry (SNVM) is an emerging quantum sensing technique which allows to measure minute magnetic fields with nanoscale resolution. We present a specific use-case of SNVM: the characterization of magnetic nanowires. Magnetic nanowires are among the essential building-blocks of contemporary spintronic devices [1] since their magnetic properties can be tuned by their geometry, and their fabrication is compatible with standard semiconductor fabrication schemes. While their topography and homogeneity can be well characterized with established techniques, it remains difficult to access their microscopic magnetic properties which are key to improve device performance. Here, we demonstrate magnetic imaging of ultra-scaled magnetic nanowires by SNVM [2]. The imaging reveals the presence of weak magnetic inhomogeneities inside in-plane magnetized nanowires that are largely undetectable with standard metrology. In this context, we will discuss the potential of SNVM for semiconductor device analysis.

[1] Parkin, S., & Yang, S. H. (2015). Memory on the racetrack. Nature Nanotechnology, 10(3), 195–198.

[2] Celano U., et al., (2021) Probing Magnetic Defects in Ultra-Scaled Nanowires with Optically Detected Spin Resonance in Nitrogen-Vacancy Center in Diamond. Nano Lett. 2021, 21, 24, 10409–10415.

Polarised neutron reflectometry characterisation of interfacial magnetism in an FePt/FeRh exchange spring

W Griggs[1], C Bull[1], C W Barton[1] , R A Griffiths[1], A J Caruana[2], C J Kinane[2], P W Nutter[1], and T Thomson[1]

[1]Nano-Engineering and Storage Technologies group, School of Computer Science, University of Manchester, UK, [2]ISIS, Rutherford Appleton Laboratory, UK

Multilayer thin film systems with tuneable interlayer coupling have the potential to be functionalised for data storage [1], high-frequency broadband signal generation [2], and skyrmionic [3] devices. One such system is an exchange spring comprising two films with mutually orthogonal anisotropy axes, where the coercivity of the hard layer is reduced by its exchange coupling to the soft layer; this is the exchange spring mechanism. Here we present temperature- and applied field-dependent polarised neutron reflectometry (PNR) data on an exchange spring comprising an FePt layer with perpendicular magnetic anisotropy (PMA) and an in-plane FeRh layer. The antiferromagnetic to ferromagnetic phase transition in FeRh enables the exchange spring to be activated at ~80 °C, providing a promising route towards heat assisted magnetic recording (HAMR) with reduced operational temperatures.

By fitting simulated spin-resolved neutron reflectivity profiles to the measured PNR data, we determine the form of the magnetic scattering length densities (mSLDs), which are interpreted in terms of the competition between anisotropy, exchange coupling, and dipolar coupling as the magnetic phase transition progresses. The PNR data are combined with magnetometry and X-ray characterisation, allowing us to determine characteristic length scales over which the exchange spring mechanism is effective at ambient and elevated temperatures (Fig. 1).

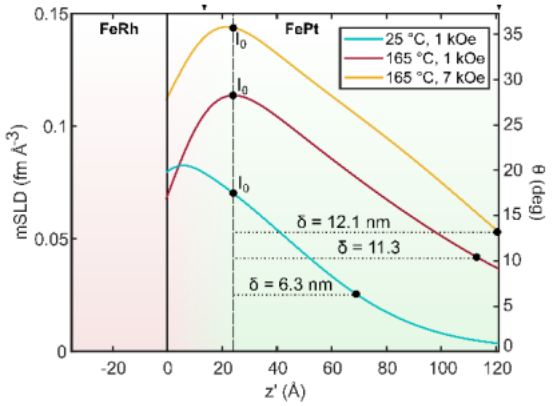

Fig. 1: The evolution of the mSLD through the depth of the FePt layer. The lengths δ characterise distance over which the mSLD decays, and hence the distance over which the FePt spins are reorientated. The right axis allows the data to be interpreted in terms of the spin angle to the easy axis.

[1] J.–U. Thiele, S. Maat, and E. E. Fullerton, Appl. Phys. Lett. 82, 2859 (2003)
[2] T. Seifert et al., Nat. Photonics 10, 483 (2016)
[3] A. Fert et al. Nature Rev. Materials 2, 17031 (2017)

Imprinting magnetic micropatterns through geometrical transformation

Volker Neu[1], Ivan Soldatov[2,3], Rudolf Schäfer[2,4], Dmitriy D Karnaushenko[1], Alaleh Mirhajivarzaneh[1], Daniil Karnaushenko[1], Oliver G. Schmidt1,5,6,7

1 Institute for Integrative Nanosciences, Germany. 2 Institute for Metallic Materials, Leibniz IFW Dresden, Germany. 3 Institute of Natural Sciences and Mathematic, Ural Federal University, Russia 4 Institute for Materials Science, TU Dresden, Germany 5 Material Systems for Nanoelectronics, TU Chemnitz, Germany. 6 Research Center for Materials, Architectures and Integration of Nanomembranes (MAIN), TU Chemnitz, Germany. 7 Nanophysics, Faculty of Physics, TU Dresden, Germany

The functionality of a ferroic device is intimately coupled to the configuration of domains, domain boundaries and the possibility for tailoring them [1,2]. We developed a novel approach which allows the creation of new, metastable multidomain patterns with tailored wall configurations through a self-assembled geometrical transformation [3]. The central idea is to bring the 2D layer architecture into an intermediate rolled up 3D tube state with multiple windings in which a simple homogeneous field magnetizes the structure. After unrolling, a multi-domain configuration is achieved (Fig. 1a).

To realize the above idea, the magnetic layer is prepared on a so-called polymeric platform (PP), which consists of sacrificial layer, hydrogel as a swelling layer and a stiff polyimide layer. It allows a self-assembled, repeatable geometrical transition in aqueous solution by simple control of the pH-value [4]. Figure 1b displays a [Co/Pt]5 multilayer sample with perpendicular magnetic anisotropy rolled into a 90 µm diameter tube. After saturation and partial magnetization reversal in a homogeneous field, a regular stripe pattern is imprinted (Fig. 1c). The field history leads to two basic outof-plane domains per winding after saturation, in which oppositely magnetized domains are additionally imprinted during the partial reversal. The positions of the inner domain transitions (Fig. 1d) encode the angle dependent switching for the given reversal field.

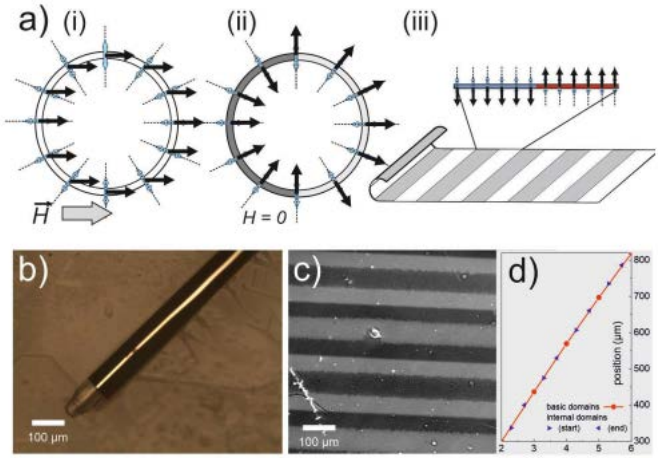

Fig. 1: Imprinting magnetic textures. (a) (i) rolled film with perpendicular magnetic anisotropy exposed to a magnetic field perpendicular to the tube, and (ii) after relaxing into the remanent state; (iii) after unwinding, a bipolar magnetic texture is imprinted. (b) [Co/Pt] on PP in rolled state. (c) Magnetic texture after unwinding (Kerr observation). (d) Analysis of domain coordination.

The process is linked to the employed magnetic anisotropy with respect to the surface normal, and the geometrical transformation connects the angular with the lateral degrees of freedom. This combination offers unparalleled possibilities for designing new magnetic or other ferroic micropatterns.

[1] A. Sarella, A. Torti, M. Donolato, M. Pancaldi, P. Vavassori, Adv. Mater. 26, 2384 (2014).
[2] K. Wagner, A. Kákay, K. Schultheiss, A. Henschke, T. Sebastian and H. Schultheiss, Nat. Nanotechnol. 11, 432 (2016).
[3] V. Neu, I. Soldatov, R. Schäfer, D.D. Karnaushenko, A. Mirhajivarzaneh, D. Karnaushenko, O.G. Schmidt, Nano Letters 21, 9889 (2021).
[4] D. Karnaushenko, N. Münzenrieder, D.D. Karnaushenko, B. Koch, A.K. Meyer, S. Baunack, L. Petti, G. Tröster, D. Makarov, and O.G. Schmidt. Adv. Matter. 27, 6797 (2015).

Microstate control via direct writing of vortices in an Artificial Spin-Vortex Ice

Holly H Holder[1], Jack C Gartside[1], Kilian D Stenning[1], Alex Vanstone[1], Troy Dion[1,2], Daan M Arroo[1,2], Francesco Caravelli[3], Hidekazu Kurebayashi[2], and Will R Branford[1,4]

[1]Blackett Laboratory, Imperial College London, UK, [2]London Centre for Nanotechnology, University College London, UK, [3]Theoretical Division (T4), Los Alamos National Laboratory, USA, [4]London Centre for Nanotechnology, UK

Traditional artificial spin ices employ macrospin-like nanoislands, with bar geometries designed to strongly favour an Ising macrospin formation [1]. Nanoislands can also support magnetic vortex states [2], with little research into bistable systems capable of supporting both textures.

We have created an Artificial Spin-Vortex Ice ('ASVI'), a novel bi-textural system, in which the energetic equivalence of Ising and vortex states within a single bar allows easy access to both textures, providing unique system control. This strongly-interacting spin-ice system can be trained via application of a global minor magnetic field loops, inducing a certain percentage of macrospins to become vortices [3]. Vortex-state islands are seen to induce fascinating changes to local magnetic switching and dynamics.

In addition to global-field creation of vortices, we demonstrate the local writing of vortices to any desired nanoisland using a Magnetic Force Microscope (MFM) tip [4]. This local control (Fig I.) allows powerful modification of the microstate and dipolar-field landscape of the system, leading to complex emergent phenomena. Results include strong, targeted modification of local coercive fields and physical system memory of tip-written state.

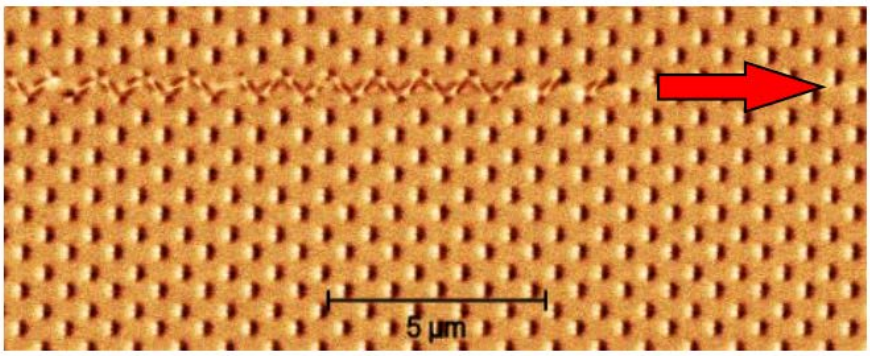

Fig. 1: MFM image of ASVI with bar lengths 600nm, thickness 20nm, widths 200nm (wide bar) and 125nm (thin bar). Vortices have been induced in a horizontal row of wide-bars via 'tip-writing' with a high-moment tip (direction of tip-writing indicated by red arrow).

[1] R. Wang, C. Nisoli, R. Freitas et al., "Artificial 'spin ice' in a geometrically frustrated lattice of nanoscale ferromagnetic islands", Nature 446, 102 (2007).
[2] T. Shinjo et al., "Magnetic Vortex Core Observation in Circular Dots of Permalloy", Science 289, 930 (2000).
[3] J. C. Gartside et al., "Reconfigurable Training and Reservoir Computing via Spin-Wave Fingerprinting in an Artificial Spin-Vortex Ice", arXiv preprint, arXiv:2107.08941.
[4] J. C. Gartside et al., "A novel method for the injection and manipulation of magnetic charge states in nanostructures", Scientific Reports 6, 32864 (2016)

Structural, chemical, and magnetic investigation of a graphene/cobalt/platinum multilayer system on silicon carbide

Philipp Weinert[1], Lukas Kesper[1], Julian Hochhaus[1], Robert Appel[1], Sergio Valencia Molina[2], Florian Kronast[2], Richard Hönig[1], Ulf Berges[1], Carsten Westphal[1]

[1]Fakultät Physik/DELTA, TU Dortmund University, Germany, [2]Helmholtz-Zentrum Berlin für Materialien und Energie GmbH, Germany

Graphene-ferromagnet interfaces like g/Co are characterized by several remarkable properties, for example enhanced perpendicular magnetic anisotropy (PMA) in the ferromagnet [1]-[3]. Another well-known way to induce PMA in Co is combining it with a high-Z non-magnetic metal such as Pt [4]. For these reasons, the combined g/Co/Pt multilayer system is highly promising in the field of graphene spintronics. In this work we investigated the structural, chemical, and magnetic properties of a g/Co/Pt multilayer system on silicon carbide (SiC) by means of low-energy electron diffraction (LEED), x-ray photoelectron spectroscopy (XPS), and x-ray photoemission electron microscopy (XPEEM) in combination with the x-ray magnetic circular dichroism (XMCD) effect.

Graphene has been prepared on SiC using the confinement controlled sublimation. Subsequently, Pt and afterwards Co was intercalated to prepare the g/Co/Pt multilayer system. After each of these steps, LEED, XPS, and ARXPS measurements have been taken. LEED revealed that Pt reconstructs in a $(4\sqrt{3} \times 4\sqrt{3})$-R30° pattern and Co in the well-known (1 × 1)-R30° pattern [3]. The XPS spectra show the formation of three types of Pt silicides as sell as the desired absence of Co silicides. ARXPS was used to prove the Co intercalation. The Co-layer of the resulting system has been analysed using XPEEM. This way the structure of domains with in-plane and out-of-plane magnetization was analysed. Figure 1 shows two of the corresponding images (Film thicknesses: T_{Co} = 2.6 nm, T_{Pt} = 0.8 nm). Two kinds of domains with different magnetic structures and different PMA strength are identified (Figure 1(a): bright and dark area). Using these

results, even larger domains with a strong PMA may be prepared and can be used in future spintronic devices.

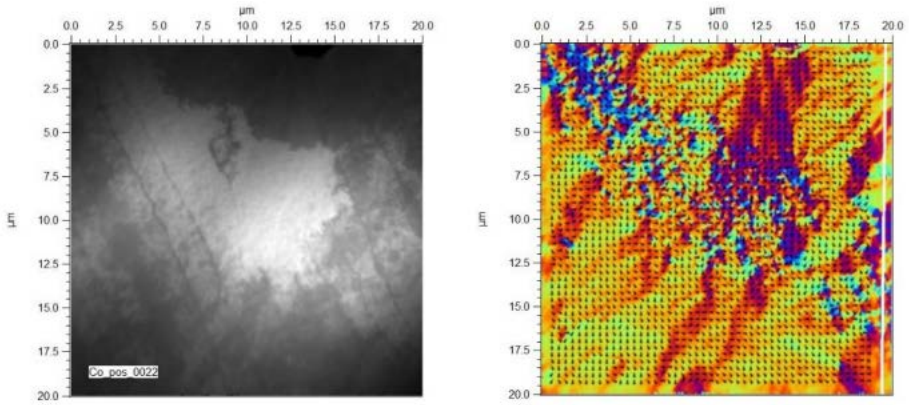

Fig. 1: XPEEM images of a g/Co/Pt multilayer system on SiC recorded at the Co L3-edge with chemical contrast (a) and contrast of the in-plane magnetization (b). Magnetization direction is indicated by colour and black arrows.

[1] Ajejas, F. et al 2018 Nano Lett. 18 5364−5372
[2] Ajejas, F. et al 2020 Interfaces ACS Appl. Mater. Inter. 12 4088−4096
[3] Hönig, R. et al 2019 Nanotechnology 30 025702 [4] Carcia, P. F. 1988 J. Appl. Phys. 63 5066

Spintronics 1

(Invited) Ferromagnetic Josephson junctions for cryogenic memory

Nathan Satchell

School of Physics and Astronomy, University of Leeds, UK

The dissipation of heat in traditional silicon (CMOS) based electronics is a major source of inefficiency and environmental impact. Superconductors are, by nature, dissipationless. Traditionally considered competing phenomena, when artificially juxtaposed a wealth of new physics at the interface between superconductors and ferromagnets emerges [1]. By combining ferromagnetism with the dissipationless property of superconductivity, superconducting spintronic memory and logic devices have potential to be both fast and highly energy efficient [2].

Here, I will present our recent results combining superconducting circuits with magnetic memory elements, such as spin-valves [3],[4]. Fig. 1 shows a pseudospin-valve Josephson junction where the information is encoded into the magnetic state of the device, but read-out is achieved by the superconducting elements of the circuit for maximum energy efficiency and compatibility with the rest of the computer. In the device, shown schematically in Fig. 1 (a), the magnetic Co and CoB layers have perpendicular magnetic anisotropy and independent switching fields, allowing the device to be configured into parallel and antiparallel magnetic configurations. By tuning the magnetic configuration, we measure in Fig. 1 (b) a difference in critical supercurrent in the device of 60%.

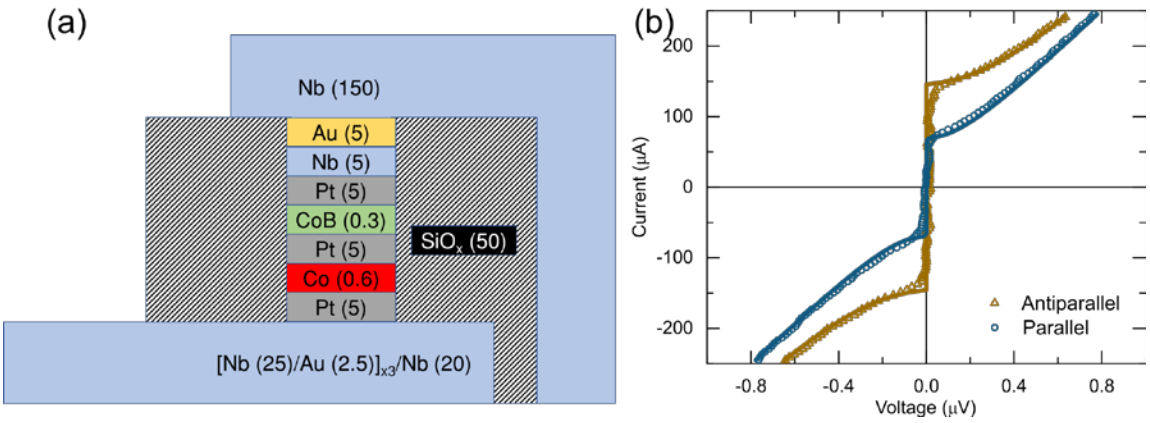

Fig. 1: (a) Schematic cross section of the pseudospin-valve Josephson junction device with layer thickness in (nm). (b) Current-voltage characteristic of the device measured at 0 applied field at 1.5 K. A difference in critical current of 60% can be achieved by tuning between parallel or antiparallel magnetic configuration. Adapted from [3].

Acknowledgement(s): This work is supported by EPSRC grant no. EP/V028138/1. This project received funding from the European Union Horizon 2020 research and innovation programme under the Marie Skłodowska-Curie Grant Agreement No. 743791 (SUPERSPIN).

Reference(s):

[1] J. Linder, and J.W.A. Robinson Nat. Phys. 11 (4), 307-315 (2015)
[2] N. Satchell Supercond. Sci. Technol. 32 2 020501 (2019).
[3] N. Satchell, et al. Appl. Phys. Lett. 116, 022601 (2020)
[4] N. Satchell, et al. Sci. Rep. 11, 11173 (2021)

Spintronic terahertz emitters exploiting uniaxial magnetic anisotropy for field-free emission and polarisation control

S M Hewett[1,2], C Bull[1,2], C-H Lin[1,2], A M Shorrock[2,3], R Ji[1,2], M T Hibberd[2,3], T Thomson[1], P W Nutter[1], and D M Graham[2,3]

[1]Nano Engineering and Spintronic Technologies Group, Dept. of Comp. Science, University of Manchester, UK, [2]Department of Physics & Astronomy & Photon Science Institute, University of Manchester, UK, [3]The Cockcroft Institute, Sci-Tech Daresbury, Keckwick Lane, UK

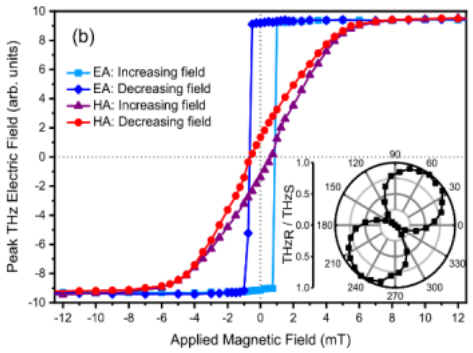

Fig. 1: E_{THz} for a CoFeB (2.5 nm)/Pt (3 nm) bilayer as a function of H_{app}, with M aligned parallel to its easy axis (EA) or hard axis (HA).

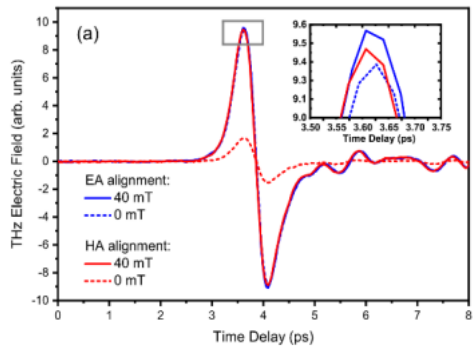

Fig. 2: Terahertz waveforms measured for EA and HA alignment of H_{app}, showing E_{THz} for $H_{app} > M_s$ and for $H_{app} = 0$.

The useful ability to generate and control pulses of broadband terahertz (THz) radiation has mediated the advance of non-invasive, investigative technologies used for material characterisation, medical diagnosis and weapon detection [1-2]. With further research, pulses of THz radiation have future application in the ultrafast control of electron spin states [3] and picosecond magnetisation switching in ferrimagnets and antiferromagnets [4]. To exploit the full potential of THz radiation, emitters are required that can generate a THz electric field of high amplitude, E_{THz}, with a broad spectral bandwidth and gapless coverage over the full THz spectral region (1-10 THz) [5]. Simple spintronic emitters consisting of ferromagnetic (FM)/nonmagnetic (NM) thin films, such as CoFeB/Pt, satisfy these requirements, producing strong THz pulses (E_{THz} < 300 kV/cm [6]) with gapless bandwidths of up to 30 THz [6] when excited by femtosecond laser pulses. In particular, E_{THz} has been shown to scale with laser fluence and the magnetic moment of the FM layer, M, to which the THz pulses are perpendicularly polarised [5]. This offers the possibility to create devices in which the THz amplitude and polarisation can be controlled, at source, through magnetic manipulation.

While many spintronic THz emission schemes utilise saturating fields, H_{app}, to maximise M, and hence E_{THz}, recent work on field shaping schemes [7-9] results in regions across the FM layer where M < Ms, and the emitted THz pulse profile is influenced by the remanent magnetisation, Mr, of the FM layer. We have investigated the THz emission characteristics of Co20Fe60B20 (2.5 nm)/Pt (3 nm) bilayer structures in this below magnetic saturation regime and reveal orientation dependence in the emission behaviour, arising from in-plane uniaxial magnetic anisotropy (UMA) of the CoFeB FM layer. By maximizing the UMA through manipulation of sputter deposition conditions and aligning the external applied field, H_{app}, with the easy axis, E_{THz} is found to reach saturation under weaker applied fields (Fig. 1). In addition, E_{THz} is seen to remain at saturation when H_{app} is removed (Fig. 2), effectively providing an emitter that requires no external magnetic field to drive emission. The development of spintronic structures that can emit broadband THz pulses without the need for an applied field is beneficial to THz spectroscopy, and facilitates the production of largearea spintronic emitters, overcoming one of the key challenges of such emitters compared to well-established sources of THz radiation [5]. Furthermore, by aligning H_{app} along the hard axis we observe a 90^0 rotation of the THz pulse polarisation as H_{app} is reduced to zero. Manipulating H_{app} therefore allows polarisation control of E_{THz}, without the need for mechanical rotation of external magnets.

[1] Woodward et al., J. Biol. Phys. 29, 257, 2003;
[2] Kawase et al., Opt. Express 11, 2549, 2003;
[3] Baierl et al., Nat. Photonics 10, 715, 2016;
[4] Wienholdt et al., PRL 108, 247207, 2012;
[5] Bull et al., APL Mater. 9, 090701, 2021;
[6] Seifert et al., Nat. Photonics 10, 483, 2016; [7] Hibberd et al., APL 114, 031101, 2019;
[8] Niwa et al., Opt. Express 29, 13331, 2021;
[9] Kong et al., Adv. Opt. Mater. 7, 1900487, 2019.

The role of proximity induced magnetism on spin transport in multilayered systems

C Swindells[1] , H Głowiński[2] , Y Choi[3], D Haskel[3], P P Michałowski[4] , T Hase[5], F Stobiecki[2], P Kuświk[2], and D Atkinson[6]

[1]University of Sheffield, UK, [2]Institute of Molecular Physics, Polish Academy of Sciences, Poland, [3]Argonne National Laboratory, USA, [4]Lukasiewicz Research Network, Warsaw, Poland, [5]University of Warwick, UK, [6]Durham University, UK

Spin transport across interfaces is fundamental to many spintronic devices. To fully exploit interfacial phenomena, such as spin-orbit torques and spin-pumping, in ferromagnetic (FM) and heavy metal systems (HM) the properties of both the HM layer and the interface must be considered, particularly in the case of perpendicularly magnetised systems [1]. Previously we showed the evolution of spin transport as a function of FM and HM thicknesses [2] and the role of insulating layers [3]. Debate remains regarding the physical basis of interfacial spin transport and the role of proximity polarisation of the HM layer [4]. A notional 'spin memory loss' term is often used to represent an interfacial contribution, while for Pt in particular, a magnetic polarisation arises in proximity (PIM) to a ferromagnetic material, opens a question about the role that PIM has upon interfacial spin phenomena, with contradictory reports that it has either a profound effect [5] or no effect [6] on spin transport.

Here we present the results of a published study [7], providing a detailed investigation into systematic spin transport and PIM in the same FM/HM samples. Structures with either a constant Pt thickness and a spacer layer thickness wedge, or a constant spacer layer and a Pt wedge were deposited. A combination of dynamic and static magnetic measurements, along with element specific resonant x-ray measurements at the APS, Argonne Lab, were used to address both the interfacial scattering contribution and the role of PIM in Pt on spin transport and to determine their relative contributions. Figs. 1 and 2 show damping and PIM data, with a persisting Pt moment with a 3nm Au layer, and a clear trend observed between the PIM and dynamic behaviour. These results highlight the role of the d-d orbital hybridisation and the induced moment for efficient interfacial transport, which is key for many spintronic applications.

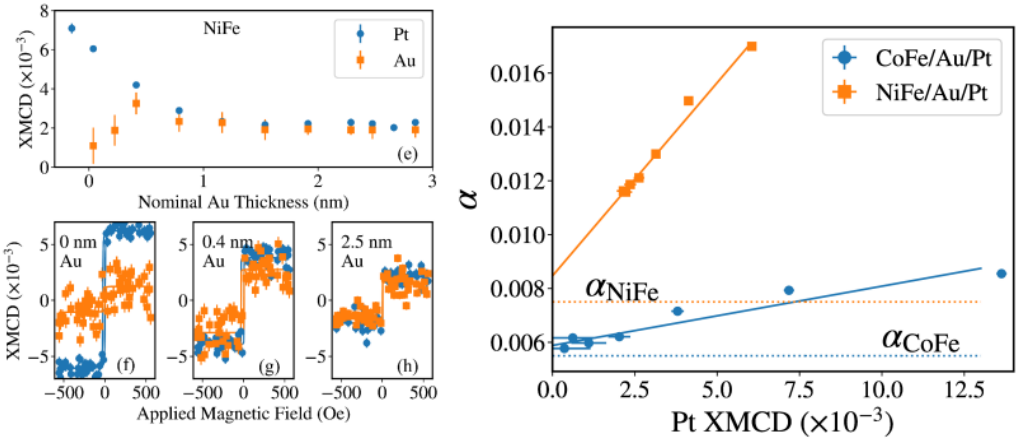

Figures: Left: Measured XMCD as a function of Au spacer thickness at both the Pt (blue) and Au (orange) L3 edges for NiFe (7 nm)/ Au / Pt (4 nm). Right: Damping and Pt XMCD for CoFe/Au/Pt and NiFe/Au/Pt. Dotted lines indicate bulk damping contributions from the ferromagnetic layer.

[1] P. Kuświk, H. Głowiński et al., J. Phys.: Condens. Matter 29 (2017)
[2] C. Swindells, A. Hindmarch, A. Gallant and D. Atkinson, Phys. Rev. B, 99, 064406 (2019)
[3] C. Swindells, A. Hindmarch, A. Gallant and D. Atkinson, Appl. Phys. Lett. 116 (2020)
[4] R. Rowan-Robinson et al., Sci. Rep. 7 16835 (2017)
[5] M. Caminale, et al., Phys. Rev. B, 94 014414 (2016)
[6] L. J. Zhu, D. C. Ralph, and R. A. Buhrman, Phys. Rev. B, 98, 164406 (2018) [7] C Swindells et al., Appl. Phys. Lett. 119, 152401 (2021)

Voltage-Controlled Skyrmionic Interconnect with Multiple Magnetic Quasiparticles

Runze Chen, Will Griggs, Yu Li, Vasilis F Pavlidis, and Christoforos Moutafis

The University of Manchester, UK

Skyrmionic devices show potential for future nanocomputing with information encoded by quasi-particles with a topological charge N, including skyrmions ($N = -1$) [1], skyrmioniums ($N = 0$) [2], and anti-skyrmionites (i.e., a double-antiskyrmion-skyrmion pair with $N = +1$) [3]. This is increasingly relevant since high-degree skyrmionic configurations have been experimentally demonstrated in liquid crystals [4] and chiral magnets [5]. Hitherto, skyrmionic non-volatile memory, neuromorphic, and nanocomputing devices have been investigated [6]. However, the efficient transmission of information with spintronic devices, e.g., spintronic interconnect devices and multiplexers, has not received as much attention. In our previous work, a notch-based skyrmionics interconnect device was proposed numerically [24]. The device performs topological filtering that enables information signal multiplexing utillising sequences of magnetic skyrmions and skyrmioniums. However, such a design would be challenged by pinning and annihilation issues at notches and edges. To address such concerns, we propose a more realistic and robust spintronic interconnect design that should also exhibit enhanced effective tunability.

In this work, we propose a skyrmionic interconnect device where multiple information signals are encoded and transmitted simultaneously by skyrmions, skyrmioniums, and anti-skyrmionites. The skyrmionic interconnect device can be pipelined via voltage-controlled-magnetic-anisotropy (VCMA) gated synchronizers that behave as intermediate registers along the pipelined interconnect. We demonstrate theoretically that the interconnect throughput and transmission energy can be effectively tuned by the gate voltage and electric current pulses. By carefully adjusting the device structure characteristics, we find that the proposed interconnect may achieve comparable energy efficiency with copper interconnects in CMOS technologies. This study provides fresh insight into the possibilities of skyrmionic devices in future spintronic applications.

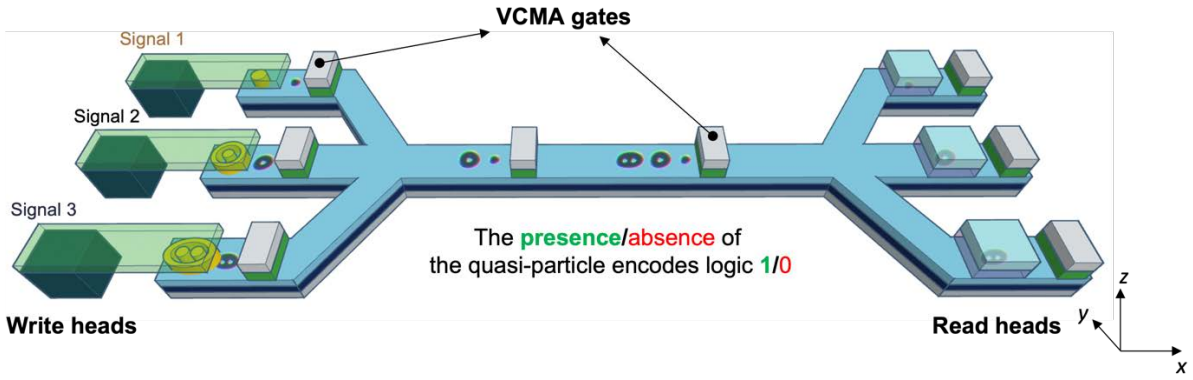

Fig. 1: Schematic drawing of the proposed VCMA skyrmionic interconnect. The proposed device comprises STT nucleation heads, VCMA-controlled gates, nano racetrack, and MTJ-based read heads.

[1] A. Fert, N. Reyren, and V. Cros, Nat. Rev. Mater. 2, 17031 (2017).
[2] B. Göbel, A. F. Schäffer, J. Berakdar, et al., Sci. Rep. 9, 12119 (2019).
[3] R. Chen, Y. Li, V. F. Pavlidis, and C. Moutafis, Phys. Rev. Res. 2, 1 (2020).
[4] D. Foster, C. Kind, P. J. Ackerman, et al., Nat. Phys. 15, 655 (2019).
[5] J. Tang, Y. Wu, W. Wang, et al., Nat. Nanotechnol. (2021).
[6] C. Back, V. Cros, H. Ebert, et al., J. Phys. D. Appl. Phys. 53, 363001 (2020).

Plenary Lecture

(Plenary) Fully-nano spintronic neural networks with radio-frequency connections

Nathan Leroux[1], Andrew Ross, Danijela Markovic[1], Dedalo Sanz-Hernandez[1], Andrew Ross[1], Juan Trastoy[1], Paolo Bortolotti[1], D. Querlioz[2], Leandro Martins[3], Alex Jenkins[4], Ricardo Ferreira[3], Alice Mizrahi[1] and Julie Grollier[1]

[1]Unité Mixte de Physique CNRS/Thales, CNRS, Université Paris Saclay, France, [2]Université Paris-Saclay, CNRS, Centre de Nanosciences et de Nanotechnologies, France, [3]International Iberian Nanotechnology Laboratory (INL), Portugal

Neuromorphic computing takes inspiration from the architecture of the brain to build miniaturized, ultra-low power hardware for artificial intelligence. In recent years, nanoscale devices that perform key functions of neurons (nonlinear activation) [and synapses (weighted sum) have been realized, with a special focus on memristive stacks. However, such nanoscale neurons and synapses are typically made from different materials, with different circuitry, making it difficult to stack them into deep networks that can perform complex classifications. Here we overcome this challenge by leveraging the multifunctionality of spintronics and show how to use the same magnetic tunnel junctions to mimic neurons and synapses, and connect them in multilayer neural networks through the radio frequency (RF) signals that these devices can transmit as well as filter and rectify in a wide frequency band (10 MHz - 60 GHz). We experimentally demonstrate direct communication between spintronic neurons and spintronic synapses. We assemble a fully nanoscale RF spintronic neural network with a hidden layer, composed of nine magnetic tunnel junctions, and show that it natively classifies RF signals with high accuracy. We demonstrate through physics-based simulations the ability of a scaled up system to classify real-world RF signals.

High Frequency Spin Dynamics

(Invited) Spin transport in a conventional superconductor

Chiara Ciccarelli

University of Cambridge, UK

I will give an overview of our work in collaboration with the Department of Materials Science and Metallurgy in Cambridge [1-5] on the spin pumping into a Nb thin film. Unlike conventional spin-singlet Cooper pairs, spin-triplet pairs can carry spin. Triplet supercurrents were discovered in Josephson junctions with metallic ferromagnet spacers, where spin transport can occur only within the ferromagnet and in conjunction with a charge current. Ferromagnetic resonance injects a pure spin current from a precessing ferromagnet into adjacent non-magnetic materials. For spin-singlet pairing, the ferromagnetic resonance spin pumping efficiency decreases below the critical temperature (Tc) of a coupled superconductor. Here we present ferromagnetic resonance experiments in which spin sink layers with strong spin–orbit coupling are added to the superconductor. We show that the induced spin currents, rather than being suppressed, are substantially larger in the superconducting state compared with the normal state and show that this cannot be mediated by quasiparticles and is most likely a triplet pure spin supercurrent. By carrying angular dependence studies of the Gilbert damping we are able to link the generation of a triplet condensate with the Rashba spin-orbit coupling.

[1] Nature Materials 17, 499 (2018)
[2] Phys. Rev. Appl., 11, 014061 (2019)
[3] Phys. Rev. B 99, 024507 (2019)
[4] Phys. Rev. X 10, 031020 (2020)
[5] Phys. Rev. B 99, 144503 (2019

Control of spin wave propagation in YIG by overlaying chiral magnonic resonators

Y Au, K G Fripp, A V Shytov and V V Kruglyak

University of Exeter, Stocker Road, UK

The discovery of switchable resonant scattering of spin waves (SWs) by chiral nanomagnet resonators a decade ago[1] is predicted to have important applications in magnonics. 1,2 However, the applications can be hindered by SW damping in the metallic ferromagnet-based magnonic medium assumed in the original proposal.[1] The recent advent of nanometres-thick patternable low-damping YIG films and the discovery of the same effect based on the resonator's dark modes 3 brings revival to this subject. The ideas are becoming particularly important in the recent rapid development of magnonics for application in neuromorphic computing, since the unique capability of chiral resonant scattering (CRS) to manipulate magnitude and phase of SWs could be used to design complex patterns of interference required by neural networks. Also, preliminary results predict that CRS demonstrates non-linear behaviour, an indispensable ingredient in neuromorphic applications. Here, we present results of application of the CRS concept to SWs propagating in YIG films / waveguides and scattered by overlaid ferromagnetic stripes / nanomagnets. Exemplary simulated data for the case of SWs propagating in a thin YIG film in the backward volume geometry is provided below (Fig. 1). The results confirm the CRS feasibility when using nanometre thick YIG films as the medium. The performance and merits of CRS will be compared to other SW manipulation mechanisms exploited in the magnonic community. The research leading to these results has received funding from the EPRSC of the UK

(Projects EP/L019876/1 and EP/T016574/1).

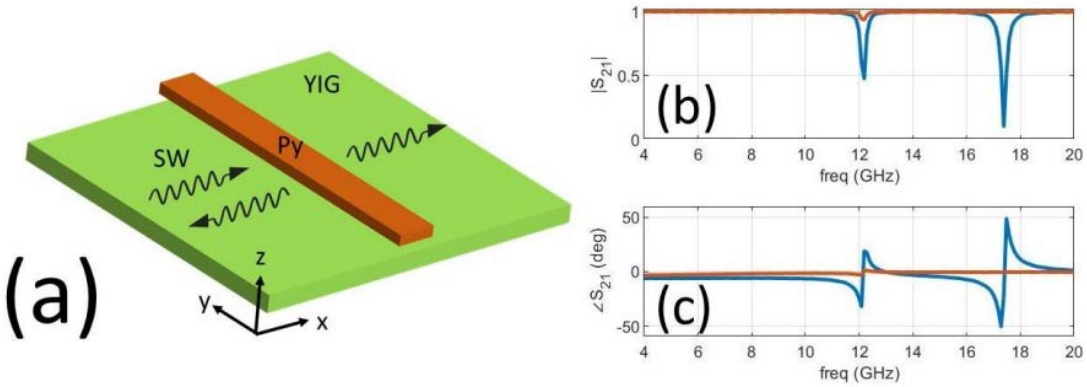

Fig. 1: (a) A 50 nm wide and infinitely long permalloy (Py) stripe is placed above a continuous film of YIG with a vertical spacing equal 5 nm between them. The thickness of the Py stripe and the YIG film are 15 and 20 nm respectively. A broadband Gaussian packet of spin waves (SWs) propagates toward +x direction. The transmission and reflection of this SW packet are recorded and Fourier transformed into frequency domain. (b) Simulated SW transmission magnitude and (c) phase for the case of the Py magnetization pointing towards -y (blue curve) and +y direction (brown curve). A 50 Oe bias field is applied in the +x direction, which also orients the YIG film magnetization in the same way.

[1] "Nanoscale spin wave valve and phase shifter", Y. Au, M. Dvornik, O. Dmytriiev, and V. V. Kruglyak, Appl. Phys. Lett. 100, 172408 (2012).
[2] "Chiral magnonic resonators: Rediscovering the basic magnetic chirality in magnonics", V. V. Kruglyak, Appl. Phys. Lett. 119, 200502 (2021).
[3] "Spin-wave control using dark modes in chiral magnonic resonators", K. G. Fripp, A. V. Shytov and V. V. Kruglyak, Phys. Rev. B 104, 054437 (2021).

Timescales and contribution of heating and helicity effect in helicity-dependent all-optical switching

Guanqi Li[1,2], Xiangyu Zheng[1,2], Junlin Wang[1,2], Xianyang Lu[2], Jing Wu[1, 2], Jianwang Cai[3], Thomas A. Ostler[4], and Yongbing Xu[2, 5,]

[1]Department of Physics, University of York, UK [2]York-Nanjing International Joint Center in Spintronics, School of Electronic Science and Engineering, Nanjing University, China [3]Institute of Physics, Chinese Academy of Sciences, China [4]College of Business, Technology and Engineering, Sheffield Hallam University, UK [5]Spintronics and Nanodevice Laboratory, Department of Electronics Engineering, University of York, UK

The heating and helicity effects induced by circularly polarized laser excitation are entangled in the helicity-dependent all-optical switching (HD-AOS), which hinders the understanding of magnetization dynamics involved. Here, by applying a dual-pump laser excitation, first with a linearly polarized (LP) laser pulse followed by a circularly polarized (CP) laser pulse, we identify the timescales and contribution from heating and helicity effects in HD-AOS with a Pt /Co /Pt triple layer. When the sample is preheated by the LP laser pulses to a nearly fully demagnetized state, CP laser pulses with a much-reduced power switches the sample's magnetization. By varying the time delay between the two pump pulses, we show that the helicity effect, which gives rise to the deterministic helicity-induced switching, arises almost instantly upon laser excitation, and exists for less than 0.2 ps close to the laser pulse duration of 0.15 ps. The results reveal that the transient magnetization state upon which CP laser pulses impinge is the key factor for achieving HD-AOS, and importantly, the tunability between heating and helicity effects with the unique dual-pump laser

excitation approach will enable HD-AOS in a wide range of magnetic material systems having wide raging implications for potential ultrafast spintronics application.

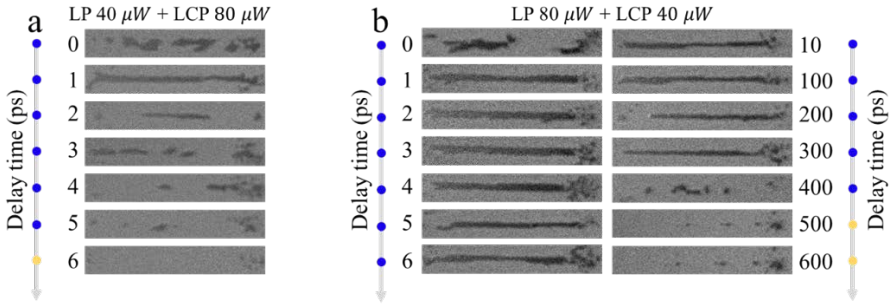

Fig. 3: HD-AOS in a Pt/Co/Pt triple layer induced by dual-pump as a function of time interval between two pulses. The first pulse is LP and the second is CP. The two panels show MOKE images of magnetic domains induced under two different combinations of LP and CP powers (a) LP 40 μW + CP 80 μW and (b) LP 80 μW + CP 40 μW under the same total power of 120 μW. The number next to each image indicates the delay time.

Reservoir Computing with an Artificial Spin-Vortex Ice

Jack C Gartside[1], Kilian D Stenning[1], Alex Vanstone[1], Troy Dion[1,2,3], Holly H Holder[1], Francesco Caravelli[4], Daan M Arroo[1], Hidekazu Kurebayashi[2], and Will R Branford[1]

[1]Imperial College UK, [2]University College, UK, [3]Kyushu University, Japan, [4]Los Alamos National Lab, USA

Strongly-interacting artificial spin systems are moving beyond mimicking naturally-occurring materials to emerge as versatile functional platforms, from reconfigurable magnonics to neuromorphic computing. Typically, artificial spin systems comprise nanomagnets with a single magnetisation texture: collinear macrospins or chiral vortices. By tuning nanoarray dimensions we achieve macrospin/vortex bistability and demonstrate a four-state metamaterial spin-system 'Artificial Spin-Vortex Ice' (ASVI). ASVI is capable of adopting Ising-like macrospins with strong ice-like vertex interactions, and weakly-coupled vortices with low stray dipolar-field. Vortices and macrospins exhibit starkly-differing spin-wave spectra with analogue-style mode-amplitude control and mode-frequency shifts of df = 3.8 GHz.

The enhanced bi-textural microstate space gives rise to emergent physical memory phenomena, with ratchet-like vortex training and history-dependent nonlinear 'echo state' training trajectories. We employ spin-wave microstate fingerprinting for rapid, scaleable readout of vortex and macrospin populations and leverage this for spin-wave reservoir computation. ASVI performs linear and non-linear mapping transformations of diverse input signals as well as chaotic time-series forecasting. Energy costs of machine learning are spiralling unsustainably, developing low-energy neuromorphic computation hardware such as ASVI is crucial to achieving a zero-carbon computational future.

Optical generation and detection of coherent propagating magnons in an antiferromagnet

R V Mikhaylovskiy[1], R Leenders[1], J Hortensius[2] , and D Afanasiev[3]

[1]Lancaster University, UK, [2]Kavli Institute of Nanoscience, Delft Technological University, The Netherlands, [3]Institute for Molecules and Materials, Radboud University, The Netherlands

Magnons, also called spin waves, are the most promising candidates for wave-based logic devices. Experiments using magnons in conventional (ferro)magnets have shown that it is possible to build small logic devices without using electrical currents and thus avoid Joule heating. In recent years, there has been a focus shift towards the use of antiferromagnets, materials with antiparallel spin alignment. Antiferromagnets allow significantly higher spin-wave propagation velocities and the possibility of terahertz operational clock-rates. However, the generation of short-wavelength coherent propagating magnons in antiferromagnets has so far remained a major challenge.

Here we report the efficient emission and detection of a nanometer-scale wavepacket of coherent propagating magnons in antiferromagnetic DyFeO3 using ultrashort pulses of light [1]. The subwavelength confinement of the laser field due to large absorption creates a strongly non-uniform spin excitation profile, enabling the propagation of a broadband continuum of coherent THz spin waves (Fig. 1a). The wavepacket features magnons with detected wavelengths down to 125 nm that propagate with supersonic velocities of more than 13 km/s into the material.

We also have derived a model for the optical generation of spin waves in an antiferromagnet. By considering different optical excitation profiles, boundary conditions, and material properties we calculated the magnon waveforms propagating from the excitation spot (Fig.1b). Furthermore, we have derived a formalism for the magneto-optical detection of these spin waves. In reflective pumpprobe geometry we have calculated the magneto-optical Kerr effect and have shown that the spin waves are selectively detected through the arising of the Bragg condition. As a result, we have demonstrated that the detected frequency of the spin waves blue shifts for increasing probe frequency. The results of our model have been confirmed experimentally by scanning over the probe photon energy and variation of the varying the angle of incidence [1].

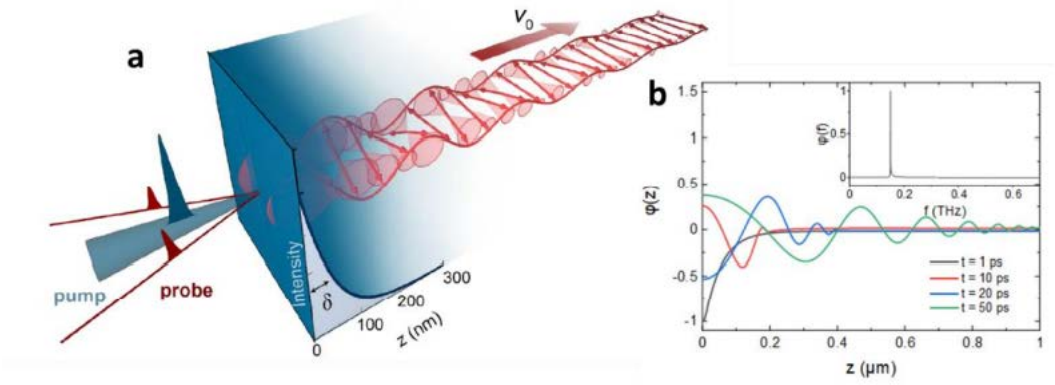

Fig.1: a, Schematic of the generation and detection of antiferromagnetic magnons excited by a strongly absorbed laser pulse. The optical penetration depth δ defines the excited region. b, Snapshots of optically excited magnons. The inset shows the corresponding spectrum at a distance z=0.2 μm.

[1] J. Hortensius, et al. Nature Physics 10, 715 (2021).

Computation and Theory

(Invited) Revealing the ultrafast domain wall motion in Manganese Gold through Permalloy capping

Sarah Jenkins[1], Ricardo Rama-Eiroa[2,3], Rubén M Otxoa[4,2], Roy W Chantrell[5], Karin EverschorSitte[1], and Richard F L Evans[5]

[1]TWIST Group, Institut fur Physik, University of Duisburg-Essen, Duisburg, Germany, [2]Donostia International Physics Center, Spain, [3]Polymers and Advanced Materials Department: Physics, Chemistry, and Technology, University of the Basque Country, Spain, [4]Hitachi Cambridge Laboratory, J. J. Thomson Avenue, UK, [5]Department of Physics, University of York, UK

Antiferromagnetic spintronic devices have the potential to greatly outperform their current ferromagnetic counterparts due to their robustness to external fields, ultrafast dynamics and potential for high data density storage. Mn2Au is one of the most promising materials for antiferromagnetic spintronics due to its ability to generate Néel spin orbit torques (SOTs)[1] meaning the magnetisation can be controlled electrically. However, a read-out of the Néel order parameter is still a challenge. One possibility for detecting the magnetisation of MnAu is by coupling the AFM to a thin FM film[2], giving the advantages of the FM and the AFM.

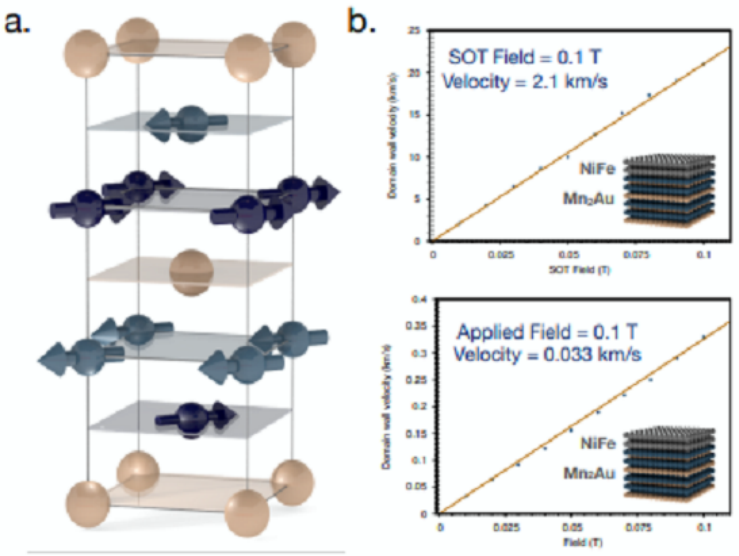

Fig. 1. (a) Magnetic unit cell of Mn2Au. The Mn atoms (atoms with arrows) form two anti-parallel sublattices aligned along the [110] and [-1-10] crystal directions. The gold coloured atoms represent Gold. (b) The domain wall velocities in a coupled MnAu and NiFe bilayer for different applied SOT fields and magnetic fields.

Here we present atomistic spin simulations that allow us to estimate the magnetic properties of Mn2Au [3]. The crystal structure of Mn2Au shows two distinct Mn sites with a 180 degree relative orientation as shown in Fig. 1 (a). Our model provides a critical temperature (Néel) of 1256 K from the ab initio values [4] of the exchange interactions. In Mn2Au due to the presence of four easy directions, the domain wall structures of 90 degrees and 180 degrees are stable. We find a narrow domain wall width of 33.16 +/- 0.085 nm at zero temperature. Coupling the MnAu to a Permalloy bilayer we simulate the coupled dynamics of a 90 degree domain wall percolating the FM/AFM bilayer. We study the domain wall dynamics in two cases, i) under the presence of a current to generate SOTs in the AFM and ii) an applied field to generate motion through the FM. In both cases the coupled domain walls of the FM and the AFM remain coupled together throughout the domain wall motion. For SOTs the domain wall moves with ultrafast dynamics, with a SOT field of 0.1T the

domain wall reaches velocities of ~2.1 km/s. Whereas, when the applied field drives the domain wall motion the FM is driving the dynamics and therefore the velocity is slower ~0.033 km/s for a 0.1T field as shown in Fig. 1 (b). These results pave the way for ultimate control of the AFM with the ability to manipulate the speed of the domain wall by either driving it with the GHz FM motion or THz AFM motion whilst also offering measurability through the coupled FM layer.

[1] J. Železný, H. Gao, K. Výborný, J. Zemen, J. Mašek, A. Manchon, J. Wunderlich, J. Sinova, and T. Jungwirth, Phys. Rev. Lett. 113, 157201 (2014).
[2] S. P. Bommanaboyena et al., Readout of an antiferromagnetic spintronics system by strong exchange coupling of Mn2Au and Permalloy, Nature Communications 12: 6539, 11 November 2021
[3] R. F. L. Evans, et al, J. Phys. Cond. Matter, 26, (2014) [4] A. B. Shick et al. Phys. Rev. B 81, 212409 (2010)

Decreasing the magnetic anisotropy of Fe_3O_4 by Co-doping?

David Serantes[1,2], Daniel Faílde[1,2], Adolfo O Fumega[1,2], Víctor Pardo[1,2], Daniel Baldomir[1,2], Beatriz Pelaz[3], Pablo del Pino[3], and Roy W Chantrell[4]

[1]Applied Physics Department, Universidade de Santiago de Compostela, Spain, [2]Instituto de Materiais (iMATUS), Universidade de Santiago de Compostela, Spain, [3]Centro Singular de Investigación en Química Biolóxica e Materiais Moleculares (CiQUS), Departamento de Física de Partículas, Universidade de Santiago de Compostela, Spain, [4]Department of Physics, University of York, UK

Doping magnetite with Co is usually regarded as an effective method to largely increase its anisotropy constant, K. In the present work we discuss the existence of a region with a decreased K value, at about 4% to 7% Co-doping, where a transition from negative to positive K occurs. Our approach simply assumes that the effective K is directly proportional to the doping fraction, which can have a different magnitude and symmetry than the parent phase. As a representative example, we focus here on the so-called macrospin model (i.e., up to dozens of nm in size, with coherent rotation of the constituent atomic magnetic moments) of $Co_xFe_{3-x}O_4$ ($0<x<1$) magnetic nanoparticles case due to its importance for a variety of applications, ranging from magnetic recording to biomedicine. Remarkably, the predicted unexpected trend is confirmed by *ab initio* electronic structure calculations. The comparison between theoretical and published experimental results is extremely good, thus supporting the assumed approach as suitable to describe such type of magnetic alloys. Lastly, it is worth to mention that while we have focused on Co-doping of magnetite as a significant example for applications, our model and predictions apply could be extended to other types of alloys with anisotropy-type change in the series, and not necessarily on nanosized dimensions.

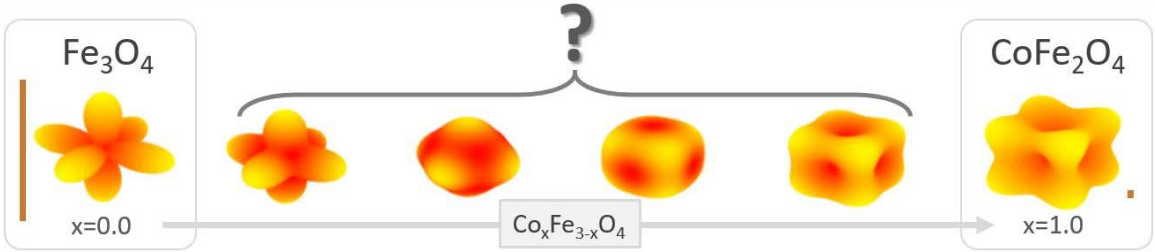

Schematic illustration of the evolution of the effective anisotropy landscape of $Co_xFe_{3-x}O_4$ nanoparticles as a function of the Co-content x. The bars for x = 0 and x = 1 represent the relative magnitudes of the anisotropy in each case.

Quantifying temperature-induced magnetic disorder effects in the anisotropy of MnBi

Christopher E Patrick

University of Oxford, UK

MnBi is remarkable for being a hard magnet, free of rare earths, whose magnetocrystalline anisotropy (MCA) increases with temperature. Starting from an in-plane magnetization at cryogenic temperature, the easy magnetization direction rotates to the uniaxial direction above 140 K and the MCA energy continues to increase until reaching a maximum at approximately 500 K [1]. Density-functional theory calculations (including a Hubbard U correction) have been used to show that this unusual behaviour follows the thermal evolution of the lattice parameters [2], but recent calculations have also found a sizeable contribution to the MCA from the free energy associated with the phonons [3]. On the other hand, a very satisfactory explanation of the temperature dependence can also be provided by the phenomenological Callen-Callen theory [4]. Here, we attempt to reconcile these different viewpoints by performing first-principles density-functional calculations at zero and finite temperature, treating the latter within the disordered local moment picture. In particular, we aim to quantify the contribution of local magnetic moment disorder to the MCA and understand its interplay with the structural and vibrational properties of MnBi.

This work supported by a Royal Society Research Grant, RGS\R1\201151.

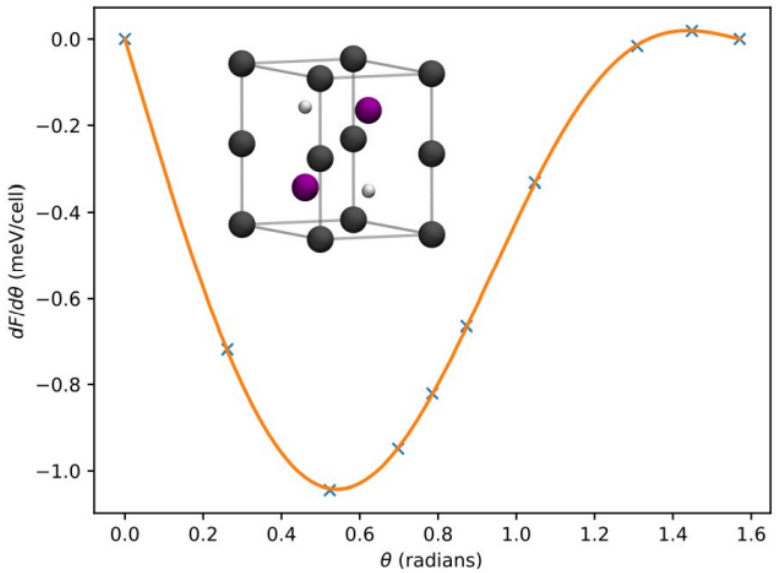

Fig. 1. An example calculation of the torque (rate of change of MCA energy with magnetization direction, shown as crosses), with a phenomenological fit, for MnBi (crystal structure shown as inset)

[1] W. E. Stutius et al., AIP Conf. Proc. 18, 1222 (1974)
[2] V. P. Antropov et al., Phys. Rev. B 90, 054404 (2014)
[3] A. Urru and A. Dal Corso, Phys. Rev. B 102, 115126 (2020)
[4] J. Barker and O. Mryasov, J. Phys. D.: Appl. Phys. 49, 484002 (2016)

Spin transport in easy-axis and easy-plane antiferromagnetic insulator thin films

Verena Brehm, and Alireza Qaiumzadeh

QuSpin, NTNU Trondheim, Norway

Due to their high-frequency excitation spectrum and the absence of stay fields, antiferromagnetic (AFM) insulators are promising candidates for magnonic applications [1].

We model an AFM monolayer inspired by the prominent example α-Fe2O3, commonly known as hematite, that undergoes two phase transitions: For very low temperatures, there is no magnetization as the N´eel vector lies in the plane, which corresponds to an easy-axis anisotropy. At the Morin temperature, the N´eel vector rotates out of plane, leading to a finite magnetization with the system being in an easy-plane phase, until at the N´eel temperature magnetic order is lost. We model the latter phase with an additional small easy-axis anisotropy that lies in the easy plane (biaxial antiferromagnet, see Figure 1 for dispersion relation.

Spin transport measurements across the Morin temperature [2] are exciting, since the magnonic modes show an anisotropy-dependent polarization [3], which has an impact on the transported angular momentum [4].

In this talk, we demonstrate both analytically and numerically (micromagnetic simulations [5]), how the magnon polarization impacts the spin transport signal across the Morin transition, in connection to N´eel vector dynamics and dispersion

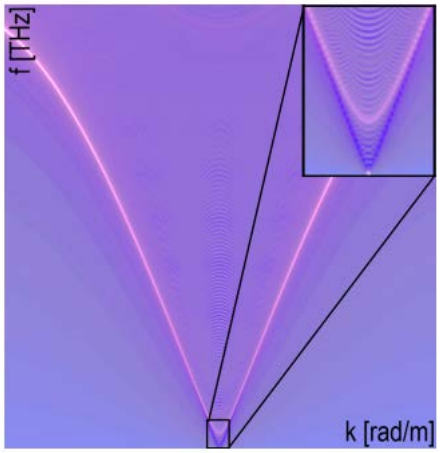

Fig. 1: Micromagnetic simulation of magnon dispersion in a typical biaxial antiferromagnet. The two antiferromagnetic magnon modes can be distinguished around the Brillouin zone centre (inset).

[1] Rezende, White. Phys. Rev. B 14 (1976)
[2] Ross et al. Jour. Mag. and Magn. Mat. 453 (2022)
[3] Rezende et al. J. Appl. Phys. 126 (2019)
[4] Lebrun, Kl¨aui et al. Nat. Comm. 11 6332 (2020)
[5] Lepadatu. J. Appl. Phys. 128 243902 (2020)

The thermodynamic properties of exchange stiffness

Sean Stansill[1, 2], and Joseph Barker[1, 2]

[1]University of Leeds, Leeds, UK, [2]Bragg Centre for Materials Research, UK

The effective temperature dependence of micromagnetic parameters such as anisotropy (K), exchange stiffness (A) and the Dzyaloshinskii–Moriya interaction (DMI) are usually written as a power law of the magnetisation. For anisotropy this is well founded, based on Callen-Callen theory[1]. For exchange stiffness and DMI the power laws are based on classical numerical models, or assumed to be the same as anisotropy. Recently there has been a lot of interest in the temperature dependence of these properties because their value affects spin textures like skyrmions.

Inferring the DMI from experimental measurements requires first deducing the exchange stiffness by fitting Bloch's law to measurements of magnetisation at finite temperature. The problem is that Bloch's law contains the zero-temperature value of exchange stiffness but is used to fit a finite temperature range over which the value of the exchange stiffness should change significantly. Another issue is that Bloch's law is derived using quantum mechanics with magnons which obey Bose statistics – numerical models typically use classical statistics for the thermal occupation of spin waves. Classical models cannot reproduce Bloch's $T^{3/2}$ law for ferromagnets or the T^2 dependence of sublattice magnetisation in antiferromagnets[2]. So, the classical thermodynamics of exchange is also a poor approximation for real materials in which the quantum distributions of magnons plays a large role.

Here we discuss a quantum implementation of atomistic spin dynamics[2], compare with classical results and present the temperature scaling of the micromagnetic exchange stiffness for both ferromagnets and antiferromagnets calculated from magnon spectra. We show antiferromagnets have similar scaling behaviour to ferromagnets and that the results using quantum statistics don't follow a power law.

Figure 1 shows the thermal behaviour of the exchange stiffness as a function of reduced sublattice magnetisation of the prototypical antiferromagnet NiO used in antiferromagnetic spintronics[3]. At low temperature (high magnetisation) the exchange stiffness is almost temperature independent when using quantum statistics in stark contrast to a power law. Figure 2 shows the sublattice magnetisation of NiO against temperature as measured by neutron diffraction[4] and simulated using atomistic spin dynamics with a quantum thermostat.

[1] H. Callen and E. Callen, J. Phys. Chem. Solids, 27, 1271 (1966)
[2] J. Barker and G. Bauer, Phys. Rev. B, 100, 140401 (2019)
[3] V. Baltz, Rev. Mod. Phys., 90, 015005 (2018)

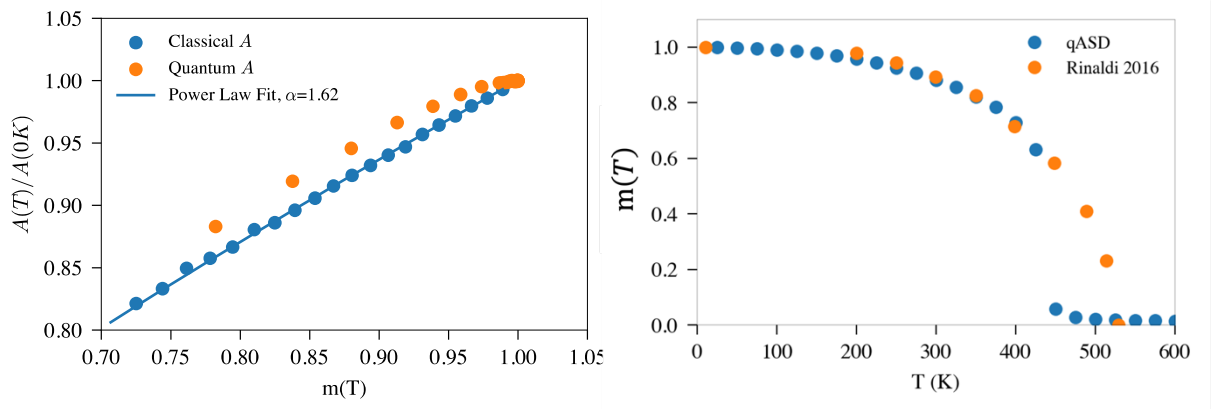

[4] N. Rinaldi-Mentes et al, *AIP Adv.*, **6**, 056104 (2016)

Tuesday 29 March 2022

(Wohlfarth Lecture) Controlling and utilising antiferromagnetic order

Peter Wadley

University of Nottingham, UK

Until recently antiferromagnetism was largely considered a theoretical curiosity. Indeed, one of the pioneers of antiferromagnetic order, Loius Neel, dubbed them theoretically interesting but without application, during his Nobel lecture. Recent advances have demonstrated that they can be both controlled and read electrically [e.g. 1,2,3] propelling them into a prominent position in spintronics research [4]. In this talk, I will present our work on the control, imaging and reading of antiferromagnetic metals, as well as discussing our latest work in addressing the remaining barriers to spintronic applications of antiferromagnets.

[1] Wadley, P. et al. Science351, 587–590 (2016).
[2] Bodnar, S. Y. et al. Phys. Rev. B99, 140409 (2019).
[3] Baldrati, L. et al. Phys. Rev. Lett. 123, 177201 (2019).
[4] J. Železný et al Nat. Phys. 14,220-228 (2018).; Baltz, V. et al. Rev. Mod. Phys.90, 015005 (2018).

Spintronics 2

(Invited) Memristor controlled mutual synchronization of spin Hall nano-oscillator arrays for neuromorphic computing and spintronic Ising Machines

Johan Åkerman

University of Gothenburg, Sweden

In my talk I will first briefly review the recent progress in mutually synchronized nano-constriction based spin Hall nano-oscillator (SHNO) chains [1] and two-dimensional arrays [2]. I will then describe how we can generate propagating spin waves from such nano-constrictions using W/CoFeB/MgO stacks where the CoFeB has sufficient perpendicular magnetic anisotropy (PMA) to change the sign of the non-linearity from negative to positive [3]. Since the PMA in W/CoFeB/MgO trilayers can be voltage-controlled, we can also tune the SHNO frequency using voltage gates on top of the auto-oscillating region. Thanks to the nano-constriction geometry the SHNO properties can hence be tuned such that the auto-oscillation mode changes continuously from localized to propagating and the associated additional damping from generating propagating spin waves leads to a giant 42% change in the effective SHNO damping using only a few Volts [4]. In our most recent work, we have now added memristive functionality to these SHNOs and demonstrated non-volatile control of mutual synchronization [5] and how this can be used for neuromorphic computing. Time permitting, I will also briefly discuss how two-dimensional SHNO networks can be used to create so-called Ising Machines [6]. Using phase-sensitive micro-Brillouin Light Scattering microscopy, such two-dimensional SHNO arrays can be efficiently phase-binarized and solve MAX-CUT problems [7].

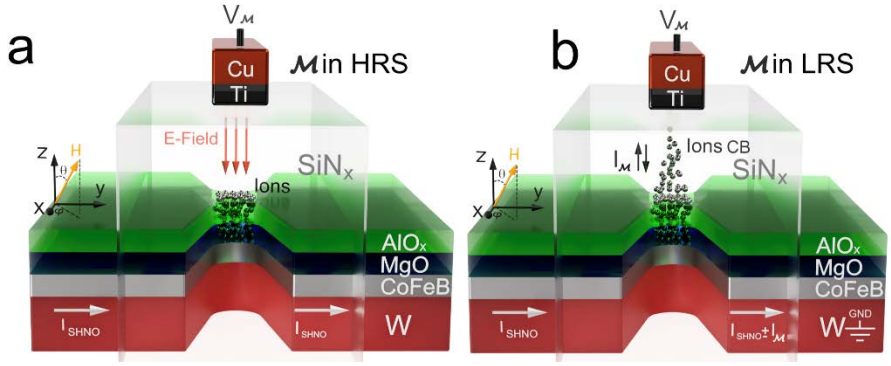

Fig. 3: a) A voltage-gated SHNO where the E-field controls the PMA of the CoFeB layer. b) A memristor-controlled SHNO where an additional memristor current adds or subtracts to the SHNO drive current [5].

[1] A. A. Awad et al, Nature Physics 13, 292–299 (2017)
[2] M. Zahedinejad et al, Nature Nanotechnology 15, 47 (2020)
[3] H. Fulara et al, Science Advances 5, eaax8467 (2019)
[4] H. Fulara et al, Nature Communication 11, 4006 (2020)
[5] M. Zahedinejad et al, Nature Materials 21, 81 (2022)
[6] D. I. Albertsson et al, Applied Physics Letters 118, 112404 (2021)
[7] A. Houshang et al, Physical Review Applied 17, 014003 (2022)

All-optical switching in Ni3Pt/Ir/Co synthetic ferrimagnets driven by spin current

M Dąbrowski[1], J N Scott[2] , W R Hendren[2], C M Forbes[2], C R J Sait[1] , A Frisk[3], D M Burn[3], P S Keatley[1], D G Newman[1], A T N'Diaye[4], T Hesjedal[5], G van der Laan[3], R M Bowman[2], and R J Hicken[1]

[1]Department of Physics and Astronomy, University of Exeter, UK, [2]School of Mathematics and Physics, Queen's University Belfast, UK, [3]Diamond Light Source, Harwell Science and Innovation Campus, UK, [4]Advanced Light Source, Lawrence Berkeley National Laboratory, USA, [5]Department of Physics, Clarendon Laboratory, University of Oxford, UK

All-optical switching (AOS) of magnetization allows the writing of magnetic bits purely by optical laser pulses without any need for an external magnetic field [1]. From the viewpoint of technological applications, rare-earth free synthetic ferrimagnets (SFi's) are highly desirable due to the low cost and relative abundance of the constituent materials, and the unparalleled tunability. Here we demonstrate multi-pulse AOS in the SFi Ni3Pt/Ir/Co, achievable independently of the light polarization and across a broad temperature range [2]. The constituent layers of the SFi are magnetically soft, which leads to unique static and dynamic magnetic properties. In particular, the existence of a negative remanence state, and its correlation with the domain structure and AOS mechanism, demonstrates the importance of magnetic anisotropy in the AOS switching process and the magnetization reversal. Timeresolved measurements indicate that AOS is mediated by the transfer of spin angular momentum between the ferromagnetic layers, which promises a new arena for the exploration of ultrafast spintronic effects down to the nanoscale, and suggests that ultrafast switching with a single laser pulse is feasible in a SFi.

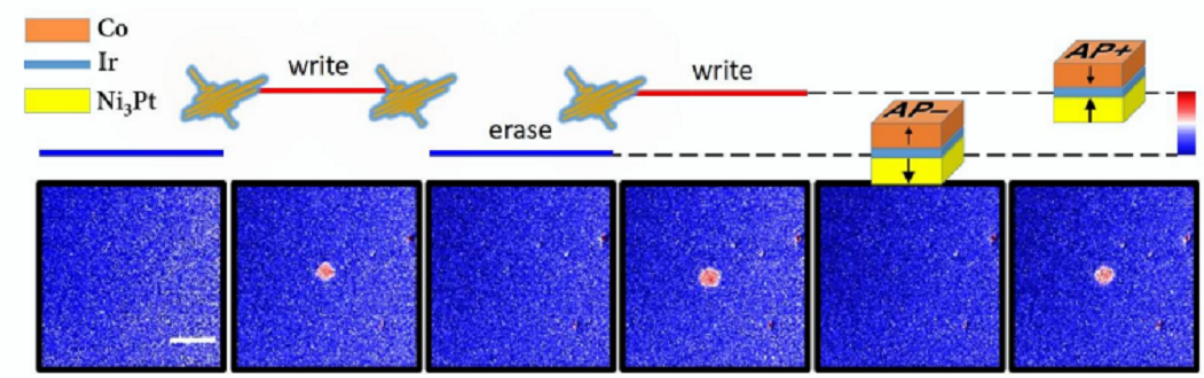

Fig. 1: Toggle switching of Ni3Pt(8.5nm)/Ir(0.5nm)/Co(1nm) between two equivalent remanent states AP+ and AP- allows writing and erasure of magnetic bits with consecutive pulses. The length of the scale bar is 20 μm.

[1] C. D. Stanciu, et al. All-optical magnetic recording with circularly polarized light. Phys. Rev. Lett. 99, 047601 (2007).

[2] M. Dąbrowski, et al. Transition Metal Synthetic Ferrimagnets: Tunable Media for AllOptical Switching Driven by Nanoscale Spin Current. Nano Lett., 21, 9210–9216 (2021).

Oblique spin injection and gate-controlled spin polarity in 1D-contact architectures

J Toscano[1,2], Daniel Burrow[1], N Natera[1,2], C R Anderson[1], V Guarochico[1], I V Grigorieva[1], and I J VeraMarun[1]

[1]Department of Physics and Astronomy, University of Manchester, UK, [2]Consejo Nacional de Ciencia y Tecnología (CONACyT), México

Spintronics promises information storage and logic operation applications. To achieve those, spins need to undergo injection, transport, detection and crucially, manipulation. Production of out-of-plane spins is possible using perpendicular magnetic tunnel junctions (pMTJ)1 with complex vertical stacking of magnetic and high SOC metals to achieve perpendicular magnetic anisotropy (PMA). Another way is by applying magnetic fields: i) before injection to exploit the anomalous spin Hall effect (ASHE)2 and give the spins a certain directionality, or ii) after injection to rotate the already-in-plane spins via spin precession 3.

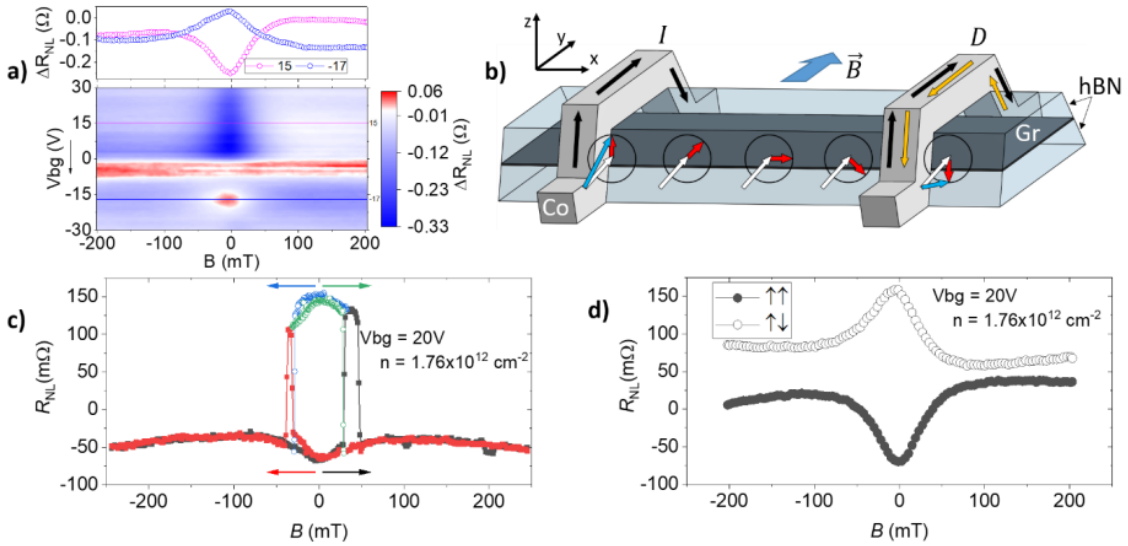

Fig. 1: a), 2D map of non-local resistance difference (Spin signal) as a function of back gate voltage and magnetic field, the polarization reverses beyond the neutrality point. b), Schematic of our 1D-contact architecture illustrating the

x- and z-components of spin at the injection point which originate an out-of-plane spin component after precession. c), Spin valve showing a Hanle-like baseline due to spin precession. d), Hanle spin precession of same data set.

In this work, we demonstrate the existence of an out-of-plane spin component just by exploiting the geometry of a 1-dimensional contact between a Ferromagnetic electrode and graphene. Such electrode has a partially vertical magnetization when climbing up and down the hBN-GrhBN heterostructure. As a result, we observe spin precession and spin-valve phenomena corresponding with spins having components both inside the plane of the device and perpendicular to it. We also observe a gate controlled spin polarity, with a reversal ocurring around the neutrality point. Such manipulation of polarity could be useful to remove the need of magnetic fields to achieve gate-controllable graphene spin logic devices 4.

Together, these observations demonstrate an effective oblique spin injection where – by means of the device architecture – an out-of-plane component of spin is introduced into a 2D surface without the need of an external magnetic field or PMA, relying exclusively on the geometry of our device architecture.

[1] J.-H. Park, et al, J. Appl. Phys., 103, 7, 07A917 (2008)
[2] K. S. Das, et al, Nano Lett., vol. 18, no. 9, pp. 5633–5639, (2018)
[3] C. K. Safeer, et al, Nano Lett., vol. 19, no. 2, pp. 1074–1082, (2018)
[4] Jinsong, X. et al, Nat. Commun., 9, 2869 (2018)

Computation with Magnetic Domain Walls and Oscillators

Aleš Hrabec[1,2,3], Zhaochu Luo[1,2], Zhiyang Zeng [1,2], Joo-Von Kim[4], Trong Phuong Dao[1,2,3], Pietro Gambardella[3], Laura J. Heyderman[1,2]

[1]Laboratory for Mesoscopic Systems, Department of Materials, ETH Zurich, Switzerland [2]Laboratory for Multiscale Materials Experiments, Paul Scherrer Institute, Switzerland [3]Laboratory for Magnetism and Interface Physics, Department of Materials, Switzerland [4] Centre de Nanosciences et de Nanotechnologies, CNRS, Université Paris-Saclay, France

In order to go beyond the traditional CMOS logic technology, novel spin-based logic architectures are being developed to provide nonvolatile data retention, near-zero leakage, and scalability. Architectures based on magnetic domain walls take the advantage of the fast motion, high density, non-volatility and flexible design of domain walls to process and store information in three dimensions. Here we demonstrate a method for performing all-electric logic operations and their cascading using domain wall racetracks [1].

Our concept is based on the recently developed chiral coupling mechanism between adjacent magnets where the magnetic anisotropy competes with the interfacial Dzyaloshinskii–Moriya interaction (DMI) in Pt/Co/AlOx trilayers [2-5]. When a narrow in-plane (IP) magnetized region is incorporated into an out-of-plane (OOP) magnetized track, it couples to its surrounding, leading to the antiferromagnetic alignment of the OOP magnetization on the left and right of the IP region. The chiral OOP-IP-OOP structure then serves as a domain wall inverter, the essential building block for all implementations of Boolean logic. Based on this principle, we realized reconfigurable NAND and NOR logic gates, making our concept for current-driven DW logic functionally complete. We also cascaded several NAND gates to build XOR and full adder gates, demonstrating electrical control of magnetic data and device interconnection in logic circuits. The functionality of logic circuits can be also expanded by the realization of a domain wall diode based on a geometrically tailored inverter [6]. We also broadened the application of chiral coupling towards dynamic computation [7]. By introducing inhomogeneous anisotropy in our system, spintronic oscillators with a chiral polar vortex ground state can be established. We investigated the mutual synchronization of such oscillators and demonstrated their potential for neuromorphic computing.

[1] Luo, Z. et al. Nature 579, 214-218 (2020).
[2] Luo, Z. et al. Science 363, 1435 (2019).

[3] Dao, P. D. et al. Nano Lett. 19, 5930-5937 (2019).
[4] Hrabec, A. et al. Appl. Phys. Lett. 115, 130503 (2020).
[5] Liu Z. et al. Phys. Rev. Appl. 16, 054049 (2021).
[6] Luo Z. et al. Phys. Rev. Appl. 15, 034077 (2021).
[7] Zeng Z. et al. Appl. Phys. Lett. 118, 222405 (2021).

Dipolar and quadrupolar spontaneous magnetic ordering in an atomic spin system mediated by light

T Ackemann[1], J G M Walker[1], G R M. Robb[1], G-L Oppo[1], G Labeyrie[2] , and R Kaiser[2]

[1]Scottish University Physics Alliance and Department of Physics, University of Strathclyde, UK, [2]Institut de Physique de Nice, Universite Cote d'Azur, France

Cold atom systems emerged as a versatile platform to address magnetic phenomena in a highly controlled environment (e.g. [1]). Many of these system use pseudo-spin and synthetic magnetic fields. We are investigating here an atomic spin system which operates with real spins and is influenced by real magnetic fields but where the coupling is significantly enhanced by interaction via the spin degrees of light. Hence spontaneous magnetic ordering can be achieved in between the situation typical for condensed matter physics (high density, high temperature) and spinor Bose-Einstein condensate (low density, very low temperature, [1]). Using an atomic ground complex enough to allow for dipolar and quadrupolar ordering, competition between these states can be studied. Hence the system might be helpful to understand complex phases with dipolar and quadrupolar character as recently discussed for $CeRh_2As_2$ [2].

The conceptually simple scheme to achieve light mediated coupling is based on a laser-cooled atomic ensemble ($T \approx 150$ μK) irradiated by a detuned laser beam. Most of the light is retro-reflected by a plane feedback mirror. A modulation of any atomic state variable will cause a phase modulation of the transmitted wave, which is converted to an amplitude modulation via diffraction in the feedback loop. This optical structure will then sustain the atomic structure via positive feedback. The parameter determining the coupling strength is the (dispersive) optical density [3]. The experiment is performed using the F=2→F'=3-line of the ^{87}Rb D_2 transition but for the theoretical interpretation a simpler F=1→F'=2 transition is used as the F=1 ground state contains already the relevant dipolar and quadrupolar components and there is no backaction of light on the higher multipoles [4].

The optical spin (or polar angle of light on the Poincare sphere determining the optical helicity) couples to a magnetic dipole moment in an atomic ground state with J>0 via optical pumping nonlinearities [4]. Anti-ferromagnetic structures are observed in zero field giving way to ferrimagnetic structures in a small Bz-field. Increasing a transverse magnetic field these dipolar structures disappear like in the transverse Ising model [4]. Linearly polarized light of zero net spin can couple to a Δm=2 coherence or magnetic quadrupole in an atomic ground state with J>1/2. The direction of local light polarization defines the axes of the quadrupole. The resulting structure is typically highly disordered (see inset in Fig. 1) but locally stripe-like, as also evidenced in numerical simulations. The modulation observed in the transmitted light indicates a spatial modulation of the quadrupole axes in the atomic structure. The transition between the phases can be first or

second order. We studied critical slowing down and growth exponents at the phase transitions [5]. The system appears to be interesting to study interaction of dipolar and quadrupolar waves.

Fig. 1: Magnetic phase diagram spanned by Bx field (x parallel to polarization of input beam) and Bz-field (z is the axis of the laser beam). AFM = antiferromagnetic dipolar phase, FM = ferri-magnetic dipolar phase, "high Bz" disordered dipolar ferri-magnetic phase, "coherence" quadrupolar phase. All phases contain excitation of both magnetic moments but their prevalence changes.

[1] J. Stenger, et al., Nature 396, 345–348 (1998); J. Kronjäger, et al., Phys. Rev. Lett. 105, 090402 (2010)

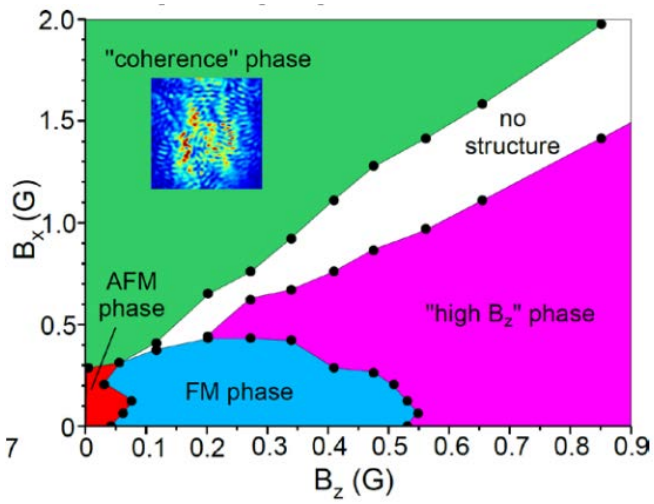

[2] Hafner et al., arXiv2108.06267 (2021)
[3] T. Ackemann et al., atoms 09, 35 (2021)
[4] G. Labeyrie et al., Optica 5, 1322 (2018)
[5] G. Labeyrie et al., to appear in Phys. Rev. A

General 1

(Invited – IEEE) Exploring the Potentials of Spin-Orbitronics

Aurélien Manchon

Aix-Marseille University, France

The ever-increasing demand for information technology for power-efficient components has led to the search for alternative solutions to mainstream microelectronics. In this context, spintronics devices stand out as competitive candidates, especially for memory and logic applications. A promising route harvests unconventional transport properties arising from spin-orbit coupling in magnetic heterostructures lacking inversion symmetry.

In these systems, typically multilayers of transition-metal ferromagnets and heavy materials (e.g., W, Pt, Ta, Bi2Se3, and WTe2), interfacial spin-orbit coupling promotes a wealth of remarkable physical phenomena: the generation of spin-orbit torques, the interconversion between spin and charge currents, and the stabilization of topological magnetic skyrmions. These effects have gathered extraordinary interest and have led to remarkable experimental breakthroughs, including extremely fast magnetic reversal, terahertz emission, and current-driven skyrmion motion. The recent synthesis of novel classes of materials, including all-oxide heterostructures, noncollinear antiferromagnets, and van der Waals heterostructures, has

profoundly enriched this vivid field of research by unlocking unforeseen forms of torques and magnetic interactions, thereby enhancing the functionalities of spin-orbitronic devices.

This lecture will provide a theoretical perspective of the advancement of the fascinating field of spin-orbitronics, focusing on two emblematic mechanisms: the spin-orbit torque and the Dzyaloshinskii-Moriya interaction. I will examine what theory and materials modeling can tell us about these two effects, and what future research directions they open. I will first introduce key concepts in spintronics, such as spin currents and spin-transfer torque, and show how spin-orbit coupling enables new physical effects of high interest for potential applications. I will present standard phenomenological descriptions of these two effects, spin-orbit torque and Dzyaloshinskii-Moriya interaction, determine the symmetry rules that govern them, and give a broad overview of the current state-of-the-art of the field from experimental and theoretical standpoints. Finally, I will explore how spin-orbitronics takes a completely new form in materials possessing low crystalline symmetries, such as Fe3GeTe2, CuPt/CoPt bilayers, and noncollinear antiferromagnets (e.g., Mn3Sn).

I hope this seminar will not only encourage electrical engineers to engage in this beguiling field of research and explore the device implications of this new technology but also reach out to scientists working in adjacent fields (terahertz science, for instance) who could bring inspiring new ideas to spintronics [1]–[5].

[1] A. Manchon, J. Železný, I. M. Miron, T. Jungwirth, J. Sinova, A. Thiaville, K. Garello, and P. Gambardella, “Current-induced spin-orbit torques in ferromagnetic and antiferromagnetic systems,” Rev. Mod. Phys., vol. 91, 035004, September 2019.

[2] A. Belabbes, G. Bihlmayer, F. Bechstedt, S. Blügel, and A. Manchon, “Hund’s rule-driven Dzyaloshinskii-Moriya interaction at 3d-5d interfaces,” Phys. Rev. Lett., vol. 117, 247202, December 2016.

[3] E. Jué, C. K. Safeer, M. Drouard, A. Lopez, P. Balint, L. Buda-Prejbeanu, O. Boulle, S. Auffret, A. Schuhl, A. Manchon, I. M. Miron, and G. Gaudin, “Chiral damping of magnetic domain walls,” Nature Mater., vol. 15, pp. 272-277, March 2016.

[4] S. Laref, K.-W. Kim, and A. Manchon, “Elusive Dzyaloshinskii-Moriya interaction in monolayer Fe3GeTe2,” Phys. Rev. B, vol. 102, 060402, August 2020.

[5] L. Liu et al., “Symmetry-dependent field-free switching of perpendicular magnetization,” Nat. Nanotech., vol. 16, pp. 277-282, January 2021.

Energy based model for Twin boundary prediction in the Sm-Fe-Co 1:12 phase

Gino Hrkac[1], Connor Skelland[1], and Thomas Schrefl[2]

[1]EMPS, University of Exeter, UK, [2]Center for Integrated Sensor Systems, Danube University, Austria

To be able to investigate the origins and effects of twins in magnetic materials, one must understand that by introducing twins, one introduces another interface and have to analyse the interface energy of a twin itself. Further one has to identify the most prominent grain boundary neighbours, 1:5, 3:29 or liquid phases.

To proof our hypothesis we started to construct an elliptical grain and calculate interfaces between 1:12 phase and the 1:5 phase. It was found that one of the interfaces is coherent below 0.2 J/m2 and the other one is semi-coherent above 0.2 J/m2. This shows that interface can be optimized for one interface but not for two. For the second case, we introduce a twin in our system but keep the orientation of our 1:12 phase the same. The total energy of this system is composed of two interfaces to the 1:5 phase, which are energetically coherent and the twin interface in the 1:12 phase, which is energetically coherent.

We start by calculating the total interface energy of surface 1, 1:12 phase to 1:5 phase coherent, 0.175 Jm2, surface two has the configuration 1:12 phase to 1:5 phase semi-coherent, 0.237 J/m2. For case one the surface 3 is zero as there is no twin. For the case 2, the twin surface has an interface energy of 0.175 J/m2. We now vary the aspect ratio. In figure 1, you can see the normalised energy increase of case 1 (circle) no twin and case 2 (diamond) with twin as function of grain size. On the right axis we have plotted the normalised energy difference delta E between Case 2 and 1. A positive value means, Case 2 is unfavourable as it needs more energy and Case 1 is preferred. A negative value is that by forming a twin Case 2 becomes more favourable which occurs between 900 and 1200 nm grain size, in agreement with experiments [1]. We have shown that the boundary where twins start to emerge are dependent on the interface energy, hence the boundary and also the shape of the grain plays an important part.

[1] Semih Ener, Konstantin P Skokov, Dhanalakshmi Palanisamy, Thibaut Devillers, Johann Fischbacher, Gabriel Gomez Eslava, Fernando Maccari, Lukas Schäfer, Léopold VB Diop, Iliya Radulov, Baptiste Gault, Gino Hrkac, Nora M Dempsey, Thomas Schrefl, Dierk Raabe, Oliver Gutfleisch, Acta Materialia 214, 116968 (2021)

Atomic Level Analysis of the Oxidation Pathways in Magnetic Fe/Fe Oxide Particles

Toby W Bird[1], Sitki Aktas[2], Shuayl Alotaibi[1], Leonardo Lari [1,3], Katie Dexter[4], Steve Baker[4], Chris Binns[5], Roland Kröger[1], and Andrew Pratt[1]

[1] Department of Physics, University of York, UK [2] Mechanical Engineering, Giresun Universitesi, Turkey [3] York JEOL Nanocentre, University of York, UK [4] Department of Physics and Astronomy, University of Leicester, UK [5] Universidad de Castilla-La Mancha, Departamento de Fisica Aplicada, Spain

Magnetic nanoparticles continue to attract a great deal of attention relating to their potential use in biomedical, environmental, and data storage applications [1,2]. Pure Fe nanoparticles have higher magnetic moments than their Fe oxide counterparts, but their reactivity currently precludes use in these applications. A deeper understanding of oxidation at the nanoscale is required and how this differs from the well-understood theory of bulk metal oxidation [3].

In this study, Fe and Fe/Fe_xO_y magnetic nanoparticles were produced under ultrahigh vacuum conditions in a gas-aggregation cluster source and size-selected using a quadrupole mass filter. As well as being cleaner than typical methods of chemical synthesis, this physical approach of magnetic nanoparticle production also allows control over geometry with cubic, cuboctahedral, and spherical shapes possible under different source conditions [4]. We have previously demonstrated that geometry and confinement effects during oxidation of an Fe core can promote ionic transport at the facets of cuboid particles leading to enhanced oxidation and shape evolution [3].

Results from aberration corrected environmental transmission electron microscopy (e-TEM) imaging of Fe/Fe_xO_y nanoparticles will be presented correlating the balance between grain boundary and lattice diffusion with oxidative behaviour. In-situ heating and exposure to a constant flow of oxygen gas allowed the particles to be imaged as they fully oxidised through the environmental capabilities of the TEM. The effect of temperature and electron beam dosage on the oxidation process were explored. The nano Kirkendall effect was also observed as well as dynamics differing from bulk theories such as Cabrera-Mott [5] and Wagner [6]. The observation of the complete oxidation of a particle, Fig 1, allowed for a calculation of the diffusion coefficient of Fe in Fe_xO_y.

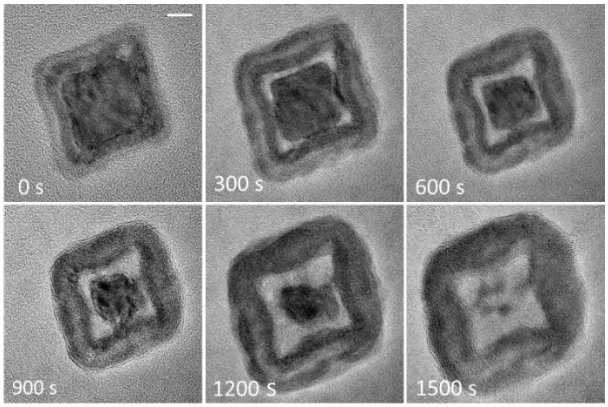

Fig 1: Complete particle oxidation after exposure to oxygen under environmental conditions. Steady depletion of the core typical in nano-Kirkendall effect. Kinetics of the growth can be measured as well as the diffusion coefficient of Fe in Fe_xO_y.

[1] M. Walker, I. Will, A. Pratt et al., ACS Appl. Nano Mater. 3, 5008 (2020)
[2] A. Pratt, Environmental Applications of Magnetic Nanoparticles, in: Frontiers of Nanoscience (Ed.: C. Binns) Vol. 6, pp.259-307 (2014).
[3] A. Pratt, L. Lari, O. Hovorka et al., Nature Mater. 13, 26 (2014).
[4] S. Aktas, S. C. Thornton, C. Binns et al. Mater. Res. Exp. 2, 035002 (2015).
[5] N. Cabrera and N.F. Mott, Rep. Prog. Phys. 12, pp.163-184 (1949)
[6] C. Wagner, Z. Phys. Chem. 21, pp. 25-41 (1933)

Optimising Laser Additive Manufacturing Process for Amorphous Magnetic Materials

Merve Özden, and Nicola Morley

Department of Materials Science and Engineering, University of Sheffield, UK

Optimization of process parameters in the laser powder bed fusion (LPBF) technique has been extensively studied using the volumetric energy input equation: E=P/ (v.t.h), which includes major build parameters; laser power (P), scan speed (v), layer thickness (t) and hatch spacing (h). Even though utilizing laser energy density to predict final properties of a specified materials is a good way to start, only considering this is not enough to optimize the process. For detailed investigation, all process parameters should be examined individually. Researchers often focus on the effect of laser power and scan speed on the final properties. This study investigates how the major process parameters influence the physical and magnetic properties of LPBF-processed Fe-based amorphous/nanocrystalline composites ($(Fe_{87.38}Si_{6.85}B_{2.54}Cr_{2.46}C_{0.77}$ (mass %)). Fig. 1 shows the hysteresis loops and the microstructures of the samples fabricated by using same E (=60 J/mm^3) and v (= 1000 mm/s) and varying P, h and t (left corner in Fig. 1). It is obvious that despite being printed with same energy density, changing h and t (Sample 1 and 2) or changing P and h (Sample 2, 3 and 4) led to different results. It was found that bulk density improves as P increases, v, t and h decreases, i.e., high E is necessary, however, greater than 80 J/mm_3 (due to the keyhole effect) and less than 45 J/mm_3 (because of the insufficient energy input to the powder bed) causes either failing parts or large and high number of pores. In addition, the magnetic properties differ significantly due to the nanocrystalline phases present in the microstructure and their size depends on the process parameters considerably. Owing to the laser scanning nature, the microstructure evolves as molten pool (MP) and heat affected zones (HAZ) resulting from the high thermal gradient occurred between laser tracks. MP forms around the scans, having Fe_2B nanograins mainly, whereas HAZ generally contains α-Fe(Si) and Fe_3Si nanocrystalline clusters. The size and quantities of those nanocrystallites determine the magnetic properties.

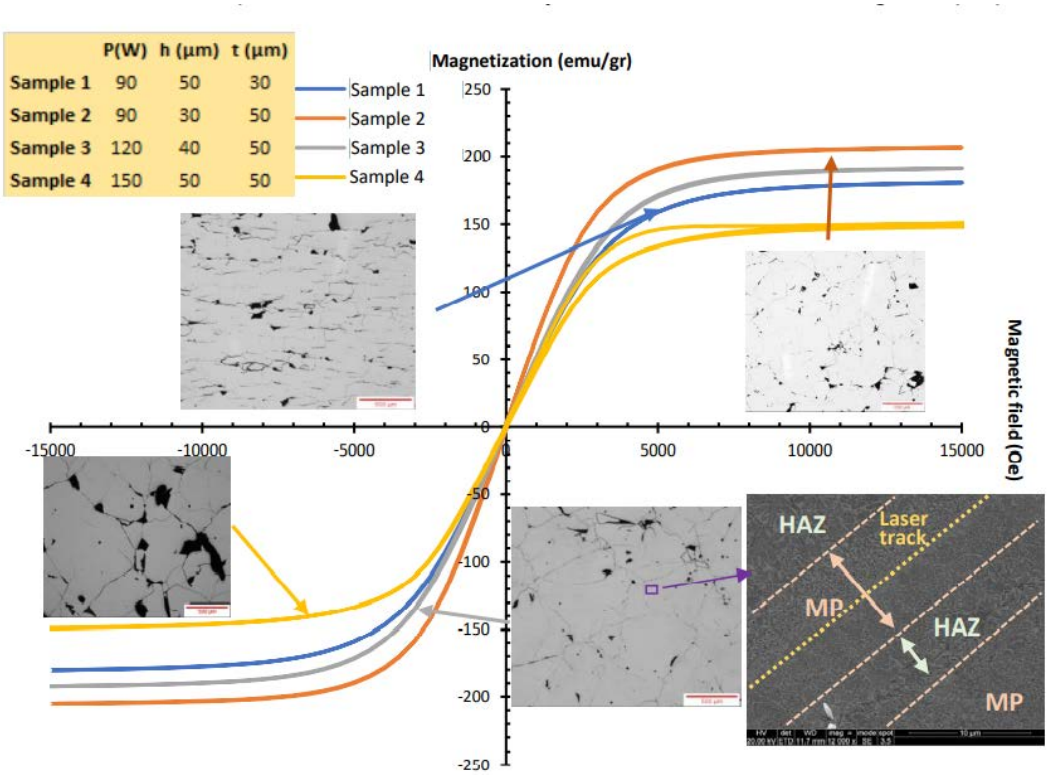

Fig. 1: Hysteresis loops and micrographs of the samples LPBF-processed with same E (=60 J/mm3) and v (=1000 mm/s).

Structural Explanation for Titanium Stability Range in $RFe_{12-x}Ti_x$

Connor Skelland, and Gino Hrkac

University of Exeter, UK

$RFe_{12-x}Ti_x$ structures are considered a promising candidate to replace $Nd_2Fe_{14}B$ as the magnet of choice for high performance electric vehicles, owing to their similar magnetic properties and reduced reliance on critical rare earth elements. Substitution of iron atoms for titanium is necessary as RFe12 structures are intrinsically unstable. Work by Buschow [1] showed that the stability range of $RFe_{12-x}Ti_x$ structures falls between x=1-1.4.

The range can be explained by examining the pattern of titanium substitutions in the crystal lattice. To investigate this, we performed energy based substitution permutation calculations, methodology in [2], on 3×3×2 supercells of $NdFe_{12-x}Ti_x$ and $SmFe_{12-x}Ti_x$. Our results showed two distinct substitution patterns across the stability range. The complete first substitution pattern is shown in Figure 1, which shows that titanium atoms align to decrease their proximity to one another. As can be seen, the resultant pattern places titanium atoms in separate cells across the crystal lattice. This preference is due to titanium-titanium interatomic interactions having an equilibrium distance ~22% higher than iron-iron interactions. Consequently, close proximity titanium pairs produce significant and energetically unfavourable stresses within the crystal lattice.

The beginning of the stability region falls roughly near the end of the first substitution pattern, at about 8Ti at.%. Beyond this point titanium atoms follow a secondary substitution pattern which results in them being positioned much closer to one another, particularly in the Z direction. The stress induced by substitutions in this pattern causes a significant expansion in the c lattice parameter. The gradual increase of stress coupled with the induced strain deteriorates the crystal structure over time and increases the probability of a phase change. We consider this the most likely cause of the low stability range seen in the $RFe_{12-x}Ti_x$ structures.

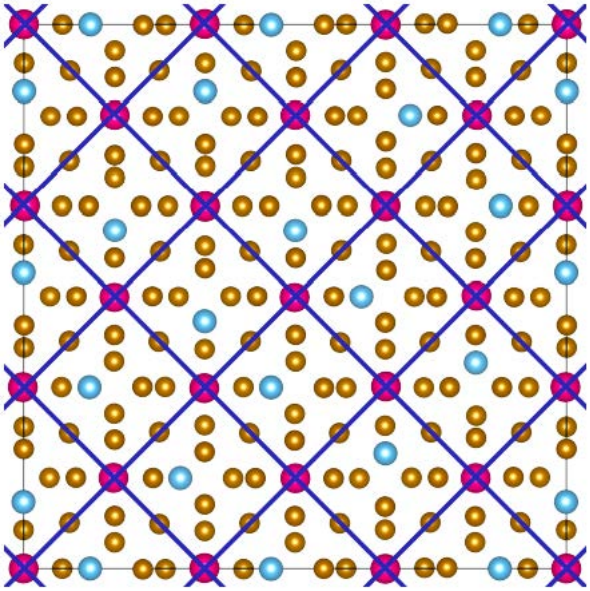

Fig 1: Visual illustration of the first substitution pattern in SmFe12–xTix at 8Ti at. % (36 titanium substitutions for a 3×3×2 structure).

[1] K. Buschow, Reports on Progress in Physics 1991, 54, 1123.
[2] C. Skelland, T. Ostler, S. Westmoreland, R. Evans, R. Chantrell, M. Yano, T. Shoji, A. Manabe, A. Kato, M. Ito, et al., IEEE Transactions on Magnetics 2018, 54, 1–5.

Invited: IEEE presentation

(Invited – IEEE) Coherent Magnonics for Quantum Information Science

Michael E Flatté

Department of Physics and Astronomy, The University of Iowa, USA

The current revolution in quantum technologies relies on coherently linking quantum objects like quantum bits (“qubits”). Coherent magnonic excitations of low-loss magnetic materials can wire together these qubits for sensing, memory, and computing. Coherent magnonics may reduce the size of superconducting qubits (which otherwise struggle with the large scale of microwave excitations) and may increase the size of spin-based qubit networks (which otherwise contend with the very short distances of dipolar or exchange interactions). Compared to photonic devices, these magnonic devices require minimal energy and space. However, efforts to exploit coherent magnonic systems for quantum information science will require a new understanding of the linewidths of low-loss magnonic materials shaped into novel structures and operating at dilution-refrigerator temperatures. This lecture will introduce the fundamental requirements for practically linking quantum objects into large-scale coherent quantum systems as well as the advantages of coherent

magnonics for next-generation quantum coherent systems (i.e., spinentangling quantum gates [1]). Other critical challenges for quantum information science then will motivate the development of coherent magnonics for quantum transduction from "stationary" spin systems to "flying" magnons and for quantum memory [2]–[4]. Finally, the advantages of all-magnon quantum information technologies that rely on manipulating and encoding quantum information in superpositions of fixed magnon number states will highlight the potential of new magnetic materials, devices, and systems.

REFERENCES

[1] M. Fukami, D. R. Candido, D. D. Awschalom, and M. E. Flatté, "Opportunities for long-range magnon-mediated entanglement of spin qubits via on and off-resonant coupling," PRX Quantum, vol. 2, Oct. 2021, Art. no. 040314.
[2] D. R. Candido, G. D. Fuchs, E. Johnston-Halperin, and M. E. Flatté, "Predicted strong coupling of solid-state spins via a single magnon mode," Mater. Quantum Technol., vol. 1, Dec. 2021, Art. no. 011001.
[3] Ö. O. Soykal and M. E. Flatté, "Strong field interactions between a nanomagnet and a photonic cavity," Phys. Rev. Lett., vol. 104, Feb. 2010, Art. no. 077202.
[4] T. Liu, X. Zhang, H. X. Tang, and M. E. Flatté, "Optomagnonics in magnetic solids," Phys. Rev. B, Condens. Matter, vol. 94, Aug. 2016, Art. no. 060405(R).

Invited: IEEE presentation

(Invited – IEEE) Symmetry Breaking by Materials Engineering for Spin-Orbit-Torque Technology

Jingsheng Chen

National University of Singapore

Electric manipulation of magnetization is essential for the integration of magnetic functionalities in integrated circuits. Spin-orbit torque (SOT), originating from the coupling of electron spin and orbital motion through spin-orbital interaction, is able to effectively manipulate magnetization. Symmetry breaking plays an important role in spintronics based on SOT. SOT requires inversion asymmetry in order to have a net effect on magnetic materials, which is commonly realized by spatial asymmetry: a thin magnetic layer sandwiched between two dissimilar layers. This kind of structure restricts the SOT by mirror and rotational symmetries to have a particular form: an "antidamping-like" component oriented in the film plane even upon reversal of the magnetization direction. Consequently, magnetization perpendicular to the film plane cannot be deterministically switched with pure electric current. To achieve all-electric switching of perpendicular magnetization, it is necessary to break the mirror and rotational symmetries of the sandwiched structure.

In this lecture, I will begin with a basic introduction of the physical origin of SOT, followed by the related symmetry analysis of a magnetic thin film in a sandwiched structure for the generation of a net SOT effect. Then I will introduce a new method—a composition gradient along the thin-film normal for breaking the inversion symmetry—to generate bulk-like SOT [1], which enables a thicker magnetic layer with high magnetic anisotropy. An overview of the methods commonly used to break mirror and rotational symmetries in order to realize all-electric switching of perpendicular magnetization will follow. I will give a detailed discussion on our methods for the realization of all-electric switching of perpendicular magnetization: the use of a spin source layer with low magnetic symmetry and low crystal symmetry, which generates an out-of-plane SOT [2]–[4]; interfacial 3m1 symmetry, which induces a new "3m" spin torque [5]; precise control of the tilting of magnetocrystalline anisotropy easy axis [6]; and a spin-current gradient along the current direction [7].

[1] L. Liu et al., "Electrical switching of perpendicular magnetization in a single ferromagnetic layer," Phys. Rev. B, vol. 101, 220402, June 2020.
[2] J. Zhou et al., "Magnetic asymmetry induced anomalous spin-orbit torque in IrMn," Phys. Rev. B, vol. 101, 184403, May 2020.
[3] J. Zhou et al., "Large spin-orbit torque efficiency enhanced by magnetic structure of collinear antiferromagnet IrMn," Sci. Adv., vol. 5, eaau6696, May 2019.
[4] Q. Xie et al., "Field-free magnetization switching induced by the unconventional spin–orbit torque from WTe2," APL Mater., vol. 9, 051114, May 2021.
[5] L. Liu et al., "Symmetry-dependent field-free switching of perpendicular magnetization," Nat. Nanotech., vol. 16, pp. 277-282, January 2021.
[6] L. Liu et al., "Current-induced magnetization switching in all-oxide heterostructures," Nat. Nanotech., vol. 14, 939-944, September 2019.
[7] S. Chen et al., "Free field electric switching of perpendicularly magnetized thin film by spin current gradient," ACS Appl. Mater. Interfaces, vol. 11, pp. 30446-30452, July 2019.

Thin Films 3

Current-induced crystallisation in Heusler alloy films for memory potentiation in neuromorphic computation

William Frost[1], Zhenyu Zhou[2], Kelvin Elphick[2,3], Marjan Samiepour[2,4] & Atsufumi Hirohata[2]

[1]Department of Physics, University of York, UK, [2]Department of Electronic Engineering, University of York, UK

Whilst great progress has been made in the reduction of crystallisation energy of Heusler alloys, they typically still require significant process to achieve the full $L2_1$ ordering. By growing on the {110} planes of a transition metal seed layer, 85% of a $Co_2FeAl_{0.5}Si_{0.5}$ (CFAS) thin film can be crystallised when deposited at a moderate temperature ~350 K [1]. In this work, current annealing has been applied to a fabricated giant magnetoresistive (GMR) pillar, whereby an applied current much greater than the typical sensing current has applied. This allows for potentiation in neuromorphic-type computing, where the value of the resistance or the MR of the pillar can inform the reader of the history of the device.

A multilayer GMR structure consisting of W (10)/CFAS (10)/W (3)/CFAS (5)/Ru (3) (thicknesses in nm) was deposited and patterned into a nanopillar junction using e-beam lithography and Ar-ion milling, measuring between (80 – 200) nm. The fabricated devices were then measured under an applied current using a HiSOL HMP-400 SMS non-magnetic probe station with a conventional DC 4-probe measurement set up. A Keithley 2400 sourcemeter was used to supply a sensing current of 50 μA and to apply annealing currents of (0.001 – 10) mA. The pulse length of the heating current was varied to change the Joule heating induced in the pillar up to 500 μs. Due to the extremely small variations in resistance, a Keithley 2182a nanovoltmeter was used for the sensing.

Fig 1(a) shows the resistance change in a (150 x 100) nm GMR pillar after the repeated current applications. At low currents of 50 μA, the same as the sensing current, very little change is observed. However, as the current intensity and pulse length increase to 500 μA and 500 μs an asymptotic decrease in the device resistance is observed. This change in irreversible and is therefore easily separated from the change in resistance incurred by simple temperature dependence. The TEM diffractogram shown in fig. 1(b) confirms that this heating has contributed to crystallisation of the CFAS layer. The {220} reflections of the CFAS are clearly visible spots, indicating a strong $B2$ texture in the layer. This is a significant improvement on the disordered/weakly crystalline as deposited state previously reported. Further results and discussion will be presented at the conference.

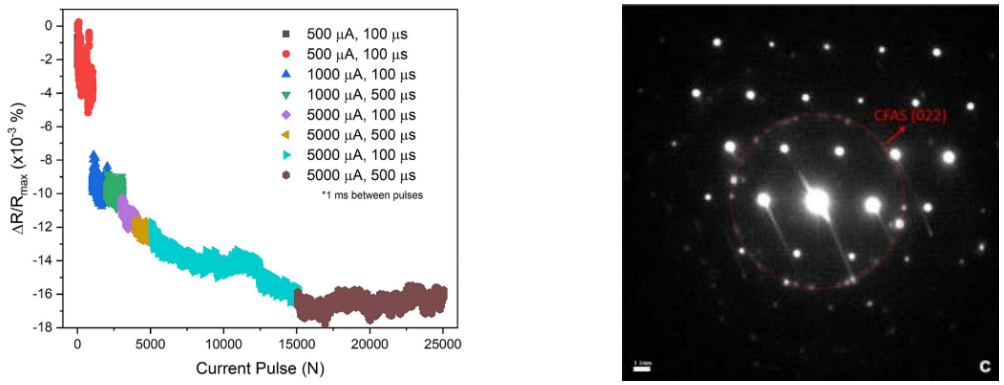

Fig 1: a) The change in the resistance of a (150 x 100) nm nanopillar after a series of current applications and b) the TEM diffractogram of the CFAS layer after current annealing, showing strong {220} reflections [2].

[1] Frost, W., Samiepour, M. & Hirohata, A *J. Magn. Magn. Mater.,* **484**, 100 (2019).
[2] Frost, W, Samiepour, M, Elphick, K, Hirohata, A, *Scientific Reports,* **11**, 17382 (2021).

Experimental Demonstration of Reservoir Computation using Emergent Domain Wall Dynamics in a Patterned Magnetic Substrate

I T Vidamour[1], C Swindells[1], G Venkat[1], E Vasilaki[2], D A Allwood[1], T J Hayward[1]

[1]Department of Materials Science and Engineering, University of Sheffield, UK, [2]Department of Computer Science, University of Sheffield, UK

Reservoir computing (RC) is a neuromorphic machine learning paradigm where computation is performed using the intrinsic memory and nonlinearity of a dynamical system. Traditionally, the dynamic system is simulated algorithmically using a sparsely connected recurrent neural network, though recent studies show this network can be substituted with a physical dynamic system, realising the paradigm in hardware. In the field of nanomagnetism, many systems have been proposed as potential candidates for RC, including spin torque oscillators (STOs) [1], skyrmion textures [2], superparamagnetic arrays [3], and individual domain walls [4]. However, aside from STOs, few of these proposed systems have been experimentally realised. Here, we experimentally demonstrate RC *in materio* using a single-layer array of interconnected permalloy nanorings with emergent domain wall dynamics [5].

First, we show how data can be encoded to the array by modulating the amplitude of an applied rotating magnetic field, and how we can extract information on the magnetic state of the array through anisotropic magnetoresistance (AMR) measurements. These measurements demonstrate that the array's dynamics have a highly non-linear response to the applied field amplitude, and that they exhibit a fading memory of past inputs, thus meeting the two critical criteria for performing RC. Next, we show how we can control the system's response through appropriate scaling of the applied magnetic field, allowing a broad range of different transfer functions between input and output, with different computational properties.

Finally, we show how these different transfer functions can be exploited to perform spoken and written digit recognition tasks with a high level of accuracy. Furthermore, through optimised scaling of the applied fields, the different computational demands of each task were able to be met on a single device. We believe that the computational versatility, relative simplicity of manufacture, as well as the wide range of available parameter space to explore makes the arrays an exciting platform for neuromorphic computation.

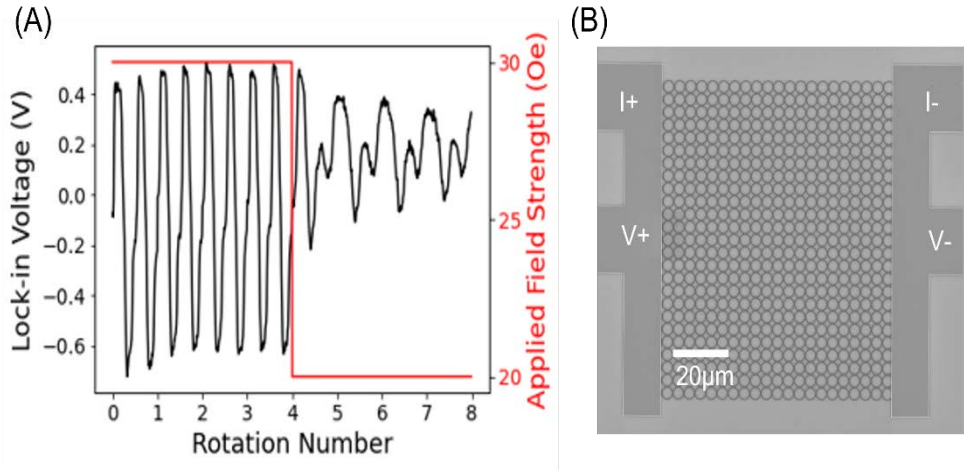

Fig 1: - (A) Measured AMR response for 4 rotations of 30 Oe applied field, followed by 4 rotations of 20 Oe applied field, showing both a nonlinear response and fading memory. (B) Micrograph of patterned nanoring array and electric contacts taken from RAITH Voyager electron beam lithography system.

[1] J. Torrejon *et al.*, "Neuromorphic computing with nanoscale spintronic oscillators," *Nature*, vol. 547, no. 7664, pp.428–431, Jul. 2017

[2] D. Pinna, G. Bourianoff, and K. Everschor-Sitte, "Reservoir Computing with Random Skyrmion Textures," *Phys. Rev. Appl.*, vol. 14, no. 5, p. 054020, Nov. 2020,

[3] A. Welbourne *et al.*, "Voltage-controlled superparamagnetic ensembles for low-power reservoir computing," *Appl. Phys. Lett.*, vol. 118, no. 20, p. 202402, May 2021, doi: 10.1063/5.0048911.

[4] Ababei, R.V. Neuromorphic computation with a single magnetic domain wall. Sci Rep 11, 15587 (2021).

[5] R. W. Dawidek *et al.*, "Dynamically-Driven Emergence in a Nanomagnetic System," *Adv. Funct. Mater.*, vol. 31, no. 8, 2021.

Obtaining additional behaviour from magnetic ring arrays for reservoir computing

G Venkat[1], I Vidamour[1], C Swindells[1], T J Hayward[1], P W Fry[2] , F Maccherozzi[3] , S S Dhesi[3] , R Allenspach[4], and D A Allwood[1]

[1]Department of Materials Science and Engineering, University of Sheffield, UK, [2]Nanoscience and Technology Centre, University of Sheffield, UK, [3]Diamond Light Source, Harwell Science and Innovation Campus, UK, [4]IBM Research-Zurich, Switzerland

Stochastic behaviour has traditionally been a limiting factor in developing nanomagnetic technology. Recently, we have shown complex probabilistic, emergent behaviour in interconnected nanowire ring arrays [1-2] which is particularly useful for a novel form of neuromorphic computing called 'reservoir computing' (RC) which is highly efficient for time domain processing of signals [3]. We have also simulated reservoir computing with such arrays for recognising spoken digits [2]. Since there is a requirement of processing different tasks and data using RC, there is a need to derive additional and varied complex behaviour from physical systems.

Here we show magneto-optic Kerr effect (MOKE) measurements of ring arrays of varying wire widths driven by in-plane rotating magnetic fields. The arrays consisted of 10 nm thick rings of $Ni_{80}Fe_{20}$ patterned with electron beam lithography. The MOKE measurement procedure involves applying a 150 Oe saturating field cycle followed by 30 cycles of a rotating field of amplitude H_{rot} [2]. Since the rotating field drives domain walls (DWs) around the rings, the clock frequency component of the Fast Fourier transform (FFT) of the Kerr

signal relates to the propagating DW state population N_{prop}. This is shown in Fig. 1(a) for different ring widths as a function of H_{rot}. The field at which saturation is observed increases with decrease in ring width due to shape anisotropy [4]. The intermediate decrease in N_{prop} is an emergent state of DWs possibly due to the formation of vortices as indicated by X-ray photoemission electron microscopy (XPEEM) image (Fig. 1(b)) for the 400 nm wide array. Furthermore, the responses of arrays with rings of different width leading to and away from the emergent state are more asymmetric as the ring width decreases.

Micromagnetic simulations using MuMax[3] of single junction rings were performed with rotating fields for 300 and 400 nm wide rings (Figs. 1(c)&(d)). We observe that while the DWs for the 300 nm rings depin from the junction and subsequently move along the ring (leading to a stochastically higher N_{prop}), the DWs for the 400 nm rings tend to stretch and remain in contact with the edges at the junction before completely depinning. This difference in DW population along with a possible role of increased relative surface roughness can explain the difference in behaviour in the MOKE responses. We expect that these varied responses from ring arrays of different widths are essential for obtaining additional processing capabilities in reservoir computing using magnetic rings.

[1] Negoita et al., J. Appl. Phys. 114, 013904 (2013).
[2] Dawidek et al., Adv. Funct. Mater., 2008389 (2021).
[3] Jensen et al., ALIFE 2018: The 2018 Conference on Artificial Life 15, (2018).
[4] Dumpich et al., J. Magn. Magn., 248, 241 (2002).

Thermal and edge roughness effects on domain wall based reservoir computing

R V Ababei[1], M O A Ellis[2], I T Vidamour[1] , D S Devadasan[1], D A Allwood[1], E Vasilaki[2], and T J Hayward[1]

[1] Department of Materials Science and Engineering, University of Sheffield, UK, [2]Department of Computer Science, University of Sheffield, UK

The complex non-linear dynamics inherent in many magnetic systems are ideal for a class of machine learning algorithms known as reservoir computing (RC) [1]. As an alternative to the increasing energy demand of deep neural networks, RC exploits a fixed network or dynamical system to transform input data so that it is linearly classifiable offering high performance with low training times. Recently it has been demonstrated that a single magnetic domain wall (DW) pinned between two anti-notches can be used to perform computation within the RC paradigm [2].

Here, we demonstrate the viability of this DW reservoir at finite temperature and with edge roughness effects. The dynamics of the DW are modelled using a 1d collective coordinates model with added thermal noise and an edge roughness field. The edge roughness field arises from an effective energy term that varies randomly along the length of the nanowire in discrete sections of 20 nm steps. The performance of the DW reservoir was tested on a simple classification task of recognising whether a datapoint is part of a sine or square wave. Fig. 1.a) shows the impact of thermal noise on RC performance since at 0K 100% accuracy is achieved. Finite temperature performance can be improved by using a larger input field scaling parameter (ΔH) and increasing the cross-sectional area of the wire, reaching 93% accuracy at ΔH=2.5 kA/m. Edge roughness again degrades performance, but optimal input field parameters can be chosen to recover a performance of 89% with ΔH=0.5 kA/m. This work validates the potential of this device for neuromorphic computing with realistic operating conditions and shows how DW devices can be optimised for such cases.

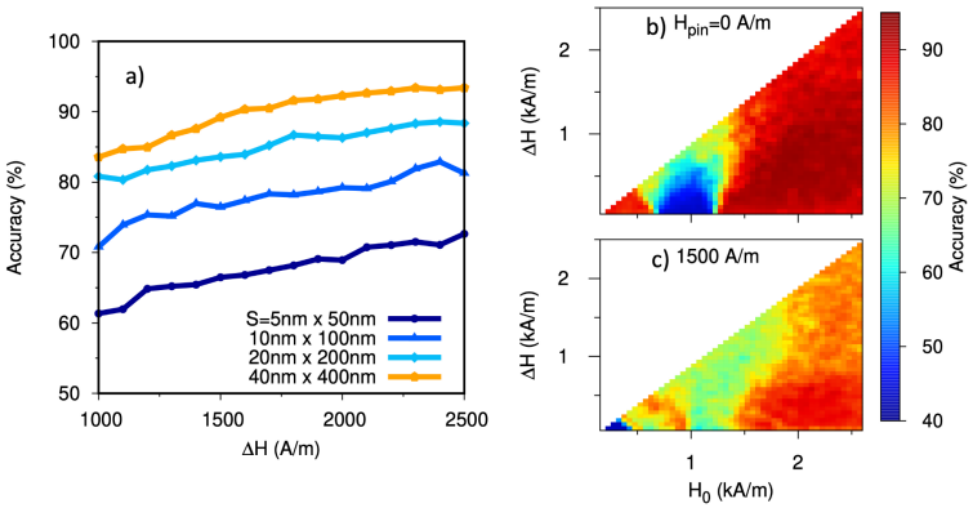

Fig. 1: a) Classification accuracy at 300K with 100 neurons as a function of input field scaling (ΔH) for increasing wire cross-section. b) and c) classification accuracy maps for edge roughness magnitudes of 0 and 1.5 kA/m respectively over a range of input field offset and scaling parameters.

[1] Grollier et al. Nat Electron 3, 360–370 (2020)
[2] Ababei et al. Sci Rep 11, 15587 (2021)

Voltage Controlled Superparamagnetic Ensembles for Low Power Reservoir Computing

A Welbourne[1], A L R Levy[3] , M O A Ellis[2] , H Chen[1] , E Vasilaki[2], M J Thompson[1] , D A Allwood[1], and T J Hayward[1]

[1]Department of Materials Science and Engineering, University of Sheffield, UK, [2]Department of Physics, École Polytechnique, France

Physical reservoir computing is gaining traction as a bio-inspired, machine-learning approach to solving the computational problems, such as speech recognition and prediction of chaotic time series, that are fundamental to modern technology [1]. Many magnetic systems fulfil the requirements of hardware-based reservoirs (non-linearity, fading memory, and a reproducible response) and single devices, subject to a temporal input sequence, can replace algorithms on complex networks of transistors [2]. This offers the potential for compact devices, with reduced energy costs.

Here, we propose voltage-controlled superparamagnetic ensembles as ultra-low-energy reservoirs. In these devices, thermal noise is utilised to drive dynamics and data input is provided by strain-mediated voltages [3]. Using an analytical model (confirmed by micromagnetics) of the response of the system [4], we simulate (Fig. 1a) the physical reservoir. By inputting a temporal sequence and training a single layer of output weights, we have performed standard machine learning benchmarks with competitive performance spoken digit recognition (TI-46) with 95 % accuracy, and chaotic time series prediction (NARMA10) with error (NRMSE = 0.42) comparable to current reservoir approaches [1,2].

We also explore how the use of a non-standard delayed feedback (where the delay time differs from the intrinsic timescale of the input) can provide substantial error reductions in chaotic time series prediction tasks. Fig. 1b illustrates how high performance (NRMSE ≈ 0.2) on the NARMA10 task can be maintained on timescales from τ = 1.4 μs (KV/K_BT = 20) to τ = 66 ms (KV/K_BT = 50) by tuning the strength of the delayed feedback. Further exploration examines the effect of temperature fluctuations on the system.

We suggest that the low energy consumption expected for these voltage-controlled and thermally-driven devices makes them ideal candidates for edge computing applications, where high performance is needed at very low latency and power.

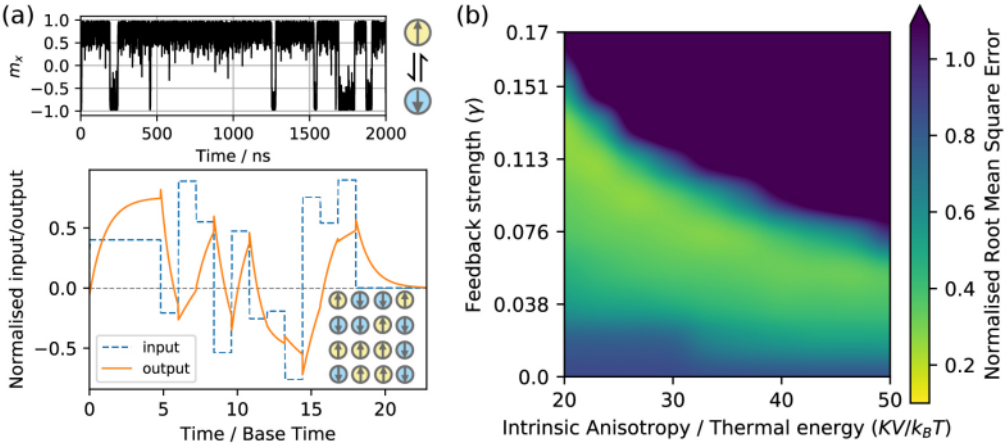

Fig. 1: (a) Superparamagnetic ensemble. Applied strain biases dwell times of individual dots in up versus down states. A reproducible non-linear response with fading memory emerges from the ensemble average of many stochastic nanodots subject to the same temporal input. (b) Performance in chaotic time series prediction (NARMA10) as a function of uniaxial anisotropy strength (normalized by thermal energy). Performance is maintained across a range of timescales by tuning the strength of delayed feedback into the reservoir.

[1] L. Appeltant, et al., Nature Communications, Vol. 2, p.468 (2011).
[2] J. Grollier, et al., Nature Electronics, Vol. 3, p.360-370 (2020).
[3] A. Welbourne, et al., Applied Physics Letters, Vol. 118, p.202402 (2021).
[4] O. Hovorka, et al., Applied Physics Letters, Vol.97, p.062504 (2010).

General 2

(Invited) Magnetic Nanoparticles as a Theranostic Platform for Cardiovascular Diseases

Alan Harper[1,2], Antonio Santana-Otero[3], Maneea E Sharifabad[2], Daniel Ortega[3,4,5], Neil D Telling[2], and David Cabrera[2]

[1]School of Medicine, Keele University, UK, [2]School of Pharmacy and Bioengineering, Keele University, UK, [3]iMdea Nanociencia, Campus Universitario de Cantoblanco, Spain, [4]Condensed Matter Physics department, Faculty of Sciences, Spain, [5]Institute of Research and Innovation in Biomedical Sciences of Cádiz (INiBICA), University of Cádiz, Spain

In this talk we will discuss how magnetic nanoparticles can improve current treatment and diagnostic methods of venous thromboembolism (VTE). VTE is a condition where blood clots formed in the veins of the legs travel through the circulatory system and lodge in the lungs, leading to significant complications and death. Current treatment of venous thromboembolism involves the systemic administration of either anticoagulants to prevent further thrombus growth, or thrombolytic enzymes to try to lyse the clot. Yet systemic circulation of both pharmacological agents often leads to major unwanted bleeding in patients.

By functionalising MNPs with anti-fibrin antibodies and the clot-busting enzyme tissue plasminogen activator (tPA), MNPs can target blood clots to deliver tPA locally and potentially reduce secondary effects associated with systemic circulation of tPa. MNPs can additionally be magnetically excited to deliver a localised heating to the blood clot to increase tPa activity, as well as breakdown the cellular barriers on the thrombus surface to all fibrinolytic enzymes to permeate deeper into the clot (Figure 1). Interestingly, immobilisation of MNPs in the structure of the clot has the potential of tracking blood clot formation by monitoring Brownian relaxation of MNPs with AC susceptometry, conferring to MNPs the potential to become a diagnostic tool in blood clotting disorders. Combining future in vitro studies in a humanised vein model and in vivo studies to confirm the biocompatibility of MNPs, we aim to demonstrate the feasibility of using MNPs as a more effective and safer theranostic approach for VTE.

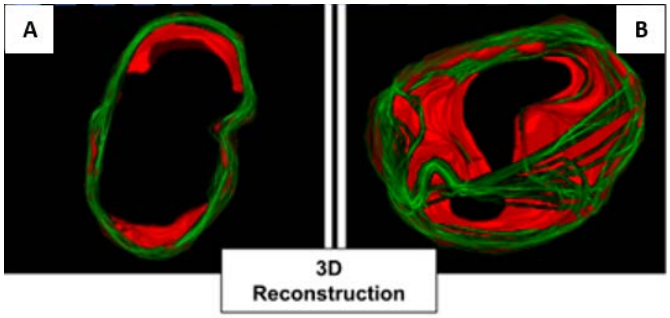

Fig. 1. 3D reconstruction of a blood clot (A) untreated or (B) treated with nanoparticle-mediated magnetic hyperthermia. Green colour: Blood clot contour; Red colour: fluorescent dextran with similar molecular weight to that of clot-busting enzymes.

This work is funded by The Wellcome Trust through a Sir Henry Wellcome Postdoctoral Fellowship and a Seed Award in Science Grant.

Elasto-Magnetic Pumps for Point-of-Care Diagnostics

Jacob Binsley, Stefano Pagliara and Feodor Ogrin

Department of Physics and Astronomy, University of Exeter UK

Microfluidic lab-on-a-chip (LOC) devices are pivotal for the progression of point-of-care (POC) diagnostics. Their effectiveness has been shown recently with the widespread advent of the lateral flow immunoassays used for rapid testing of COVID-19[1]. However, depending on passive flow generation such as capillary forces does not easily allow for prolonged operation times or constant flow rates.

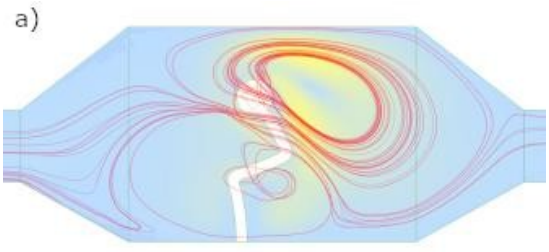

We have seen in recent decades, a surge in the development of integrated pumping solutions; miniature on-board pumps which can enhance the capability of POC devices outside of laboratory environments[2]. Pumping and swimming on this scale is non-trivial. Heavily damped Aristotlean mechanics must be considered and fluid flow must be generated through a non-reciprocal sequence of pump motions.

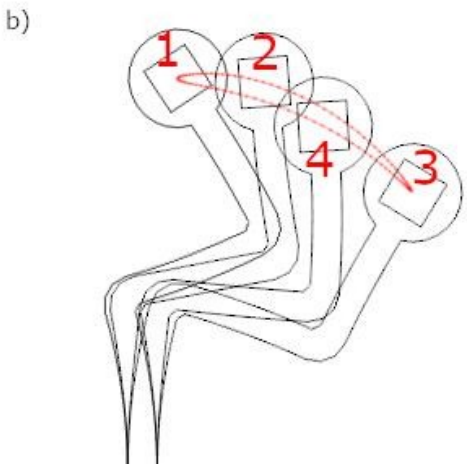

We have developed a possible novel pumping solution and have fabricated and tested an experimental, elasto-magnetic

micropump inspired by Purcell's 3-link swimmer[3]. This design, consisting of 3 elasticated links made from PDMS, is coupled to an external magnetic driving field via the inclusion of a small Neodymium Iron Boron magnet. When provided with a weak, uniaxial oscillating driving field with flux density of 10s of gauss and frequency in the range of 10s of Hz, the device produces tuneable and reversible fluid flow.

During our most recent investigations, we modelled this system numerically using COMSOL Multiphysics to not only verify our experiments, but to explore the device more deeply and gain an understanding of how this system may be optimised. These new numerical results will be the main subject of this talk and offer valuable and very visual insight into bio- inspired pumping mechanisms for lab-on-a-chip POC devices.

The device is outlined in the attached figure, a) represents the fluid motion at one point in time during operation, b) represents the non-reciprocal motion of the pump, tracing the centre of the pump head through the sequence $1 \longrightarrow 4$.

[1] Andryukov, Boris G. "Six decades of lateral flow immunoassay: from determining metabolic markers to diagnosing COVID-19." AIMS microbiology 6.3 (2020): 280.
[2] Boyd-Moss, Mitchell, et al. "Self-contained microfluidic systems: a review." Lab on a Chip 16.17 (2016): 3177-3192.
[3] Binsley, Jacob L., et al. "Microfluidic devices powered by integrated elasto- magnetic pumps." Lab on a Chip 20.22 (2020): 4285-4295.

SAR determination from temperature measurement using repeated heating-cooling cycles

Sergiu Ruta 1, Yilian F. Afonso 2, Samuel E. Rannala 3, Sabino Veintemillas-Verdaguer 4, M. Puerto Morales 4, David Serantes 5, Luc ía Gutié rrez 2, Roy W Chantrell 3

1 College of Business, Technology and Engineering, Sheffield Hallam University, UK 2 Department of Analytical Chemistry, Universidad de Zaragoza, Spain 3 Department of Physics, University of York, UK 4 Materials Science Institute of Madrid (ICMM/CSIC), Spain 5 Applied Physics Department, Universidade de Santiago de Compostela, Spain

In recent years magnetic hyperthermia has been proposed to help a range of biomedical applications such as a non-invasive alternative for cancer treatment. Accurate knowledge of the heating performance of magnetic nanoparticles (MNPs) under AC fields is critical for the development of hyperthermia-mediated applications. Usually, the heating efficiency reported in terms of the specific absorption rate (SAR) is obtained from the temperature variation (ΔT) vs. time (t) curve (fig. 1a). Most estimates are based on simplified temperature dynamics such as adiabaticity (initial slope) or assuming Newton's law of cooling where the temperature evolution is defined as:

$$\frac{dT}{dt} = -a(T - T_{env}) + S_0,$$

where a stands for a characteristic relaxation time of the system, and S0 is defines the heating source (SAR) and T_{env} is the environmental temperature. Such estimates are subjected to huge uncertainty due to dynamic changes in the sample or even from the measurement device/environment. For example, large variations in the heating efficiency of a given batch of particles have been reported when measured in different laboratories [1], under a priori the same experimental conditions.

In general, to have a correct description of the temperature evolution during hyperthermia protocol we need a detailed temperature profile both in time and space. This requires solving the full heat diffusion equation or the bioheat equation if the magnetic nanoparticles are in a biological environment [2]. We show, based on simulated heat diffusion, that for general magnetic hyperthermia conditions the heat profile is not uniform inside the sample. As a consequence the determination of SAR as described above leads to large errors (figure 1c).

In this work, we present a novel protocol, in which simple temperature measurements combined with eq. 1 can be used to obtain a more reliable SAR value, independent of environmental conditions (e.g. the device/laboratory). The proposed protocol is based on a set of repeated heating-cooling cycles as illustrated in figure 1b. To validate the protocol test cases are generated by numerically solving the heat diffusion equation considering the liquid, sample holder and surrounding environment (air). Although the temperature profile is not uniform, during a single heating-cooling cycle, there is a minimum variation in the spatial temperature profile between the final heating and the initial cooling processes. This allows for eq. 1 to be used at the transition from heating to cooling, leading to a more precise SAR determination. Examples of the error in determining SAR using a single (1c) or repeated heating-cooling cycles (1d) are shown in figure 1. The protocol has been successfully applied to experimental data of magnetite particles in liquid samples.

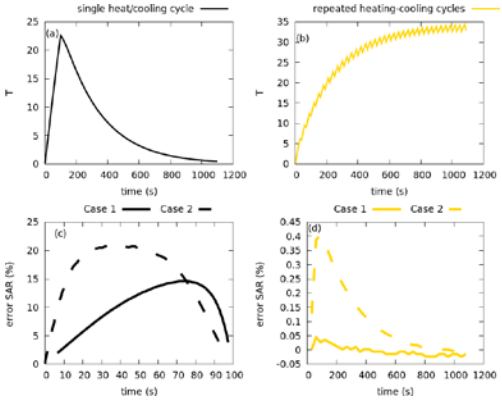

Figure 1: Diagram showing the single heat/cooling cycle (a) and the new protocol of repeated heating-cooling cycles (b). Examples of error in SAR determination based on equation 1 for two test cases using the single heat/cooling cycle(c) and repeated heating-cooling cycles (d).

The proposed protocol will enable more accurate comparison of the SAR data generated by different laboratories. Also, the new protocol can detect any time variation of SAR as for example during cluster formation during hyperthermia procedure, or variation of particle properties over time.

[1] Wells, J.; Ortega, D.; Steinhoff, U.; Dutz, S.; Garaio, E.; Sandre, O.; Natividad, E.; Cruz, M. M.; Brero, F.; Southern, P., et al. Int J Hyperthermia 2021, 38, 447–460.
[2] Pennes, H. H. Journal of applied physiology 1948, 1, 93–122.

Thinking Magneto-ionics: Neuromorphic Functionalities in Magnetic Nitride Films

Julius de Rojas[1,2], Zhengwei Tan[1], Alberto Quintana[3,4], Enric Menéndez[1] and Jordi Sort[1,5]

[1]Departament de Física, Universitat Autònoma de Barcelona, Spain [2]Department of Physics, Durham University, UK [3]Department of Physics, Georgetown University, USA, [4]Institut de Ciència de Materials de Barcelona (ICMAB-CSIC), Campus UAB, Spain.[5]Institució Catalana de Recerca i Estudis Avançats (ICREA), Pg. Lluís Companys 23, Spain

Magneto-ionics is an emerging field where an applied electric field is used to drive ions into and out of a target material, undergoing changes in stoichiometry, oxidation state, and crystal structure, in turn producing large, cyclable, and low-energy tuning of magnetic properties. Here, we will present nitrogen-based magneto-ionics in transition metal nitride thin films (CoN & FeN) biased under liquid electrolyte gating. Nitrogen magneto-ionics can undergo reversible *on-off* ferromagnetic transitions more quickly than their oxygen-based counterparts (Co_3O_4) while using less energy.[1,2] This is attributed to the relatively smaller energy barrier for ion diffusion and the lower electronegativity of nitrogen when compared with transition metal oxide films. In addition, nitrogen magneto-ionics transports ions via a remarkable plane-wave-like

migration front, allowing for the imprinting of magnetic spin textures or possible implementation in 3D memory devices. We will further show that sub-second nitrogen magneto-ionics can be achieved by decreasing the CoN film thickness down to 25 nm, an improvement of 1 order of magnitude. Finally, we will show that pulsed DC biasing reveals neuromorphic functionalities. The cumulative effects of pulsed DC biasing at frequencies between 1 – 100 Hz allows for spike time-dependent plasticity (learning and forgetting functionalities), and, in the case of thin CoN films (≤ 50 nm) pulsed at high frequencies (≥ 100 Hz), for *learning while under deep sleep* (with zero external energy input). The competition between high ionic transport rates in CoN films and the DC pulse frequency results in a balancing act between the generation (*on*) and partial depletion or recovery (*off*) of ferromagnetism, producing a controllable ion accumulation effect at the interface between the films and the electrolyte.[3] Practically, this can be viewed as a logical function which allows the device to toggle between auto-learning or forgetting as-needed, with zero external energy input. This constitutes a novel approach to emulate specific neural functionalities (*e.g.*, learning under deep sleep) that are not easily achievable using other classes of materials currently employed in neuromorphic computing applications.

[1] de Rojas, J. et al. Voltage-driven motion of nitrogen ions: a new paradigm for magneto-ionics. Nature Communications 11, 5871 (2020).
[2] de Rojas, J. et al. Magneto-Ionics in Single-Layer Transition Metal Nitrides. ACS Applied Materials & Interfaces 13, 30826–30834 (2021).
[3] Z. Tan et al. Brain-inspired magneto-ionics: emulation of stimulated and post-stimulated neural learning. Submitted (2021).

Posters

Topic: Bulk Magnetic Materials

(P1) Band magnetism in doped GdTSi compounds

Sergey Platonov[1], Anatoly Kuchin[1], Roman Mukhachev[1,2], Alexey Lukoyanov[1,2], Alexey Volegov[1,2], Vasilii Gaviko[1,2], Mari Yakovleva[1]

1. Institute of Metal Physics of Ural Branch RAS, Ekaterinburg, Russia, 2. Ural Federal University, Ekaterinburg, Russia

The GdTSi intermetallic compounds crystallize in the tetragonal CeFeSi-type structure (*P4/nmm*) which is built from alternating (001) layers with the sequence: Gd-Si-T2-Si-Gd-Gd-Si-T2-Si-Gd (T = Ti, Mn, Fe, Co)[1]. The hybridization between Si *p* and T 3*d* states causes the absence of the magnetic moment of Fe or Co in the GdTSi compound. Thus, the magnetic properties of the GdTSi compounds depend on the interatomic distances, as well as on the number of 3*d* electrons. It is of interest to study the magnetic, magnetothermal and structural properties of the $GdFe_{1-x}T_xSi$ substitutional alloys with T = Ti[1], V, Cr, Fe, Ni with different atomic radii (1.462, 1.346, 1.282, 1.274, 1.246 Å) and the number of 3*d* electrons (2, 3, 5, 6, 8). Equiatomic alloys GdCrSi and GdVSi do not seem to exist[1]. GdNiSi crystallizes in the orthorhombic TiNiSi-type crystal structure[1].

In the $GdFe_{1-x}T_xSi$ systems, T = Cr, V, Ti[2], the lattice parameter *c* increases rapidly and the parameter *a* slightly decreases, while for the $GdFe_{1-x}Ni_xSi$ system, the parameter *c* noticeably decreases and the parameter *a* slightly increases with increasing content of T. It was found that the Curie temperature T_C sharply increases from 130 K to 255 K and 250 K for $GdFe_{1-x}Cr_xSi$ and $GdFe_{1-x}V_xSi$ and decreases to 98 K for $GdFe_{1-x}Ni_xSi$ when *x* changes from 0 to 0.5, 0.3, and 0.3, respectively. This result is explained within the framework of the mechanism proposed to explain a similar sharp increase of T_C up to 185 K in the $GdFe_{1-x}Ti_xSi$, *x*=0-0.1 system[2]. Calculations of the electronic structure indicated that the Fermi level E_F for GdFeSi is localized on the right slope of the density of states $N(E)$ peak[2]. In the rigid band shift method, when Fe is replaced by Ti[2], V, Cr or Ni in GdFeSi, E_F shifts to the left or to the right along the slope due to the smaller or larger number of 3*d* electrons in the Ti (2), V (3), Cr (5) or Ni (8) atoms compared to the Fe (6) atom. As a result, the density of states at the Fermi level $N(E_F)$ and, therefore, T_C in the $GdFe_{1-x}T_xSi$ systems increases with T=Ti, V, Cr or decreases with T=Ni, within the framework of the model of effective *d–f* exchange interaction in R-3*d* metal intermetallics, in which $T_C \sim N(E_F)$[3]. Earlier[2], we assumed that the possible maximum increase of T_C, which can be caused by the monotonic increase of $N(E_F)$, was not realized in the $GdFe_{1-x}Ti_xSi$ system because of the solubility limit $x \sim 0.1$. In the present work, we confirm this assumption in the case of the other 3*d* elements T = V, Cr, Ni having the atomic radius smaller and therefore the solubility higher than Ti.

This study was supported by the grant of Russian Science Foundation No. 18-72-10098, https://rscf.ru/en/project/18-72-10098/

[1] S. Gupta, K. Suresh, Review on magnetic and related properties of RTX compounds, J. Alloys Compd. 618 (2015) 562-606.
[2] A.G. Kuchin, S.P. Platonov, A.V. Lukoyanov, A.S. Volegov, V.S. Gaviko, R.D. Mukhachev, M.Yu. Yakovleva, Remarkable increase of Curie temperature in doped GdFeSi compound, Intermetallics 133 (2021) 107183.
[3] A. Cyrot, M. Lavagna, Density of states and magnetic properties of the rare-earth compounds RFe_2, RCo_2 and RNi_2, J. de Phys. 40 (1979) 763-771.

(P2) Tailoring the structural and magnetic properties of $CoFeNi_{0.5}AlCr_*$

Mark Anis, James Harris, Aris Quinata-Nedelcos, Yunus Azakli, Zhaoyuan Leong and Nicola Morley

Department of Materials Science and Engineering, University of Sheffield, UK

Multi-component alloys (MCAs) contain > 4 elements in near equimolar fractions which can lead to single or dual phase alloys. In dual phase alloys, the interplay between individual phase stabilities can lead to promising magnetic properties [1,2], which requires further investigation. Structural and magnetic properties changes in the CoFeNi0.5AlCrx alloy were investigated as a function of Cr concentration (x: 0.25, 0.5, 0.75, and 1.0) and post-synthesis heat treatment: 1423K for 5 or 10 hours and furnace cooled or water quenched. This temperature was chosen as a minimum in the Gibbs free energy difference between the solid solution and the B2 phase is calculated and observed for x: 0.5at 1423K; with this the HT can be employed to stimulate nanoprecipitate formation. Past work suggests that magnetisation is maximised just before the compositions where nanoprecipitates stabilise.

Our results confirm that nanoprecipitates were observed in x: 0.5 via SEM (Fig 1a). The water quenched 10hrs (WQ10) and furnace cooled 5 and 10h (FC5 and FC10) samples showed nanoparticles within a matrix. The water quenched 5hrs (WQ5) alloy had no clear separation of phases which corresponded with the broad Curie temperature transition observed and is consistent with expected solid solution stability above 1410K.

In general, Cr addition to CoFeNi0.5Al moved stability from single-phase to dual-phase BCC. The phases correspond to two magnetic phases inferred through the experimental MT curves: i. High Curie temperature (Tc) almost independent of Cr, ii. Low Curie temperature decreasing with increasing Cr (Fig 1b). These are expected to be FeCr and AlCoNi rich from our enthalpy-of-mixing pair analysis.

For the magnetocaloric properties, it was found that Cr decreased the change in entropy (ΔS) for both magnetic transitions. For all the alloys, the lower Curie temperature had a smaller ΔS compared to the higher Curie temperature but a larger refrigerant capacity due to a wider temperature transition. CoFeNi0.5AlCr0.25 possesses the highest magnetisation which agrees with our hypothesis, and the two Curie temperature peaks were within 100K of each other, such that the ΔS curves overlapped giving a wider temperature range, and a refrigerant capacity of 150 J/K. Thus tuning the two transitions to be <100 K of each other increases the refrigerant capacity.

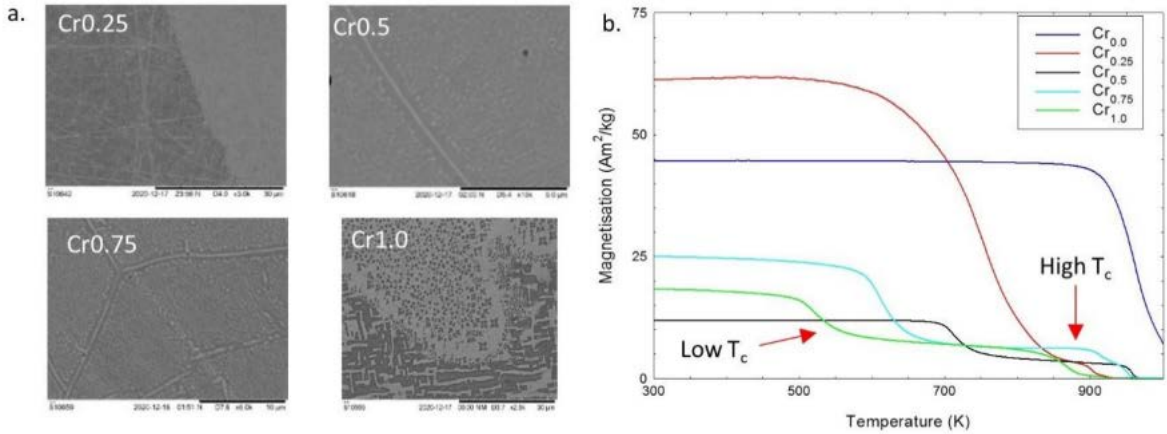

Fig 1a. SEM images of CoFeNi0.5AlCrx alloys and 1b. Magnetisation as a function of temperature for an applied field of 250 Oe.

[1] N. A. Morley, C. R. B. Lim, J. Xi , A. Quintana-Nedelcos, Z. Leong, Sci Rep, 10, 14506, (2020)
[2] A Quintana-Nedelcos, Z Leong, N. A. Morley, Materials Today Energy 100621 (2021)

(P3) Unravelling magnetoelectric effects in doped M-type hexaferrites

O Alsaqer [1,2], and S A Cavill[1]

[1]Department of Physics and Astronomy, University of York, York, UK, [2]Department of science and technology, University College at Nairiyah, University of Hafr Albatin, Saudi Arabia

The field of magnetoelectric (ME) multiferroicsis driven by the promise of controlling magnetism using applied electric fields, offering the possibility of a new generation of ultra-low power devices. Among the few room temperature single-phase ME multiferroics reported, hexaferrites show potential for device applications as they exhibit a low field ME effect at room temperature [1]. The most common hexaferrite, the M-type, is arranged in different repeating sequences of basic building blocks; the R and S layers. Fe3+ cations occupy both octahedrally (Oh) and tetrahedrally (Td) co-ordinated sites in the S block (Wyckoff positions 2a and 4f1) and octahedral sites (12k and 4f2) in the R block. The Sr ion located at the 2d positions strongly distorts the octahedral site located at 2b, giving rise to a bipyramidal 5-fold co-ordination which induces a large uniaxial magnetic anisotropy parallel to the caxis. However, Co2+ and Ti4+ substitutions for Fe3+ dramatically alter the magnetic properties. Ti substitutions at the 12k sites decrease the exchange coupling between spins in the R and S blocks, whilst the Ti and Co substitutions change the magnetic anisotropy from uniaxial to an easy cone of magnetization tilted away from the c-axis. The result is to stabilize a conical magnetic structure [2], which is of high interest in the field of magnetoelectrics.

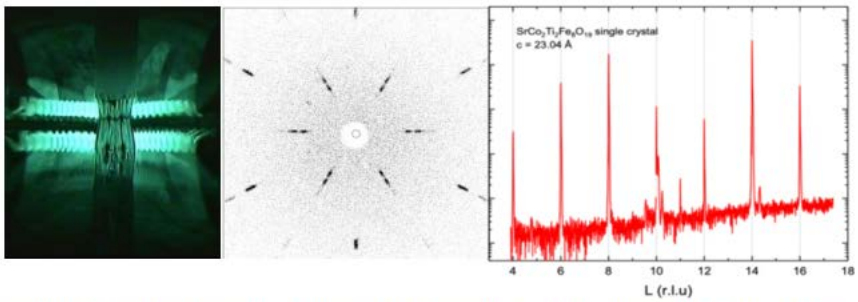

Figure 1: (a) Zone float growth of $SrFe_8Co_2Ti_2O_{19}$ single crystal. (b) Laue diffraction pattern from crystal grown in (a). (c) Diffraction pattern along L (c-axis).

In this work we present a variable temperature VSM study of Ti - Co doped SrM (SrTi2Co2Fe8O19) and un-doped (SrFe12O19) bulk single crystals grown by the high-pressure floating zone method, see Fig.1a. For the undoped sample collinear magnetic order is observed over the full temperature range (6K – 380K) with strong c-axis anisotropy. For the doped system the sample exhibits an easy cone of magnetization and below room temperature step like anomalies are observed in the M-H loops which we believe are indicative of a metamagnetic transition of the spin cone to either a fanlike structure or collinear order as discussed in [3]. Such features usually are associated with electrical polarization of the material via the inverse Dzyaloshinskii – Moriya model.

[1] Y. Kitagawa et al. Nat. Mater. 9, 797 (2010)
[2] M. Soda et al. Phys. Rev. Lett. 106, 087201 (2011)
[3] Y. Tokunaga et al. Phys. Rev. Lett. 105, 257201 (2010)

(P4) Magnetic Structure and Highly Unusual In-field Behaviour of D-type Erbium Disilicate

Manisha Islam[1], Monica Ciomaga Hatnean[1], Nicholas d'Ambrumenil[1], Pascal Manuel[2], Fabio Orlandi[2], Dmitry Khalyavin[2], Jacques Ollivier[3], Björn Fåk[3], Boris Malkin[4], Geetha Balakrishnan[1], and Oleg Petrenko[1]

[1]Department of Physics, University of Warwick, UK, [2]ISIS Facility, STFC Rutherford Appleton Laboratory, UK, [3]Institut Laue-Langevin, France, [4]Kazan Federal University, Russia

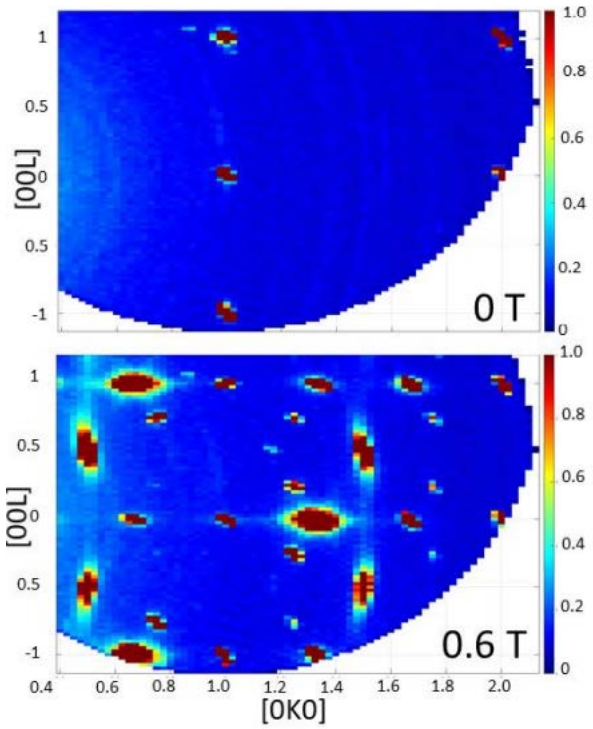

Fig. 1: Intensity maps of single crystal in-field neutron diffraction of Er2Si2O7 measured on IN5 at ILL, with H//a. Magnetic integer (0kl) peaks are observed at zero field until the magnetisation plateau region is reached. The plateau then stabilises at 0.6 T, accompanied by additional magnetic peaks with fractional, non-integer indices. Some of these non-integer peaks are not resolution limited, suggesting shorter-range magnetic correlations

The rare-earth disilicates form seven different crystalline polymorphs and have been found to have promising luminescent and optical properties, making them possible candidates for crystal scintillators and the detection of gamma and X-rays. Despite their interesting polymorphic characteristics, little is known of the magnetic properties of these compounds due to their complex structural phase diagram. The magnetic rare-earth ions within the majority of rare-earth disilicates are arranged in a distorted honeycomb structure, giving potential for fundamental magnetism interest.

Initial predictions of a magnetic order below 1.8 K with a proposed q=0 four-sublattice antiferromagnetic arrangement of the magnetic moments [1] have been recently confirmed via zero-field powder neutron diffraction measurements [2]. Here, both polycrystalline and single crystals of the monoclinic D-type Er2Si2O7 have been synthesised [3] and investigated using powder and single crystal neutron scattering techniques as well as magnetisation measurements.

Our H//a single crystal magnetisation measurements reveal a plateau at 1/3 of saturation, accompanied by a significant increase of the magnetic unit cell. Figure 1 illustrates the dramatic change in the single crystal neutron diffraction patterns when the narrow plateau stabilisation is reached. The magnetic non-integer peaks indexed as (0, k+1/2, l+1/2), (0, k+1/3, l) and (0, k+2/3, l), where k and l are integers during the plateau are surprising as only four sublattices have been confirmed in zero field. We also report that our

crystal field measurements, observed via inelastic neutron scattering suggest an almost ideal Ising system. The dispersionless low-energy excitations low temperature spectrum also demonstrates Ising-like behaviour in lower and higher fields and significantly softens on the magnetisation plateau.

[1] M. J. M. Leask, P. R. Tapster, and M. R. Wells, J. Phys. C Solid State 19, 1173 (1986).
[2] G. Hester, T. N. DeLazzer, et al. Phys. Condens. Mat. 33, 405801 (2021).
[3] M. C. Hatnean, O. Petrenko, et al. Cryst. Growth. Des. 20, 6636-6648 (2020).

Topic: Carbon-based Materials and Molecular Magnetism

(P5) The Impact of Finite Phonon Lifetimes on the Spin Dynamics in Single-Molecule Magnets

Rizwan Nabi, Jonathan M Skeltona, and Nicholas F Chiltona

Department of Chemistry, The University of Manchester, UK

The design of nanoscale information storage devices based on molecular magnets requires preparation of materials with well-designed spin-phonon interactions such that magnetic memory persists at ambient temperatures. Understanding the fine details of spin-phonon coupling is thus crucial in designing new materials for this task. Of crucial importance for molecular spin dynamics is the phonon density of states, which directly impacts the timescale of magnetic memory, and a core part of this is the knowledge of phonon linewidths (lifetimes). Many works use a fixed empirical linewidth of ca. 10 cm^{-1} [1], but others have suggested a strong temperature and energy-dependence to the phonon linewidth [2] (Equation 1). However, the phonon linewidths are, in principle, accessible from first-principles calculations; albeit at extraordinary computational cost. By judiciously choosing a compact, high-symmetry molecular magnet, we have been able to directly tackle this problem, and have performed the full third-order force constant calculations for the high-performance Dy(III) single-molecule magnet, [Dy(bbpen)Br] [1]. We find that the linewidths vary on the order of 0.1 to 10 cm^{-1}, as a function of both energy and wavevector, but the approximation proposed in Equation 1 is far from reality (Figure 1a). These calculations enable us to calculate a fully ab initio phonon density of states (Figure 1b) with which we will subsequently analyse the spin-phonon dynamics.

$$\gamma = (\hbar\omega_j)^2 e^{\frac{\hbar\omega_j}{k_B T}} \Big/ \left(e^{\frac{\hbar\omega_j}{k_B T}} - 1\right)^2 \qquad \text{Equation 1}$$

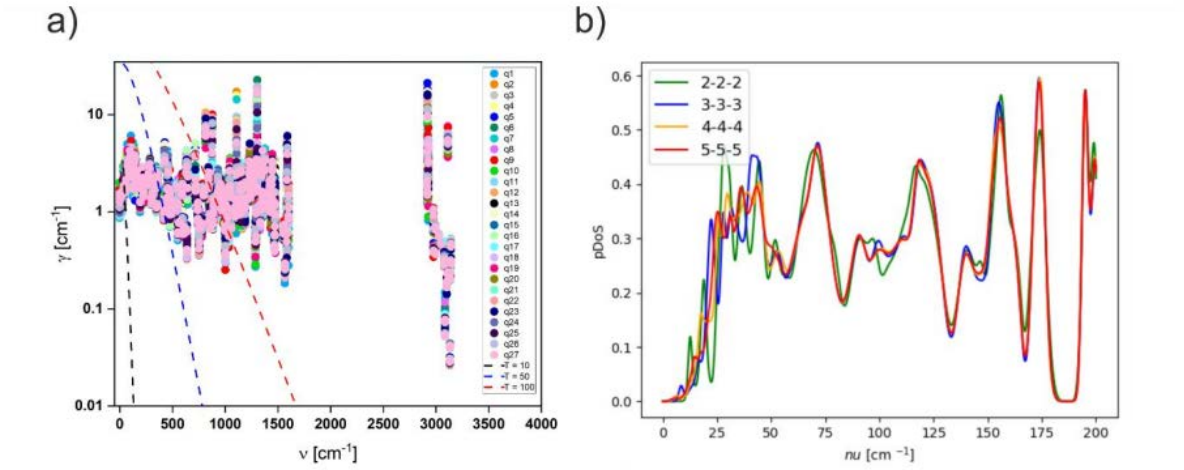

Fig 1: a) Phonon linewidth at unique q vectors in a 5×5×5 mesh of reciprocal space. Dashed lines are plots of Equation 1 at 10 K (black), 50 K (blue), and 100 K (red). b) Low energy pDOS using DFT-calculated line widths for 2×2×2, 3×3×3, 4×4×4, and 5×5×5 meshes of reciprocal space.

[1] D. Reta, J. G. C. Kragskow and N. F. Chilton, J. Am. Chem. Soc., 2021, 143, 5943.
[2] A. Lunghi, F. Totti, R. Sessoli and S. Sanvito, Nature Commun., 2017, 8, 14620.
[3] J. Liu, Y.-C. Chen, J.-L. Liu, V. Vieru, L. Ungur, J.-H. Jia, L. F. Chibotaru, Y. Lan, W. Wernsdorfer, S. Gao, X.-M. Chen and M.-L. Tong, J. Am. Chem. Soc., 2016, 138, 5441

(P6) Characterisation of magnetic relaxation on extremely long timescales

William J A Blackmore, Sophie Corner, Peter Evans, Jack Emerson-King, Gemma Gransbury, David Mills, and Nicholas F Chilton

Department of Chemistry, School of Natural Sciences, University of Manchester, UK

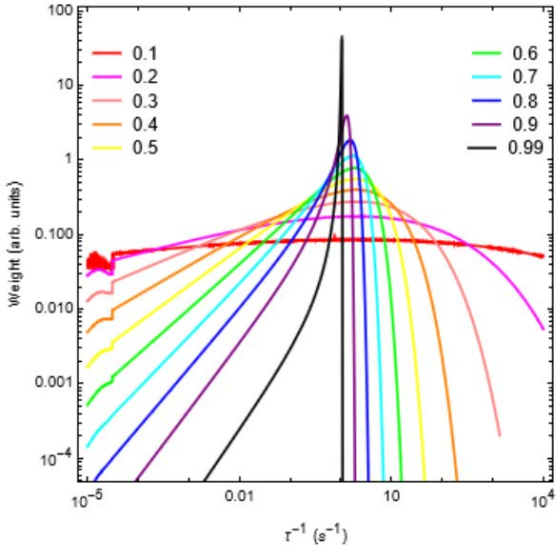

Figure 1: Distribution of the stretched exponential function for τ^*= 1 and different indicated values of β.

Recent advances in the field of single-molecule magnets have led to the development of very slow relaxing species. However, challenges remain in understanding the effect that the local environment has on the quantum tunnelling of magnetisation (QTM) and Raman processes in these materials. This is partly due to the extremely long relaxation times τ that are now being observed. On these timescales, DC decays modelled by the stretched exponential function are used:

$$M(t) = M_{eq} + M_0 \exp\left[-\left(\frac{t}{\tau^*}\right)^{\beta}\right]$$

where τ^* is the "characteristic tau" and β is the stretching factor that parameterises the spread of relaxation rates. For τ^* of the order of a week or longer, it is not feasible to measure DC decays all the way to equilibrium (M_{eq}). Whilst we can calculate M_{eq} theoretically, one cannot model how M(H) approaches M_{eq} for these timescales. This leads to an increasingly large asymmetry and width of the distribution of the rate (Fig. 1), such that the measured τ^* becomes increasingly meaningless. We investigate the distribution of the stretched exponential function to develop a more realistic measure of τ. We compare this to the AC-like

waveform technique pioneered by Hilgar et al to determine the accuracy of our calculated relaxation time [1]. We will also present low-temperature magnetometry measurements of the high-performance SMM $[Dy(Cp^{ttt})_2][BArF]$ [2] secured in eicosane to test this method, and dissolved in dichloromethane and difluorobenzene to explore the effect solvating $[Dy(Cp^{ttt})_2][BArF]$ has on the relaxation processes.

[1] J. Hilgar, A. Butts and J. Rinehart, PCCP. 40, 22302 (2019). Z
[2] C. Goodwin et al., Nat. 548, 439 (2019).

(P7) Intrinsic Magnetism of Spider Dragline Silks

Varun Ranade[1], Ram J Choudhary[2], and Kamal P Singh[1]

[1]Indian Institute of Science Education and Research (IISER) Mohali, India, [2]UGC DAE Consortium for Scientific Research Indore Centre, India

Silk biomaterials have gained a lot of interest in material and biomedical engineering due to their incredible mechanical, optical, biodegradable and biocompatible properties. However, the intrinsic magnetic properties of spider silk have remained unknown. In present work, we studied the intrinsic magnetic properties of pristine spider dragline silks using a SQUID magnetometer and observed that spider dragline silks show ferromagnetism at room temperature without any magnetic doping. A comprehensive elemental analysis of dragline silks revealed absence of any d-block and f-block element in pristine silk. It was confirmed that ferromagnetism in spider dragline silk originate due to carbon radicals formed because of microscopic defects in protein structures. Interestingly, we observed that spider silks exhibit ferromagnetic character over a wide range of temperatures from 5 K up to 400 K. This implies that silk might bring a substantial advance in biomedical and technological sectors including applications like creating silk-based micro/nano-robots for drug delivery and preparing organic magnetic sensors. These findings also hint at the possibility of spiders ingeniously using the ferromagnetic properties of its dragline silk for magnetoreception.

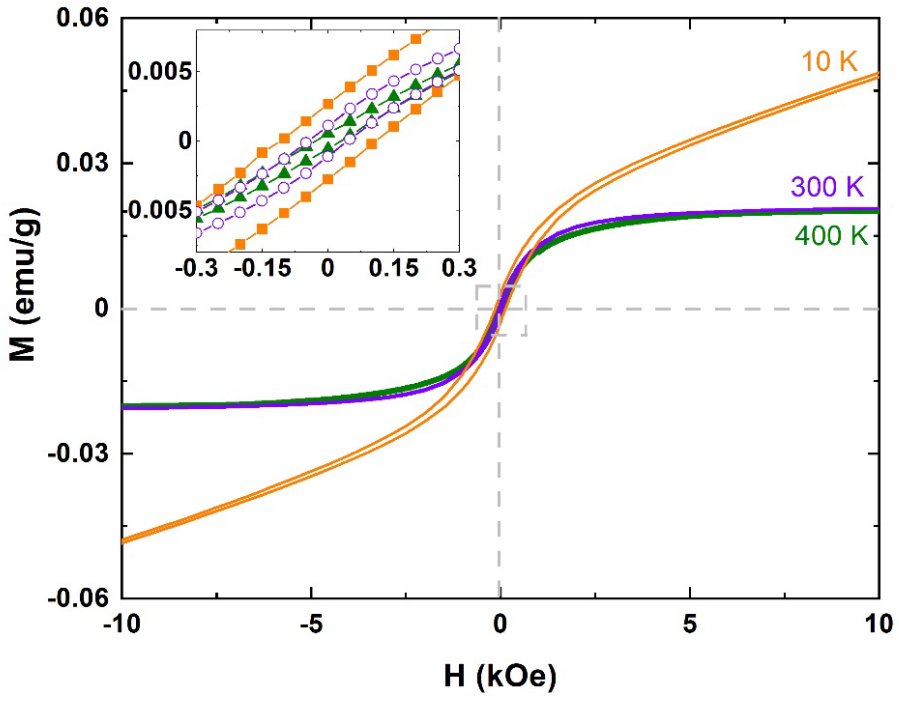

Comparison of Magnetic Hysteresis at Different Temperatures: M-H curves of spider silk at 10 K, 300 K and 400 K. The hysteresis (inset) indicates ferromagnetic character of spider silk at all temperatures. At low temperatures, the magnetization does not saturate even at high magnetic fields and keeps increasing linearly.

(P8) Magnetic and Structural Effects of Boron Migration in C60/CoB/C60 Structures

Daniel Roe[1], Andrew Caruana[2], Sean Langridge[2], and Oscar Cespedes[1]

[1]University of Leeds, UK, [2]ISIS Neutron and Muon Source, UK

Here we study the use of C_{60} as a matrix in which light boron ions can move in and out of to tune magnetic properties of CoB thin films. Initial research has focussed on confirming that B will diffuse from CoB to C_{60} in C_{60}/CoB/C_{60} trilayers when the sample is annealed. In the future, we aim to achieve this via a gate voltage. Similar control of the magnetic and electrical properties of many different materials such as organic semiconductors and complex oxides has already been achieved using ionic liquids [1,2]. Replacing ionic liquids with C_{60} will allow for: UHV deposition, greater functional temperature range and molecular monolayers for nanoscale devices. Current magnetic characterisation shows an increase in saturation magnetisation after annealing which could suggest either migration of boron leading to cobalt-rich regions and/or improved cobalt crystallinity. X-Ray reflectivity shows changes in fringe depth and shape without much change in angular separation, which could be attributed to density changes within the layers. In Raman spectroscopy we observe an increase in the intensity around the C_{60} Hg(1) peak (200-400 cm-1) after annealing at 300° C. This could be an indication of boron carbide formation as boron ions diffuse into the C_{60} layers [3]. This could open new paths of research in nanocarbon thin film batteries and supercapacitors. We will verify the boron migration, changes in the profile of the structure and magnetisation throughout the annealing process by using Polarised Neutron Reflectivity (PNR) with in-situ annealing. Here we aim to utilize the large neutron absorption cross section of B to determine its distribution throughout the sample [4].

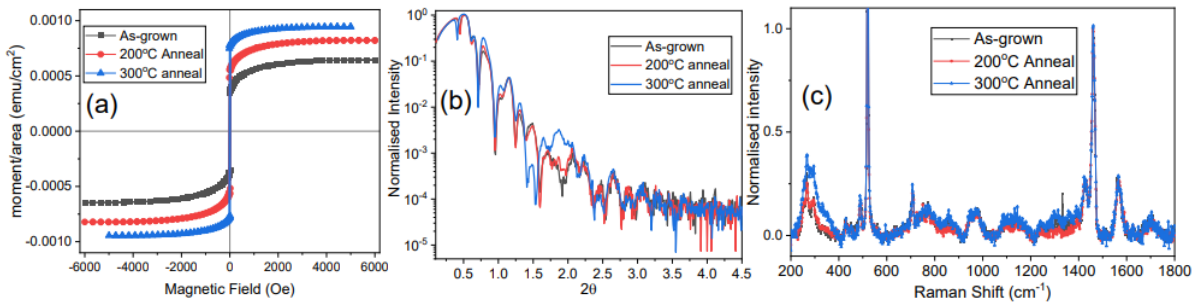

Fig. Initial measurements comparing 3 identical samples of C60(200 Å)/CoB(250 Å)/C60(200 Å) with different post-growth annealing: as-grown, 200oC anneal for 1 hour and 300oC anneal for 1 hour. (a) Room temperature SQUID hysteresis loops. (b) X-Ray Reflectometry. (c) Raman spectroscopy using a 532 nm green laser.

[1] C. H. Ahn, Electrostatic modification of novel materials. Rev. Mod. Phys. 78, 1185 (2006)
[2] C. Leighton, Electrolyte-based ionic control of functional oxides. Nature Materials 18, 13 (2019)
[3] H. Werheit, Raman effect in icosahedral boron-rich solids. Sci. Technol. Adv. Mater. 11, 2 (2010)
[4] T. Zhu, the study of perpendicular magnetic anisotropy in CoFeB sandwiched by MgO and tantalum layers using polarized neutron reflectometry. Appl. Phys. Lett. 100, 202406 (2012)

Topic: Computational and Theoretical Magnetism

(P9) Longitudinal spin fluctuations in atomistic spin models

David R Papp, Richard F L Evans, and Roy Chantrell

Department of Physics, University of York, UK

Heat Assisted Magnetic Recording (HAMR) is a solution to the increasing demand for data storage mechanisms, dictated by fast paced growth in file formats used internationally. The Curie temperature properties of a material can be determined through atomistic simulations, which is done with the use of an integrator model that simulates the spin fields in a system as it evolves with time. The most prominent integrator model, the Landau-Liftshitz-Gilbert (LLG) integrator [1] has limitations in that it does not consider the role of platinum moments in calculations, and thus a new approach, the Longitudinal Spin Fluctuations (LSF) model [2], [3] has been devised to account for them. The research done shows the progress made on appropriate methods to implement the LSF for use in atomistic simulations of HAMR, which would yield more accurate results for materials commonly used in magnetic recording instances such as $L1_0$ FePt.

The Longitudinal Spin Fluctuations (LSF) model builds upon the fundamental strengths of the well-established (LLG) equation and aims to correct the short-comings by considering spin fluctuations more readily in atomistic simulations of magnetic materials. The research done shows that this is especially important in materials such as $L1_0$ FePt, where the platinum atoms undergo strong fluctuations due to the presence of a strong exchange field. [2] Including platinum degrees of freedom in atomistic simulations of FePt leads to more accurate results, which aids in accurately modelling Heat Assisted Magnetic Recording (HAMR) in FePt recording media. Preliminary Curie temperature simulation results are shown in Figure 1.

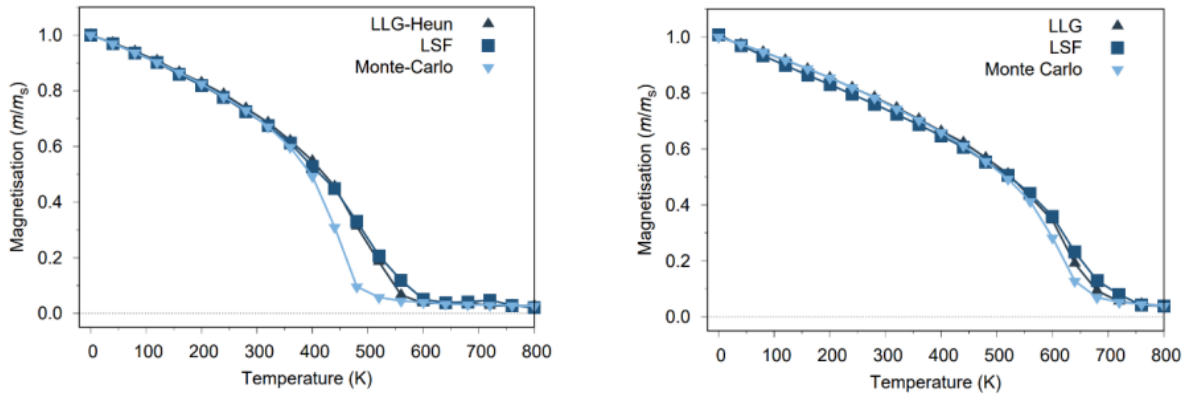

Figure 1 – Left: Curie temperature simulation of $L1_0$ FePt, showing good agreement between the LLG-Heun and LSF integrators. Right: Curie temperature simulation of BCC Fe. Both simulations required bespoke parametrisation (based on material) of the Landau Hamiltonian used to calculate longitudinal fluctuations.

[1] T. Gilbert, A phenomenological theory of damping in ferromagnetic materials, IEEE Transactions on Magnetics 40, 3443 (2004).
[2] M. O. A. Ellis, M. Galante, and S. Sanvito, Role of longitudinal fluctuations in L10 fept, Phys. Rev. B 100, 214434 (2019).
[3] P.-W. Ma and S. L. Dudarev, Longitudinal magnetic fluctuations in langevin spin dynamics, Phys. Rev. B 86, 054416 (2012).

(P10) Atomistic simulations on the effects of grain size in HAMR

David R Papp, Richard F L Evans, and Roy Chantrell

Department of Physics, University of York, UK

Atomistic simulations of heat assisted magnetic recording (HAMR) were done to determine what properties different sized grains have on the outcome of the efficiency in storing and writing data. It is difficult to increase the areal density of conventional magnetic recording media because the boundaries between the 0's and 1's become less clear, leading to error. The HAMR process involves heating the grains to their Curie temperature: TC = 704.8K ±4.3K. At this temperature, they exhibit a smaller temperature dependent magnetic anisotropy [1] which makes writing data that is stable for more than 10 years viable. HAMR is a candidate to address the increasing importance for new data storage technology to be developed because there is a rapid increase in the size of data consumed due to social media, online video streaming etc.

The challenge lies in finding the best possible grain dimensions and configurations in order to minimise the constraining effects of the magnetic recording quadrilemma [2]. The research done finds that L10 FePt grains with diameter of 3nm and a height of 5nm are suitable dimensions for HAMR, after testing grain sizes between 3nm to 12nm in diameter. Figure 1 shows the render of a grain undergoing a typical magnetic switching process, and Figure 2 shows a general summary of what magnetic recording looks like for different sized grains.

Figure 1 - a grain with dimensions 5nm in diameter and 10nm in height showing evidence of switching. The blue dots represent spins that have their original magnetisation whereas the gold dots represent spins that have reversed their direction.

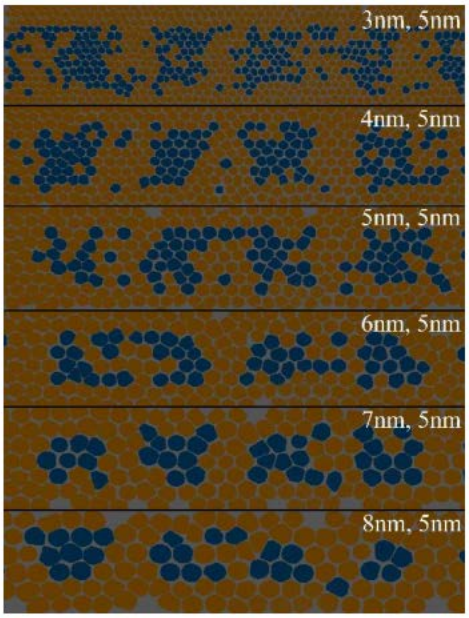

Figure 2 - HAMR simulations done on varying grain diameters (with height fixed at 5nm). The regions of blue and gold (blue representing spins pointing up and gold representing spins pointing down) are more distinct towards higher grain sizes, which is expected behaviour according to the magnetic recording quadrilemma.

[1] J. Barker, R. F. L. Evans, R. W. Chantrell, D. Hinzke, and U. Nowak. Atomistic spin model simulation of magnetic reversal modes near the curie point. Applied Physics Letters, 97(19):192504, 2010.

[2] R. F. L. Evans, R. W. Chantrell, U. Nowak, A. Lyberatos, and H.-J. Richter. Thermally induced error: Density limit for magnetic data storage. Applied Physics Letters, 100(10):102402, 2012.

(P11) Collective Skyrmion Motion Under the Influence of an Additional Interfacial Spin-Transfer Torque

Callum R. MacKinnon[1, *], Katharina Zeissler[2,3], Simone Finizio[4], Jörg Raabe[4], Christopher H. Marrows[2,3], Tim Mercer[1], Philip R. Bissell[1] & Serban Lepadatu[1]

[1] Jeremiah Horrocks Institute for Mathematics, Physics and Astronomy, University of Central Lancashire, U.K. [2] School of Physics and Astronomy, University of Leeds, UK [3]Bragg Center for Materials Research, University of Leeds, UK [4]Swiss Light Source, Paul Scherrer Institut, 5232 Villigen, Switzerland

Skyrmions have clear advantages for future spintronic devices over domain walls in terms of information carrying and storage, however there are still many open questions left and inherent challenges in the transition to applications.

We show the effect of an additional interfacial spin-transfer torque (ISTT) [1], combined with the well-established spin-orbit torque (SOT) and bulk spin-transfer torque (STT), on skyrmion collections is significant [2] and compares well with experimental results [3]. Using a skyrmion collection with a range of skyrmion diameters, we show experimental results are in good agreement with modelling when including the ISTT and cannot be reproduced by using the SOT alone. This is shown in FIG.1. in which there is little to no overlap between the SOT modelled results and the experimental results, in marked contrast to the ISTT results. We also show that for skyrmion collections the velocity is approximately independent of diameter, in marked contrast to the motion of isolated skyrmions, as the group of skyrmions move together at an average group velocity. Moreover, the calculated skyrmion velocities are comparable to those obtained in experiments [3] when the ISTT is included, whilst modelling using the SOT alone shows large discrepancies with the experimental data. Our results thus show the significance of the interfacial spin-transfer torque in ultrathin magnetic multilayers, which is of similar strength to the spin-orbit torque, and both significantly larger than the bulk spin-transfer torque. We further conclude that the ISTT in an imperative spin-torque contribution which should be included in all future micromagnetic modelling to recreate experimental results.

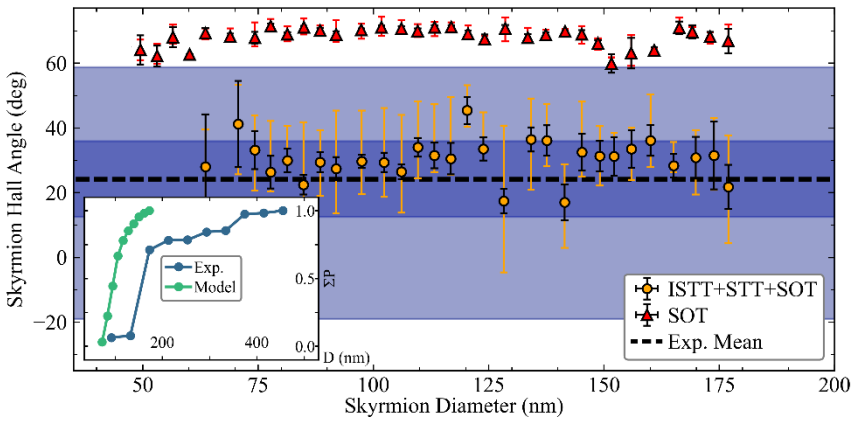

Fig. 1. A detailed viewpoint of the Skyrmion Hall angle as a function diameter at the average current density used in experiments, $J_C = 2\times10^{11}$ A/m^2. The dashed horizontal line is the mean experimental SkHA, with the inner blue horizontal band showing standard error on the mean, and lighter blue outer band showing the spread (quartile 1 to quartile 3). This is compared to the solid disks showing modelling results with ISTT+STT+SOT, and solid triangles for SOT-only

[1] C. R. MacKinnon, S. Lepadatu, T. Mercer, and P. R. Bissell. *Phys. Rev. B* **102**, 214408 (2020).
[2] C. R. MacKinnon, K. Zeissler, S. Finizio, J. Raabe, *et al. arXiv.* 2106.08046 (2021).
[3] K. Zeissler, S. Finizio, C. Barton, A. J. Huxtable, *et al. Nat. Commun.* **11**, 428 (2020).

(P12) 3D FDTD-LLG modelling of electromagnetic shock waves

L. Jones, T. Roberts and F.Y. Ogrin

School of Physics and Astronomy, University of Exeter, UK

There is a growing need in high frequency tuneable microwave materials for applications in the areas of microwave electronics, transformation optics, photonics. Due to their intrinsic RF phenomena, such as FMR, ferromagnetic thin films have always been of great interest and led to a great amount of experimental research very often supported by numerical simulations. While purely magnetostatic solvers, such as OOMMF or Mumax, have always been the standard benchmark tools and usually provide a precise description of the magnetisation processes in thin-film ferromagnetic structures, these systems are however limited in applications where full electromagnetic solutions are required, especially when the material properties are extremely non-uniform (e.g., dielectric/metal interfaces). In such cases one needs to consider a modelling approach where a full solution of Maxwell equations is needed alongside the materialistic equations, such as e.g., Landau-Lifshits-Gilbert (LLG) providing the relation between the magnetisation and the magnetic field. Here we demonstrate such a model [1, 2] which uses 3D finite-difference-time-domain (FDTD) approach together with LLG to find the exact solutions for magnetisation dynamics in ferrites as part of metallic structures. And as an example, we demonstrate a phenomenon of a shock-wave forming and propagating in a coaxial waveguide actuated by a high-voltage pulse. We explore the parameter space of the effect and show the main properties of the wave, and how it can be optimised for the particular design of the system. The results of the simulation are compared with the experimental data obtained on a real life system [3].

[1] M. M. Aziz, Progress in Electromagnetics Research B 15, (2009) 1–29
[2] https://www.maxllg.com/
[3] M R Ulmasculov et. al 2017 J. Phys.: Conf. Ser.830 012027

(P13) Current-induced resonance in long conductive ferromagnetic nano-wires

Mohammad Alneari[1], and Mustafa M Aziz[2]

[1]Department of Physics, University of Exeter, UK, [2]Department of Engineering, University of Exeter, UK

Conductive ferromagnetic nanostructures form important constituents in electromagnetic (meta)materials and composites. They offer higher moments and permeabilities for high frequency applications in communications and wave absorption [1]. They are also compatible with semiconductor fabrication methods for integration into devices. Understanding the magnetisation dynamics and resonance mechanism in the magnetic nanostructures enable tailoring of the magnetic and dielectric properties of the material or composite for targeted bandwidths, scattering properties and size in electromagnetic applications. Electromagnetic wave interaction with conductive ferromagnetic structures is complex due to coupling of both the electric and magnetic fields with the magnetic material. This leads to non-uniform electromagnetic fields with different skin depths in the material (both non-magnetic and magnetic) [2] that control the resonance mechanism and modes. Using an electromagnetic micromagnetic numerical approach based on the finite-difference time-domain method, we previously revealed that resonance in long ferromagnetic nano-prisms, excited by a plane wave at normal incidence, is induced mainly by coupling with the wave's electric field [3,4].

In this work we therefore focus on studying the current-induced ferromagnetic resonance in long circular cobalt nano-wires with diameters 50 – 500 nm by solving the coupled system of the Landau-Lifshitz-Gilbert (LLG) equation and quasi-static Maxwell's equations in finite elements using Comsol Multiphysics (see Fig. 1). The effective field in the LLG equation includes the contributions of the magnetocrystalline anisotropy, exchange fields, magnetostatic fields and current induced fields (and reciprocally induced currents from

magnetisation precession). The resonance mechanisms in the nano-wires, frequencies and their size dependence will be studied by evaluating the local and integrated power dissipation spectra, and by comparison to simplified analytical models of exchange curling and thin-film modes.

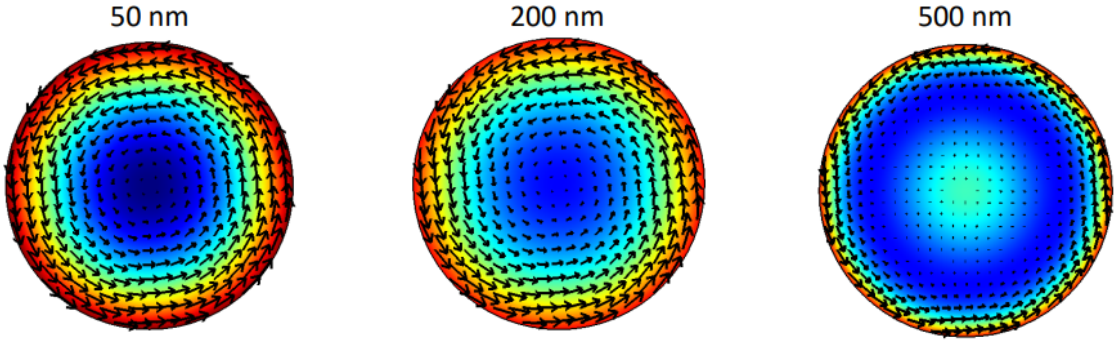

Fig. 1 Dynamic magnetisation in long cobalt cylinders with different diameters following excitation by an axial current with 70 GHz Gaussian time profile and amplitude corresponding to an incident plane wave with 0.1 mT field. The intensity plot represent the current density distribution. This figure shows that the magnetisation becomes confined to a circumferential region corresponding to the magnetic skin depth with increasing cylinder size.

[1] A. N. Lagarkov, and K. N. Rozanov, J. Magn. Magn. Mater. 321, 2082 (2009).
[2] L. Kraus, G. Infante, Z. Frait, and M. V´azquez, Phys. Rev. B 83, 174438 (2011).
[3] M. M. Aziz, and C. McKeever, Phys. Rev. Appl. 13, 034073 (2020).
[4] M. M. Aziz, and C. McKeever, J. Phys. D: Appl. Phys. 54, 345003 (2021)

(P14) Free-Energy Landscapes of Nanomagnetic Skyrmion Host Systems

Ioannis Charalampidis[1,2], and Joseph Barker[1,2]

[1]School of Physics and Astronomy, University of Leeds, UK, [2]Bragg Centre for Materials Research, University of Leeds, UK

Magnetic skyrmions are circular magnetic ‘spin textures’ which have been proposed for use as information carries in spintronic devices [1]. To use them in devices, it is vital that their creation, annihilation and motion can be accurately controlled [1]. This remains challenging as material defects can cause skyrmions to become stuck, destroyed or can even spontaneously generate new skyrmions. Most theoretical and computational models assume a perfect, defect-free material interfaces with idealised magnetic parameters. In our work, we are using atomic scale magnetic simulations to explore how defects and spatial variations of magnetic parameters affect skyrmions. Currently, we are looking to understand how defects modify the free energy landscape which the skyrmions move in. Do defects form energy minima or maxima which trap or repel skyrmions? Do they disturb the landscape making the motion more difficult?

We have combined a classical Heisenberg spin model solved with Monte Carlo techniques with an enhanced sample technique known as metadynamics [2],[3]. This allows the free energy surface to be explored in a set of collective coordinates in systems where there are many degrees of freedom [2],[3]. Traditionally this has been used to understand how molecules bind to surfaces, but we use it to explore how spin textures interact with defects. By introducing the material defects, material imperfections (lattice mismatches and vacancies) and impurities (both magnetic and non-magnetic), their effect upon the skyrmions creation and stability are expected to be studied. Ultimately this “metadynamical” analysis of skyrmion host systems is aimed to provide a way to tune these systems, to magnify any interactions required for the stabilisation of skyrmions and diminish the role of defects which may trap or annihilate skyrmions.

[1] Fert, A., Reyren, N. & Cros, V. "Magnetic skyrmions: advances in physics and potential applications. " Nat Rev Mater 2, 17031 (2017). https://doi.org/10.1038/natrevmats.2017.31

[2] Laio, A., Parrinello, L. "Escaping free-energy minima." PNAS 99 (20), 12562-12566 (2002). https://doi.org/10.1073/pnas.202427399
[3] Bussi, G., Laio, A. "Using metadynamics to explore complex free-energy landscapes". Nat Rev Phys 2, 200–212 (2020). https://doi.org/10.1038/s42254-020-0153-30

(P15) A route towards stable homochiral topological textures in A-type antiferromagnets

Jack Harrison[1], Hariom Jani[2], and Paolo G Radaelli[1]

[1]Clarendon Laboratory, Department of Physics, University of Oxford, UK, [2]Department of Physics, National University of Singapore, Singapore

Topological magnetic textures show great potential as data carriers in next-generation post-Moore technology. Whilst examples of such textures are abundant in ferromagnets, their antiferromagnetic (AFM) counterparts are elusive and yet more promising for spintronics applications. , Controlling the chirality of the topological textures present in material systems is critical to move them consistently and reproducibly via spin-torques as is required for practical applications. Establishing platforms wherein a wide array of these textures can be stabilised and exploited is key to developing this technology.

Recently, we made the pioneering experimental discovery of a family of AFM topological textures in α-Fe_2O_3, at room temperature. They can be reversibly nucleated by executing a Kibble-Zurek quench across a spin-reorientation transition. Whilst exciting, the discovered topological textures are multi-chiral and exist in a non-uniform AFM background of trivial magnetic domains. This makes it difficult to control them in a targeted manner curtailing their practical usability. Hence, an outstanding challenge is to develop a material platform that can stabilise isolated AFM topological textures in a uniform background and afford precise control over their chirality, size, and stability.

We will present our recent micromagnetic and analytical models for topological textures in the broad class of A-type antiferromagnets and apply these to the specific case of α-Fe_2O_3 (an emerging material for AFM spintronic applications), focusing on the role of the interfacial Dzyaloshinskii-Moriya interaction (iDMI). We found that the family of experimentally observed textures in this system have improved stability and enforced homochirality in the presence of iDMI (Figure 1a-c). We determined optimal material parameters to simultaneously achieve small feature sizes and stability against perturbations. In the presence of iDMI, previously unobserved antiferromagnetic skyrmions (Figure 1d) were found to be stable for an accessible range of material parameters, opening a promising route towards post-CMOS device applications of skyrmions in natural antiferromagnets.

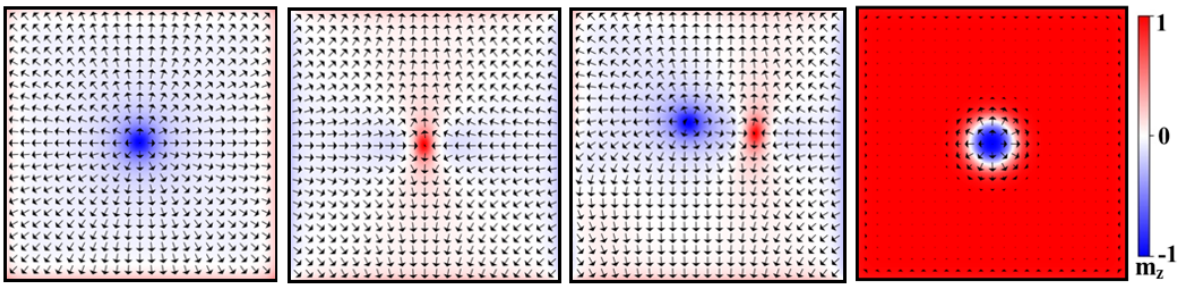

Fig 1. The family of topological textures stabilised in our simulations of A-type antiferromagnets using material parameters appropriate for α-Fe_2O_3.[7] Images a)-c) show the modification of previously observed textures (merons, antimerons and bimerons, respectively) in the presence of iDMI.[6] d) shows the novel antiferromagnetic skyrmion predicted to be stable in this system for a physically reasonable set of material parameters.

[1] C. H. Back et al., Jphys D: Applied Physics **53**, 363001 (2020)
[2] X. Zhang et al., JPhys: Condens. Matter **32**, 143001 (2020)
[3] J. Barker and O. Tretiakov, PRL **116,** 147203 (2016)
[4] X. Zhang et al., Sci. Repts **6**, 1 (2016)
[5] R. Msiska et al., arXiv:2110.07063v1 **[cond-mat.mes-hall]** (2021)
[6] H. Jani et al., Nature **590**, 74 (2021)
[7] J. Harrison et al. arXiv:2111.15520 **[cond-mat.mtrl-sci]** (2021)

(P16) Multiscale Modelling of the Antiferromagnet Mn_2Au

Joel Hirst[1], Unai Atxitia[2], Sergiu Ruta[1,4], Jerome Jackson[3], and Thomas Ostler[1]

[1]Materials & Engineering Research Institute, Sheffield Hallam University, UK, [2]Dahlem Center for Complex Quantum Systems and Fachbereich Physik, Freie Universitat Berlin,[3] STFC Daresbury Laboratory, UK

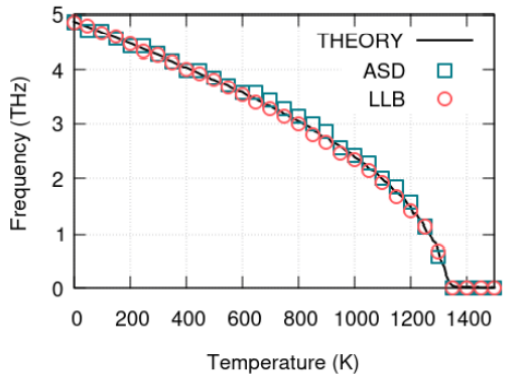

***Figure 1**: Temperature dependent AFMR results computed using atomistic and LLB models compared to analytical estimates.*

Antiferromagnetic (AFM) materials are strong candidates for next generation data storage and processing. They remain robust to external fields and have intrinsically fast THz magnetisation dynamics. Simulations of AFM dynamics using atomistic models have been used for several years [1,2], but are generally restricted to system sizes of tens of nanometers. Micromagnetic models based on the LLG equation are unable to account for changes in the magnetisation length and are therefore not appropriate to be used in scenarios where the temperature changes dynamically or where there is a spatial variation in temperature, thus requiring a new approach.

In this work, we present the first full multiscale model of the AFM Mn2Au. Mn2Au has been drawing much attention from the community largely because its ground state properties are preserved well above room temperature. We use values for the exchange interaction and anisotropy taken from ab-initio calculations as input into an atomistic model - from which we calculate the temperature dependant equilibrium parameters including the magnetisation, susceptibilities and exchange stiffness. These are then used as inputs into an AFM LLB model.

Our results show that the calculated Néel temperature of 1340 ± 10 K is in good agreement with previous experimental results [3]. We have determined the exchange stiffness through calculations of the temperature dependence of the domain wall width. As a key test of the transverse dynamics, we calculated the temperature-dependence of the antiferromagnetic resonance (AFMR) frequency, which is in excellent agreement with the results of the atomistic and analytical models, as shown in Figure 1. We also show that the modified longitudinal effective damping parameter in the LLB model as derived by Jakobs & Atxitia [4] yields excellent agreement between the longitudinal relaxation in both atomistic and LLB frameworks.

The development of this methodology is an important step forward in micromagnetic modelling where there are spatial and/or temporal variations in temperature, which lead to localised variations in the magnetisation. For example, in studies of ultrafast magnetisation dynamics or the dynamics of magnetic structures, such as domain walls under thermal gradient - which have been proposed for use in the next generation of logic and memory devices [5,6]. We show that the LLB model gives good agreement to atomistic results, as seen in Figure 2, which are computationally heavy and noisy for finite temperature DW simulations.

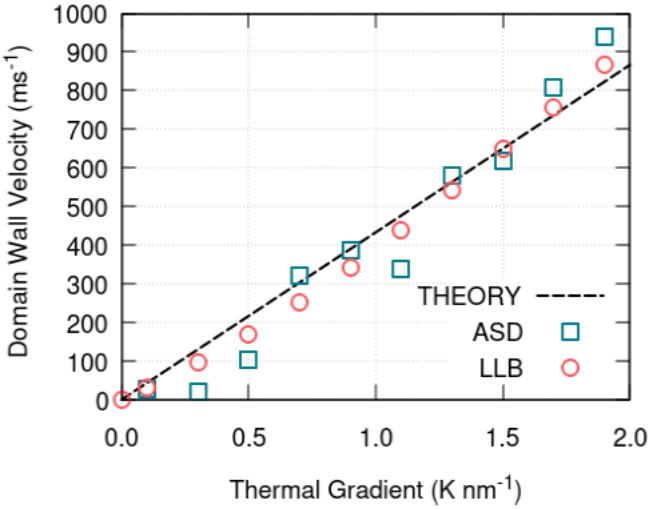

Figure 2: DW velocity due to a thermal gradient from atomistic, LLB and analytical models.

[1] Kazantseva, N. et al. Phys. Rev. B 77. (2008): 184428.
[2] Szunyogh, L. et al. Phys. Rev. B 79. (2009): 020403.
[3] Barthem, V.M.T.S. et al. Nature Communications 4. (2013).
[4] Jakobs, F. & Atxitia, U. Private Communication.
[5] D. A. Allwood, et al. Science 309. 5741(2005): 1688-1692.
[6] Stuart S. P. Parkin, Science 320. 5873(2008): 190-194.

(P17) Effect of geometry on magnetism of Hund's metals: A case study with BaRuO3

Hrishit Banerjee[1], Hermann Schnait[2], Markus Aichhorn[2], and Tanusri Saha-Dasgupta[3]

[1]Yusuf Hamied Department of Chemistry, University of Cambridge, UK, [2]Institute of Theoretical and Computational Physics, Graz University of Technology, Austria, [3]S. N. Bose National Centre for Basic Sciences, India

In order to explore the effects of structural geometry on properties of correlated metals we investigate the magnetic properties of cubic (3C) and hexagonal (4H) $BaRuO_3$. While the 3C variant of $BaRuO_3$ is ferromagnetic below 60 K, the 4H phase does not show any long-range magnetic order, however, there is experimental evidence of short-range antiferromagnetic correlations. Employing a combination of computational tools, namely density-functional theory and dynamical mean-field theory calculations, we probe the origin of contrasting magnetic properties of $BaRuO_3$ in the 3C and 4H structures. Our study reveals that the difference in connectivity of RuO_6 octahedra in the two phases results in different Ru-O covalency, which in turn influences substantially the strengths of screened interaction values for Hubbard U and Hund's rule J. With estimated U and J values, the 3C phase turns out to be a ferromagnetic metal, while the 4H

phase shows paramagnetic behaviour with vanishing ordered moments. However, this paramagnetic phase bears signatures of antiferromagnetic correlations, as confirmed by a calculation of the magnetic susceptibility. We find that the 4H phase is found to be at the verge of antiferromagnetic long-range order, which can be stabilized upon slight changes of screened Coulomb parameters U and J, opening up the possibility of achieving a rare example of an antiferromagnetic metal.

[1] Effect of geometry on magnetism of Hund's metals: A case study with BaRuO3, Hrishit Banerjee, Hermann Schnait, Markus Aichhorn, Tanusri Saha-Dasgupta, arXiv:2111.04408 , 2021

(P18) The effect of transmitted Spin Wave to Transient retrograde motion of skyrmions in multilayer wave guides

L Huang, G Burnell and C H Marrows

School of Physics and Astronomy, University of Leeds, UK

One of the tools to move a skyrmion is an injected current [1,2], which gives rise to the risk of producing excessive heat. On the other hand, spin-waves (SW) are a promising way to drive skyrmions without producing such high temperatures and hence affecting the performance of a skyrmionic device [3,4]. The dataset and characteristic analysis we present concern SW driven skyrmion motion simulations by OOMMF[5] with fixed parameters, D=1.5 mJ/m^2, M_S=1004 KA/m, A=3.6 pJ/m, Ku=1 MJ/m^3, damping constants α = 0.03, track width (40-100 nm). The sizes of relaxed skyrmions are from 20nm to 23nm when the track widths increase from 40nm to 100nm, so there remains more than 5 nm between the skyrmion to each sample upper edge at initial stage. In Fig 1, the skyrmion displacement with time along the SW propagation direction for various track width is shown. When the track width >50 nm, the skyrmion will initially move opposite to the SW propagation direction before moving forward at longer times. Fig 2 shows the acceleration of SW-driven skyrmion and the SW transmission T through the skyrmion vs time. It is significant that with decreasing transmission, the skyrmion starts having positive acceleration which has a same direction of SW propagation. By using the traditional Thiele equation, the transmitted SW is well considered but the reflected SW is always ignored. [6] Considering the linear momentum transfer torque from the reflected SW, the lower SW Transmission leads to weaker force that pull the skyrmion moving towards the SW resource, and more possible let the reflected SW drives skyrmion away from SW resource. The skyrmion retrograde motion gives a possible observation result in the future and gives a guidance about the interesting role of reflected SW.

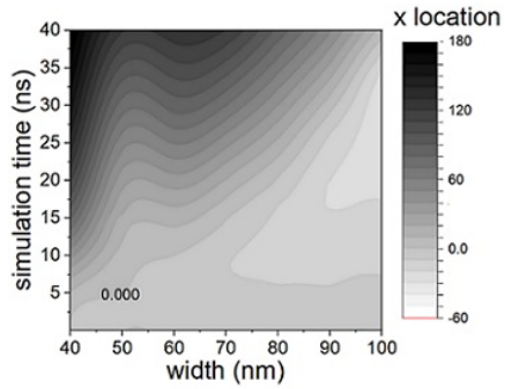

Fig 1. Time-dependent skyrmion displacement for various magnetic track widths

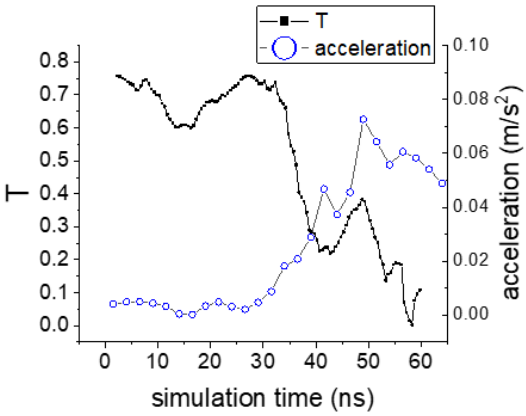

Fig. 2: Time-dependent skyrmion acceleration on 100 nm width track and the SW transmission data.

[1] S. Mühlbauer, B. Binz, F. Jonietz, Science, Vol.330, p1648(2010)
[2] E. Karin, G. Markus, R. A. Duine, Phys. Rev. B, Vol.84, p064401(2011)
[3] X. Zhang, J. Müller, J. Xia, New J. Phys., Vol.19, p065001(2017)
[4] L. Kong, R. Zhao, Appl. Phys. Lett., Vol.116, p192407(2020)
[5] M. Donahue, D. Porter, National Institute of Standards and Technology (1999)
[6] A.A. Thiele, Phys. Rev. Lett, Vol.30, p230(1973)

(P19) The Micromagnetic Effect of Magnetoelasticity on Antiferromagnets

R Mackay, J Barker, and S Fitzgerald

University of Leeds, UK

Spintronic devices have the potential to permit faster and more energy efficient data storage and transfer. Antiferromagnets have desirable properties, namely their resistance to interference by stray fields (meaning increased density accessible data storage is possible) and THz spin dynamics [1] which makes them a great candidate for spintronic devices. When designing devices, magnetic domain formation and propagation needs to be well understood. In ferromagnets, it is well understood that domains form to reduce magnetostatic energy and can be manipulated magnetically, electrically or through strain. In antiferromagnets, there is no magnetostatic energy to minimise. Instead, the existence of antiferromagnetic domains is thought to be magnetoelastic in origin. Magnetoelastic phenomena is poorly understood in the literature—in particular the dynamics of domains in the presence of defects [2].

We aim to explore domain formation and dynamics in this important class of magnetic materials via magnetoelastic coupling to an applied strain field. This will be implemented at the micromagnetic length scale using a specialist computational technique called phase field modelling [3]. This uses the free energy directly instead of the Hamiltonian energy. The phase field approach includes both micromagnetic and continuum considerations for the inclusion of defects within the model. Complimentary atomistic spin dynamics calculations on superlattices with defects included will be used to verify the phase field model—similar to standard micromagnetic problems. Spin dynamics calculations have a good theoretical foundation for thermodynamics but do not permit device sized simulations. By including dynamic strain fields and lattice defects within the phase field model, we expect to be able to understand magnetic domain dynamics for the design of spintronic devices as seen experimentally [4].

[1] K. Olejník, T. Seifert, Z. Kašpar, V. Novák, P. Wadley, R. P. Campion, M. Baumgartner, P. Gambardella, P. N˘emec, J. Wunderlich, J. Sinova, P. Kužel, M. Müller, T. Kampfrath, and T. Jungwirth, Terahertz electrical writing speed in an antiferromagnetic memory, Sci. Adv. 4, eaar3566 (2018)
[2] O. Gomonay and D. Bossini, Linear and nonlinear spin dynamics in multi-domain magnetoelastic antiferromagnets, J. of Phys. D: App. Phys. **54**, 37 (2021)
[3] J. Wang and J. Zhang, A real-space phase field model for the domain evolution of ferromagnetic materials, Int. J. Solids Struct. 50, 3597 (2013)
[4] K. Olejník, V. Schuler, X. Marti, V. Novák, Z. Kašpar, P. Wadley, R. P. Campion, K. W. Edmonds, B. L. Gallagher, J. Garces, M. Baumgartner, P. Gambardella & T. Jungwirth,
[5] Antiferromagnetic CuMnAs multi-level memory cell with microelectronic compatibility, Nat. Comms. 8, 15434 (2017)

(P20) Coherent spin states path integral spin dynamics

Thomas Nussle[1,2], and Joseph Barker[1,2]

[1]School of Physics and Astronomy, University of Leeds, UK, [2]Bragg Centre for Materials Research, University of Leeds, UK

Atomistic spin dynamics is a classical model that approximates the magnetisation of a given compound as a collection of localised and immobile magnetic moments interacting with each other through a set of local interactions [1]. This formalism is a powerful tool for understanding magnetisation dynamics in magnetic materials. However, it is based on classical assumptions which make it difficult to incorporate quantum properties in a non ad-hoc fashion [2].

These classical methods neglect the quantum nature of objects, for example ignoring the incommutability of spins. With experimental measurements of quantum effects up to 40K [3] in antiferromagnetic systems, we aim to include these effects. Starting from quantum mechanics in the framework of path integrals, one can recover an equivalent classical system of dimension N+1 for a quantum system of dimension N, as is the case in statistical sampling methods such as Quantum Monte Carlo [4] or dynamical methods such as Path Integral Molecular Dynamics [5]. The former method being a statistical sampling method has very poor scaling, but in the case of Path Integral Molecular Dynamics, simulating much larger systems is not uncommon.

Using the basis of coherent spin states [6] and path integral formalism so as to recover a continuous description of the partition function of our system, we are building a similar model for atomistic spin dynamics in order to recover quantum properties of magnetic systems, especially at low temperatures or for systems where these are of higher fundamental importance such as antiferromagnets, without having to sacrifice the ability to simulate device size objects.

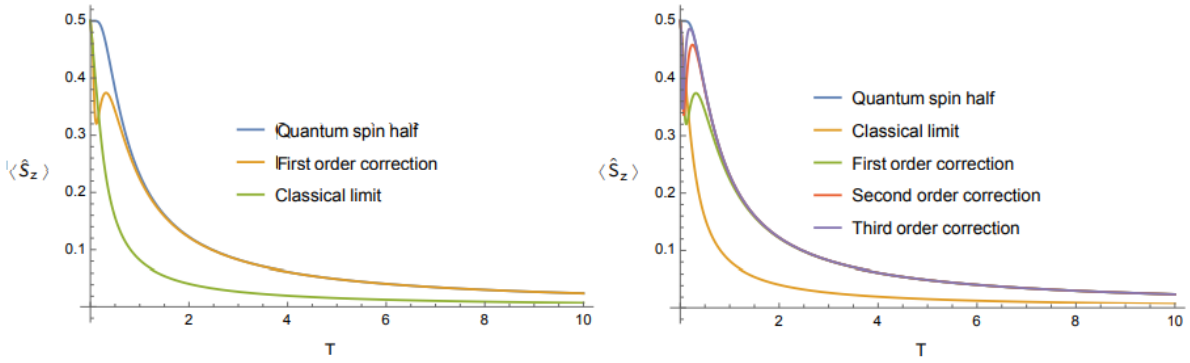

Figure 1: Expectation value of spin along z-axis as a function of temperature: classical, quantum and path integral models

[1] O. Eriksson, A. Bergman, L. Bergqvist, and J. Hellsvik, Atomistic Spin Dynamics: Foundations and Applications, 1st ed. (Oxford University Press, Oxford, 2017)
[2] J. Barker and G. E. W. Bauer, Phys. Rev. B 100, 140401 (2019)
[3] O. G. Shpyrko, E. D. Isaacs, J. M. Logan, Y. Feng, G. Aeppli, R. Jaramillo, H. C. Kim, T. F. Rosenbaum, P. Zschack, M. Sprung, S. Narayanan, and A. R. Sandy, Nature 447, 68 (2007).
[4] J. Gubernatis, N. Kawashima, and P. Werner, Quantum Monte Carlo Methods: Algorithms for Lattice Models (Cambridge University Press, Cambridge, 2016).
[5] M. E. Tuckerman, D. Marx, M. L. Klein, and M. Parrinello, J. Chem. Phys. 104, 5579 (1996)
[6] Y. Lee Loh and M. Kim, American Journal of Physics 83, 30 (2015)

(P21) Breaking through the Mermin-Wagner limit in 2D van der Waals magnets

Sarah Jenkins[1,2,3], Levente Rozsa[4], Unai Atxitia[5], Richard F L Evans[1], and Elton Santos[6]

[1]Department of Physics, University of York, UK [2]TWIST Group, Institut fur Physik, Johannes Gutenberg Universitat, Germany, [3]TWIST Group, Institut fur Physik, Universitat Duisburg-Essen, Campus, Germany, [4]Institut fur Physik, Universitat Konstanz, Germany, [5]Dahlem Center for Complex Quantum Systems and Fachbereich Physik, Freie Universitat Berlin, Germany, [6]Department of Physics, University of Edinburgh, UK

The Mermin–Wagner theorem [1] states that long-range magnetic order should be suppressed at finite temperatures in the 2D regime, when only short-range isotropic magnetic interactions exist. 2D magnetic materials have generated significant interest in recent years following their first experimental realisation in monolayer CrI_3[2]. Thermodynamically stable 2D magnetic materials could allow for the development of spintronic devices with unprecedented power efficiency and computing capabilities. In such systems, the existence of magnetic ordering is typically attributed to the presence of a significant magnetic anisotropy [3], which is known to introduce a spin-wave gap. Importantly, the theorem is only valid for systems of infinite size, as directly stated by Mermin and Wagner [1], where the Curie temperature is shown to be T = 0K. However, common understanding is that the theorem also excludes the alignment of spins in the sample sizes studied experimentally which are only a few microns in size [2], suggesting that such systems are indistinguishable from infinite.

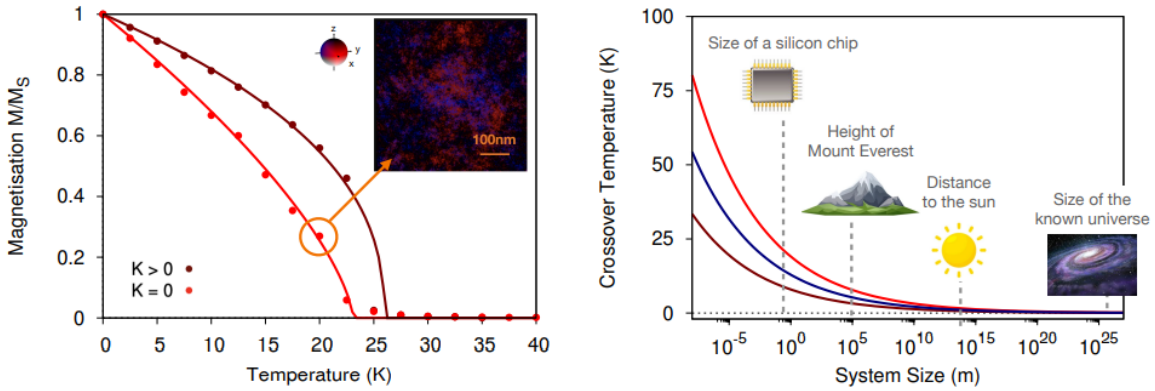

Fig 1. (a) Simulated temperature-dependent intrinsic magnetisation with and without anisotropy for a 1000nm * 1000 nm flake size. The inset shows a visualisation of the magnetic spin configurations at 20K for the 1000 * 1000 nm flake. (b) Size scaling of the simulated crossover temperature for the different 2D lattices.

Here, we show using numerical simulations and analytic calculations that spins remain aligned with each other at moderate temperatures in micrometre-scale flakes of 2D materials even in an isotropic spin model, circumventing the assumed Mermin-Wagner limit. Surprisingly we find that the crossover temperature, where the magnetisation changes from ferromagnetic to paramagnetic ordering, is weakly dependent on system size with samples of micrometre size having a well-defined magnetic moment that is stable on nanosecond timescales. For a typical 2D vDW magnet with an intrinsic ordering temperature of 25K, a system with area (10^{12} m^2) still has an ordering temperature around 1 K which is still accessible experimentally. Our findings challenge the widely held assumption that a significant magnetic anisotropy is required to observe magnetic ordering in 2D systems [1], opening up a huge range of 2D magnetic materials previously assumed to be unsuitable for applications.

[1] Mermin, N. D. & Wagner, H. Phys. Rev. Lett., 17, 1133–1136, (1966).
[2] Wei, S. et al. Mater. Res. Express, 6, 122004 (2019)
[3] Torelli, D., Thygesen, K. S. & Olsen, T. Comput. Mater. 6, 045018, (2019).

(P22) Ab-inito and atomistic spin dynamics characterisation of antiferromagnetic materials Mn2Au and CuMnAs

Sergiu Ruta[1], Jerome Jackson[2], Joel Hirst[1], and Thomas Ostler[1]

[1]College of Business, Technology and Engineering, Sheffield Hallam University, UK, [2]STFC Scientific Computing Department, Daresbury Laboratory, UK

Antiferromagnetic (AFM) materials are magnetically ordered systems with parallel magnetisation in sub-lattices and a net-zero overall magnetisation. Discovered by Louis Neel [1] in 1948, ´ AFMs have become of interest due to the high frequency antiferromagnetic resonance mode, which is often in the THz domain, resulting in fast magnetisation dynamics. As a result of these high frequency dynamics, AFMs have been proposed for information transport applications via electrons (spintronics) [2] or spin waves (magnonics) [3]. Exciting AFM systems with an electric current or ultra-fast laser pulse can lead to a fast response of the system, emitting THz signal or even switching the magnetic configuration [4]. In this work, we characterise two promising AFM materials Mn2Au and CuMnAs. Both have in-plane AFM ordering that is maintained at room temperature, with an Neel temperature (´ TN) above 300K (∼550K for CuMnAs and ∼ 1500K for Mn2Au). First, we parametrize the Heisenberg Hamiltonian using ab initio density functional theory, which is used as the basis for the atomistic spin dynamics modeling. The ab-initio calculations were done using 1) quasiparticle self-consistent GW (QSGW) via the full-potential linearised muffin-tin orbital (FP-LMTO) code Questaal [5] and 2) the fully-relativistic Korringa-Kohn-Rostoker package SPR-KKR [6].

For the SPR-KKR method, the inter-atomic magnetic interactions (Heisenberg exchange integrals) are evaluated using the magnetic force theorem independently for ferromagnetic, antiferromagnetic (the true ground state) and paramagnetic configurations. The results indicate comparable exchange parameters and to some degree independent of the configuration used.

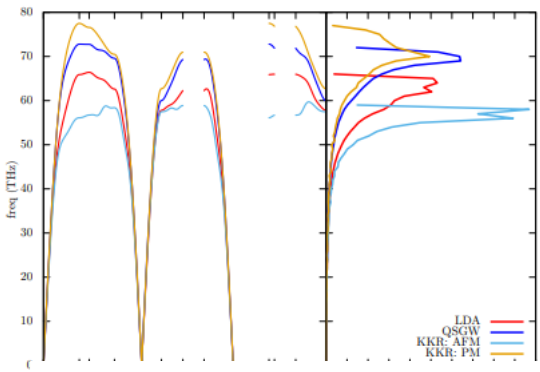

Fig 1: Spin-wave dispersion (left) and magnon density of state (right) for Mn2Au. The results are computed using AFM and PM exchange parameters from SPRKKR and AFM parameters from QSGW.

In the second part, we use atomistic spin dynamics to determine the Neel temperature TN and the spin waves for different parametrisation mentioned above. The Neel ´ temperature is in the experimental range of about 1500K, with the mention that the atomic configuration becomes unstable just below 1000K and direct measurement of TN is not possible. An alternative way to validate the exchange parameters is via spin wave (SW) dispersion relations, which can be computed at any temperature. In figure 1, we show the SW and magnon density of state at 0K (similar results at 300K), indicating a very good agreement at a lower frequency (below 40 THz) and differences up to 10Thz at the high range.

[1] Neel, L. In ´ Annales de physique, 1948; Vol. 12, pp 137–198.
[2] Olejnık, K.; Seifert, T.; Kaspar, Z.; Nov ˇ ak, V.; Wadley, P.; Campion, R. P.; Baumgartner, M.; ´ Gambardella, P.; Nemec, P.; Wunderlich, J., et al. ˇ Science advances 2018, 4.
[3] Barman, A.; Gubbiotti, G.; Ladak, S.; Adeyeye, A. O.; Krawczyk, M.; Grafe, J.; Adelmann, ¨ C.; Cotofana, S.; Naeemi, A.; Vasyuchka, V. I., et al. Journal of Physics: Condensed Matter 2021.
[4] Walowski, J.; Munzenberg, M. ¨ Journal of Applied Physics 2016, 120, 140901.
[5] Pashov, D.; Acharya, S.; Lambrecht, W. R.; Jackson, J.; Belashchenko, K. D.; Chantis, A.; Jamet, F.; van Schilfgaarde, M. Computer Physics Communications 2020, 249, 107065.
[6] Ebert, H.; Kodderitzsch, D.; Min ¨ ar, J. ´ Reports on Progress in Physics 2011, 74, 096501.

(P23) Investigating the exchange through the amorphous inter-granular phase in NdFeB permanent magnets

J B Collings, R W Chantrell, R F L Evans

The University of York, UK

Highly coercive permanent magnets such as Nd2Fe14B have significant industrial applications as e.g., the motors of electric vehicles, or the generators of wind turbines. Such uses are indicative of their role in renewable energy [1]. In many applications these magnets are required to retain their magnetisation at high temperatures, and the low Curie temperature, T_C = 585 K, of Nd2Fe14B, can be a limiting factor [1]. Furthermore, the rare-earth element content in their structure means they are expensive to produce [1].

An important aspect thought to affect the properties of permanent magnets is the exchange between grains of the material across the inter-granular phase. Experimental data suggests that there can be a significant fraction of around 30 % Fe in the inter-facial grain boundary which may lead to a significant reduction in the coercivity [2]. In this research the effects of the Fe concentration have been investigated to understand the contributing factors to the coercivity of these important permanent magnets.

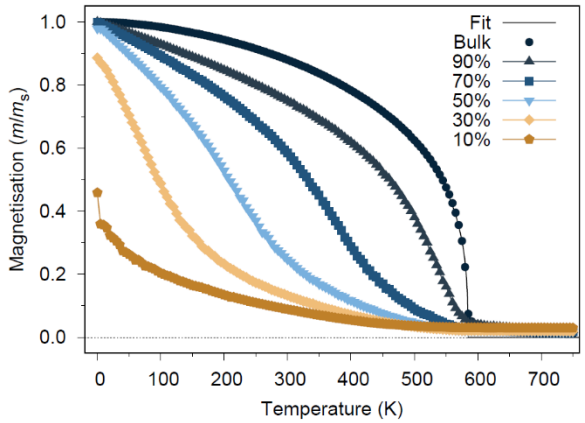

Fig 1: The Curie temperature decreases for lower Fe densities. The different initial gradient between the bulk and other densities is due to the inclusion of spin-temperature rescaling. The thin layer also retains magnetisation past its T_C. Also note that the lowest iron densities fail to reach saturation magnetisation at 0K.

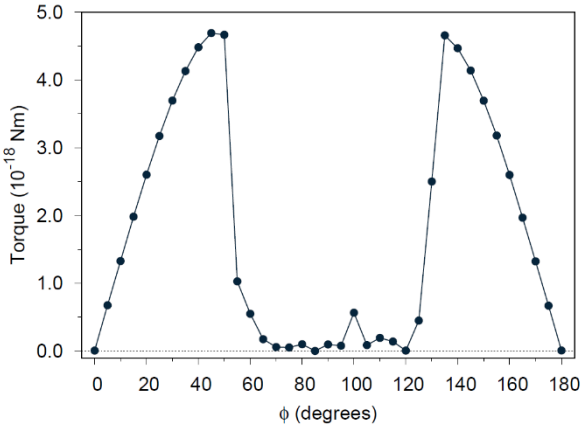

Fig 2: Calculation of the torque vs set constraint angle collapses at angles near 90 degrees. This is indicative of the formation of a domain wall leading to a cancellation of the torque which occurs due to anisotropy.

To do this initially, atomistic simulations of bilayer systems were undertaken using the Vampire software package [3]. The first simulation consisted of a thin ~2 nm layer on top of a bulk ~12nm layer. The iron density in the thin layer was varied, and anisotropy as well as spin-temperature rescaling [4] were removed to better simulate an amorphous phase. Magnetisation vs temperature curves were calculated for the thin layer and compared to that of the bulk of the system, see Fig.1. The investigation of the features of Fig.1 are a large part of the research being presented. The next simulation involved simply adding a bulk layer on – top to sandwich the thin layer between two grains. By constraining one bulk layer to 180 degrees and varying the magnetisation angle of the other from 0-180 degrees then plotting the torque, see Fig.2, the inter-

granular exchange coupling can be calculated as the integral. However, the inclusion of anisotropy as a factor complicates this calculation, and this is the subject of further investigation.

[1] O. Gutfleisch et al, Advanced Materials 23, 821 (2011)
[2] T. Woodcock et al, Acta Materialia 77, 111 (2014)
[3] R. F. L. Evans et al, Journal of Physics: Condensed Matter 26, 103202 (2014)
[4] R. F. L. Evans, U. Atxitia, and R. W. Chantrell, Phys. Rev. B 91, 144425 (2015)

(P24) Higher-order Magnetic Anisotropy in Soft-hard Nanocomposite Materials

Nguyen Thanh Binh[1], Sarah Jenkins[2], Sergiu Ruta[1] , Richard F L Evans[1], Roy W Chantrell[1]

[1]Department of Physics, University of York, UK 2University of Duisburg-Essen, Germany

Properties of higher-order magnetic anisotropy constants in soft-hard nanocomposite materials still attract much debate [1]. We investigated the magnetic anisotropy in a $L1_0$/A1 FePt system using the VAMPIRE software package [2]. An elongated, faceted cylindrical core-shell was constructed with a $L1_0$-FePt core of varied size surrounded by an A1-FePt shell. The system exchange interaction was 3-dimensional and accounted up to the third nearest neighbours. A 2-ion Fe-Pt anisotropy component was incorporated to the system Hamiltonian following Mryasov et al. [3]. The angular dependence of the restoring torque was calculated from 0K to 1000K in 5K steps using a constrained Monte-Carlo integrator. Temperature-dependent anisotropy constants were then determined from fitting to the system torque as a function of the constrained angle.

We find that the core-shell structure exhibits an unexpected 4^{th} -order anisotropy term of which magnitude depends on the core-size ratio R. The K_2/K_1 ratio, with K_1 and K_2 being the 2^{nd} and 4^{th} -order anisotropy constant respectively, displays a non-monotonic pattern with a peak occurring at $R \sim 0.55$ [Fig.1]. We find that K_2 scales with $(M/M_s)^{\sim 2}$ at temperatures below T_c - a remarkable deviation from the established Callen-Callen theory [4] which instead predicts a scaling with $(M/M_s)^{10}$. A simple analytical model shows the 4^{th} -order term to arise from canting of the core and shell magnetisation. Further, the model demonstrates that the magnitude of the 4th -order term is proportional to $K^{1\,2}/J$, with J the exchange coupling. Given that the 2-ion K_1 term scales approximately with M^2 and J with M^2, the predicted scaling exponent is 2 in agreement with the simulations. Generally, the 4^{th} -order anisotropy constant is shown to exhibit a strong dependence on the system geometry, thus suggesting that the Callen-Callen power law is not universal and valid only for single-ion anisotropies.

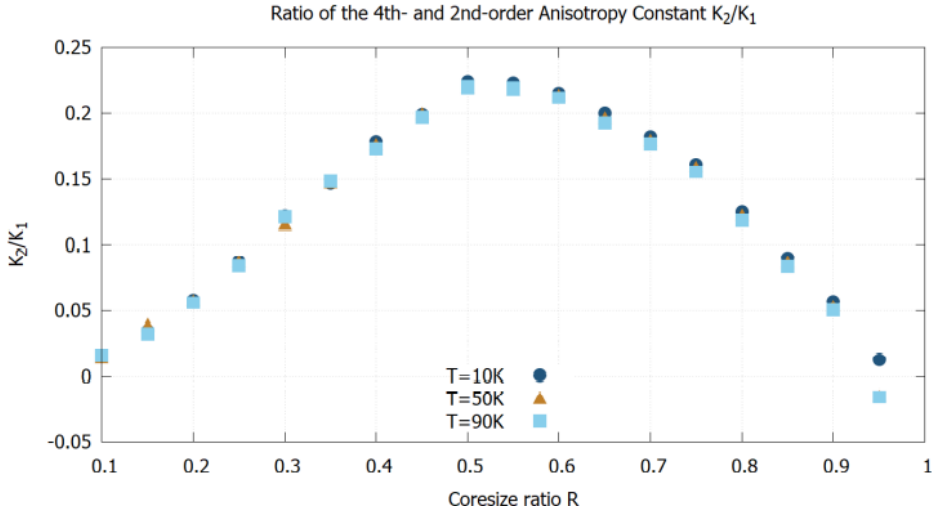

Fig.1: A low temperature scan displays a non-monotonic dependence of K2/K1 on core size ratio R with a peak at $R \sim 0.55$.

[1] Richter et al., J. Appl. Phys. 109, 07B713 (2011)

[2] Evans et al., Journal of Physics: Condensed Matter, 26, 103202 (2014). More information about VAMPIRE can be found at: http://vampire.york.ac.uk/features/
[3] Mryasov et al., Europhys. Lett., 69 (5), pp. 805–811 (2005)
[4] Callen et al., J. Phys. Chem. Solids, 16, 310 (1960)

(P25) Switching Efficiency in Coreshell $L1_0$/A1-FePt Grain

Nguyen Thanh Binh[1], Sarah Jenkins[2], Sergiu Ruta[1] , Richard F L Evans[1], Roy W Chantrell[1]

[1]Department of Physics, University of York, UK 2University of Duisburg-Essen, Germany

Iron Platinum in the $L1_0$-phase ($L1_0$-FePt) is being extensively investigated for potential applications in Heat-Assisted Magnetic Recording (HAMR) [1]. However, it is found challenging to reduce grain size to below 10nm because of reducing thermal stability and, consequently, switching efficiency. In addition, a recent study discovered a size-dependent effect of surface segregation of Pt which decreases anisotropy and further destabilises the grain [2]. Therefore, in this research we aim to study computationally the impact of surface disorder on switching efficiency in sub-10nm FePt grain.

Our simulations are performed by the VAMPIRE software package [3]. Elongated, faceted cylindrical FePt grains are created with three different configurations in order to investigate the effect of varying size and adding surface disorder. The very strong 2-ion Fe-Pt anisotropy component of FePt, which is the origin of the exceptionally high uniaxial anisotropy of the material, is incorporated into the system Hamiltonian following Mryasov et al.'s treatment [4]. A laser pulse of varied duration is applied to switch the spin, and after 100 trials the switching efficiency of the grain in each configuration is calculated.

Preliminary data in [Fig.1] shows that as a laser pulse being applied to heat up the material, the switching efficiencies of FePt grains in all 3 configurations will increase sharply around the Curie temperature region and finally converge, but at a probability lower than the ideal 100%. This indicates a noticeable chance of switching error in the grain of sub-10nm sizes, which is detrimental for HAMR data function. Reducing the grain size does induce higher switching error rate. This effect, however, could be mitigated by surface engineering – in this case the addition of a disorder A1 shell around the ordered $L1_0$ grain. Further works including varying the laser pulse duration and studying the effect of temperature-rescaling in simulations are being carried out to achieve a complete description of switching efficiency.

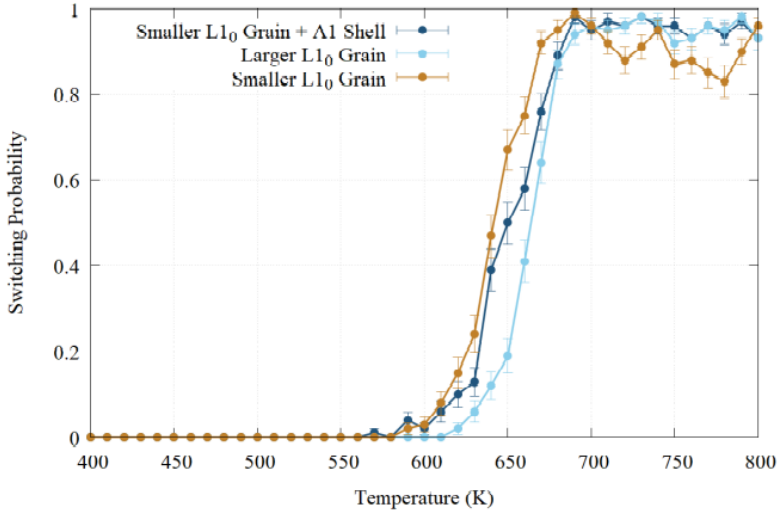

Fig.1: The switching efficiency for 3 different configurations of the investigated FePt grain with the applied laser pulse of 0.5ns.

[1] D. Weller et al., Journal of Vacuum Science & Technology B, 34, 060801 (2016)
[2] H.S-Amin et al., Scripta Materialia 135 (2017) 88–91

[3] Evans et al., Journal of Physics: Condensed Matter, 26, 103202 (2014). More information about VAMPIRE can be found at: http://vampire.york.ac.uk/features/
[4] Mryasov et al., Europhys. Lett., 69 (5), pp. 805–811 (2005)

(P26) Electronic Heat Bath Simulations for Ultra-fast Spin Dynamics

Jackson Ross, Roy W Chantrell and Richard F L Evans

Department of Physics, University of York, UK

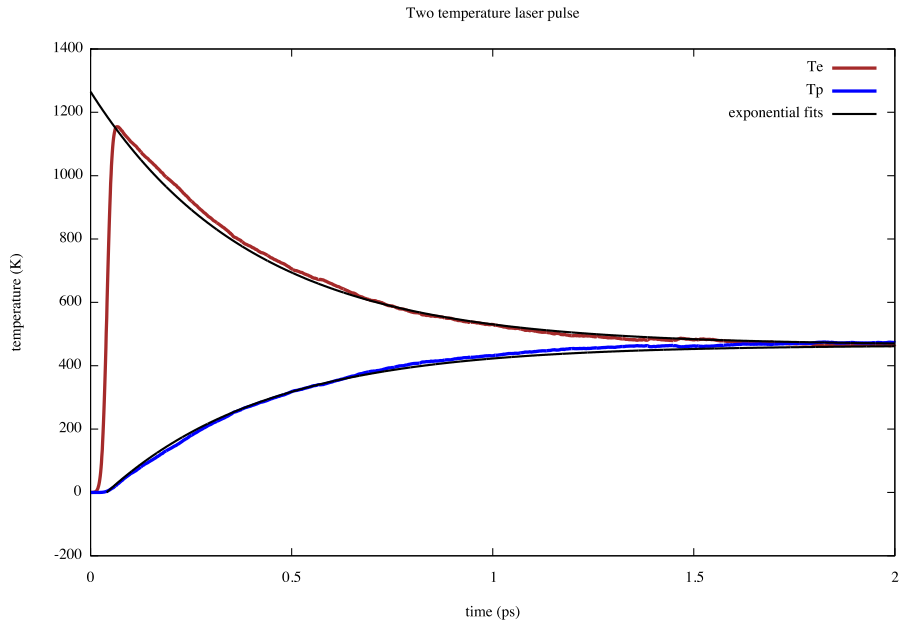

Fig 1. Simulation from laser heating showing electron (Te) and lattice (Tp) temperature compared to exponentially decaying fits. The small deviations represent localized pockets of non-equilibrium that—when coupled to a spin system—could assist magnetic nuclei formation.

Atomistic modelling makes common use of Langevin Dynamics—a Gaussian distribution of small changes to the effective field term in the spin Hamiltonian—to simulate the effects of thermal fluctuations on atomic magnetic moments in a material (1). Such a model is simple to add to any finite-temperature simulation: at pico-second timescales, the thermal impact on atomic spins is uncorrelated in space or time—the thermal effect on spin *a* at time *t* is completely unrelated to the thermal effect on spin *b* at time *t + 1.* In general, however, the thermal fluctuations in a material are correlated through collective motions of electrons in the system. Taking these localized and time dependent influences into account is a requirement for improving ultra-fast spin dynamic simulations in the femtosecond time scale. To advance a solution to this problem, we present on the use of an explicitly determined conduction band electron environment for the purpose of correlating thermal effects in metals. Currently, our environment simulates charge and heat transport in metals on ultra-fast time scales during severe non-equilibrium caused from applied electric fields or laser-heating pulses. Electron motion is calculated using simple Newtonian equations of motion (2); the electron-electron and electron-lattice relationship is parametrized using constants derived from experimental data (3)(4). Our environment successfully reproduces the popular two-temperature model used to simulate laser-heating of experimental samples (fig. 1) with the added advantage of considering local correlation effects. In the future, this will offer the ability to include correlated spin effects not possible in Langevin Dynamics.

[1] R F L Evans *et al* 2014 *J. Phys.: Condens. Matter* **26** 103202

[2] M van Kampen *et al* 2005 *J. Phys.: Condens. Matter* 17 6823
[3] W Miao *et al* 2019 *Phys. Rev. B* 99, 205433
[4] L Jiang *et al* 2005 *ASME. J. Heat Transfer* 127(10): 1167.

(P27) An ab initio study of anomalous magneto-volumetric behaviour of ferrimagnetic $Ni_{31}Mn_{25}Sn_8$ alloy

M Friák[1], M Mazalová[1,2], I Miháliková[1,2], N Masničák[1,2], M Golian[1,2], L Knoflíčková[1], F Zažímal[1,2], A Zemanová[1], I Turek[1], O Schneeweiss[1], J Kaštil[3], J Kamarád[3], and M Šob[2,1]

[1]Institute of Physics of Materials, v.v.i., Czech Academy of Sciences, Czech Republic, [2]Faculty of Science, Masaryk University, Czech Republic, [3]Institute of Physics, v.v.i., Czech Academy of Sciences, Czech Republic

We have performed a quantum-mechanical study of disordered ferrimagnetic $Ni_{31}Mn_{25}Sn_8$ martensite. Employing the supercell approach combined with the special quasi-random structure concept for modeling of disordered states we have determined thermodynamic, magnetic, structural, elastic and vibrational properties of the studied material. Its atomic and magnetic configuration is found to exhibit rather anomalous pressure-induced increase of the total magnetic moment, i.e., the total magnetic moment increases with decreasing volume. This highly unusual trend in the total magnetic moment is revealed despite of the fact that the magnitudes of local magnetic moments of atoms decrease with decreasing volume (as is common in magnetic systems). The origin of the identified anomalous phenomenon may be related to (i) the ferrimagnetic nature of the magnetic state when the parallel and antiparallel magnetic moments nearly compensate each other and (ii) chemical disorder that leads to different local atomic environments and, consequently, also to different local magnetic moments and their different response to hydrostatic pressures (the antiparalell moments are more sensitive to pressures). The studied state is mechanically and dynamically stable (no imaginary-frequency phonons) but, regarding its thermodynamic stability, it is an excited state (see M. Friák et al., Mater. Trans. (2022) in press, doi:10.2320/matertrans.MT-MA2022006).

Topic: Correlated Electron Systems

(P28) Site-specific Kondo and Spin-flip spectral signatures in chains of magnetic molecules on Au (111) surface

Yingzheng Gao, Tommaso Gorni, Sergio Vlaic, Dimitri Roditchev, Luca De' Medici, and Stéphane Pons

Laboratoire de Physique et d'Etudes des Matériaux, LPEM, France and PSL Research University, CNRS, France

When a magnetic molecule is deposited on a surface, Kondo effect occurs if the spin degree of freedom of magnetic molecule is coupled with the conduction electrons of the substrate. In that case, the magnetic moment tends to be cancelled. If the spin degree of freedom of the molecule is not coupled with conduction electrons, the spin state can be deduced from the detection of the spectroscopic signature of the spin-flips (SF) during the tunnelling process of the electrons through the molecule0.

We have used scanning tunnelling microscope (STM) to study chains of bonded Iron (II) 5,15-(di-4-bromophenyl)-10,20-(di-4-pyridyl) porphyrin molecules on Au(111) surface. By moving the chain of molecules at various locations of the reconstructed surface, we could drive the ground state of the molecules between Kondo and magnetic states. Our density functional theory (DFT) calculations suggest that the molecule exhibits low spin doublet state (S=1/2) and high spin triplet state (S=1) depending on the absorption configuration. Only low spin doublet should be giving rise to Kondo physics. This result could give to insight for the control of spin states of molecular chains in spintronic devices.

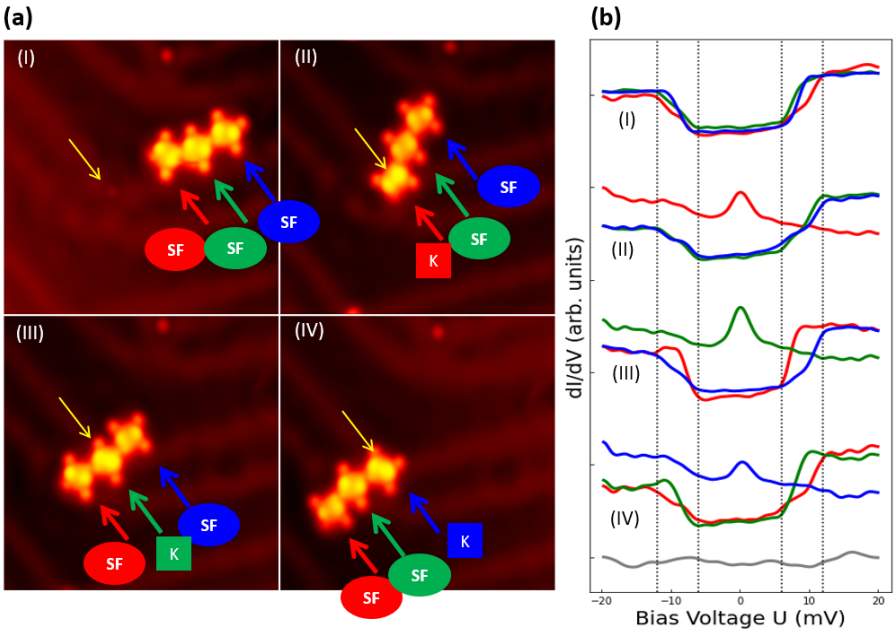

Fig1. (a) Topography image (setpoint I=20pA V=125mV) of bonded trimer molecules in different configurations labelled from (I) to (IV) on Au (111) surface. Molecules in trimer are marked by thick red, green, and blue arrows respectively, the specific site of surface is marked by thin yellow arrow. In (I) none of molecules is on specific site, in (II)-(IV) red, green, and blue marked molecule is on specific site respectively. K or SF indicate that the corresponding molecule shows Kondo or SF signature. (b) dI/dV spectra of trimer molecules in different configurations, grey spectrum taken on Au (111) surface. Kondo physics in scanning tunnelling spectroscopy (STS) experiments is evidenced by a sharp spectral feature near the Fermi level, i.e., a peak near zero bias (Abrikosov-Suhl resonance)0. SF are detected as symmetric conductance steps at low bias0.

[1] Heinrich, A, et al. (2004-10-15). "Single-Atom Spin-Flip Spectroscopy". Science. 306 (5695): 466–469

[2] Jacob, David, and Joaquin Fernández-Rossier. "Competition between Quantum Spin Tunneling and Kondo Effect." European Physical Journal B, vol. 89, no. 10, 2016, p. 210.

[3] Tsukahara, Noriyuki, et al. "Adsorption-Induced …on an Oxidized Cu(110) Surface." Physical Review Letters, vol. 102, no. 16, 2009, pp. 167203–167203.

Topic: Correlated Electron Systems

(P29) Reconfigurable stripe array metamaterial for control of surface acoustic wave propagation

Y Au[1], E R Gilroy[2], O S Latcham[1] , A V Shytov[1], T J Hayward[2], and V V Kruglyak[1]

[1]Department of Physics and Astronomy, University of Exeter, UK, [2]Department of Materials Science and Engineering, University of Sheffield, UK

Devices for control of surface acoustic wave (SAW) propagation would benefit greatly from metamaterials that are reconfigurable, non-volatile and involve fabrication of minimal complexity. To meet these requirements, we propose a metamaterial consisting of an array of nickel stripes formed atop LiNbO3 substrate (Fig. 1a). The spacing between stripes is large enough to aid fabrication but is small enough to maintain a significant magneto-dipolar coupling between adjacent stripes. This coupling leads to formation of two collective precessional eigenmodes. The lower (higher) frequency mode is characterised by in-phase (out-of-phase) oscillation of the in-plane component of the magnetisation in the nearest neighbour stripes, irrespective of whether they are magnetised parallel or antiparallel to each other. In contrast, the magneto-

elastic field acting on this dynamic magnetisation is determined by the orientation of the static magnetisation in individual stripes. One can use this dependence to control which of the two collective precessional modes couples to propagating SAWs by switching the relative magnetisation orientation of neighbouring stripes, thus achieving switchable attenuation and phase shift of SAWs propagating through the structure at designated frequencies (Fig. 1b and c). The design provides a proof of concept for manipulation of SAWs using static magnetization configuration and opens avenues to more sophisticated device architectures. In future, this concept could play a substantial role in the emerging integrated phononic circuitry. The research leading to these results has received funding from the EPRSC of the UK (Project EP/L019876/1 and EP/T016574/1).

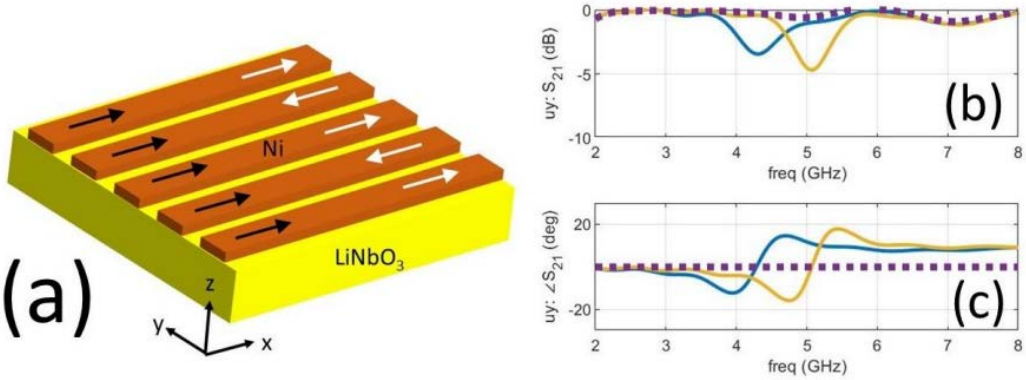

Fig. 1. (a) The Ni stripe array (width=250 nm, spacing=100 nm, thickness=30nm) formed on a 41° YX $LiNbO_3$ substrate hosts a Love mode propagating along the +x direction and polarized along the ±y direction. The nearest neighbour stripes are magnetized along x direction, either parallel or antiparallel to each other, as shown by the black arrows and white arrows, respectively. (b) Comsol simulated Love wave transmission magnitude and (c) phase shift across a 9 μm distance in x direction for the case of parallel (blue solid curve) and anti-parallel (yellow solid curve) magnetization alignment under zero bias field. The dotted curve corresponds to the same set of data with a 5 kOe bias field applied in the x direction.

(P30) Exchange constant determination using multiple-mode FMR perpendicular standing spin waves

H J Waring, Y Li, N A B Johansson, I J Vera-Marun, C Moutafis , and T Thomson

University of Manchester, UK

The exchange constant (A_{ex}) is recognised as one of the fundamental properties of magnetic materials [1]. However, its accurate experimental determination remains a particular challenge. In thin films, recent literature uses dynamic measurements exploiting Perpendicular Standing Spin Waves (PSSWs) to extract A_{ex}, typically through a measurement of the first order PSSW mode and a subsequent analysis assuming rigid surface pinning is present (Kittel model) [2,3]. Here, we present a systematic study of multiple PSSW modes in NiFe films using Vector Network Analyser-Ferromagnetic Resonance Spectroscopy (VNA-FMR) as a function of thickness (t_{NiFe}) and capping layer material (uncapped, Ta, Pt) [4]. An example of measured PSSW resonances is shown in Fig. 1a. It is shown that an analysis of PSSW resonant modes using the Kittel model provides an A_{ex} that varies with mode number, t_{NiFe} and capping layer material (Fig. 1(b-d)). This is clearly inconsistent with the physical expectation that the A_{ex} of a material is single valued for a given set of thermodynamic conditions (temperature etc.). To resolve this inconsistency, we use a more general exchange boundary condition [5] (of which the Kittel model is a particular case) and show through a comprehensive set of micromagnetic simulations that a dynamic pinning mechanism originally proposed by Wigen [6] is able to reproduce the experimental results using a single value of A_{ex}. Our findings support the

utility of short wavelength PSSWs to determine the A_{ex} in thin films, though indicate that the A_{ex} obtained has a weak dependency on the material immediately adjacent to the magnetic layer.

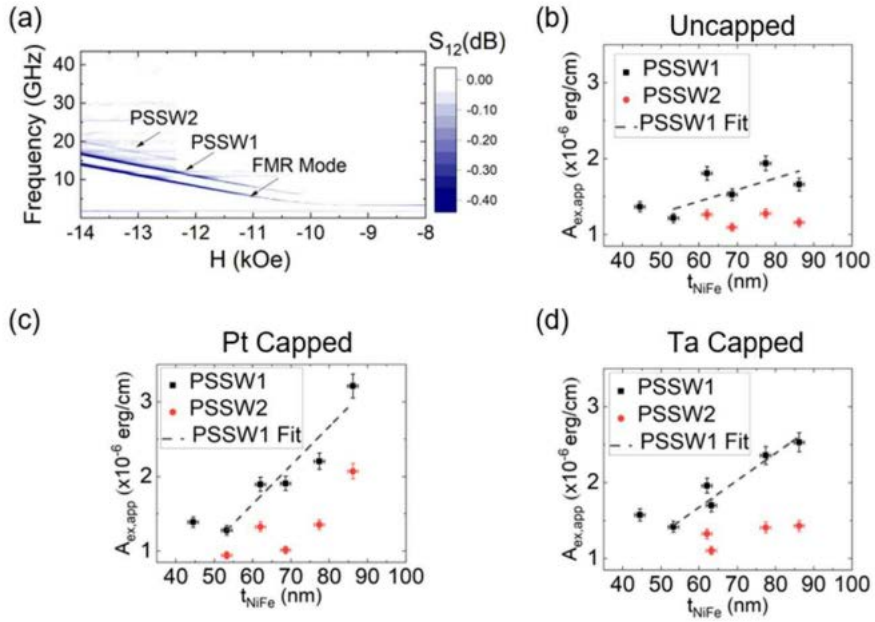

Fig 1: a) Out-of-plane spin-wave spectra of a Ta capped NiFe thin film with t_{NiFe}=77 nm as a function of applied field and frequency. (b-d) The variation in apparent exchange constant ($A_{ex,app}$) determined using the Kittel model for each capping layer case.

[1] J. M. D. Coey, Magnetism and Magnetic Materials (2010).
[2] I. S. Maksymov et al., Phys. E Low-Dimensional Syst. Nanostructures 69, 253 (2015).
[3] C. Kittel, Phys. Rev. 110, 1295 (1958).
[4] H. J. Waring et al. (Submitted).
[5] G. T. Rado et al., J. Phys. Chem. Solids 11, 315 (1959).
[6] P. E. Wigen, et al. Phys. Rev. Lett. 9, 206 (1962).

(P31) Enhancing the zero field resonances in synthetic antiferromagnets

Harry J Waring, Paul Nutter, and Tom Thomson[1]

University of Manchester, UK

Synthetic Antiferromagnets (SAFs), engineered structures of antiferromagnetically RKKY exchange-coupled ferromagnet/non-magnet/ferromagnet thin films, hold great promise for device applications [1,2]. In addition, they are fabricated using processes that are compatible with current technologies, such as STT-MRAM [3]. The magnetisation dynamics of SAFs are of particular interest as in addition to the conventional acoustic (Kittel) mode SAFs possess a higher order resonant (optic) mode which has recently been shown to exceed 20 GHz [3,4], close to those required for 5G networks [5]. In this work we demonstrate that even higher zero-field optic modes are possible by further optimising the properties of the constituent material layers and interfaces of the SAF structure. Specifically, we show results from a study to optimise the deposition parameters of the Ru layer. The SAF studied in this work possesses the structure Ta (2 nm)/CoFeB(4 nm)/Ru(0.4 nm)/CoFeB(4 nm)/Pt(5 nm), where the samples were produced using magnetron sputtering. The static magnetic properties were measured by Vector-VSM with the structural properties examined using XRR. Fig.1 shows a 2D frequency vs field map of the S_{12} parameter obtained from

our broad band vector Network Analyser (VNA-FMR) instrument. The results show a zero-field frequency optic mode at (29.71 ± 0.03) GHz representing an increase of approximately 40% over our previous value of (21.13 ± 0.01) GHz and a significant enhancement on the previously reported literature record [4]. These new results demonstrate the potential of magnetisation dynamics in SAF structures for applications requiring frequencies compatible with 6G mobile communications.

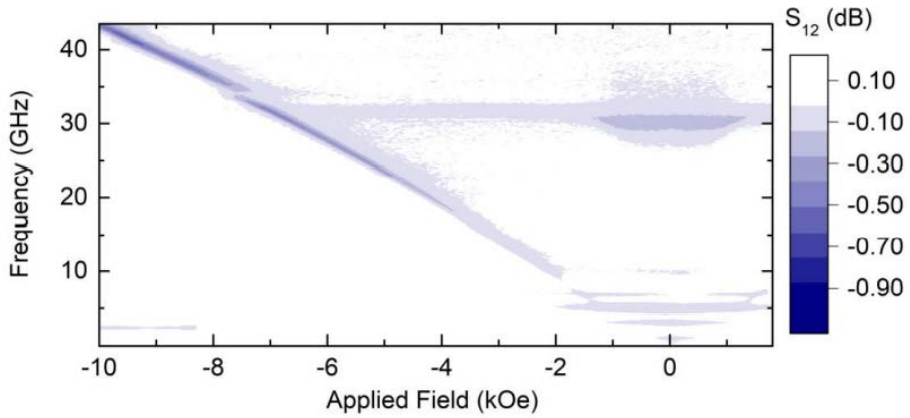

Fig 1. 2D map of the resonant spectra of a Ta(2 nm)/CoFeB (4 nm)/Ru(0.4 nm)/CoFeB(4 nm)/Pt(5 nm) SAF stack as a function of applied field and frequency.

[1] R. A. Duine et al., Nat. Phys. 14, 217 (2018).
[2] S. Li et al., Adv. Funct. Mater. 26, 3738 (2016).
[3] H.J. Waring et al., Phys. Rev. Appl. 13, 034035 (2020). [4] A. Zhou et al., J. Magn. Magn. Mater. 547, 168955 (2021). [5] J. Zhang et al., Sci. China Inf. Sci. 60, 1 (2017).

(P32) Theory of THz-Driven Rare-Earth Dynamics in $RFeO_3$

N R Vovk[1], E V Ezerskaya[2], R V Mikhaylovskiy[1]

[1]Department of Physics, Lancaster University, UK, [2]Department of Physics, V. N. Karazin Kharkiv National University, Ukraine

One of the most intriguing issues of modern data storage technologies is the creation of devices that allow information recording in an ultrafast way and with minimal energy losses. From the theory of magnetism, we know that the existence of the exchange interaction between neighbouring spins is responsible for creating a long-range magnetic ordering. Therefore, one of the possible realizations of ultrafast recording could be the switching of the exchange between the spins with subsequent writing in the form of a standard “0,1” binary code.

In this regard, the Rare Earth Orthoferrites (REO) compounds can be promising recording media due to their intrinsic properties like a strong exchange interaction between 3d iron and 4f rare-earth magnetic ions. As has been shown recently in [1,2] by using ultrashort intense coherent THz radiation (See Fig.1 a) one can modify REO f-d exchange and induce a strongly nonlinear regime of spin dynamics with subsequent switching of the magnetic order. In this way, theoretical description of nonlinear dynamics behaviour of coupled 4f rare-earth ions orbitals and 3d Iron ions spins has become an important subject to investigate.

However, to the present moment, only the role of Iron spins dynamics has been well understood, but the rare-earth subsystem's role has remained largely unexplored. Here, based on the theoretical formalism proposed in [3], we derive and calculate the response of the rare-earth orbitals to the strong THz excitation.

Thus, by using mean-field theory approximation, we have got a thermodynamic potential of the system which we used to obtain the set of equations of motion to describe the dynamics of rare-earth subsystem. Then by solving them numerically, we were able to model the behaviour of coupled rare-earth and Iron subsystems (See Fig.1b).

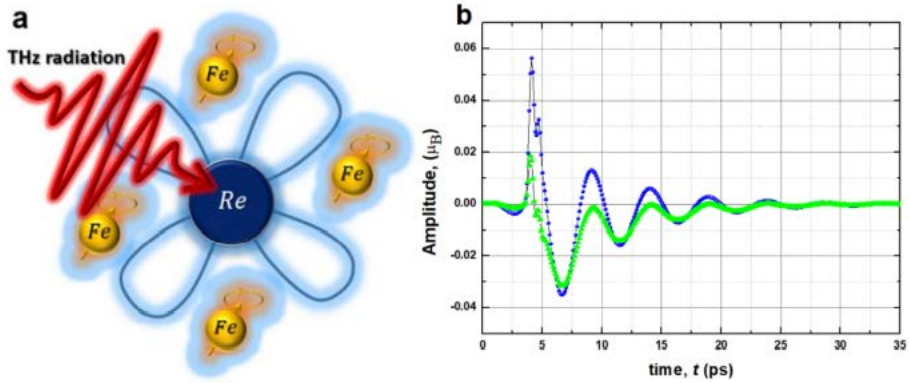

Fig.1 (a, b). Panel a shows the general idea of how strong THz radiation excites heavy Rare Earth ions and therefore modulates the f-d exchange interaction with Iron ions. Panel b shows calculated dynamics of rare-earth magnetic moment components μx and μy driven by realistic waveform of the THz pulse. The non-symmetric deflection of the moments, producing nonlinear torque on the iron spins, is obtained.

[1] S. Baierl, et al. Nature Photonics 10, 715 (2016).
[2] S. Schlauderer, et al. Nature 569, 383 (2019).
[3] A. M. Balbashov, et al. Sov. Phys. JETP 68, 629–638 (1989).

(P33) Tuneable NiFe Multilayers for High Frequency Applications

Matthew R McMaster, William R Hendren, Jade N Scott, Robert M Bowman

School of Mathematics and Physics, Queen's University Belfast, UK

Characterisation and control of the electromagnetic properties of synthetic magnetic structures at gigahertz frequencies is advantageous for the simulation and design of components for high frequency applications, such as shielding materials in magnetic recording. In such applications it is desirable to have a high saturation magnetisation, low coercivity, high permeability and near zero magnetostriction. A typical material is Ni_xFe_{100-x} alloys where x ~ 80 provides near zero magnetostriction but also relatively low magnetisation. However, multilayer structures such as $Ni_{80}Fe_{20}/Ni_{20}Fe_{80}$ may benefit some static properties such as magnetisation while retaining low magnetostriction [1]. The purpose of this work is to investigate the dynamic properties of such structures and thus explore the possibility of better performing materials through multilayer design.

We present a systematic study of the ferromagnetic resonance (FMR) of sputter deposited thin film NiFe bilayers of the form $Ni_xFe_{100-x}/Ni_yFe_{100-y}$. Of particular interest are layer combinations involving both fcc and bcc crystal structures, since studies on single films of Ni_xFe_{100-x} have shown dramatically increased damping of the FMR when Ni content is reduced across the transition from fcc to bcc near x = 40, figure 1. Magnetic and material properties were measured using FMR [2], vibrating sample magnetometry and X-ray diffraction, with the aim of determining the relation between microstructure and the static and dynamic magnetic properties. A result that was not to be expected from the single layer studies was that the FMR response of certain bilayers was strong even when the bcc NiFe layer was the dominant layer in the structure (figure 2). The possibility of incorporating the best properties of both layers in this way has significance for achieving an optimised material design.

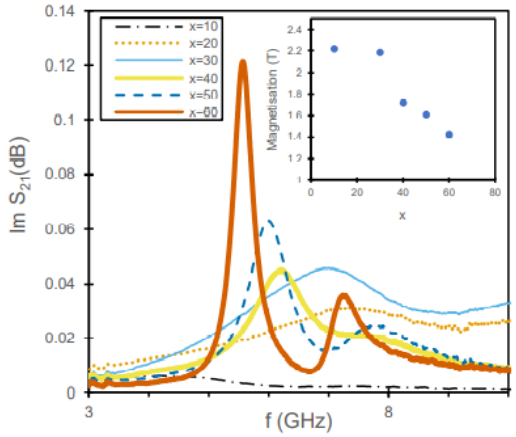

Fig. 1: FMR spectra of 100nm Ni_xFe_{100-x} single layer thin films. Note that all measurements were performed at an applied field H=253Oe. Magnetisation trend is inset.

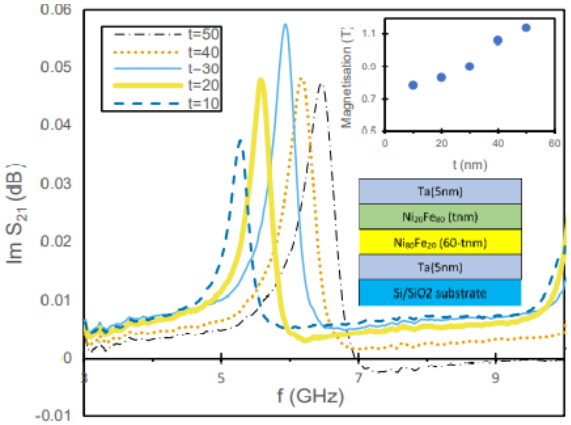

Fig. 2: FMR spectra of $Ni_{80}Fe_{20}$(60-t nm)/$Ni_{20}Fe_{80}$(t nm) thin films with varying bcc layer thickness, t. Note that all measurements were performed at an applied field of 253Oe. Magnetisation trend and structure schematic is inset.

[1] C.B. Hill. "Manipulation and Magnetostriction of NiFe Films for Advanced Reader Shielding Applications". PhD Thesis. QUB. 2013
[2] Y. Ding et al. J. Appl. Phys. 96. (2004).

(P34) Magnetisation dynamics in thin ferromagnetic films with Hybrid Anisotropy

Daniel Bangay, Jaime Leon, Harry J. Waring, Thomas Thomson

NEST Group, University of Manchester, UK

Hybrid anisotropy thin film heterostructures with a high perpendicular anisotropy fixed layer and an in plane low anisotropy free layer have become structures of considerable interest for applications in spin torque oscillators (STOs) [1] and magnetic bit patterned media [2]. It has been suggested that structures with hybrid anisotropy can take advantage of the best properties of both in plane and out of plane polarising layers in STOs [3]. Exchange coupled $[Co/Pd]_8$-Pd-NiFe films such as those shown in Fig.1 (a) can achieve such a hybrid anisotropy [4]. Furthermore, the dynamic properties of these films can be easily tuned by varying the Pd "exchange break" layer thickness.

Here, we investigate the magnetisation dynamics of such hybrid anisotropy structures in the direct exchange coupled limit, where there is no Pd spacer layer. The samples were fabricated by DC magnetron sputtering. Vector Vibrating Sample Magnetometry (V-VSM) was used to verify ferromagnetic coupling, and a Vector Network Analyser Ferromagnetic Resonance (VNA-FMR) setup was used to investigate magnetization dynamics.

We identify a single resonance mode in the FMR spectrum, which is expected in the directly exchange coupled limit. In Fig.1 (b) we plot the resonance frequency for several fixed fields, as a function of the field angle, where 0˚ is in-plane and 90˚ is out of plane. It is seen that the resonance frequency is minimal at both 0˚ and 90˚ with a maximum between 30˚ to 45˚. The properties of resonances in our hybrid anisotropy structures are a complex combination of the properties of the individual layers. Thus, we see an effective 'easy' axis low-frequency resonance along the easy axes of the NiFe and $[Co/Pd]_8$ layers (0˚ and

90˚ respectively), and an increase in the resonance frequency as the field angle varies between these values. This interpretation agrees well with preliminary micromagnetic simulation results.

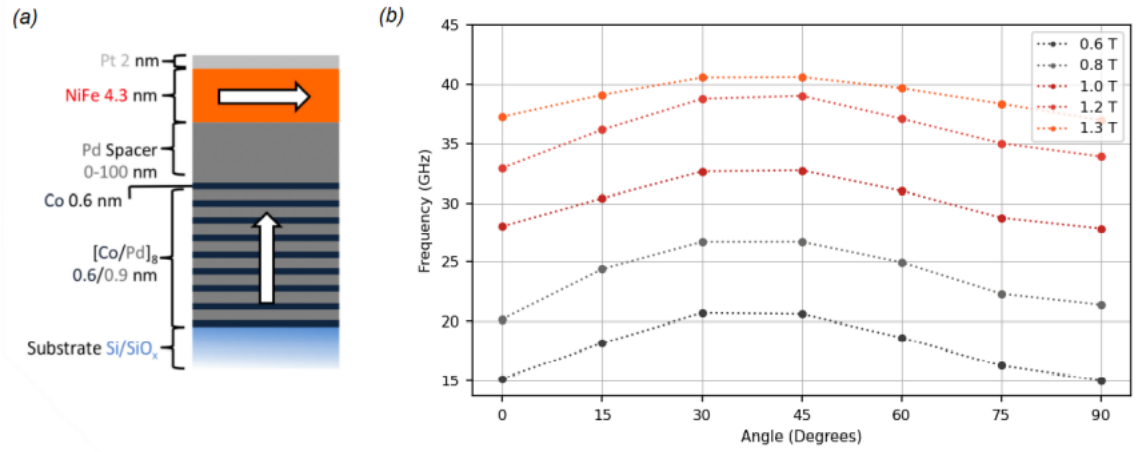

Fig 1 (a) Schematic representation of $[CoPd]_8$-Pd-NiFe films used in this study. (b) Plot showing the field angle dependence of resonance frequency for several applied fields.

[1] K. J. Lee, O. Redon, and B. Dieny, Appl. Phys. Lett. 86, 022505 (2005)
[2] T. Thomson, B. Lengsfield, H. Do, and B. D. Terris, J. Appl. Phys. 103, 07F548 (2008)
[3] Y. Zhou et al., Appl. Phys. Lett. 92, 262508 (2008)
[4] C. Morrison, J. J. Miles, T. N. Anh Nguyen, et al., J. Appl. Phys. 117, 17B526 (2015)

(P35) The THz-driven nonlinear spin wave propagation in an antiferromagnet

Y Saito, and R V Mikhaylovskiy

Lancaster University, UK

In recent years, thanks to the technology of lasers, many breakthroughs on the interaction between terahertz (THz) electromagnetic field and antiferromagnets were reported. Particularly, the intense THz emission, generated by the tilted pulse front method, enabled driving spin dynamics directly without optical pump. The excited antiferromagnet resonance surpassed the linear regime and the nonlinearity in the antiferromagnetic orthoferrite was experimentally observed [1]. However, the theoretical analysis of non-local spin deflection propagation from the excitation region has not been revealed sufficiently. We model the spatial distribution of the THz-driven spin deflection in the rare-earth orthoferrites and its time development.

We solved a partial nonlinear differential equation for the quasi-ferromagnet mode in the weak ferromagnets. We assume a metallic antenna for the amplification on the crystal surface, which forms the exponential distribution of both magnetic and electric filed [2]. As a result, the ultrashort THz pulse flipped the magnetic vector around the antenna and the spin waves with non-zero wavenumber were generated at the edge of the moving domain wall. At the conference, we will discuss the results under various amplitudes, orientations and origins of the external field and discuss the specification of spin wave generated by the nonlinearity.

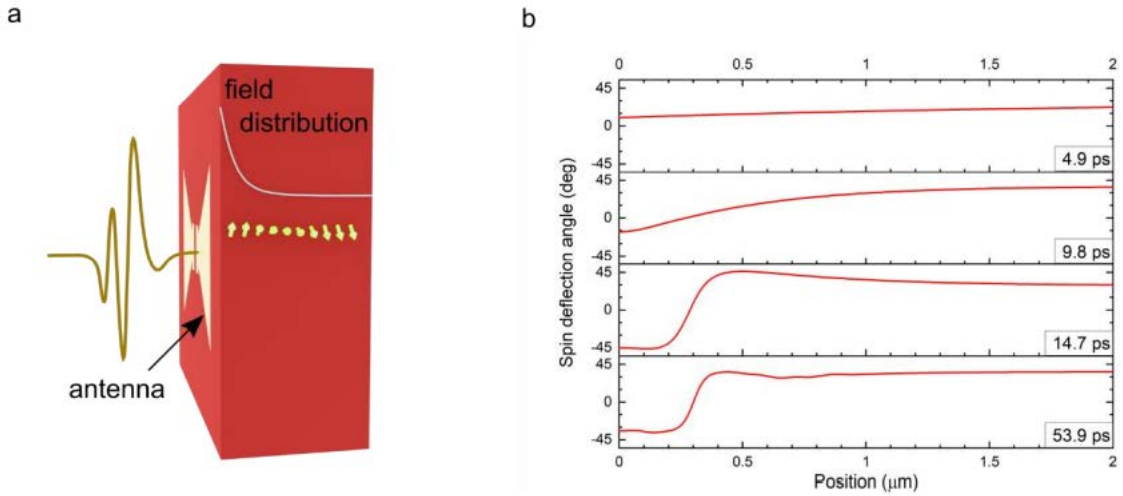

Fig 1 a, the geometry to achieve non-uniform THz distribution. b, Snapshots of excited spin waves emitted from the THz excitation region.

[1] S. Baierl, et al. Nature Photonics 10, 715 (2016).
[2] S. Schlauderer, et al. Nature 569, 383 (2019).

Topic: Nanoparticles

(P36) Signature of coexistent Ferromagnetism and Superconductivity in Bi coated Ni nanoparticles

Laxmipriya Nanda[1], Pratap K Sahoo[1], and Kartik Senapati[1]

[1]School of Physical Sciences, National Institute of Science Education and Research, HBNI, India

Competition between the superconducting (S) and ferromagnetic (F) orders at the interface of S-F hetero-structures gives rise to several interesting physical phenomena. A few examples are (i) damped oscillatory behaviour of superconducting order parameter in ferromagnet and (ii) long range spin triplet supercurrent in ferromagnet. These effects have been widely studied in S-F thin film multilayer structures [1, 2]. However, there are fewer reports on exploring the S-F hetero-structures in nanoscale geometries such as nanoparticles and nanowires. In the literature, coexistence of superconductivity and Ferromagnetism has been observed in Pb/PbO core-shell nanoparticles [3] and Sn/SnO core-shell nanoaprticles [4] where Pb and Sn were the superconducting components, respectively. In these studies, however, ferromagnetism is not the bulk property of the oxide shells. Rather, ferromagnetism originates from defects and oxygen vacancies at the interface of metal and the corresponding oxide in these core-shell structures. Therefore, studies of superconducting proximity effect are not possible in these material combinations. For this one needs to have nanoparticle of a well established bulk ferromagnetic material coated with a superconducting layer or vise-versa. In particular, it could be interesting to study how the induced superconducting order behaves in a confined magnetic nanostructure. The practical difficulty with studying such F-S nanostructures would be to achieve a clean enough interface which is absolutely imperative to see the superconducting proximity effect. There are not many chemical routes available to fabricate F-S core-shell structures where both superconducting and ferromagnetic orders are established bulk properties of the materials. In this context, here we attempt to fabricate and characterize a superconductor coated bulk ferromagnetic nanoparticle system, where Ni is the ferromagnetic component and $NiBi_3$ is the superconducting component coated on the Ni nanoparticles. We have found earlier [5, 6] that a bulk superconducting phase $NiBi_3$ grows naturally on Ni by diffusion reaction process when Bi is deposited on the Ni surface. Since the superconducting phase

($NiBi_3$, with $T_c \sim 4.2$ K) forms into the ferromagnetic Ni surface, the interface between $NiBi_3$ and Ni is expected to be very clean. Nickel nanoparticles were prepared from the thin film of Ni deposited on Si/SiO2 substrate using solid state de-wetting method. Magnetization(M) vs Magnetic field(H) characterization on these isolated nanoparticles indicated superparamagnetic behaviour, due to single domain nature of ferromagnetic nanoparticle and inter-particle interactions. Subsequently Bismuth was thermally evaporated onto these nickel nanoparticles at elevated temperatures to enhance diffusion and formation of $NiBi_3$. The $NiBi_3$ was confirmed by variable glancing angle X-ray diffraction and Transmission Electron Microscopy on Bismuth coated Nickel nanoparticles. Since these are isolated particles spread on a substrate the only way to look for superconducting signal was Magnetization(M) vs Temperature(T) measurement, which confirmed a superconducting transition below 3K.

[1] A.I. Buzdin. In: Reviews of Modern Physics 77 (2005), pp. 935–976.
[2] F. S. Bergeret et al. In: Reviews of Modern Physics 77 (2005), pp. 1321–1372.
[3] Chien-Kang Hsu et al. In: Journal of Applied Physics 109 (2011), 07B528.
[4] Xiao-Liang Wang et al. In: J. Phys. Chem. C 114 (2010), pp. 14697–14703.
[5] Vantari Siva et al. In: Journal of Applied Physics 117 (2015), p. 083902.
[6] Vantari Siva et al. In: Journal of Applied Physics 119 (2016), p. 063902.

(P37) High-Moment Films Produced by Depositing Gas-Phase Nanoparticles

Raúl López-Martin[1], Benito S Burgos[1], José A De Toro[1], Peter Normile[1], Andrew Pratt[2], and Chris Binns[1]

[1]Universidad de Castilla-La Mancha, Departamento de Fisica Aplicada, Instituto Regional de Investigación Científica Aplicada (IRICA), Spain, [2]University of York, Department of Physics, UK

There is a need in many industries for soft magnetic materials with a high saturation magnetisation that exceeds that of currently available alloys. A promising candidate is nanostructured FeCo produced by co-depositing gas-phase nanoparticles of one element and an atomic vapour of the other. Such films have been studied by magnetometry and synchrotron radiation methods and they have been demonstrated to have a saturation magnetisation that exceeds the Slater-Pauling limit. They also have a soft magnetic behaviour resulting from the random anisotropy direction of the deposited nanoparticle building blocks. The films do not form magnetic domains and their magnetic switching is more rapid than that in conventional films. The latest developments and the technological applications of the films will be discussed.

(P38) Magnetic nanoparticles for spin Seebeck based thermoelectrics

M Awad, and K. Morrison

Physics Department, Loughborough University, UK

Thermoelectric generation is an energy harvesting method that could utilize waste heat from sources such as lighting and engines to increase the efficiency of various technologies.[1] Whilst solid-state thermoelectric generators benefit from reliability (non-mechanical source of energy), their relatively low efficiencies present a limitation to widespread applications.

In 2008, it was shown that a spin current is generated in a ferromagnetic (FM) film placed under a temperature gradient – the spin Seebeck effect (SSE). This is typically detected by the inverse spin Hall effect (ISHE), where this spin current is injected from the ferromagnetic film into an adjacent non-magnetic metals (such as Pt) and the spin current is converted to a measurable charge current[1].

The spin Seebeck effect has been suggested as a potential direction for thermoelectrics due to scalability with area and physical separation of the electric and thermal conductivities that control the efficiency of such a

device. What is new in the spin Seebeck device (Fig. 1) is that it has a scalability different from that of conventional Seebeck devices, in that the output power is proportional to area perpendicular to the temperature gradient. However, there are still several drawbacks, such as limitations on the efficiency of spin conversion by the inverse spin Hall effect and spin injection from the ferromagnetic to the paramagnetic detection layer(s).

The goal of this work is to make composites of Pt/FM nanoparticles to explore additional scalability of the spin Seebeck effect in bulk composites[2]. Additionally, to enhance the quality of the Pt/FM interface using chemical routes (Fig. 1) to develop an easy, affordable, and scalable spin Seebeck based devices for energy harvesting[3]. I will outline and discuss initial results, including a study of size dependence of different NPs, as well as the potential applications of such spin Seebeck thermoelectrics, their basic design, and the measurement of device efficiency.

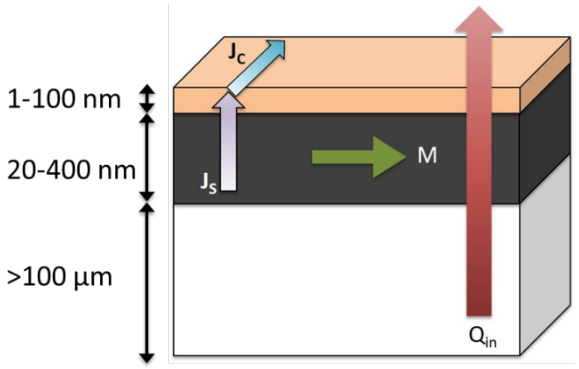

Fig 1 – Left: Schematic of a simple spin Seebeck based device. Right: schematic of the one-pot synthesis method of Fe_3O_4 nanoparticles.

[1] K. Uchida et al., 455, 778–781 (2008).
[2] S. R. Boona, K. Vandaele, I. N. Boona, D. W. McComb, and J. P. Heremans, Nat. Commun., 7, 13714 (2016).
[3] D. K. Kim, M. Mikhaylova, Y. Zhang, and M. Muhammed, Chem. Mater., 15, 1617–1627 (2003).

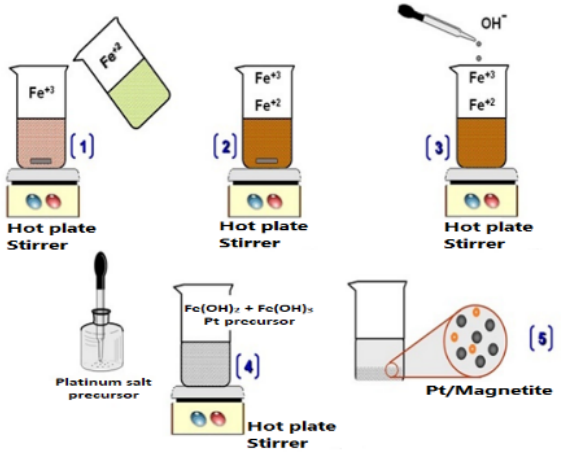

(P39) Synthesis, characterisation and biofunctionlisation of $BaTiO_3$ – $CoFe_2O_4$ magnetoelectric nanoparticles for biomedical applications.

Samyog Adhikari, Le Duc Tung and Nguyen TK Thanh*

Biophysics Group, Department of Physics & Astronomy University College London, UK and UCL Healthcare Biomagnetics and Nanomaterials Laboratories, UK

Magnetoelectric nanoparticles (MENP) have magnetic and electric properties coupled together.[1] Here, the significant coupling between the two properties will allow direct control of ferroelectricity and magnetism. MENP are of significant interest in biomedical applications as they exhibit new functionalities such as magnetic field control of electric polarisation used in on-demand drug release among others.[2] Although there are several ways of achieving the magnetoelectric (ME) effect, combining a magnetic material with a ferroelectric one in a core-shell structure has gained significant interest in recent years due to its large ME effects.[3] The magnetic phase used in this study will be cobalt ferrite (CF) due to its high magnetostrictive coefficient and the ferroelectric phase barium titanate (BT) due to its high piezoelectric coefficient.[4, 5]

First, we present an optimisation of the synthesis protocol for the ferroelectric and the ferrimagnetic phase to control morphology of the nanoparticles. The effect of morphology and size on the properties of MENP will be studied by using different characterisation techniques (TEM, SQUID, STM, XRD, Raman, DLS).

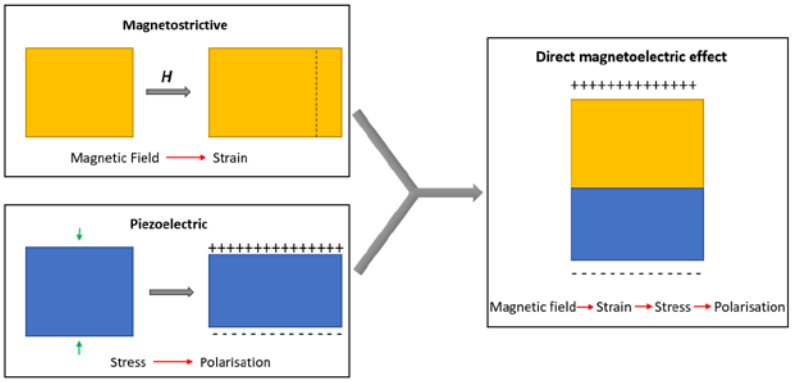

Fig 1: Schematic of magnetoelectric coupling causing direct magnetoelectric effect.

When a magnetic field is applied on a MENP, CF undergoes magnetostriction which causes the material to strain and elongate. This mechanical energy is transferred to BT which then exhibits polarisation. This is called strain mediated magnetoelectric coupling (figure 1). The shape and size of the core-shell nanostructure is controlled using synthetic parameters.

[1] Spaldin NA. Magnetic materials: fundamentals and applications. Cambridge university press; 2010 Aug 19.
[2] Kolishetti N, Vashist A, Arias AY, Atluri V, Dhar S, Nair M. Recent advances, status, and opportunities of magneto-electric nanocarriers for biomedical applications. Molecular aspects of medicine. 2021 Nov 4:101046.
[3] Wang P, Zhang E, Toledo D, Smith IT, Navarrete B, Furman N, Hernandez AF, Telusma M, McDaniel D, Liang P, Khizroev S. Colossal Magnetoelectric Effect in Core–Shell Magnetoelectric Nanoparticles. Nano Letters. 2020 Jul 8;20(8):5765-72.
[4] Pan Q, Xiong YA, Sha TT, You YM. Recent progress in the piezoelectricity of molecular ferroelectrics. Materials Chemistry Frontiers. 2021;5(1):44-59.
[5] Bozorth RM, Tilden EF, Williams AJ. Anisotropy and magnetostriction of some ferrites. Physical Review. 1955 Sep 15;99(6):1788.

(P40) Magnetic anisotropy in relation to nanoparticle agglomeration and hyperthermia

David Serantes

Applied Physics Department and Instituto de Materiais (iMATUS), Universidade de Santiago de Compostela, Spain

Since the magnetic response of a system of magnetic nanoparticles may change significantly due to agglomerate formation, as in the case of the heating performance under AC fields [1], awareness of the agglomeration likelihood of the magnetic colloid is crucial for several applications. The problem is that it is often estimated through the ratio between magnetic dipole-dipole and thermal energies, therefore missing the key factor that the magnetic moment may fluctuate internally and thus hamper the agglomeration process [2]. This is to say, that the key role of the magnetic anisotropy constant (K) is neglected. In this work we perform a theoretical study, based on the comparison between the involved timescales (i.e., inner-particle magnetic relaxation vs. entire particle rotation and displacement), about how the threshold size for magnetic agglomeration, d_{aggl}, is influenced by the K value [3]. In addition, based on the key role of the magnetic anisotropy on hyperthermia performance we also simulate the heating capability, as non-agglomerated particles would be desirable for the application.

Scheme illustrating how the comparison of relaxation times may be correlated with the active part of the particle size distribution, and thus with agglomeration likelihood [2].

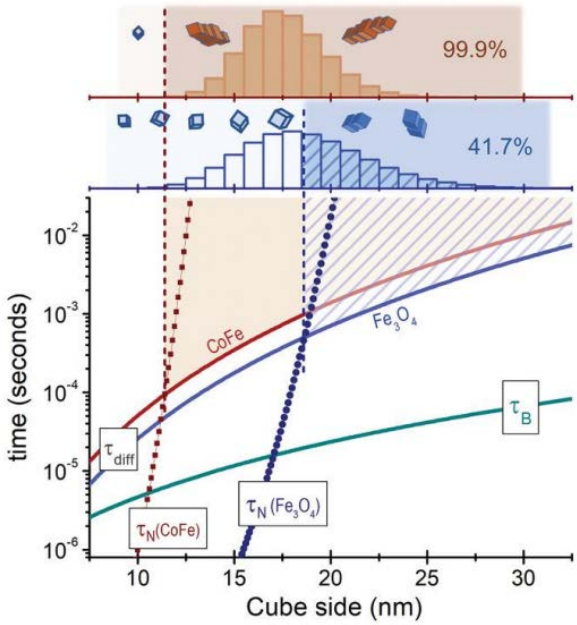

[1] D. Serantes et al., J. Phys. Chem. C 118, 5927-5934 (2014).
[2] P. B. Balakrishnan et al., Adv. Mater. 32, 2003712 (2020). [3] D. Serantes and D. Baldomir, Nanomaterials 11, 2786 (2021).

Topic: Spintronics

(P41) Growing and characterising magnetic tunnel junction structures

Meg Smith[1], Charlotte Bull[1], Matt Spink[2], Paul Nutter[1], Chris Allen[2,3], and Tom Thomson[1]

[1]Nano Engineering and Spintronic Technologies (NEST) group, Department of Computer Science, University of Manchester, UK, [2]Diamond Light Source Ltd, Diamond House, Harwell Science & Innovation Campus, UK, [3]Department of Materials, University of Oxford, UK

Spin-transfer-torque magnetoresistive random access memory (STT-MRAM) and Spin-orbittorque magnetoresistive random access memory (SOT-MRAM) have enormous potential as non-volatile data storage technology due to their scalability, energy efficiency, and fast read/write speed [1]. However, the problem of the magnetic recording trilemma associated with HDD media remains and will emerge as an issue to overcome for the future development of ultra-high-density STT/SOT-MRAM [1]. To improve such devices further, their key component, the magnetic tunnel junction (MTJ), must first be optimised; one way to achieve this is to ensure interfacial lattice matching between the MgO barrier and ultra-thin film (≤1.5 nm) CoFeB to obtain perpendicular magnetic anisotropy (PMA) in the MTJ structure [1]. To fabricate MTJ structures, it is essential to understand how each of the individual layers contributes to the stack's overall functionality; for example, smooth, pinhole-free MgO (~1 nm) tunnel barriers are important to achieving sufficiently high tunnelling magnetoresistance ratios [2].

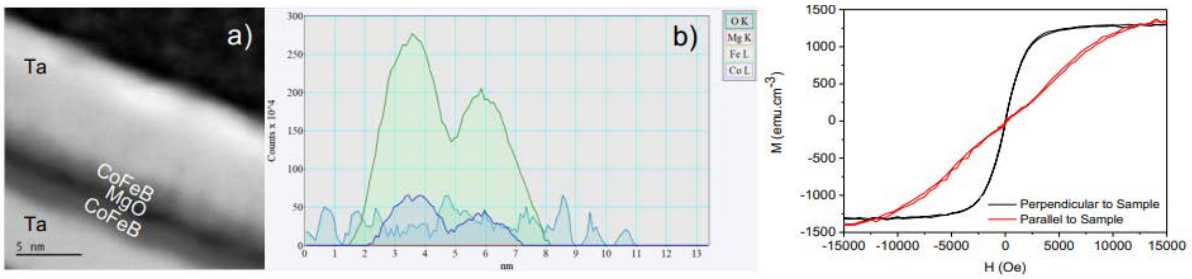

Fig. 1. (a) STEM high-angle annular dark field image showing the individual layers that form the MTJ, showing continuous CoFeB and discontinuous MgO layers (b) Integrated intensity of the EELS core-loss edges taken from a line scan through the MTJ.

Fig. 2. Magnetic hysteresis loop for an MTJ film annealed to 340°C and measured by VSM, applying a 20kOe field perpendicular (black) and parallel (red) to the sample surface.

Prototype MTJs have been improved by optimising the sputter growth conditions of the CoFeB and MgO layers. MTJs consisting of ($Pt(3nm)/Ta(5nm)/Co_{20}Fe_{60}B_{20}(0.8nm)/MgO(1nm)/Co_{20}Fe_{60}B_{20}(0.7nm)/Ta(5nm)$) have been grown at room temperature on Si/SiO_2 (290nm) substrates. The thicknesses of the MTJ layers were identified using X-ray reflectivity (XRR), and the magnetic properties have been investigated using vibrating sample magnetometry (VSM). Scanning transmission electron microscopy (STEM) has been used to investigate the MTJ structure (Fig.1); this experiment found that all the expected layers are present, but that interfacial roughness degraded the ultrathin CoFeB and MgO layers, as the MgO layer became discontinuous. Based on this result, the Ta deposition parameters have been optimised to produce a smoother seed layer with a view to producing higher quality, smoother interfaces. In the next phase, the MTJs will be annealed at temperatures between 300°C and 400°C to achieve strong interfacial PMA as shown by previous research, Fig.2, where annealing the MTJ to a temperature of 340°C produces strong interfacial PMA. As optimisation and characterisation of MTJ films are essential for developing novel film structures for STT-MRAM and SOT-MRAM, point contacts are lithographically patterned to perform CIPT measurements on MTJ films [3]. The overall goal of this project is to study the magnetoresistance ratio dependence with annealing conditions.

[1] D. Apalkov et al. Proc. IEEE 104,1796-1830 (2016).
[2] S. Ikeda et al. Appl. Phys. Lett. 93, 082508 (2008).

[3] D. C. Worledge et al. Appl. Phys. Lett. 83, 84 (2003)

(P42) Spintronic terahertz emitters exploiting uniaxial magnetic anisotropy for field-free emission and polarisation control

S M Hewett[1,2], C Bull[1,2], C-H Lin[1,2], A M Shorrock[2,3], R Ji[1,2], M T Hibberd[2,3], T Thomson[1], P W Nutter[1], and D M Graham[2,3]

[1]Nano Engineering and Spintronic Technologies Group, Dept. of Comp. Science, University of Manchester, UK, [2]Department of Physics & Astronomy & Photon Science Institute, University of Manchester, UK, [3]The Cockcroft Institute, Sci-Tech Daresbury, Keckwick Lane, Daresbury, Warrington

The useful ability to generate and control pulses of broadband terahertz (THz) radiation has mediated the advance of non-invasive, investigative technologies used for material characterisation, medical diagnosis and weapon detection [1-2]. With further research, pulses of THz radiation have future application in the ultrafast control of electron spin states [3] and picosecond magnetisation switching in ferrimagnets and antiferromagnets [4]. To exploit the full potential of THz radiation, emitters are required that can generate a THz electric field of high amplitude, ETHz, with a broad spectral bandwidth and gapless coverage over the full THz spectral region (1-10 THz) [5]. Simple spintronic emitters consisting of ferromagnetic (FM)/nonmagnetic (NM) thin films, such as CoFeB/Pt, satisfy these requirements, producing strong THz pulses (ETHz < 300 kV/cm [6]) with gapless bandwidths of up to 30 THz [6] when excited by femtosecond laser pulses. In particular, ETHz has been shown to scale with laser fluence and the magnetic moment of the FM layer, M, to which the THz pulses are perpendicularly polarised [5]. This offers the possibility to create devices in which the THz amplitude and polarisation can be controlled, at source, through magnetic manipulation.

While many spintronic THz emission schemes utilise saturating fields, Happ, to maximise M, and hence ETHz, recent work on field shaping schemes [7-9] results in regions across the FM layer where M < Ms, and the emitted THz pulse profile is influenced by the remanent magnetisation, Mr, of the FM layer. We have investigated the THz emission characteristics of Co20Fe60B20 (2.5 nm)/Pt (3 nm) bilayer structures in this below magnetic saturation regime and reveal orientation dependence in the emission behaviour, arising from in-plane uniaxial magnetic anisotropy (UMA) of the CoFeB FM layer. By maximizing the UMA through manipulation of sputter deposition conditions and aligning the external applied field, Happ, with the easy axis, ETHz is found to reach saturation under weaker applied fields (Fig. 1). In addition, ETHz is seen to remain at saturation when Happ is removed (Fig. 2), effectively providing an emitter that requires no external magnetic field to drive emission. The development of spintronic structures that can emit broadband THz pulses without the need for an applied field is beneficial to THz spectroscopy, and facilitates the production of largearea spintronic emitters,

overcoming one of the key challenges of such emitters compared to well-established sources of THz radiation [5]. Furthermore, by aligning Happ along the hard axis we observe a 90⁰ rotation of the THz pulse polarisation as Happ is reduced to zero. Manipulating Happ therefore allows polarisation control of ETHz, without the need for mechanical rotation of external magnets.

[1] Woodward et al., J. Biol. Phys. 29, 257, 2003;
[2] Kawase et al., Opt. Express 11, 2549, 2003;
[3] Baierl et al., Nat. Photonics 10, 715, 2016;
[4] Wienholdt et al., PRL 108, 247207, 2012;
[5] Bull et al., APL Mater. 9, 090701, 2021;
[6] Seifert et al., Nat. Photonics 10, 483, 2016;
[7] Hibberd et al., APL 114, 031101, 2019;
[8] Niwa et al., Opt. Express 29, 13331, 2021;
[9] Kong et al., Adv. Opt. Mater. 7, 1900487, 2019.

(P43) A 3D magnetic field sensor based on one single spin–orbit torque device

Ruofan Li, and Long You

School of Optical and Electronic Information, Huazhong University of Science and Technology, China

With the conventional transistor approaching its physical limits, the heterogeneous integration technology opens a new way and has been an industry trend in the post-Moore law period. Tremendous efforts have been devoted to this field including the integrations of sensors, MEMS, optoelectronics, RF and mm-wave devices. On the other hand, for the artificial intelligence system, sensor-enabled perceptual ability is as important as the learning ability and reasoning ability. Actually, the detection of three-dimensional (3D) magnetic field is more practical than that of 1D magnetic field. Traditional approaches for the detection of 3D magnetic fields require multiple sensors to obtain the magnitude of the magnetic field components along the three axes (x, y, and z), or to use a magnetic flux guide to deflect the magnetic field to the detection direction of planar sensors, making the set-ups bulky. However, these solutions have the problem that the three measured magnetic field components are not orthogonal or not in the same spatial position.

Here, a single memristive spin–orbit torque device composed of a HM/CoFeB/MgO heterostructure for sensing a vector magnetic field is demonstrated. A vector magnetic field is composed of two in-plane (IP, H_x or H_y) components and one out-of-plane (OOP, H_z) component. These three elements can lead to continuous multiple intermediate magnetization states in the CoFeB layer with the switching mode of domain wall motion or domain nucleation, modulating the associated anomalous Hall effect resistance (R_H) [1, 2]. Moreover, R_H has a linear response with H_x, H_y and H_z. We derive the net contributions to R_H from each of the three orthogonal components. Based on the measured resistance, the magnitude of the three field components can be obtained, implementing the detection of the 3D magnetic field. Our compact 3D magnetic field sensor exhibits low 1/f noise, good linearity and sensitivity within a certain range in the *x*, *y* and *z* directions, respectively.

[1] R. Li, S. Zhang, S. Luo, Z. Guo, Y. Xu, J. Ouyang, M. Song, Q. Zou, L. Xi, X. Yang, J. Hong and L. You, *Nat. Electron.* 4, 179–184 (2021).
[2] S. Zhang, Y. Su, X. Li, R. Li, W. Tian, J. Hong and L. You, *Appl. Phys. Lett.* 114, 042401 (2019).

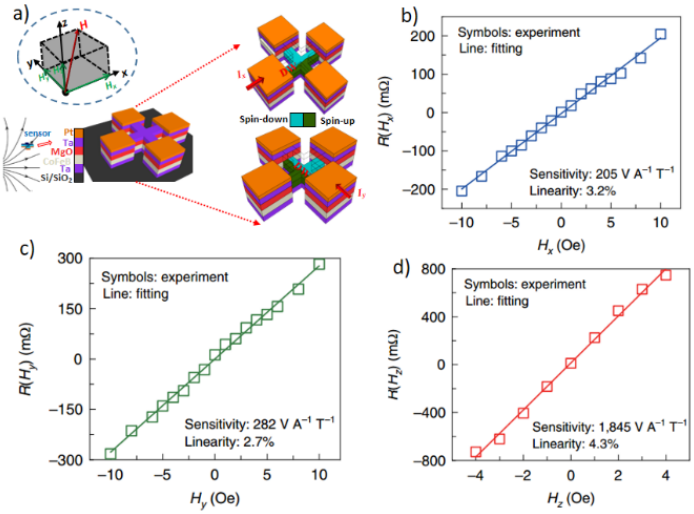

Fig. 1. Three-dimensional magnetic field sensing based on a ta/coFeB/MgO heterostructure. a) Schematic of the 3D sensor placed in a vector magnetic field. b) The net resistance component $R(H_x)$ as a function of H_x. c) The net resistance component $R(H_y)$ as a function of H_y. d) The net resistance component $R(H_z)$ as a function of H_z.

(P44) Extrinsic contributions to spin Hall angle in Cu induced by impurities

J Harknett, M G Greenaway, and K Morrison

Physics Department, Loughborough University, UK

The spin Hall effect (SHE) is a phenomenon of increasing interest in spintronics in which a spin current can be generated from a charge current in nonmagnetic materials without using ferromagnets. The efficiency of the SHE is defined by the ratio of the spin current, J_s, induced to the charge current, J_c, otherwise known as the spin Hall angle (SHA = J_s/J_c). For there to be efficient spintronics devices, a larger value of the SHA is sought after. For pure metals, such as Pt or β-Ta, large SHAs have been reported [2],[3] due to high intrinsic spin-orbit coupling, however these are often not practical for widescale use. A giant SHE was reported for Au in 2008,[4] which was attributed to extrinsic spin-scattering (skew scattering). Following on from this, there have been several studies on increasing SHA in otherwise poor materials such as Cu or Au, that are well suited as interconnects for electronics. For example, Niimi et al. reported that Cu doped with a small amount of Bi had a SHA as high as -0.24 [5].

It has been suggested by Fert and Levy [6], that the SHA is induced by resonant skew scattering of the 6p orbitals on Bi impurities in Cu. In this case, the SHE comes from the asymmetric and symmetric scattering probabilities in channels of odd and even angular momentum (l). Along with skew scattering, another contribution to the SHE is side-jump scattering, which is proportional to the impurity concentration, with concentrations up to and potentially beyond 10% [6,7]. For impurities such as Ta in Cu, the concentration could exceed 10% increasing the SHA from a skew scattering dominated contribution to the SHE to include side-jump effects.

We will outline the calculation of these values in some example doped Cu alloys and compare to experimental results. We will show using density functional theorem (DFT) to simulate materials with various levels of doping how applying the Friedel's sum rule and phase shift model can be used to calculate the scattering contribution to the SHA and the effect that the concentration of the dopant has on this value. The advantage of this approach is that it would allow us to engineer the SHA via doped materials in order to optimise it for use in more efficient spintronic devices.

Figure 1: Spin Hall effect in a nonmagnetic material (NM), where J_c is the charge current and J_S^{SHE} is the spin current generated.[1]

[1] T. C. Chuang et al., Phys. Rev. Research 2, 032053(R) (2020);
[2] A. Hoffman, IEEE Trans. Magn., 49, pp. 5172-5193 (2013);
[3] L. Liu et al., Science 336, 555 (2012);
[4] T. Seki et al., Nat. Mater. 7, 125 (2008);
[5] Y. Niimi et al., Phys. Rev. Lett. 109, 156602 (2012);
[6] A. Fert and P. M. Levy, Phys. Rev. Lett. 106, 157208 (2011); [7] P. M. Levy et al., Phys. Rev. B 88, 214432 (2013).

(P45) Atomistic simulations of spin-orbit torque switching of Pt/MnPt bilayers

Richard F L Evans[1], Carenza E Cronshaw[1], and Sarah Jenkins[1,2]

Department of Physics, University of York, UK Institut für Physik, Universität Duisburg-Essen, Germany

Antiferromagnetic spintronics is a new field of research which uses spintronic effects to manipulate the magnetic properties of antiferromagnets [1-3]. The interaction of magnetic materials and electrical currents is extremely complex, with a wide variety of effects such as the spin Hall effect, the Rashba effect, anisotropic magnetoresistance, spin transfer and spin orbit torques, all with their origins in spin orbit coupling. This is even more complex in the case of antiferromagnets where there are no magnetic stray fields and the presence of ultrafast dynamics. Here we present atomistic simulations [4] of interfacial spin-orbit torque switching of $L1_0$ MnPt / Pt bilayers. The model includes an exact representation of the crystal structure and collinear antiferromagnetic ground state of MnPt suitably oriented to have an interfacial spin-orbit torque from the neighbouring Pt layer to enable electrical switching between the two easy axis directions. We find that the reversal speed and threshold strongly depends on the strength of the spin-orbit torque field and also the strength of the magnetocrystalline anisotropy which acts to stabilise the MnPt. Figure 1 (left) shows a visualisation of the average magnetic ground state spin structure achieved after simulated cooling of the MnPt to zero K, with an easy axis along the 001 crystal direction. Dynamic atomistic simulations of spin-orbit torque switching using the Landau-Lifshitz-Gilbert equation in Figure 1 (right) show different switching timescales based on the strength of the spin-orbit torque, which is directly proportional to the current density. We will present additional calculations of the effects of thermal fluctuations on the switching and the role of Gilbert damping on the waiting and reversal times to gain a better understanding of SOT induced switching from a theoretical perspective.

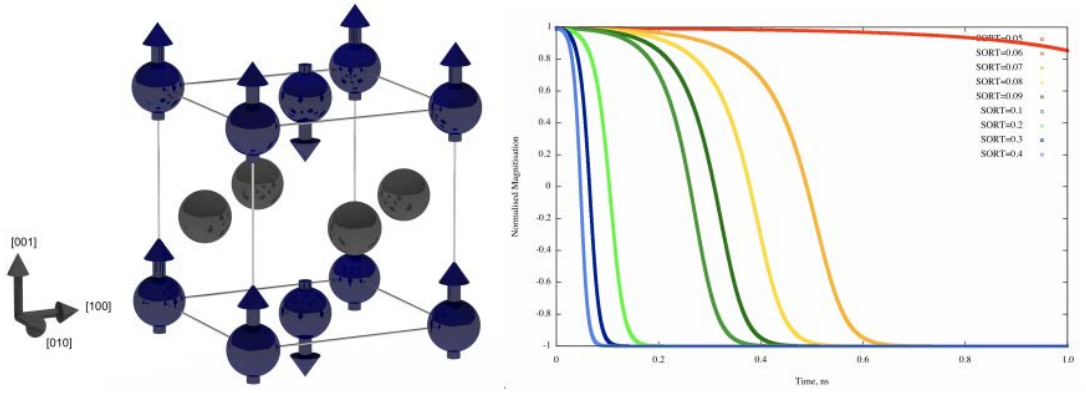

Fig 1. Visualisation of groundstate magnetic structure of L10 MnPt showing spin directions and non-magnetic Pt atoms (left). Atomistic simulations of switching dynamics of MnPt for different strengths of spin-orbit torque field (right) showing a non-linear dependence of the waiting-time on the current.

[1] T. Jungwirth, X. Marti, P. Wadley, and J. Wunderlich, Nature Nanotechnology 11, 231 (2016)
[2] V. Baltz et al, Rev. Mod. Phys. 90, 015005 (2018)
[3] T. Jungwirth et al, Nature Physics 14, 200 (2018)
[4] R. F. L. Evans et al J. Phys.: Condens. Matt. 26, 103202 (2014)

(P46) Investigating ballistic transport in 1D graphene/FM spin injectors

Daniel Burrow, Jesus C Toscano-Figueroa, Noel Natera-Cordero, Chris R Anderson, Victor H Guarochico-Moreira, Thomas Thomson, Irina Grigorieva, and Ivan J Vera-Marun

University of Manchester, UK

Despite its great promise for spintronics, experimental values for spin transport parameters extracted from graphene are currently significantly below theoretical predictions. Our group recently reported encouraging results from a novel spintronic device architecture that constitutes a fully encapsulated single layer graphene (SLG) channel and employs one-dimensional (1D) ferromagnetic contacts (Fig. 1a) [1]. Encapsulation of the channel in hexagonal boron nitride (hBN) preserves the quality of the graphene, resulting in long range charge and spin transport, while adoption of 1D contacts mitigates many of the problems associated with 2D tunnel contacts, such as doping [2, 3]. In addition, the geometry of the contact area places transport across the junction in the ballistic regime. This not only allows for achieving sizeable contact resistance (R_c) without the need for tunnel barriers, but also opens the possibility of studying previously unexplored phenomena such as quantized conductance across the 1D graphene/FM junction. Here we detail further results from our novel device architecture with a focus on the behaviour on the 1D FM/graphene junction at low temperature. Measurements of contact resistance while sweeping back gate voltage imply a strong dependence of R_c on carrier density that becomes more pronounced as temperature is decreased (Fig. 1b); this indicates the possibility of tuneable spin injection through manipulation of the Fermi level in the graphene region adjacent to the contacts [1, 3]. Additionally, in voltage bias spectroscopy measurements on 1D contacts in single layer and bilayer graphene (BLG) devices, we observe quantized conduction through the junction in no applied magnetic field, a previously unreported result in such devices. These results may offer new insight into the spin injection process in 1D contacts.

[1] Guarochico-Moreira, V. H., et al. (2021). *Tuneable spin injection in high-quality graphene with one-dimensional contacts*. http://arxiv.org/abs/2109.08827
[2] Wang, L., et al. (2013). *One-Dimensional Electrical Contact to a Two-Dimensional Material*. Science, 342(6158), 614–617.

[3] Xu, J., et al. (2018). *Spin inversion in graphene spin valves by gate-tunable magnetic proximity effect at one-dimensional contacts*. Nature Communications, 9(1), 2869.

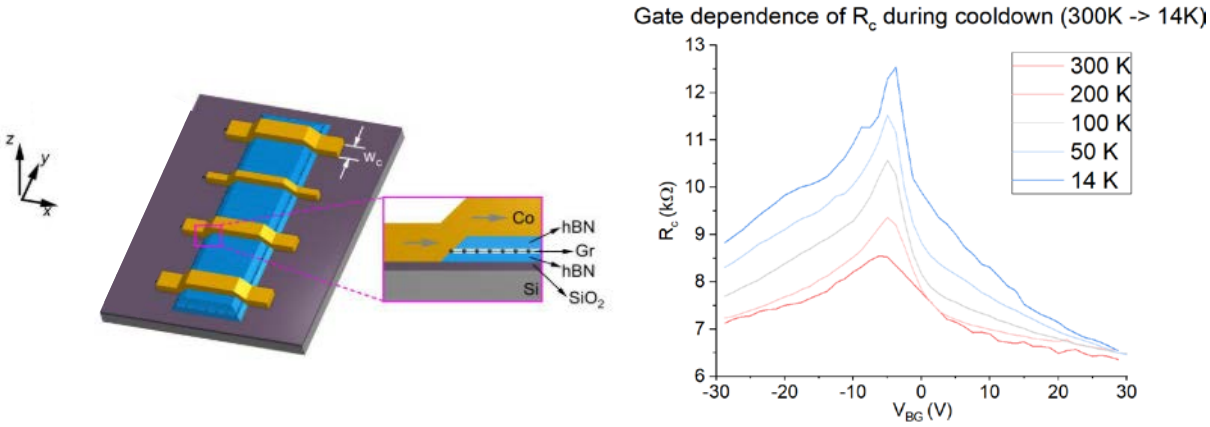

Fig 1: (a) 3D schematic and 2D cross section (inset) of the device architecture. Figure adapted from [1]. **(b)** Gate voltage profiles taken at various temperatures to illustrate the evolution of R_c as the temperature is decreased.

(P47) Magneto-Optic Imaging of Coupled Domains in BaTiO3(111)/CoFeB Heterostructures

Robbie Hunt[1], Kévin Franke[1], Philippa M Shepley[1], Andrew J Bell[2], Thomas A Moore[1]

[1]University of Leeds, School of Physics and Astronomy, UK, [2]University of Leeds, School of Chemical and Process Engineering , UK

Ferroelectrics have been the subject of great interest to the field of thin film magnetism for the purpose of electric field control of magnetism 1. Magnetic thin films with a high magnetostriction deposited onto ferroelastic substrates couple strongly to the strain transferred at the interface. When deposited onto ferroelectrics the individual ferromagnetic domains have differing strain orientations resulting in a one-to-one mapping of the local ferroelectric domain onto the local magnetization with the possibility to control the behaviour of the magnetization purely through the application of a voltage to the ferroelectric 2. This degree of control presents an avenue by which more efficient spintronic devices could be designed.

Previous work has focused on using $BaTiO_3(100)$ as the substrate in which the polarization can rotate by 90° either in or out of the plane. In this work, we deposit films of $Co_{40}Fe_{40}B_{20}$ on $BaTiO_3(111)$ oriented substrates in which the projection of the polarization at the surface of the substrate can rotate through a 60° or 120° angle from one domain to the other. Using magnetooptic Kerr microscopy we can obtain magnetic contrast in adjacent domains and determine the magnetic easy axes through the angular dependence of the remanent magnetization. This study reveals that there are two distinct anisotropy states that must be dependent on the polarization of the ferroelectric a quasi-perpendicular state where the spin rotation is 120° and close to perpendicular to the ferroelectric domain wall, seen in figure 1a, and a quasi-parallel state with a spin rotation of 60° that is close to parallel in figure 1b. The acute angle between the easy axes of adjacent domains, Δ, is 60° in both states. Furthermore, we can swap the contrast between longitudinal and transverse configurations to show that it is possible to initialize the domains in either head-to-head or tail-to-tail configurations dependent only on how the magnetic field is applied with respect to the ferroelectric domains. Understanding these domain configurations lays the groundwork for voltage control of coupled domains in $BaTiO_3(111)$/CoFeB devices.

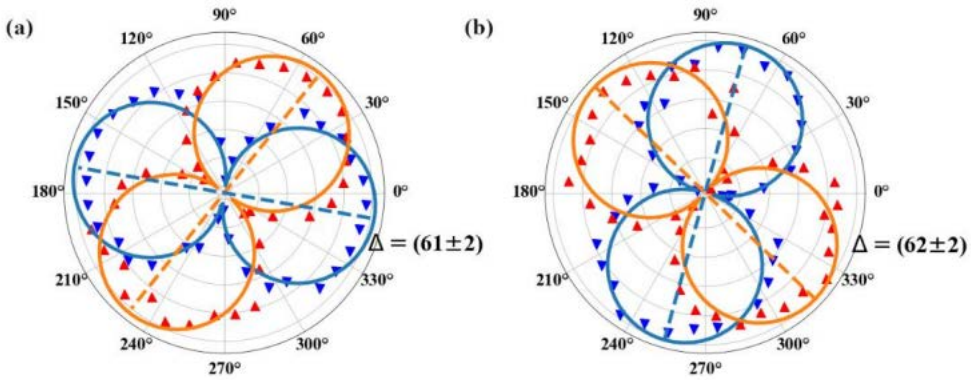

Fig 1. Polar plots of two different regions of the same sample demonstrating quasiperpendicular (a) and quasiparallel (b) behavior. Up and down triangles represent adjacent ferroelectric domains.

[1] M. Ghidini, F. Maccherozzi, X. Moya, L. C. Phillips, W. Yan, J. Soussi, N. M´etallier, M. E. Vickers, N. J. Steinke, R. Mansell, C. H. W. Barnes, S. S. Dhesi, and N. D. Mathur, Advanced Materials 27, 1460 (2015).

[2] R. Streubel, D. K¨ohler, R. Sch¨afer, and L. Eng, Phys. Rev. B 87, 054410 (2013).

(P48) Combined spin transfer torque and spin orbit torque for low power magnetisation dynamics in magnetic tunnel junctions

Andrea Meo[1,2], Roy W Chantrell[2], Jessada Chureemart[1], and Phanwadee Chureemart[1]

[1]Department of Physics, Mahasarakham University, Thailand, [2]Department of Physics, University of York, UK

Spin transfer torque magnetoresistive random access memories (STT-MRAM) have been proposed as a universal memory able to replace silicon-based technologies from the slow to the fast end of the memory hierarchy. Magnetic tunnel junctions (MTJs) are the key structure used in STT-MRAM and provide the low power consumption, long retention times, high endurance and downscaling potential [1]. However, STT-MTJs suffer of long incubation and stochastic delays, and the large current densities that cross the MTJ stack required for fast writing operations cause degradation of the tunnel barrier. These factors limit the reliability and switching speed of STT-MRAMs. An alternative is represented by spin orbit torque MRAMs (SOT-MRAMs), which promise faster switching, low error rates, and endurance of the barrier [2,3]. The writing mechanism relies on SOT induced by an in-plane current flowing in a metallic layer adjacent to the MTJ and does not require the electric current to flow across the MTJ. However, SOT-MRAM is a three terminal device and as such has a larger footprint, requires a symmetry-breaking mechanism to achieve deterministic switching in perpendicular systems and it consumes more power for switching. A possible solution to overcome the limitations affecting STT- and SOT-MRAMs is to combine these two effects in a single device. Here we perform atomistic spin simulations of magnetisation dynamics induced by combination of SOT and STT in CoFeB-based MTJs. Within the model the effect of SOT is introduced as a Slonczewski formalism, whereas the effect of STT is included via a spin accumulation model. We investigate a CoFeB/MgO/CoFeB MTJ coupled with a heavy metal layer where the charge current is injected into the plane of the heavy metal to induce SOT, meanwhile the other charge current flows perpendicular into the MTJ structure and is responsible for STT (Figure 1(a)). Our results reveal that SOT can assist the precessional switching induced by spin polarised current within a certain range of injected current densities yielding a low power, efficient and fast reversal on the sub-nanosecond timescale (Figure 1(b)). The combination of STT and SOT gives a promising pathway to improve high performance CoFeB-based devices with high speed and low power consumption.

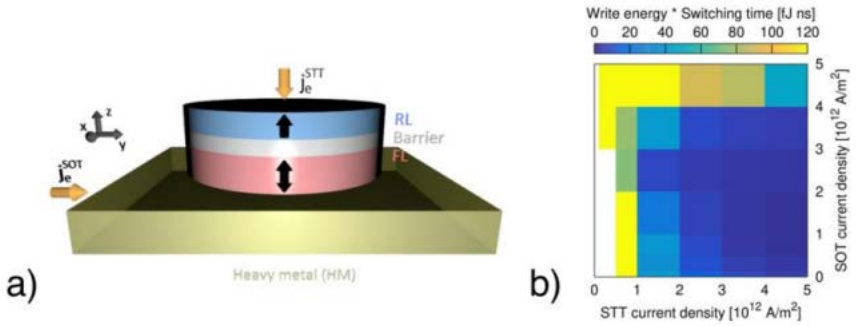

Fig 1: (a) Schematic of combined SOT-STT MTJ. The in-plane current j_e^{SOT} flowing through the heavy metal induces the spin current by SOT, the perpendicular current j_e^{STT} injected into the MTJ is responsible for STT. Brass colour depicts the heavy metal (HM), red and light blue represent the free layer (FL) and reference layer (RL) of the MTJ respectively, light grey refers to the MTJ barrier. (b) Write energy*total switching time as a function of j_e^{STT} and j_e^{SOT} for a MTJ diameter of 20nm. The palette gives the energy*switching time and ranges from efficient switching (blue) to inefficient writing (yellow). White regions correspond to no switching.

[1] S. Bhatti et al, Mater. Today 20, 530–548 (2017)
[2] A. Manchon et al, Rev. Mod. Phys. 91, 035004 (2019)
[3] K. Garello et al, In 2018 IEEE Symposium on VLSI Circuits, vol. 54, 81–82 (IEEE, 2018)

(P49) Thermodynamic properties and switching dynamics of perpendicular shape anisotropy MRAM

Wayne Lack, Roy W Chantrel, Richard F L Evans, and Sarah Jenkins

University of York, UK

Magnetoresistive RAM is a non-volatile memory technology that stores a bit as a magnetic state of a ferromagnetic CoFeB free layer which can either align or anti-align with a fixed magnetisation CoFeB layer, where these two layers sandwich a non-magnetic MgO layer, shown in figure 1a. The modern market consists mainly of dynamic and static RAM which are both volatile technologies and draw large amounts of power in high performance computing clusters. MRAM is ultrafast and durable while scaling to smaller volumes than the limitations of SRAM and DRAM allow, attracting significant research and development. [1] To achieve practical applications, MRAM must display a high thermal stability, high tunnel magnetoresistance ratio and a low writing current while scaling to competing volumes. A recent development with potential to achieve this scalability is to use tower structures with height greater than the diameter, which allows the perpendicular shape anisotropy and the interfacial perpendicular magnetic anisotropy to favour out-of-plane magnetisation direction. [2] For reliable MRAM satisfying the three requirements above, the switching mechanism at operational temperatures needs to be understood. This study uses atomistic simulations which model the tower structure using two anti-ferromagnetically coupled CoPt layers to pin the fixed CoFeB layer, with a monolayer either side of the MgO with enhanced exchange coupling and uniaxial anisotropy. The free layer thickness is varied to observe emerging trends as the towers are scaled down. The system is modelled using a spin Hamiltonian with thermal fluctuations and dipole fields included with the LLG. [3] We have found in figure 1b (i) that the susceptibility of the free layer varies hugely as the volume is increased, but dividing these taller towers into smaller local regions in figure 1 b(ii) we find smaller and correlated curves. This shows the magnetisation is non-uniform throughout the tower, which may suggest a non-uniform magnetisation mode. In figure 1 c (i) we see snapshots of the reversal process at 50 Kelvin demonstrating nucleated domain wall reversal mode in taller towers, compared to smaller towers in figure 1 c (ii) where the switching is coherent.

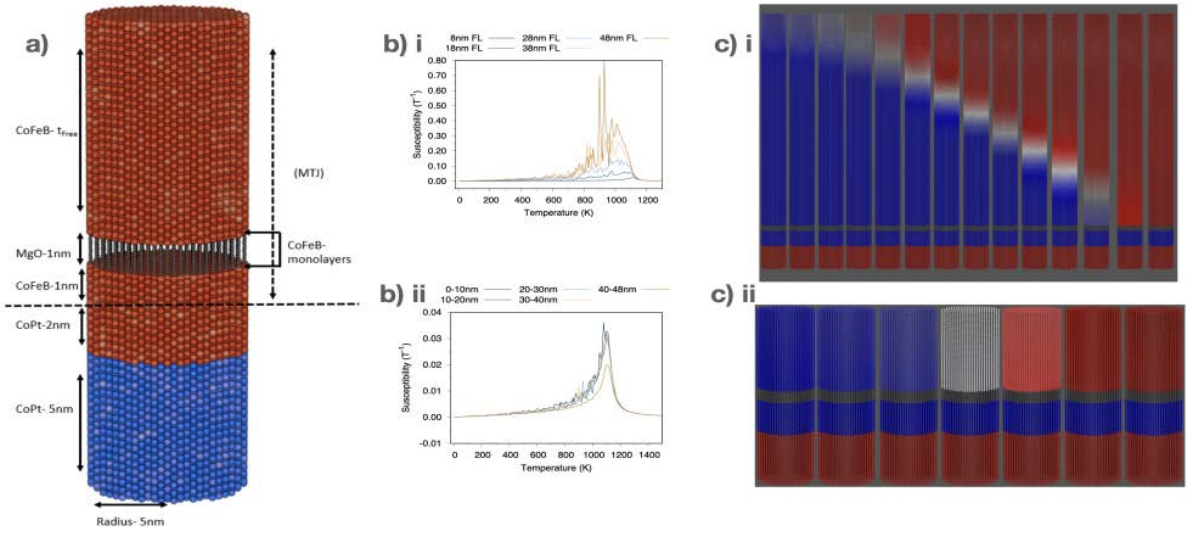

Fig 1. a) shows the dimensions and structure of the PSA MRAM simulated, b) i shows the susceptibility for the whole free layer while ii shows the susceptibility of local 10nm chunks of the tallest tower. c) i Shows nucleated reversal in the tallest tower and ii shows coherent rotation in the smallest tower.

[1] K. Watanabe et al, Nature Communications, 9, article no. 663, 2018
[2] N. Perrissin et al, Nanoscale, issue 25, 2018
[3] R. F. L Evans et al, journal of physics: condensed matter, volume 26, number 10, 2014

(P50) Ultrafast magnetization dynamics in $Ni_{80}Fe_{20}$/Neodymium bilayer films

Lulu Cao[1], Qian Chen[2], Yuting Gong[3], Zhaocong Huang[1], and Ya Zhai[1]

1. School of Physics, Southeast University, China 2. Nanofabrication facility, Suzhou Institute of Nano-Tech and Nano-Bionics, Chinese Academy of Sciences, China 3. Jiangsu Provincial Key Laboratory of Advanced Photonic and Electronic Materials, School of Electronic Science and Engineering, China

Recently, as the most important physical quantity in spintronics, spin current has been extensively studied. The transmission of a spin current across the interface between materials is usually determined by the spin-mixing conductance at the interface. To improve the efficiency of spin transport or injection, control of the spin-mixing conductance at the interface is critically essential. Previous reports have proposed that an antiferromagnetic interface facilitates the spin transmission at the interface [1-2] of ferromagnetic/nonmagnetic (FM/NM) bilayers. In ferromagnetic/rare earth (FM/RE) structures, the magnetic moment of the RE materials is induced by adjacent FM layer, such that they are antiparallel to each other, resulting in a spontaneous antiferromagnetic interface. The relationship between the spontaneous antiferromagnetic interface and the spin-mixing conductance in FM/RE systems lack thorough research.

The ultrafast magnetization dynamics in $Ni_{80}Fe_{20}$/neodymium (Py/Nd) bilayer films were studied by using the time resolved magneto-optical Kerr effect (TRMOKE). Results show that the antiferromagnetic interface was suppressed by the increasing Zeeman field, which led to the decrease of interface spin-mixing conductance. This research demonstrates the key role that the antiferromagnetic interface plays in the spin transmission in FM/RE structures.

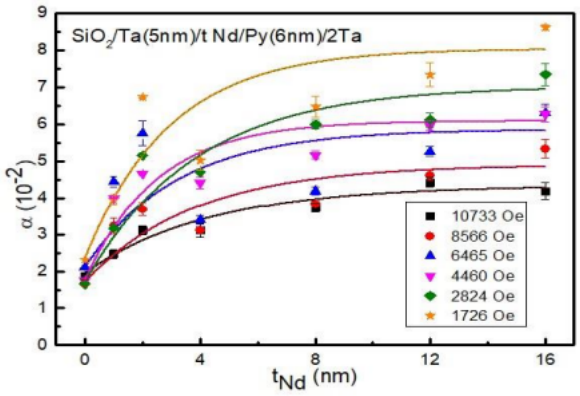

Fig. 1 Dependence of the Nd layer thickness in relation to magnetic damping (α) at varying magnetic fields.

[1] W. W. Lin, K. Chen, S. F. Zhang, C. L. Chien. Enhancement of Thermally Injected Spin Current through an Antiferromagnetic Insulator. Phys. Rev. Lett. 116, 186601 (2016).

[2] Y. Wang, D. P. Zhu, Y. M. Yang, K. Lee, R. Mishra, G. Go, S. H. Oh, D. H. Kim, K. M. Cai, E. L. Liu, S. D. Pollard, S. Y. Shi, J. M. Lee, K. L. Teo, Y. H. Wu, K. J. Lee, H. Yang. Magnetization switching by magnon-mediated spin torque through an antiferromagnetic insulator. Science 366, 1125–1128 (2019).

(P51) Spin Torque Nano Oscillators as MIMO sources for 5G telecommunications

Amelia Winterburn[1], Chris Foxley[2], David Bonham[2], Andrea Meo[3], and Richard F L Evans[2]

[1]BT Research, Adastral Park, UK, [2]Department of Physics, University of York, UK, [3]Department of Physics, Mahasarakham University,Thailand

The move to 5G and the rise of smart devices is putting pressure on wireless network operators to supply suitable bandwidth without large energy requirements. The need for new high-frequency, low-power alternatives to current communications hardware is clear. Spin torque nano oscillators (STNOs) are small bilayer ferromagnetic devices that can emit microwave electromagnetic radiation in the presence of a static magnetic field and a dc current induced spin transfer torque [1,2]. Here we present macrospin micromagnetic simulations of a single STNO device investigating the transient response and frequency of the emitted field as a function of the Gilbert damping and strength of the spin transfer torque based on the model of Taniguchi et al [3] . We perform a systematic study of the magnetization dynamics as a function of current, damping and external magnetic field strength to assess the suitable parameter ranges for 5G communications. We find that STNOs can produce stable oscillations at low GHz frequencies, with an elliptical precession of the magnetisation, as shown in Fig. 1. Relaxation to stable oscillation is found to be only a few cycles allowing for fast modulation of the signal (up to 170 MHz). For a given external applied field and damping, we find a region of high sensitivity to the strength of the spin transfer torque, allowing for current controlled signal modulation at GHz rates. Systematic simulations show that optimal efficiency is found for low Gilbert damping and large currents. This early stage work requires further exploration into thermal and non- collinear effects, power considerations, tuneability and array interference, however, early indications are that STNOs are a very promising technology for wireless microwave communications.

Fig. 1: Dynamic simulations of a STNO device. (a) Schematic of the simulated device structure showing spin polariser layer, oscillating free layer and coordinate system. (b) Time dependence of the magnetisation under the action of a STT field, showing relaxation to stable oscillation. (c) Time dependence of the cycle frequency, showing a characteristic time $\tau \sim 5$ns fitted by $f(t) = A\exp(-t/\tau) + B$. (d) Detail of the magnetisation dynamics at equilibrium, showing a small non-sinusoidal oscillation of the z-component of the magnetisation due to the device symmetry.

[1] T. Chen et al Proceedings of the IEEE 104, 1919 (2016) [2] Z. Zeng, G. Finocchio, and H. Jiang, Nanoscale 5, 2219 (2013) [3] T.Taniguchi and H.Kubota, Japanese Journal of Applied Physics 57, 053001 (2018)

Topic: Thin films/General submission

(P52) Development of a variable frequency, low current, low volume hysteresis loop tracer

Daniel M. Clarke, and Gonzalo Vallejo-Fernandez

Department of Physics, University of York, UK.

A variable frequency, low current, low cost, high sensitivity magnetometer has been developed [1]. The system uses three MnZn ferrite rods to enhance the maximum field achievable by up to a factor 6 compared to the case where no ferrites are used. The system was tested using a suspension of magnetite nanoparticles in water. The magnetic response of the particles was investigated as a function of the maximum applied field and the frequency of operation. Volumes as low as 7 µl are required to obtain a signal to noise ratio of 8(47 kHz)/3(111 kHz) for a fluid with a saturation magnetisation of 1.07 emu/cm^3. Fields as high as 420 Oe can be applied by passing a current as low as 2.5 A through the primary coil at all operating frequencies.

A resonant circuit is used to create an alternating current at a series of defined frequencies. The primary coil is 140 mm long, inner diameter of 10 mm, and 280 turns over three layers built on a PEEK former. Litz wire (200 strands, 0.071 mm width/strand) was used to reduce the effective impedance and negate the skin-depth effect. Two secondary coils wound in opposition were used to measure the sample signal as well as the field amplitude. Each coil consists of 18 turns of 0.2 mm copper wire. The high field (160 Oe/A), low current requirement is achieved through the use of three 40 mm long, 6 mm wide MnZn ferrite rods (Fair Rite, Material 78) [2]. This material provides a flux density of 4800 G at 5 Oe and 25°C measured at 10 kHz. A schematic of the primary and secondary coils is shown in Figure 1(a) while some of the measured

hysteresis loops at 47 kHz are shown in Figure 1(b). The full description of the apparatus and the obtained data will be presented in the full paper.

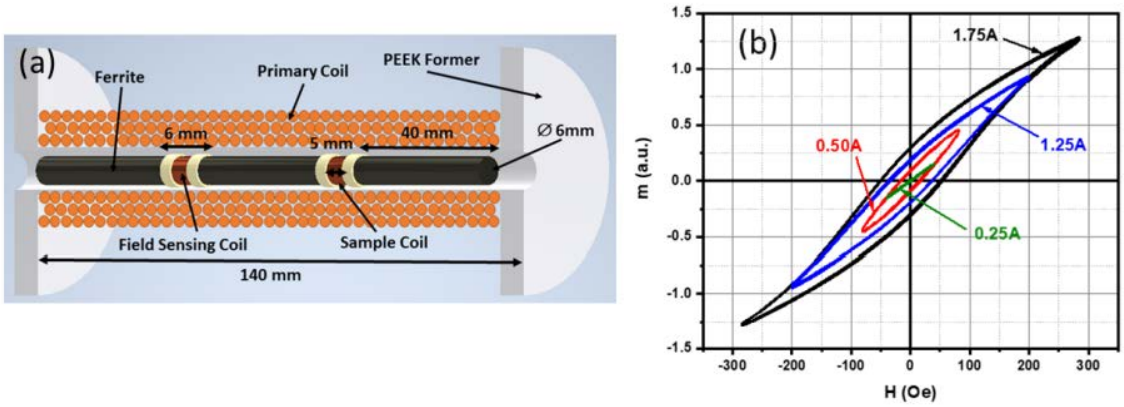

Fig 1. (a) Schematic diagram of the sensing setup and (b) Typical hysteresis loops measured at 47 kHz.

[1] D. M. Clarke, and G. Valllejo-Fernandez, submitted to J. Magn. Magn. Mater.
[2] http://www.fair-rite.com/78-material-data-sheet/

(P53) ISIS Neutron and Muon Source: The one-stop Magnetism Characterisation Shop

Helen Walker, Christy Kinane, Goran Nilsen, and Sean Langridge

ISIS, STFC, Rutherford Appleton Laboratory, Oxford, United Kingdom

The ISIS Neutron and Muon Source is a world-leading centre for research in the physical and life sciences. ISIS produces beams of neutrons and muons that study the structure and dynamics of materials at the atomic level using a suite of instruments. Most importantly the unique fundamental properties of both probes make them ideal for studying magnetism in all of its myriad forms. ISIS is free for UK and RoI users, including transport and accommodation; and we also allow proposals from PhD level (with supervisor overview) upwards. We also welcome beamtime applications from industrial and commercial customers.

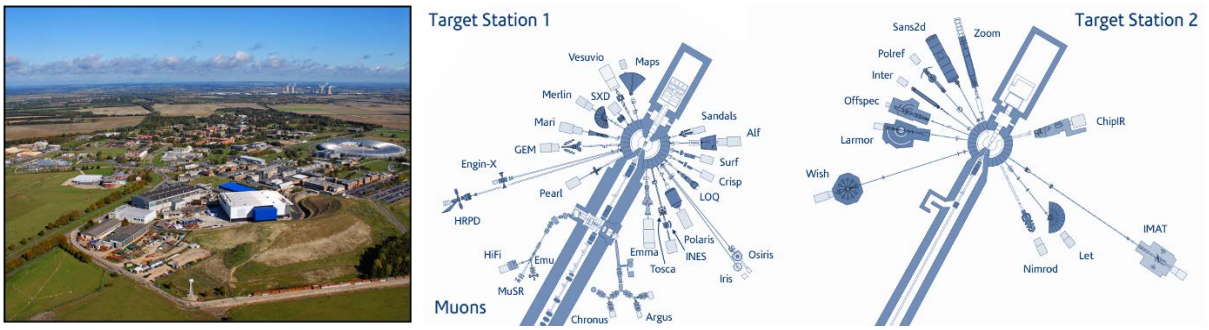

The Next Proposal deadline is the 20th of April 2022! Apply at the URL below:

https://www.isis.stfc.ac.uk/Pages/Apply-for-beamtime.aspx

Please contact any of the authors for more information and direction towards scientists working on the relevant instruments. Remember PhD students can apply!

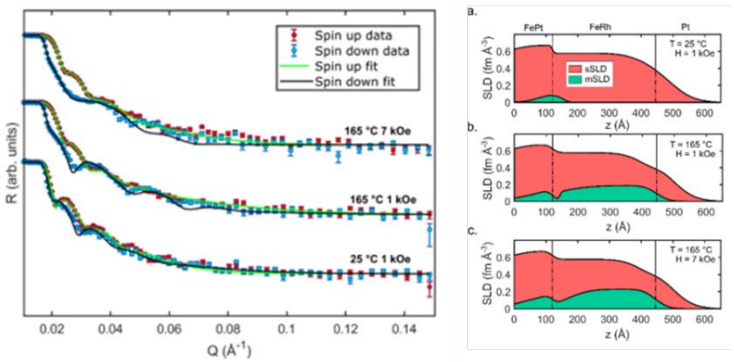

FePt/FeRh exchange springs Griggs *et al* accepted for publication in Physical Review Materials 2022

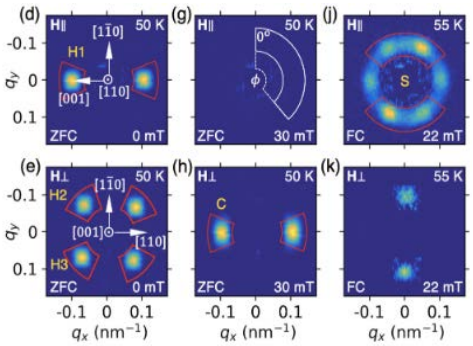

Zn-substituted skyrmion host Cu2OSeO3 Birch *et al*/PRB (2020)

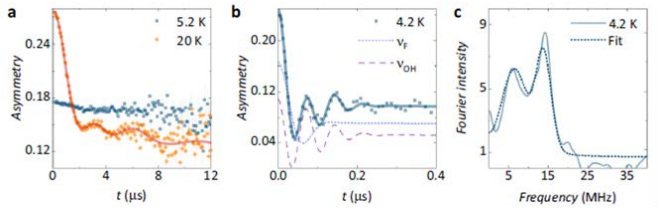

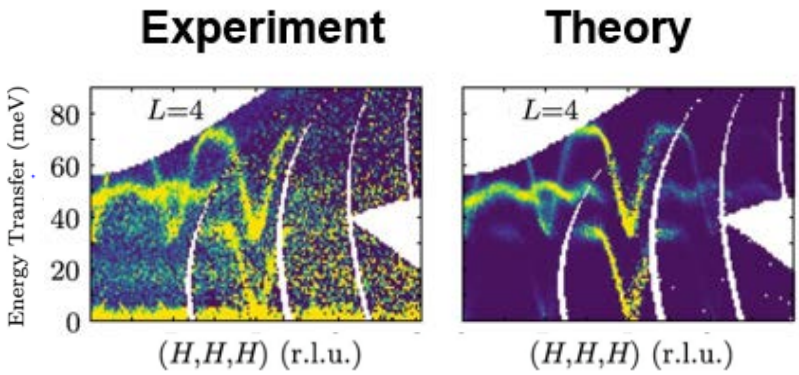

Magnons in YIG, Princep npj Quantum

From magnetic order to quantum disorder in the Zn-barlowite series of S = 1/2 kagomé antiferromagnets. Time-dependent zero-field muon asymmetry for Cu4(OH)6FBr. npj Quantum Materials 2020, 74

Topic: Thin Films and nanostructures

(P54) Magnetoelectric Coupling in Inorganic/Organic Hybrid Composite Thin Films

Muireann de h-Óra, Ahmed Kursumovic, Aliona Nicolenco, Jordi Sort, and Judith L. MacManus-Driscoll

University of Cambridge, UK

Magnetoelectric thin films can be used for various flexible electronics and biomedical applications but are limited by achieving strong magnetoelectric coupling at room temperature in a simple device. We report on the formation of a hybrid magnetoelectric system based on a new three-step grow-etch-fill process. First, a

vertically aligned nanocomposite thin film containing a magnetostrictive $CoFe_2O_4$-based material and a sacrificial passive component (MgO) is grown. Then the MgO is etched out, to leave a mesoporous structure having 10's nm dimensionality, and then a ferroelectric polymer PVDF-TrFE is coated onto the mesoporous structure.

Our study shows a novel approach to high performance magnetoelectric composites. The films have advantages over previous composites of the same composition of having much higher density of interfaces for more effective strain coupling between the ferroelectric and magnetostrictive phases at directional, high-quality interfaces between the two materials. Also, the ability to more carefully tune and change the magnetic anisotropy in the $CoFe_2O_4$ films to design strong magnetoelectric coupling is demonstrated.

(P55) Controlling Piezoelectric Love Waves in Magnetoacoustic Devices

O S Latcham, Y Au, A V Shytov, S Horsley, V V Kruglyak

University of Exeter, UK

We study the scattering of piezoelectric Love waves from isolated magnetic stripes and arrays of those. Typically, these surface acoustic waves have long lifetimes and can be coupled – via magnetostrictive effects - to the magnetization dynamics within a thin magnetic stripe, as shown in Fig.1. The coupling is enhanced in the vicinity of the Kittel resonance of the stripe, which can be tuned via the externally applied magnetic field. We analyse the reflection, transmission and losses, including radiation into the bulk, for Love waves propagating through the stripe-substrate interface. The scattering coefficients spectra exhibit asymmetric (Fano) lineshapes (reflection) and Lorentzian (transmission, absorption) near the magnetoelastic anti-crossing. We identify that, for waves emitted from the coupled interface, the emitted power has a dominant contribution from the bulk inelastic decay channel. This contributes heavily to the suppression of resonant magnetoelastic signatures in the scattering, playing a similar role to Gilbert damping. When the stripes are arranged into periodic arrays the magnetoelastic signatures are resonantly enhanced due to Bragg scattering, which also result in magnetoelastic Borrmann and induced transparency effects [1]. We identify a non-leaky branch below the first phononic band gap (see Fig.2) that is protected from Brekhovskikh attenuation [2]. This is reflected in the scattering coefficients, where an increase in attenuation can be observed above the first phononic band gap.

The research leading to these results has received funding from the EPSRC of the UK (Projects EP/L019876/1 and EP/T016574/1).

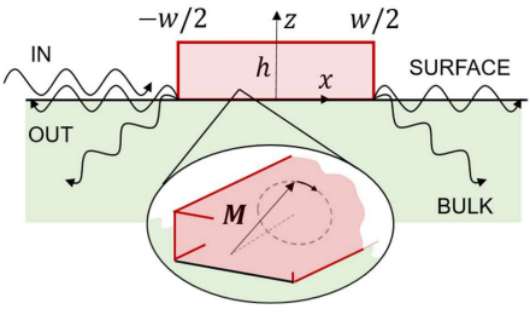

Fig.1: A magnetic stripe, with precessing magnetization $\boldsymbol{M}$, thickness h and width w, is situated atop a piezoelectric substrate. Incident surface acoustic waves ('IN') are scattered into surface and bulk modes.

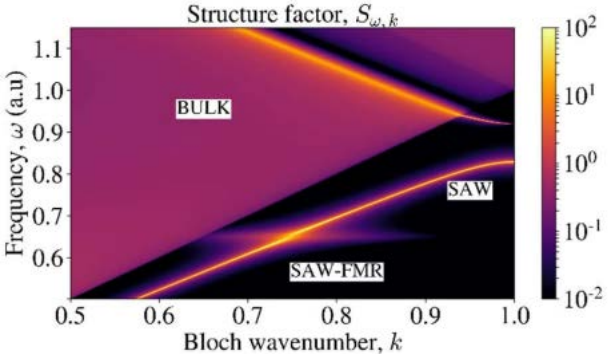

Fig.2: Elastic structure factor $S_{w,k}$, of an infinite array of stripes. The lowest surface branch ('SAW') is separated from the bulk continuum ('BULK') at $k = \pi/a$. The magnetic anticrossing is labelled 'SAW-FMR'

[1] O. S. Latcham, Y. I. Gusieva, A. V. Shytov, O. Y. Gorobets, and V. V. Kruglyak, "Hybrid Magneto-acoustic metamaterials for ultrasound control," Appl. Phys. Lett. 117, 102402 (2020)
[2] A. A. Maznev, "Band gaps and Brekhovskikh attenuation of laser-generated surface acoustic waves in a patterned thin film structure of silicon", Phys. Rev. B 78, 155323 (2008)

(P56) Vortex dynamics in microscopic magnetic thin film spherical shells

Katie Lewis, Conor McKeever, J Roy Sambles, Alastair Hibbins, and Feodor Y Orgin

Department of Physics and Astronomy, University of Exeter, UK

The ability to create materials with tuneable magnetic responses has received considerable attention due to the potential applications in microwave signal processing, magnetic memory and sensors [1]. This work aims to experimentally verify the high dynamic susceptibility observed at high frequencies [tens of GHz] that has been predicted by micromagnetic simulation in thin magnetic shells when vortices are present (Figure 1a) [2].

Nanosphere lithography and sputtering [3] were used to make arrays of microscopic shells (Figure 1b). To obtain the necessary vortex configuration in the structure, the hysteresis was measured as a function of thickness. It was found that for thicknesses above 30 nm the switching field is above 0 Oe, and vortex structures can be formed with no bias field.

The dynamic properties were experimentally investigated using VNA-FMR spectroscopy. The array of hemispherical shells is excited, and the dynamic modes present in vortex configuration are measured. The results are produced for varying external applied biasing fields, within the vortex region and the saturation regions, and compared with the numerical simulations.

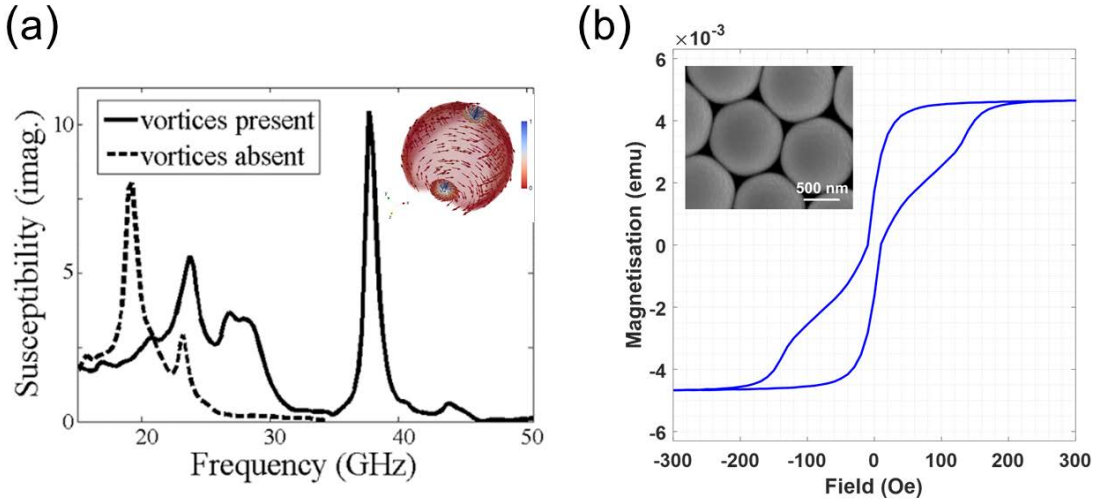

Fig 1: A) Micromagnetic simulations for dynamic susceptibility in the absence and presence of vortices [2]. Insert shows magnetic distribution of a vortex state with curling moments in plane and small out of plane moments at the cores. B) Magnetic response of a 780 nm monolayer of magnetic spherical shells with Permalloy thickness of 30 nm with varying applied magnetic field. A nucleation field can be seen around 50 Oe, the switching magnetisation indicating the presence of a vortex state. Insert shows the fabricated monolayer hexagonal array.

[1] Maksymov, I.S. and Kostylev, M., 2015. *Physica E: Low-dimensional Systems and Nanostructures, 69,* pp.253-293.
[2] McKeever, C., Ogrin, F.Y. and Aziz, M.M., 2019. *Physical Review B*, *100*(5), p.054425.
[3] Weekes, S.M., Ogrin, F.Y., Murray, W.A. and Keatley, P.S., 2007. *Langmuir 23*(3), pp. 1057-1060.

(P57) Spin pumping between two identical CoFe layers separated by an Ag layer

K Alsaeed, and AT Hindmarch

Department of Physics, Durham University, UK

Magnetisation processes including rotation of magnetisation, and dynamic propagation of domains walls in magnetic materials are regulated by the precessional damped motion of magnetic moments [1, 2] about an effective field. In thin-film systems, when a ferromagnetic (FM) layer is in contact with non-magnetic (NM), and excited with a microwave, spin-current is transmitted across the interface. This process is known as spin pumping and results in the transmission of energy and angular momentum [3]. The structure of both the FM and NM layers greatly affects spin pumping, with the change of crystalline structure affecting both spin-pumping and two-magnon scattering [2]. Two-magnon scattering is the energy transfer from uniform-to-nonuniform precessional modes. This study focuses on understanding the spin-pumping contribution to the damping between two identical 10 nm thick CoFe magnetic layers separated by Ag. The precessional dynamics were measured using ferromagnetic resonance, as illustrated in the figure1A.The thickness of the Ag interlayer has a considerable impact on the damping parameter. Spin-pumping between the two identical FM layers occurs when the Ag layer thickness corresponds to an AF coupling peak and leads to enhancement of the damping in our samples. As a result of the AF coupling across the Ag layer, stationary spin-wave modes in anti-phase are formed due to the Ruderman-Kittel-Kasuya-Yosida (RKKY) interaction into the effective fields similar to that modelled in [4]. This shows up as an additional 'bump' term to the frequency-dependence of the resonance linewidth over a certain frequency range as shown in frame C of the figure; frames B and D show conventional linear dependence when the Ag thickness is below (B) or above (D) the RKKY coupling peak thickness. In contrast to reference [4], the FM layers are in a saturated state, both magnetized along the applied field direction yet the spin-pumping contribution to the damping persists.

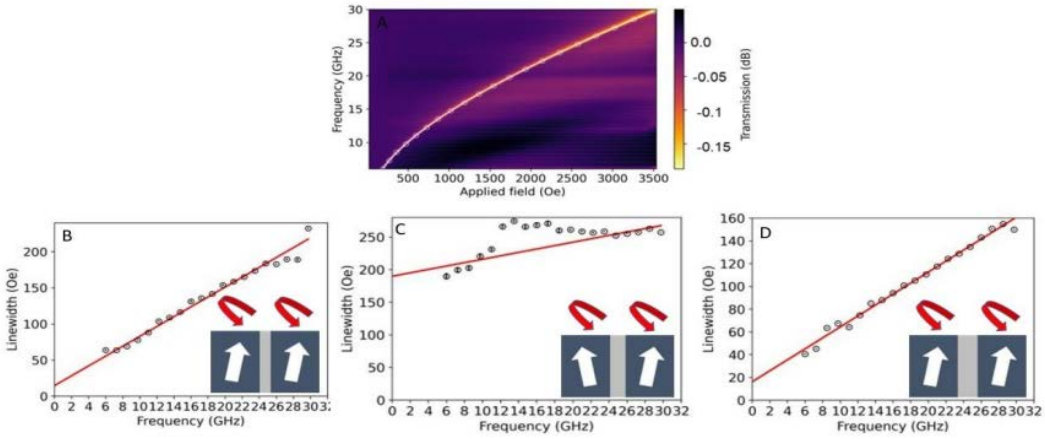

Fig1(A): Shows resonance datapoints and Kittel fit overlayed according to the relation between the field and the frequency, (B, C, D) show with and without the additional bump term in the frequency dependent linewidth from spin pumping in three different Ag layer thickness.

[1] Tokaç, M., et al., Interfacial Structure Dependent Spin Mixing Conductance in Cobalt Thin Films. Physical Review Letters, 2015. 115(5): p. 056601.

[2] Azzawi, S., et al., Evolution of damping in ferromagnetic/nonmagnetic thin film bilayers as a function of nonmagnetic layer thickness. Physical Review B, 2016. 93(5): p. 054402.

[3] Conca, A., et al., Separation of the two-magnon scattering contribution to damping for the determination of the spin mixing conductance. Physical Review B, 2018. 98(21): p. 214439.

[4] Chiba, T., G.E.W. Bauer, and S. Takahashi, Magnetization damping in noncollinear spin valves with antiferromagnetic interlayer couplings. Physical Review B, 2015. 92(5): p. 054407

(P58) Paradigm of Magnetic Domain Wall-Based In-Memory Computing

Xiangyu Zheng, Junlin Wang, Guanqi Li, Xianyang Lu, Wenjia Li, Yichuan Wang, Li Chen, Haihong Yin, Jing Wu, and Yongbing Xu

While conventional microelectronic integrated circuits based on electron charges approach the theoretical limitations in foreseeable future, next-generation non-volatile logic units based on electron spins have the potential to build logic networks of low power consumption. Central to this spin-based architecture is the development of a paradigm for in-memory computing with magnetic logic units. Here, we demonstrate the basic function of a transistor logic unit with patterned Y-shaped NiFe nanowires by gate-controlled domain-wall pinning and depinning. This spin-based architecture possesses the critical functionalities of transistors and can achieve a programmable logic gate by using only one Y-shaped nanostructure, which represents a universal design currently lacking for in-memory computing.

KEYWORDS: in-memory computing, spin-based transistor, programmable nano-logic unit, domain-wall logic, permalloy

(P59) A Study of the Dispersive Nature of the Voigt Effect in Thin Magnetic Films

N Collings[1] and M R Parker[2]

[1]retired from University of Cambridge, Cambridge, UK, [2] retired from University of S Alabama, Mobile, USA

It seems hard to believe that, after more than a hundred years from the time of its discovery, there is still no reliable published information on the Voigt effect [1] in common transition metals, alloys and compounds over a range of wavelengths at optical frequencies.

Ellipsometric measurements of this 2nd order magneto-optical effect have been made in transmission, at room temperature, on various vacuum-deposited thin films of Fe, Co, and Ni. In all three materials, there is considerable dispersion in both the Voigt rotation and ellipticity in the visible and near-IR regions of the spectrum. The data have been used to construct the complex Voigt contributions to the optical conductivity and the latter have been found to be described reasonably well in the near infrared region by using Heaviside force-modified classical dispersion theory (Fig. 1).

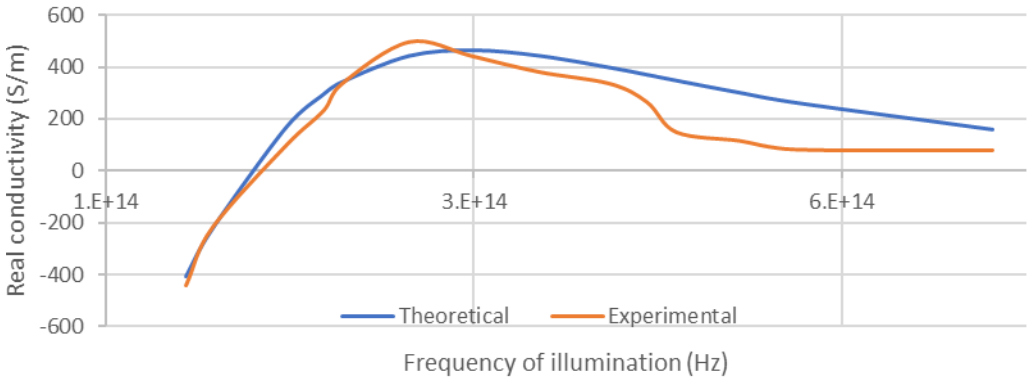

Fig. 1 The real Voigt conductivity of Iron versus the frequency of the illumination

We examine, in detail, microscopic aspects of the second-order tensor elements of that theory and show how a combined study of the (complementary) Kerr and Voigt effects could, in principle, lead to an unambiguous determination of the plasma (ω_p), cyclotron (ω_c) and relaxation (ω_R) frequencies. Both Kerr and Voigt effect measurements lead to a simple determination of the relaxation frequency; the data arising from either effect, *on its own*, however, does not lead to an unambiguous determination of either.

The validity of this theory is further underlined, here, by taking the zero -frequency asymptotes of the Kerr and Voigt conductivities and, using the Heisenberg Uncertainty Principle, and some simple reasoning, showing that, at temperatures well below the quantum limit, ($T \ll \hbar\omega_c / k$), they lead to recognized forms for the quantum Hall effect and quantum linear magnetoresistance.

Additionally, on a more speculative level, an argument is presented (along the lines of that used for the zero-frequency asymptotes), that, at optical frequencies in the quantum region, there is reason to suppose that the Voigt effect may not, necessarily, always be a quadratic function of field. It is a relatively simple matter to show that, for both first and second-order magneto-optical effects, the magneto-optical rotation reflects the field dependence of the optical conductivity. This fact is used in reviewing, briefly, a couple of possibly supportive examples taken from the literature.

[1] W. Voigt, Magneto- und Elektro-Optik (B. G. Teubner, Leipzig,1908)

(P60) Exploring magnetic responses in interconnected magnetic nanoring arrays

C Swindells[1], I T Vidamour[1], G Venkat[1], T J Hayward[1], and D A Allwood[1]

[1]Department of Materials Science and Engineering, University of Sheffield, UK

Domain wall dynamics form a rich area of nanoscale magnetic phenomena, with many useful applications such as logic gates [1], racetrack memory [2] and sensors [3]. This richness is observed in magnetic nanoring structures, in which, for example, complex domain wall motion [4] and spin wave modes [5] have been studied. More recently, the domain wall population of an array of interconnected magnetic rings has been observed to be an emergent property of the array and proposed to be a possible vehicle for performing reservoir computing [6]. However, to fully utilise such an array, it is critical to first understand the physics governing the system, as well as exploring potential magnetic characterisation which may provide useful reservoir outputs.

Here we present the results of a study into the magnetic response of a range of interconnected magnetic ring arrays (see fig) with an amplitude-varying rotating magnetic field. Using both static and dynamic techniques, principally magnetoresistance (see fig), we demonstrate the complex physics presented in the system as a result of the relative number of vortex and onion states. Additionally, understanding the time-varying magnetoresistance response in the frequency domain provides insight into the stochastic nature of domain wall dynamics.

Varying parameters such as wire width of the rings, we show how the interplay between these parameters and the rotating field affect the overall system response, and therefore their usability for computational applications. Our work provides evidence that the emergent behaviours of nanoring ensembles can be tuned in order to obtain bespoke nonlinear dynamics, potentially allowing optimisation of reservoirs for different computational tasks.

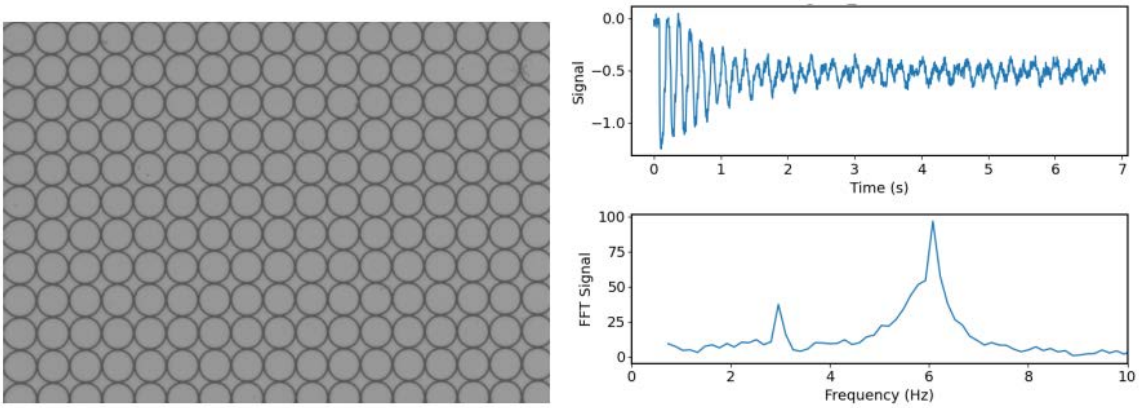

Fig 1: Left: Scanning Electron Microscope image of a nanoscale magnetic ring array, patterned using electron beam lithography. Right: Anisotropic magnetoresistance measurement of an array, with a circular magnetic field of 30 Oe at 3 Hz showing a complex response, and the associated Fourier spectrum.

[1] D Allwood et al., Science 309.5741 (2005): 1688-1692.
[2] SP Parkin et al., Science 320.5873 (2008): 190-194.
[3] M Diegel et al., IEEE Transactions on Magnetics 45.10 (2009): 3792-3795.
[4] J-M Hu et al,. Nano letters 16.4 (2016): 2341-2348.
[5] C Tian et al., Nanotechnology 31.14 (2020): 145714.
[6] R. W. Dawidek et al., Adv. Funct. Mater., vol. 31, no. 8, 2021.

(P61) Structural and magnetic properties of MBE grown Co_2FeSi/Si(111) films

I Azaceta, V K Lazarov, and S A Cavill

Department of Physics and Astronomy, University of York, UK

Full Heusler alloys such as Co2FeSi (CFS) have high Curie temperatures and a predicted 100% spin polarization at the Fermi level making them ideal candidates for spintronic devices [1]. Moreover, CFS has a huge potential for large scale integration into spintronic devices due to the excellent lattice match with Si. The half-metallicity is predicted to be a feature of the L21 ordering of CFS which is significantly reduced when the Fe-Si sublattice is disordered i.e., B2 ordering. Typically, CFS grows in the B2 phase at low temperatures (T< x), and transitions to the L21 phase with thermal annealing between 500°C and 700°C. However, at these annealing temperatures Si diffusion from the substrate reduces the magnetization and spin polarization close to the interface [2].

In this work, we study the magnetic and structural properties of epitaxial CFS films grown on Si(111) substrates at room temperature by MBE. Using X-ray diffraction (XRD) and aberrationcorrected scanning transmission electron microscopy (STEM), we show that the as-prepared films exhibit mixed L21 and B2 ordering without the need of annealing. When the L21 ordering is present, we observe a reduction of the ferromagnetic resonance (FMR) linewidth. Interestingly, even at a low growth temperatures of<130°C, interfacial effects have an impact on the magnetic anisotropy of the films which act to switch the magnetic easy axis (EA) from [10-1] to [1-10]. HAADF-STEM images show the changes at the CFS/Si interface as a function of the growth temperatures. Further microscopy experiments are currently under way in order to fully correlate the magnetic and structural properties of the CFS/Si heterostructure.

[1] B. Balke, S. Wurmehl, G. H. Fecher, C. Felser, and J. Kübler, Sci. Technol. Adv. Mater. **9**, 014102 (2008)
[2] B. Kuerbanjiang et al, Appl. Phys. Lett., 108, 172412 (2016).

(P62) Optimisation of CoFe/IrMn bilayers For Tunnel Anisotropic Magnetoresistance (TAMR) Applications

Benjamin W Wilson, Jade N Scott, William R Hendren, and Robert M Bowman

Queen's University Belfast, UK,

Increasing the areal density of hard disk drives (HDD) requires improving the writability of smaller bits and the ability to read these bits. This can only be achieved by reducing the size of conventional tunnelling magnetoresistance (TMR) sensors.

A possible solution is tunnel anisotropic magnetoresistance (TAMR), which arises due to a change of density of states at the Fermi level when a magnetic sublattice rotates with respect to the crystal field [1]. Very large TAMR signals have been observed at low temperatures that utilises an IrMn based magnetic tunnel junction (MTJ) [2] which if optimised at room temperature would remove the requirement for a second ferromagnetic (FM) electrode and thus reducing the size of the sensor.

We use the atomistic simulation package, VAMPIRE [3], in conjunction with vibrating sample magnetometry, ferromagnetic resonance (VNA-FMR) and x-ray diffraction (XRD) to investigate and optimise Ni80Fe20 and Co70Fe30 FM thin films deposited via magnetron sputtering. Ir20Mn80 has been grown on top of the FM layer and magnetically annealed to show the increase in magnetisation and to induce exchange bias in the system, figure 1.

Grain size analysis through XRD has shown that a Ru(5nm) seed results in large grains within the CoFe layer of 317Å, resulting in a shift of the Co70Fe30 (111) peak to a lower angle indicating an increase in the lattice constant. Whereas Ta(5nm) and Ta(5nm)/Ru(5nm)/Ta(5nm) seed layers produce a similar grain size of approximately 87Å. However, the multi-layered Ta/Ru/Ta seed provides a marked increase in the magnetisation and decrease in coercivity of the CoFe layer, figure 2.

As each layer of the structure is simulated, experimentally confirmed and finally optimised, we come closer to a functional room temperature TAMR structure which will pave the way for increased data storage and future technologies.

[1] Phys. Rev. Letts 100, 087204 (2008)
[2] Nature Mat. 10, 347 (2011)
[3] R. F. L. Evans et al., Appl. Phys. Lett. 104, 082410 (2014)

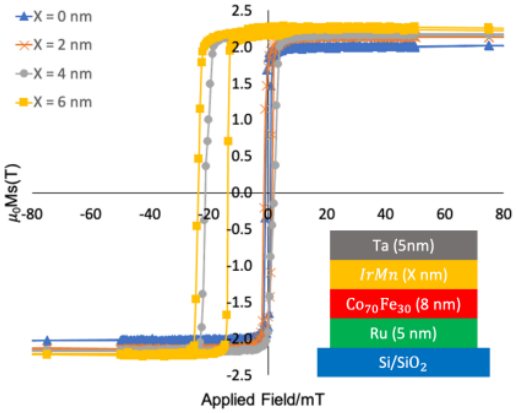

Figure 1 Magnetic hysteresis loops demonstrating exchange bias for the structure in the inset. As the thickness of the AFM layer increases, the coercivity increases until a decrease at 6nm of IrMn but with a massive shift in the loop.

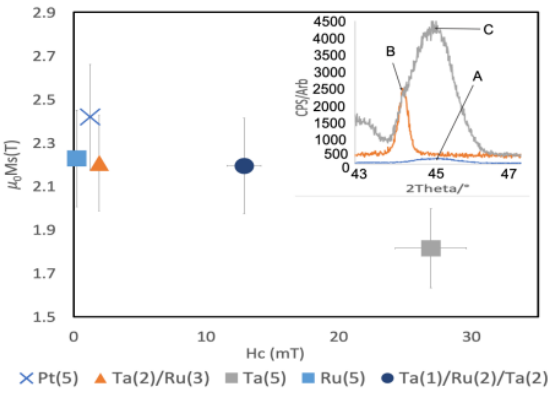

Figure 2 Plot of Ms against Hc for various seed layers of total thickness, 5nm for the following structure: Seed-Layer(5)/Co70Fe30(8)/Ta(5). Inset is 2theta XRD scan for three seed layers; A: Ta(5), B: Ru(5) and C: Ta(5)/Ru(5)/Ta(5).

(P63) Phase Coexistence and Transitions between Anti- and Ferromagnetic States in a Synthetic Antiferromagnet

Christopher E A Barker[1], Craig Barton[2], Eloi Haltz[1], Olga Kazakova[2], Thomas A Moore[1], and Christopher H Marrows[1]

[1]School of Physics and Astronomy, University of Leeds, UK, [2]National Physical Laboratory, UK

Skyrmions—topologically protected vortex-like spin structures—have been proposed as the new information carriers in racetrack memory devices [1]. In order to realise such devices a small size, high speed of propagation, and minimal deflection angle are required. Modelling has shown that synthetic antiferromagnets (SAFs) present the ideal materials system to realise these aims [2]. However, their magnetic compensation makes observation of skyrmions difficult and indeed this was only recently achieved [3]. There is thus significantly more to understand about the behaviour of synthetic antiferromagnets and the skyrmions therein. Here we present a comprehensive magnetic force microscopy (MFM) study of a SAF multilayer composed of 20 magnetic layers alternating between CoB and CoFeB each coupled antiferromagnetically with a Ru spacer layer to the one above and below. The SAF undergoes a phase transition between the compensated antiferromagnetic state and its field polarised ferromagnetic state as a field is applied. MFM shows that in our samples this is as a result of defect-driven bubble nucleation where FM ordered regions nucleate and then expand to cover the entire film. Once the FM regions exceed a critical size they collapse into a skyrmion/stripe domain pattern and so retain a net zero magnetisation. At a narrow range of fields, e.g., as shown in Fig. 1 we observe a phase coexistence between the compensated AF state and the net-zero magnetisation FM state. As the magnetic field is increased, we go on to observe isolated skyrmions at fields below saturation as expected in a FM system. These results give perspective on the ferromagnetic nature of skyrmions observed in systems at fields just below saturation and can help to inform the observation of true antiferromagnetic skyrmions.

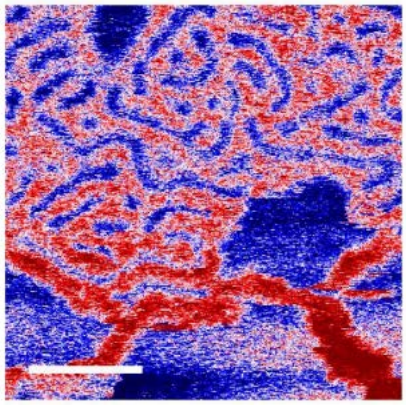

Fig. 1: Mixed phase state of our SAF system acquired at 43 mT, where red/blue texture is FM domain structure that has expanded from nucleated bubbles and the regions of uniform blue are the remaining SAF areas. Scale bar is 1 μm.

[1] S. P. Parkin et al., Science 320, 190 (2008)
[2] X. Zhang et al., Nature Communications 7, 10293 (2016)
[3] W. Legrand et al., Nature Materials 19, 34 (2020)

(P64) Structural and Magnetic Properties of CoIrMnAl Heusler Alloy Epitaxial Films Fabricated with Magnetron Sputtering for Spintronics Applications

David Lloyd[1], Kelvin Elphick[1], Ren Monma[2,3], Tufan Roy[4], Kazuya Suzuki[3,5], Tomoki Tsuchiya[5,6], Masahito Tsujikawa[4,5], Shigemi Mizukami[3,5,6], Masafumi Shirai[4,5,6] and Atsufumi Hirohata[*,1]

[1]Department of Electronic Engineering, The University of York, UK [2]Department of Applied Physics, Graduate School of Engineering, Tohoku University, Japan [3]WPI Advanced Institute for Materials Research (AIMR), Tohoku University, Japan [4]Research Institute of Electrical Communication, Tohoku University, Japan [5]Center for Spintronics Research Network (CSRN), Tohoku University, Japan [6]Center for Science and Innovation in Spintronics (CSIS), Core Research Cluster (CRC), Japan

A major area of research in the field of spintronics is the development of materials used for the fabrication of magnetic tunnel junctions (MTJ). Current uses for MTJs are data storage read heads and non-volatile memory devices such as MRAM [1]. Emergent computing technologies are already setting the demand for new MTJ electrode materials, namely, extremely high TMR ratios at room temperature [2]. Low temperature TMR ratios in excess of 2600% have been observed experimentally in half-metallic ferromagnetic materials [3]. The reduction in TMR ratio with temperature is thought to be due to loss of spin polarisation and desirable magnetic order at the interface of the electrode and the MgO tunnelling barrier [4]. Therefore, it is critical that any potential electrode material be a close crystallographic match to MgO and present consistent electronic character across a range of interfacial conditions.

A potential candidate for MTJ electrodes are quaternary Heusler alloys with equiatomic stoichiometry [5] i.e., having chemical formula XX'YZ. Recent theoretical studies have found that quaternary Heusler alloys of the form CoIrMnZ (Z= Al, Si, Ga, Ge) have near perfect spin polarisation due their half-metallic nature and have Curie temperatures above room temperature [6]. The fully ordered bcc-structure of these alloys is an excellent match to MgO. While swap-disorder within the unit can be used to tune the magnetic properties [7].

Here we have successfully deposited thin films of CoIrMnAl (50nm) at room temperature with B2 chemical ordering using sputter deposition [8]. In-situ annealing at 500-600°C yields a lattice constant approximating the theoretical values. Magnetic measurements showed ferrimagnetic ordering and a Curie temperature of 400K; which is ~70% of the predicted value. Cross-section scanning transmission electron microscopy reveal that B2 ordering is localised to the interfacial region (~17nm) of the film. This holds promise for further improvement of the magnetic properties towards the theoretical predictions.

[1] D. Apalkov, B. Dieny, and J.M. Slaughter, Proc. IEEE 104, 1796 (2016).
[2] M. Zabihi, et al, IEEE Trans. Comput. 68, 1159 (2019).
[3] H. Liu, et al, J. Phys. D. Appl. Phys. 48, 164001 (2015).
[4] Y. Miura, K. Abe, and M. Shirai, Phys. Rev. B 83, 214411 (2011).
[5] V. Alijani, et al, Phys. Rev. B 84, 224416 (2011).
[6] T. Roy, et al, J. Magn. Magn. Mater. 498, 166092 (2020).
[7] S. Yamada, et al, Phys. Rev. B 100, 195137 (2019).
[8] R. Monma, et al, J. All. Com. 868, 159175 (2021)

(P65) All optical switching in transition metal synthetic ferrimagnetic multilayer systems with enhanced interlayer exchange coupling

Connor R J Sait[1], Maciej Dąbrowski[1], Jade N Scott[2], William R Hendren[2], Paul S Keatley[1], Robert M Bowman[2], and Robert J Hicken[1]

[1]School of Physics and Astronomy, University of Exeter, UK [2]School of Mathematics and Physics, Queen's University Belfast, UK

Ultrafast all optical switching (AOS) offers the potential to switch materials with perpendicular magnetic anisotropy (PMA) and large coercivity, without the need to generate large magnetic fields. AOS is therefore of interest for future magnetic hard disk technology where the fields generated by inductive write heads are limited to the order of 1.5T.

Recently, transition metal synthetic ferrimagnets (TM SFis) with ferromagnetic Ni_3Pt and Co layers were shown to have a negative remanence (NR) temperature band, below which multiple pulse AOS occurs over a broad temperature range [1]. These materials establish a new direction for AOS in SFi materials, as previous works focus on SFis containing rare earth elements, or other SFis that lack the capacity for tuneable magnetic properties. However, as yet single pulse AOS has not been demonstrated in TM SFis.

Figure 4: AOS achieved by sweeping the laser beam with fluence 9 mJ/cm^2 (a) left and, (b) right circularly polarized beam with 2.5ps pulse width, and 250kHz repetition rate across the surface of the TM SFi Pt(5nm)/5x[Ni(0.6nm)/Pt(0.3nm)]/Ni(0.6nm) /Ir(0.4nm)/Co(0.9nm)/Ir(3nm) at 289K, taken using wide field Kerr microscopy.

Here we examine TM SFis of composition [Ni/Pt]/Ir/Co in which the [Ni/Pt] multilayer has replaced the Ni_3Pt layer used previously. The interlayer exchange coupling through the Ir is enhanced, suggesting that fewer pulses may be required for AOS [2]. We have established that the NR temperature is close to, and in some case above room temperature (RT) depending on the particular layer properties. Early results show helicity independent, multiple pulse AOS between antiparallel states just below RT. Furthermore, TR-MOKE measurements on these new TM SFis and reference [Ni/Pt] and Co films show that the ultrafast demagnetisation behaviour is in line with those reported previously [1]. A search for the laser pulse characteristics required for single pulse AOS is currently in progress.

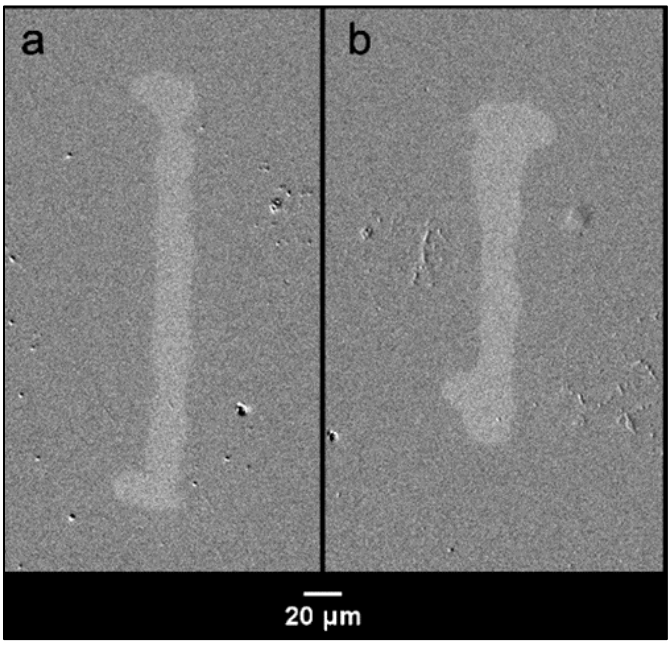

[1] M. Dąbrowski, et al. Nano Lett., 21, 9210–9216 (2021)
[2] R. F. L. Evans, et al. Appl. Phys. Lett., 104, 082410 (2014)

(P66) Skyrmions, stripe domains and AFM-FM phase coexistence observed in a synthetic antiferromagnetic system using Lorentz transmission electron microscopy

Kayla Fallon[1], Eloi Haltz[2] , Christopher E. Barker2 , Damien McGrouther1 , Thomas Moore2 , Gavin Burnell2 , Christopher Marrows2 , and Stephen McVitie1

[1]SUPA, School of Physics and Astronomy, University of Glasgow, UK, [2]School of Physics and Astronomy, University of Leeds, UK

Magnetic skyrmions, particle-like swirls of magnetisation, have been successfully stabilised in ferromagnetic multilayer stacks but two fundamental characteristics of skyrmions in this system limit their potential as information carriers in next generation technology. Firstly, a large magnetostatic energy limits their minimum size, and secondly, their topological charge results in a skyrmion Hall effect causing their trajectory to be difficult to control with skyrmions to drifting to device edges [1]. By moving to synthetic antiferromagnetic (SAF) constructions, where the multilayer consists of thin ferromagnetic layers antiferromagnetically coupled to each other (giving zero net magnetisation and no skyrmion Hall effect due to cancelling topological charge), these limitations can be overcome [2].We have studied a SAF consisting of ten repeats of the base unit [Ru(7)/Pt(8)/CoFeB(10)/Ru(7)/Pt(8)/CoB(16)] (numbers are thickness in Å). We mapped the evolution of the magnetisation of the SAF, as an external magnetic field was applied, using Lorentz transmission electron microscopy (LTEM). In a field of 35 mT skyrmions begin to become visible. A dense array of skyrmions is clear in Fig. 1(a), which is a defocused Fresnel LTEM image of the sample in a 54 mT out-of-plane field. Fourier-space analysis shows the dominant frequency of the image to be 6.2 μm^{-1}, corresponding to an average skyrmion size of 80 nm. As the field is increased further the magnetisation expands into worm-like domains before saturation is reached, a domain periodicity of 160 nm is measured from these images. In the differential phase contrast (DPC) mode of LTEM, the thicknessprojected magnetic induction can be measured quantitatively. Measuring changes in this quantity reveals the alignment of the layers of the SAF (ferromagnetic (FM) or antiferromagnetic (AF)). Fig. 1(b) shows a DPC image of the sample in a 93 mT out-of-plane field, where across the image we measure regions of low DPC signal (shaded red) which is consistent with local AF alignment of the layers and regions with strong DPC signal showing stripe domains typical of the FM phase. Our measurements suggest coexistence between the AF and FM phases of the SAF. DPC measurements performed at a range of field values show the fraction of the sample with FM alignment gradually increases until 120 mT before the sample saturates at 180 mT.

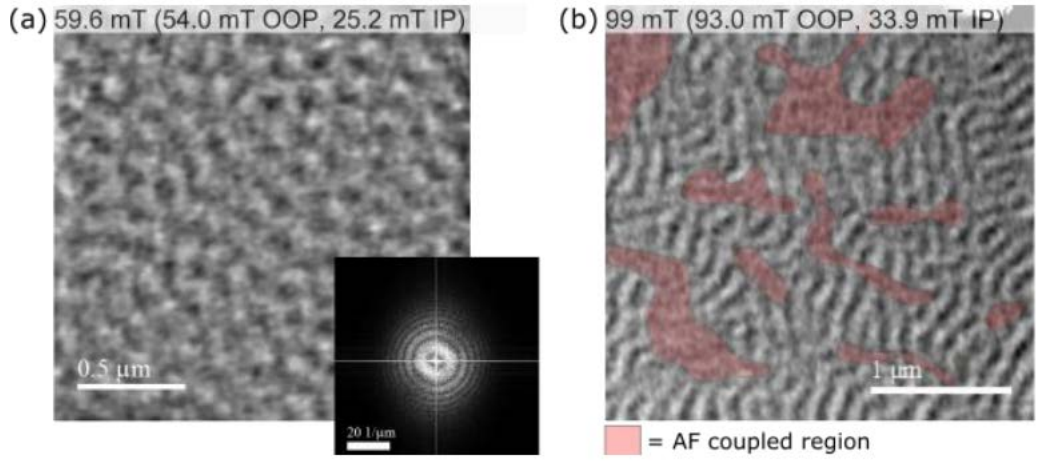

Fig 1. Lorentz TEM images of a skyrmionic SAF material. (a) A Fresnel image with a dense skyrmion array visible, length-scale information (80 nm skyrmion size) can be extracted via FFT inset on right. (b) A DPC image where phase co-existence is visible; the red areas have low signal, indicative of AF alignment.

[1] Jiang, W. et al. Direct observation of the skyrmion Hall effect. Nat. Phys. 13, 162–169 (2017).
[2] Legrand, W. et al. Room-temperature stabilization of antiferromagnetic skyrmions in synthetic antiferromagnets. Nat. Mater. 19, 34–42 (2020)

(P67) Scanning Probe Microscopy Studies of Ion-Patterned FeRh

Adrian Peasey[1], William Griggs[1], Thomas Thomson[1], and Rantej Bali[2]

[1]Nano Engineering and Spintronic Technologies Research Group, University of Manchester, UK, [2]Institute of Ion Beam Physics and Materials Research, Germany

Antiferromagnetic (AF) spintronic devices are an active area of study at present, and FeRh is one of the most promising materials for these devices. There is a need for stable, non-volatile devices to provide room temperature storage, and metamagnetic phase change materials present a possible solution in the form of antiferromagnetic anisotropic magnetoresistance (AF-AMR) memory [1]. The AF state produces no stray magnetic fields and is itself insensitive to externally applied fields, however in the ferromagnetic (FM) state the electron spins can be aligned by an external field due to the presence of a net magnetic moment in the lattice [1].

Materials such as FeRh are able to be reversibly and reliably transitioned between the AF and FM states using controlled temperature changes [2]. Equiatomic FeRh is an antiferromagnet at room temperature and transitions to a ferromagnet at around 370K, with the transition temperature approximately 10K higher during heating than cooling [3]. The phase does not change uniformly, with the FM state forming nucleations which expand to cover the whole device as it is heated, and these may be characterised using magnetic force microscopy [4].

The room temperature magnetic ordering may be manipulated by irradiating the surface with light noble gas ions, which introduce lattice disorder leading to ferromagnetic regions [5]. Lithography may be coupled with this technique to produce magnetic patterns without significantly altering the topography, allowing such films to be used in devices such as multilayer stacks. This work provides nanoscale characterisation of patterned FeRh through scanning probe microscopy techniques.

The first aspect of the work uses magnetic force microscopy to observe the effect of thermally cycling a patterned device and demonstrates the persistence of the ferromagnetic structures over multiple cycles. The second makes use of the secondary effect that the electrical resistivity of FeRh films is significantly different between the two states [6], allowing the local magnetic configuration to be measured via electrical measurements. The metallic conduction required the development of bespoke conductive microscopy techniques, which have been used to probe the local resistivity of this sample.

[1] X. Marti et al., Nat. Mater. 13, 367, (2014)
[2] M. Fallot and R. Hocart, Rev. Sci. 77, 498, (1939)
[3] J. Kouvel and C. Hartelius, J. Appl. Phys. 33, 1343, (1962)
[4] J. Warren et al., Sci. Rep. 10, 4030, (2020)
[5] W. Griggs et al., APL Mater. 8, 121103, (2020) [6] J. Arregi et al., J. Phys. D: Appl. Phys. 51, 105001, (2018)

(P68) Spintronic Computing @ Sheffield

T J Hayward1, D A Allwood[1], E Vasiliki[2], M O A Ellis[2], A Welbourne[1], G Venkat[1], C Swindells[1], I T Vidamour[1] , and L Manneschi[2]

[1]Department of Materials Science and Engineering, University of Sheffield, UK, [2]Department of Computer Science, University of Sheffield, UK

Spintronic Computing @ Sheffield is a multidisciplinary, collaborative project at the University of Sheffield between researchers from the Functional Magnetic Materials Group, Department of Materials Science and Engineering and the Machine Learning Group, Department of Computer Science. Working with collaborators from both national and international institutions, and technology companies such as IBM, our projects aim to explore how the functional properties of nanoscale magnetic devices can be harnessed to realise novel, energy efficient computational devices. In this poster we will present a high-level overview of our work.

Nanomagnetic devices are inherently non-volatile and can exhibit a range of complex non-linear behaviours when exposed to external stimuli. This combination of functional behaviour and inherent memory make them well-suited to mimicking brain-like computational operations in neuromorphic devices. We will present our efforts to create the components of feed-forward neural networks (i.e. synapses and neurons) using magnetic nanowire devices. We will also illustrate how a range of different systems can be harnessed for reservoir computing, an evolution of recurrent neural networks that is ideal for hardware-based realisations. These will include voltage-controlled superparamagnetic ensembles [1], interconnected nanoring ensembles [2] and single domain wall oscillators [3]. Novel devices also require both extensive theoretical characterisations to explore their computational strengths, as well as bespoke learning rules to harness these for applications, and we will outline our work in these areas [4].

Finally, we will present our efforts to realise other, non-neuromorphic, computational approaches in nanomagnetic hardware. Magnetic textures such as vortex domain walls in soft magnetic nanowires have internal degrees of freedom that can encode binary data. We will show how careful design of nanowire geometries allows the creation of conventional logic gates that exploit this [5]. Furthermore, while stochastic behaviour is both ubiquitous in nanomagnetic devices, and is generally detrimental to their performance, it can be turned into a functional property when considering the stochastic computing paradigm, which encodes floating point numbers in random binary bitstreams. This allows individual domain wall logic gates to perform complex mathematical operations that would usually require extended networks, as well as devices that naturally evaluate Bayes' theorem.

[1] A. Welbourne et al., Appl. Phys. Lett., Vol. 118, p.202402 (2021).
[2] R. W. Dawide et al., Adv. Funct. Mater., vol. 31, no. 8, (2021).
[3] R. Ababei et. al., Scientific Reports 11, 15587 (2021).
[4] L. Manneschi et. al., IEEE Transactions on Neural Networks and Learning Systems, doi: 10.1109/TNNLS.2021.3102378.
[5] K. Omari et. al., Adv. Funct. Mater 29, 1807282 (2019).

(P69) Stochastic Computing and Machine Learning with Magnetic Domain Wall Devices

A Welbourne[1], M O A Ellis[2], M Chambard[1], S J Kyle[1], M Drouhin[1], L T Haigh[1], A M Keogh[1], A Mullen[1], P W Fry[3], F Maccherozzi[4], T Forest[4], E Vasilaki[2], D A Allwood[1], and T J Hayward[1]

[1]Department of Materials Science and Engineering, , University of Sheffield, UK [2]Computer Science, University of Sheffield, UK, [3]Electronic and Electrical Engineering, University of Sheffield, UK, 4 Light Source, Harwell Science and Innovation Campus, UK

Non-volatile logic and memory devices based on domain wall (DW) motion have technological promise [1,2], but stochastic behaviour, which typically has to be overcome for proper device functionality, has impeded development [3]. Here, we propose that the intrinsic stochastic behaviours of these devices can be harnessed to perform computation.

Fig. 1a shows that a notch defect in a nanowire provides a tunable stochastic element, where varying the propagation field tunes the pinning probability of a DW continuously from 100 % to 0 %. We explore the use of this element in two paradigms: In the first, we demonstrate hardware-based “stochastic computing”, where floating-point numbers are encoded as the average value of random digital bit streams, and individual logic gates perform complex mathematical operations that would require extended networks of gates in conventional logic. The uncorrelated random bitstreams naturally produced by the stochastic DW pinning (i.e. by the presence or absence of DWs at device output) are challenging to generate in conventional CMOS devices [4]. We demonstrate DW AND gates based on this nanowire architecture that allow multiplication of the encoded values (Fig. 1b).

In the second paradigm, we make use of the stochastic element as a binary stochastic synapse in a neural network. Despite the success of artificial neural networks, they are significantly limited by their energy cost [5]. A potential solution is the use of physical devices, such as this tunable element, that can mimic brain-like behaviour. A model of the synapse is used to demonstrate how repeated sampling of the stochastic neural network leads to a convergence to the performance of an analogue network in recognizing handwritten digits (Fig. 1c). This is verified experimentally on a physical device by repeatedly sampling a single hardware synapse.

In summary, our work demonstrates how the intrinsically stochastic nature of DW pinning allows the realisation of two stochastic computing paradigms using devices where random processes occur naturally, thus providing a potential alternative to implementing stochastic computing and machine learning with conventional CMOS architectures.

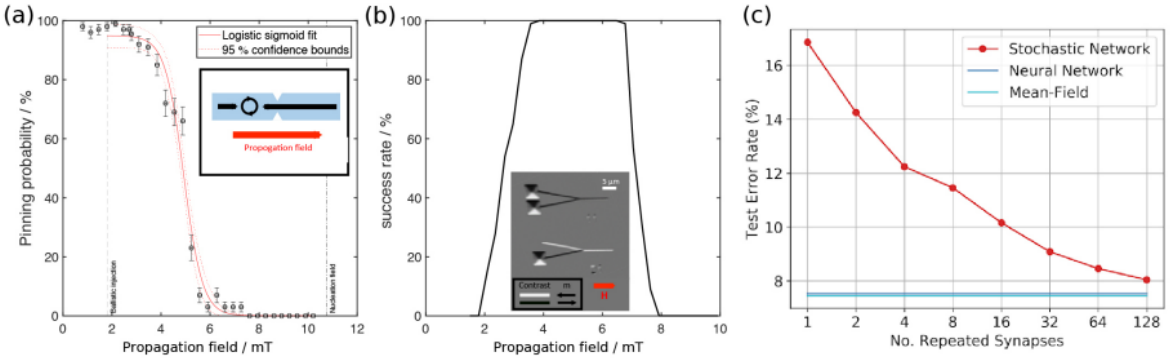

Fig. 1: (a) Notch defects in 400 nm wide (20 nm thick) permalloy nanowires provide sites with tunable pinning probability. DWs arriving at the notch under increasing propagation fields pin with probability following a logistic sigmoid-like decrease. (b) Operational range of a DW-based AND gate. For walls propagated in the range ~4–7 mT, the gate behaves deterministically as an AND gate. PEEM images (inset) illustrate this functionality. (c) The test error rate of classifying handwritten digits using a stochastic single-layer network as a function of the number of repeated synapses.

[1] D. A. Allwood, et al., Science, Vol. 309, p.1688-1692 (2005).
[2] S. S. P. Parkin, et al., Science, Vol. 320, p.190-194 (2008).
[3] T. J. Hayward and K. A. Omari, J. Phys. D. Appl. Phys., Vol.50, p.084006 (2017).
[4] A. Alaghi and J. P. Hayes, IEEE Trans. Comput. Des. Integr. Circuits Syst., Vol.37, p.139-46 (2013).
[5] Aly et al. Proc. IEEE 107 (2019)

(P70) Engineering exchange bias at the NiO/Fe_3O_4 interface by the varying surface termination of MgO

Barat Achinuq[1], Adam Kerrigan[2], Irene Azaceta[2], Dirk Backes[3], Stuart Cavill[2], Gerrit van der Laan[3], Thorsten Hesjedal[1] and Vlado K. Lazarov[2]

[1]Department of Physics, University of Oxford, UK, [2]Department of Physics, University of York, UK, [3]Diamond Light Source Ltd, Harwell Science and Innovation Campus, UK

Oxide heterostructures are of interest for developing new functional materials due to their rich physical properties. The Fe_3O_4/NiO/MgO heterostructure is an excellent candidate for spintronic applications due to the half-metallic properties of Fe_3O_4 and exchange bias between ferrimagnetic Fe_3O_4 and antiferromagnetic NiO. Thin films of NiO and Fe_3O_4 were grown on MgO(111) and MgO(001) substrates by molecular beam epitaxy. A zig-zag interface of Fe_3O_4/NiO is formed when grown on polar MgO(111) substrates, while an atomically flat interface is favoured when grown on MgO(001). We show a nearly two-fold increase of coercivity and exchange bias in the case of the zig-zag interface compared to a flat interface. The results are correlated with the atomic structure of the interface by employing aberration-corrected atomic resolution scanning transmission electron microscopy, supported by *ab initio* electronic calculations. X-ray magnetic linear dichroism measurements at the Ni-$L_{2,3}$ edge indicate that the spins of NiO on MgO(111) are canted at the Fe_3O_4/NiO interface, while retaining their bulk-like properties away from the interface. These findings make the engineering of spin alignment and magnetic properties at interfaces possible, by simply using different polar oxide surface terminations as a growth platform, serving as an excellent method for device engineering.

(P71) Pinning sites and defect phenomena on 2D magnetic materials

Leopoldine Parczanny, and Elton J G Santos

Institute for Condensed Matter Physics and Complex Systems, School of Physics and Astronomy, The University of Edinburgh, UK

There has been extensive research into introducing artificial pinning centres in bulk magnetic materials in order to enhance the critical current density at high applied magnetic fields and therefore improving their suitability for a range of technological applications such as microwave devices, generators and transformers [1] [2]. However, how pinning sites affect the magnetic properties of recently discovered 2D materials [3,4] remains elusive as well as the impact of differing defect sizes, concentrations and potential effects on device applications. Here we develop a theoretical framework based on atomistic methods [5] able to simulate the magnetic properties of 2D magnets under different conditions taking into account interactions with external driving forces, e.g., electrical currents and magnetic fields. We can simulate 'on demand' irregularly shaped defects with atomic resolution with customisable concentration, sizes and distributions that are randomly located over the sample. This was done by creating a Voronoi diagram techniques over the size of the system to be simulated with randomly placed seeds. Different 2D magnetic materials, such as CrI_3, $CrBr_3$ and $Cr_2Ge_2Te_6$ were examined with this code to investigate how their magnetic properties change with varying defect concentrations and their suitability on device applications.

[1] Cooley, L.D. and Motowidlo, L.R. (1999), Advances in high-field superconducting composites by addition of artificial pinning centres to niobium–titanium. Supercond. Sci. Technol., 12, R135.
[2] Cardwell, D.A. and Hari Babu, N. (2008), Improved magnetic flux pinning in bulk (RE)BCO superconductors. AIP Conference Proceedings, 986, 543.
[3] Huang, B., Clark, G., Navarro-Moratalla, E., Klein, D.R., Cheng, R., Seyler, K.L., Zhong, D., Schmidgall, E., McGuire, M.A., Cobden, D.H. et al. (2017) Layer-dependent ferromagnetism in a van der Waals crystal down to the monolayer limit. Nature, 546, 270- 273.
[4] Gong, C., Li, L., Li, Z., Ji, H., Stern, A., Xia, Y., Cao, T., Bao, W., Wang, C., Wang, Y. et al. (2017) Discovery of intrinsic ferromagnetism in two-dimensional van der Waals crystals. Nature, 546, 265-269
[5] Evans, R.F.L., Fan, J.W., Chureemart, P., Ostler, T.A., Ellis, M.O.A. and Chantrell, R.W. (2014), Atomistic spin model simulations of magnetic nanomaterials. J.Phys.: Condens. Matter, 26, 103202

(P72) Two-dimensional magnetic order in Cr-based chalcogenides.

Jan Phillips[1,2], Adolfo O. Fumega[3], and Víctor Pardo[1,2]

[1]Applied Physics Department, Universidade de Santiago de Compostela, Spain.[2] Instituto de Materiais (iMATUS), Universidade de Santiago de Compostela, Spain.[3] Department of Applied Physics, Aalto University, Finland

Long-range ferromagnetic order in the single-layer limit has been reported in different chromium-based chalcogenides with layered structure. Ab initio calculations based on the density functional theory of different Cr-based chalcogenides are analysed approaching the two-dimensional limit. A wide range of stoichiometries and different structures has been considered. Their dynamic stability, -in particular in the 2D limit-, and electronic structure will be discussed, but the main focus of the study will be on which cases our calculations predict an out-of-plane magnetic anisotropy that could lead to a long-range ferromagnetic order in the two-dimensional limit. The analysis will be complemented with additional tuning parameters, such as strain, pressure, the stability of charge density waves (CDW) [1], stoichiometry and other different structural details. We will discuss what parameters work in favour or against the appearance of a two-dimensional ferromagnetic order and provide some general remarks applicable to the whole transition metal chalcogenide family of materials.

[1] Adolfo O. Fumega, Jan Phillips, Victor Pardo, “Controlled two-dimensional ferromagnetism in 1T-CrTe2: the role of charge density wave and strain”, J. Phys. Chem. C 124, 21047 (2020).

(P73) POLREF: Time of flight Polarised Reflectometer for Magnetism in Thin Films

C Kinane, and A Caruana

STFC, Rutherford Appleton Laboratory, UK

Polarised Neutron Reflectometry (PNR) measures surfaces, buried interfaces and layers, yielding information about layer thicknesses, densities, surface/interface roughness and interdiffusion. Uniquely it can provide the magnetic equivalents of these quantities, including the total in-plane magnetisation [1,2]. A large variety of thin-film phenomena can be investigated using the POLREF beamline, including topological insulators, proximity-induced and fundamental magnetism, superconductivity and spintronic devices. Furthermore, POLREF can perform off-specular PNR and specular Polarisation Analysis (PA) measurements. In principle, if the problem can be made flat and is in the right length scales (~1 nm – 200 nm) then it can be measured

by PNR. The POLREF time of flight PNR beamline is located in the second target station at the ISIS Neutron and Muon source [3,4]. With a polarised wavelength band of 2-15Å (P_{Eff}~98%), low instrument backgrounds of $I/I_0 < 10^{-7}$ and a resolution of dQ/Q better than 1%, Q_{MAX} = 0.25-0.3 Å^{-1} is routinely accessible for small (10x10 mm) samples within reasonable count times. The POLREF beamline has gone through several recent upgrades. Upgrades of the spin flippers and analyser system have improved the capability of the beamline to measure samples with larger moments or weaker spin-flip signals when using the PNR and PA modes. The 1D linear detector efficiency has also been upgraded and now is fully commissioned into the user program providing full off-specular capability in the NR and PNR (see Figure 1) modes and some off-specular PA capability (the maximum Q_x being restricted by the analysing mirror). Here, we will present the current capabilities of the POLREF beamline, including science highlights and how to get access to the ISIS neutron facility and POLREF beamline.

[1] J.F. Ankner, G.P. Felcher, J. Magn. Magn. Mater, 200, 741-754 (1999)
[2] S. J. Blundell and J. A. C. Bland, PRB, 46, 3391 (1992)
[3] J.R.P. Webster et al, Eur. Phys. J. Plus, 126: 112 (2011)
[4] https://www.isis.stfc.ac.uk

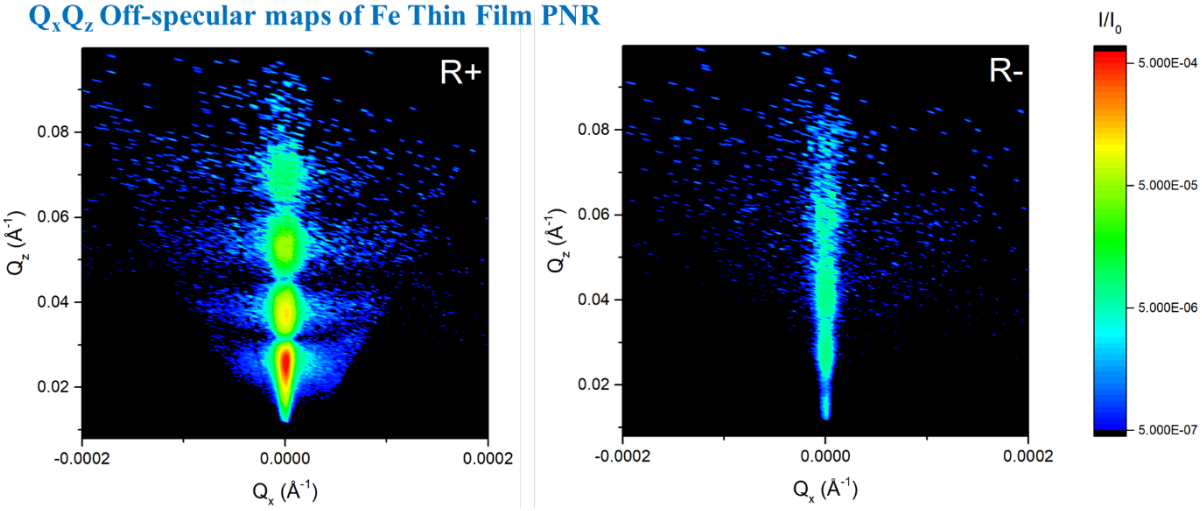

(P74) Refl1d: Advanced Neutron and X-ray reflectivity modelling with Bayesian Uncertainty analysis

A J Caruana [1], P A Kienzle[2], and B B Maranville[2]

[1]ISIS Neutron and Muon Source, UK, [2] NCNR, NIST, Gaithersburg, USA

Refl1d [1] is an advanced reflectivity modelling and fitting python package than can be used to fit both Neutron (Non-Polarized – NR, Polarized – PNR and with Polarization analysis – PA) and X-ray scattering data. Basic slab-based models can easily be constructed with additional magnetic properties, such as dead layers or decoupled magnetic interfaces, which are readily integrated into the basic modelling. Beyond the standard slab-based modelling, Refl1d allows for the use of custom functional profiles to describe complex structural and magnetic scattering length density (SLD) profiles – e.g., helical magnetism (see Figure below). Refl1d has many other modelling features such as mixed area models, multi-data set fitting and free interface spline profiles, to name a few.

With the fitting engine supplied by bumps [2], Markov Chain Monte Carlo (MCMC) Bayesian uncertainty analysis can be performed, providing information on parameter uncertainties, correlations, and model uncertainties, by using the DREAM [3] algorithm. Furthermore, the DREAM algorithm can be used as a very robust fit engine, with the ability to minimize very complex fit spaces.

Here we will show some examples of simulating and fitting X-ray, NR, PNR and PA data and further describe the features of Refl1d including some of the more recent additions to the package – such as usability improvements to the GUI and speed gains from numba based reflectivity calculations. Finally, future developments, including standardization via reproducible serialized models and integration with the ORSO [4] file format, will be discussed.

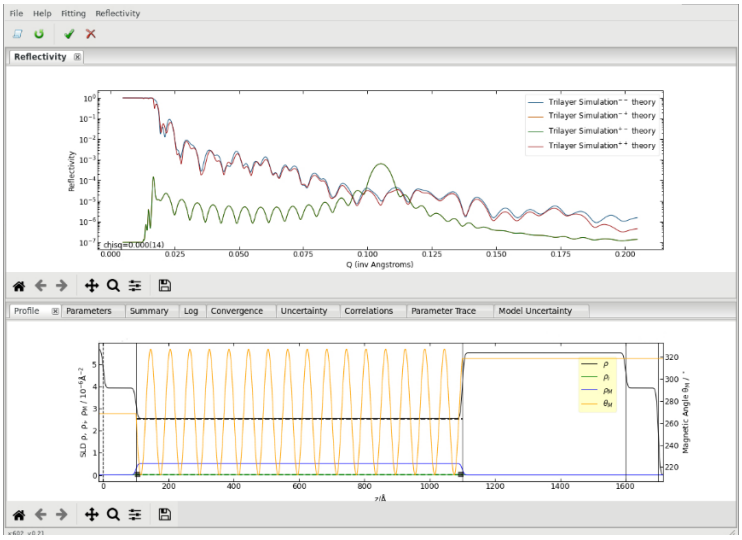

[1] Kienzle, P.A., Krycka, J., Patel, N., & Sahin, I. (2011). Refl1D (Version 0.8.15) [Computer Software]. College Park, MD: University of Maryland. Retrieved Nov 30, 2021.

[2] Kienzle, P.A., Krycka, J., Patel, N., & Sahin, I. (2011). Bumps (Version 0.8.1) [Computer Software]. College Park, MD: University of Maryland. Retrieved Nov 30, 2021.

[3] Vrugt, J. A.; Ter Braak, C. J. F.; Diks, C. G. H.; Robinson, B. A.; Hyman, J. M.; Higdon, D. International Journal of Nonlinear Sciences and Numerical Simulation, 2009, 10 (3), 273–290.

[4] Open Reflectometry Standards Organisation (ORSO) - https://www.reflectometry.org/

(P75) Fine-tuning of the compensation point in ferrimagnetic TbFe alloys by He^+ irradiation and surface to bulk ratio

Paweł Sobieszczyk*, Michał Krupiński

Institute of Nuclear Physics Polish Academy of Sciences, Poland

*visiting academic at the University of York

Over the last two decades, the interest of the 3d-transition metal (TM) - rare earth(RE) alloys has been emerged due to their possible applications in magneto-optical recording and ultrafast laser switching [1]. The most interesting properties for the magnetic reorientation process occurs at the compensation temperature (T_n) where the alloy shows no net magnetization. The value of the compensation point can be controlled through the composition, structure and thickness of the alloy thin film [2]. In the studies, we explore other possibilities of tuning the compensation point, namely by He^+ ion irradiation and by surface to bulk ratio adjustment. We investigated a 20-nm-thick Tb_xFe_{1-x} alloy film with perpendicular magnetic anisotropy, irradiated with doses ranging from 5×10^{13} to 5×10^{15} ions per cm^2. The changes in compensation point caused by the irradiation were explained with the help of atomistic simulation [4]. Based on the same model we also studied the changing in compensation point in the nanospheres of Tb_xFe_{1-x} with diameters (D) ranging from 3 nm to 12 nm. We observed that T_n depends on the diameter of the nanoparticle as 1/D, which may be attributed to changes in the spin direction on the particle surface. The results performed in atomistic approach were also confirmed with the mean-field approximation.

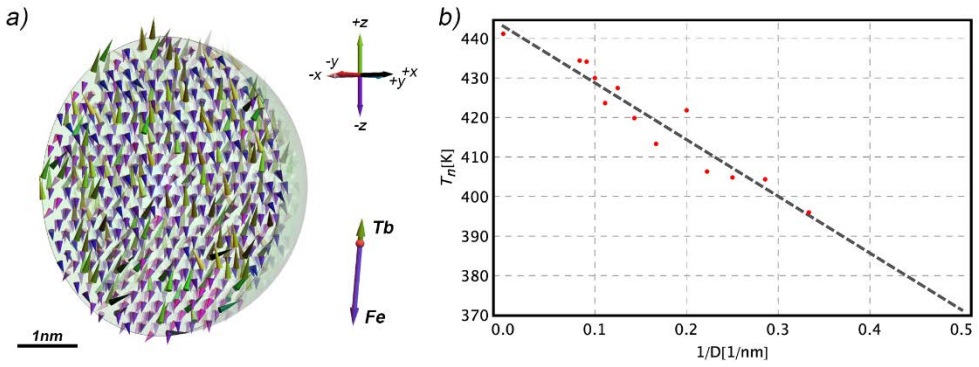

Fig. a) Distribution of spins in the ferrimagnetic $Tb_{24}Fe_{76}$ nanoparticle at T=100K.

b) Compensation point as a function of nanosphere diameter (D).

[1] S. Mangin, M. Gottwald, C.-H. Lambert, D. Steil, V. Uhlir, L. Pang, M. Hehn, S. Alebrand, M. Cinchetti, G. Malinowski, Y. Fainman, M. Aeschlimann, and E. E. Fullerton, Nat. Mater. **13**, 286 (2014).

[2] M. Heigl, C. Mangkornkarn, A. Ullrich, M. Krupinski, M. Albrecht, AIP Advances 11, 085112 (2021).

[3] M. Krupiński, J. Hintermayr, P. Sobieszczyk, and M. Albrecht, Phys. Rev. Mat. **5**, 024405 (2021)

[4] T. A. Ostler, R. F. L. Evans, R. W. Chantrell, U. Atxitia, O. Chubykalo-Fesenko, I. Radu, R. Abrudan, F. Radu, A. Tsukamoto, A. Itoh, A. Kirilyuk, T. Rasing, and A. Kimel, Phys. Rev. B **84**, 024407 (2011).

Topic: Topological Materials for Spintronics

(P76) Antiferromagnetic Materials Optimisation for Next Generation Low Power Electronic Devices Using First-Principles Simulation

Leuan Wilkes, and Keith McKenna

Department of Physics, The University of York, UK

In recent years, antiferromagnetic materials have become a more active area of research for their potential applications in memory devices [1]. These materials have an array of interesting spintronic properties, and can be used as a basis for (antiferromagnetic spintronic) memory storage devices [2]. These devices could offer unique advantages over existing computational architecture, including excellent energy efficiency compared to modern charge-based memory architecture, increased switching speeds and resistance to the influence of external stray magnetic fields [3], the latter of which MRAM devices struggle with [4]. The materials need to be stable, have significant magnetic anisotropy energy and have Spin-Hall effects that can change the magnetic state.

Here, we employ first principles materials simulation to predict the structure, stability, magnetic anisotropy and spin transport properties of a wide range of Mn-based alloys. Calculations are performed using density functional theory as implemented in the VASP code [5,6]. For promising materials we also plan to investigate the effects intrinsic defects as well as interfaces relevant to device. So far, MnIr and MnAl have been characterised in terms of stable configurations and magnetic anisotropy in part or completely, with a total maximum MAE of 0.2meV/atom and 0.05meV/atom to one significant figure respectively.

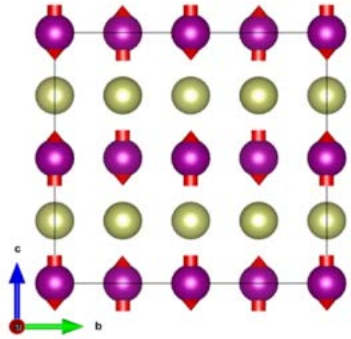

Fig 1: an example of antiferromagnetic magnetization configuration in L_{10} MnIr

[1] J. Kim, K. Kondou, Y. Otani and J. Puebla, "Spintronic devices for energy-efficient data storage and energy harvesting," Communications Materials, vol. 1, no. 24, 2020.
[2] M. Jiang, H. Asahara, S. Sato, S. Ohya and M. Tanaka, "Suppression of the field-like torque for efficient magnetization switching in a spin–orbit ferromagnet," Nature Electronics, vol. 12, no. 3, pp. 751-756, 2020.
[3] S. Fukami, V. O. Lorenz and O. Gomonay, "Antiferromagnetic spintronics," Journal of Applied Physics, vol. 128, no. 7, pp. 126-129, 2020.
[4] J. Janesky, "Impact of External Magnetic Fields on MRAM Products," Freescale Semiconductor, Austin, Texas, 2007.
[5] J. F. Georg Kresse, VASP the GUIDE, Wien, Austria: Universitat Wien, 2005.
[6] "VASP homepage," VASP Software GmbH, 2021. [Online]. Available: https://www.vasp.at/. [Accessed July 2021].

(P77) Measurement of the Skyrmion Pseudo-Liquid Phase using Resonant Elastic X-ray Scattering

Jack Bollard, and Richard Brearton

Resonant elastic X-ray Scattering is a powerful technique to provide surface sensitive information on the state and structure of an existing magnetic lattice. This can be used to study the magnetic configuration known as the skyrmion, an energetically stable vortex with a myriad of exciting properties in next generation information carriers. Understanding magnetic phases of matter is a crucial focus in the development of magnetic devices. In a synchrotron-based experiment, the skyrmion lattice of a Cu2OSeO3 sample was successfully created, this was followed by drastic changes in magnetic field, the lattice was observed melting into a state of matter not experimentally seen before. This was in-line with theoretical calculations and previous preliminary experiments. This highly disordered state is believed to be due to the devolution of the lattice structure.

In Diamond Light Source, Resonant elastic x-ray scattering was conducted with right circular polarised x-rays of energy 928-933eV incident onto a Cu2OSeO3 sample, targeted at the Cu L3-edge. Changes in the magnetic field strength, orientation and temperature allowed for a complete mapping of both phase diagram, and the path taken through it. skyrmions typically exist in either a lattice state, Bloch-type, or a sparsely populated gas state, Neel-type. Here we present a highly disordered skyrmion lattice. This skyrmion pseudo-liquid has been completely mapped in a small pocket of field and temperature. This exists just below the Curie Temperature where the skyrmion lattice becomes highly disordered and less energetically dominant. This state was induced through the use of alterations to the system, such as drastic changes in magnetic field, who's effect has also been mapped. In this state, it was observed that the diffracted intensity from the conical peak would reduce. This agrees with theoretical calculations of the skyrmion fabric becoming more disordered when they do not exist in the conical phase.

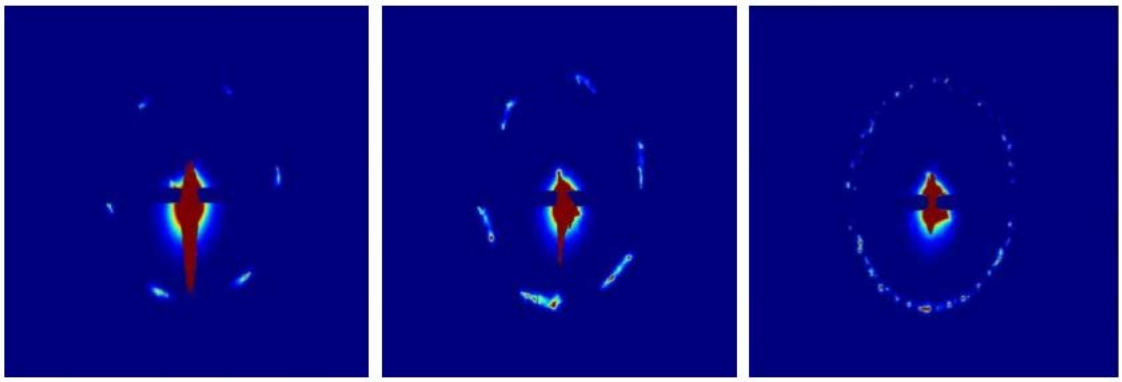

Fig 1: The Diffraction intensity of the sample is the defining characteristic of the state. In the first image, the skyrmion exists in a conical phase, with a central Bragg peak, and exceptional bleeding in the detector. As the field is adjusted, multiple co-existing lattices are present in the sample. Finally in the correct conditions, the skyrmion lattices show no preferred order, and are considered a pseudo-liquid.

Gold Sponsors:

Silver Sponsor:

Institute of Physics
37 Caledonian Road, London N1 9BU
Telephone: +44 (0)20 7470 4800
iop.org/conferences

Registered charity number 293851 (England & Wales) and SC040092 (Scotland)